

AD _____

CONTRACT NUMBER DAMD17-94-C-4126

TITLE: Model for Trauma Patient Simulation and Fluid
Resuscitation

PRINCIPAL INVESTIGATOR: Brian L. Robey

CONTRACTING ORGANIZATION: Southwest Research Institute
San Antonio, Texas, 78228-0510

REPORT DATE: November 1996

TYPE OF REPORT: Final

PREPARED FOR: Commander
U.S. Army Medical Research and Materiel Command
Fort Detrick, Frederick, Maryland 21702-5012

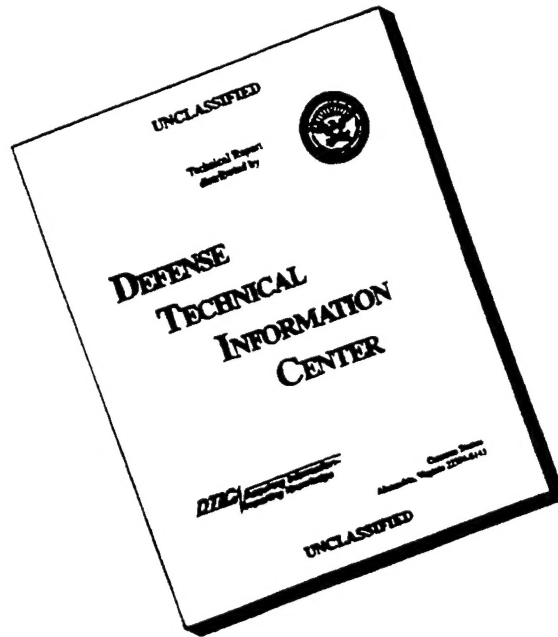
DISTRIBUTION STATEMENT: Approved for public release;
distribution unlimited

The views, opinions and/or findings contained in this report are those of the author(s) and should not be construed as an official Department of the Army position, policy or decision unless so designated by other documentation.

19961220 101

DTIC QUALITY INSPECTED 1

DISCLAIMER NOTICE



THIS DOCUMENT IS BEST QUALITY AVAILABLE. THE COPY FURNISHED TO DTIC CONTAINED A SIGNIFICANT NUMBER OF PAGES WHICH DO NOT REPRODUCE LEGIBLY.

REPORT DOCUMENTATION PAGEForm Approved
OMB No. 0704-0188

Public reporting burden for this collection of information is estimated to average 1 hour per response, including the time for reviewing instructions, searching existing data sources, gathering and maintaining the data needed, and completing and reviewing the collection of information. Send comments regarding this burden estimate or any other aspect of this collection of information, including suggestions for reducing this burden, to Washington Headquarters Services, Directorate for Information Operations and Reports, 1215 Jefferson Davis Highway, Suite 1204, Arlington, VA 22202-4302, and to the Office of Management and Budget, Paperwork Reduction Project (0704-0188), Washington, DC 20503.

1. AGENCY USE ONLY (Leave blank)		2. REPORT DATE November 1996	3. REPORT TYPE AND DATES COVERED Final (1 Sep 94 - 18 Sep 96)	
4. TITLE AND SUBTITLE Model for Trauma Patient Simulation and Fluid Resuscitation			5. FUNDING NUMBERS DAMD17-94-C-4126	
6. AUTHOR(S) Brian L. Robey			8. PERFORMING ORGANIZATION REPORT NUMBER	
7. PERFORMING ORGANIZATION NAME(S) AND ADDRESS(ES) Southwest Research Institute San Antonio, Texas 78228-0510				
9. SPONSORING/MONITORING AGENCY NAME(S) AND ADDRESS(ES) Commander U.S. Army Medical Research and Materiel Command Fort Detrick, Frederick, MD 21702-5012			10. SPONSORING/MONITORING AGENCY REPORT NUMBER	
11. SUPPLEMENTARY NOTES				
12a. DISTRIBUTION / AVAILABILITY STATEMENT Approved for public release; distribution unlimited			12b. DISTRIBUTION CODE	
13. ABSTRACT (Maximum 200 SwRI performed mathematical modeling and simulation research aimed at developing a trauma patient simulator (TPSIM) for the Life Support Trauma and Transport (LSTAT) Army evacuation platform. The purpose of this research was to develop methods for predicting changes in hemodynamic parameters during and after blood loss. Prediction of hemodynamic parameters based on blood volume changes was the first step in the development of an automated fluid resuscitation system. The research focused on the refinement of a passive system model of cardiovascular hemodynamics and fluid exchange and the design and development of an ancillary model to simulate neural and hormonal control during hemorrhagic shock. Both neural network and fuzzy logic approaches were studied to model neural and hormonal control. This combination of passive and control system models was referred to as the TPSIM. The TPSIM was developed with animal hemorrhagic shock data found in the literature. Additional animal data would be required for model refinement and validation.				
14. SUBJECT TERMS Trauma Patient			15. NUMBER OF PAGES 279	
			16. PRICE CODE	
17. SECURITY CLASSIFICATION OF REPORT Unclassified	18. SECURITY CLASSIFICATION OF THIS PAGE Unclassified	19. SECURITY CLASSIFICATION OF ABSTRACT Unclassified	20. LIMITATION OF ABSTRACT Unlimited	

Short Summary Report
DARPA Contract No. DAMD17-94-C4126
Southwest Research Institute
Project No. 12-6711

Report Date: 6 November, 1996

Project Title: Adaptive Mathematical Model for Trauma Patient Monitoring and Fluid Resuscitation

Principal Investigator: Brian L. Robey, Biosciences and Bioengineering Department

Organization: Southwest Research Institute
P.O. Drawer 28510
6220 Culebra Rd.
San Antonio, Texas 78228
Phone: 210-684-5111

Period of Performance: 1 September, 1994 to 8 November, 1996

Total Contract Amount: \$347,393.00

Amount Expended through 10/25/96: \$202,329.31

Summary of Work Performed:

SwRI performed mathematical modeling and simulation research aimed at developing a trauma patient simulator (TPSIM) for the Life Support Trauma and Transport (LSTAT) Army evacuation platform. The purpose of this research was to develop methods for predicting changes in hemodynamic parameters (e.g., mean arterial pressure, hematocrit, cardiac output, and oxygen debt) during and after blood loss. Prediction of hemodynamic parameters based on blood volume changes was the first step in the development of an automated fluid resuscitation system. The research focused on the refinement of a passive system model of cardiovascular hemodynamics and fluid exchange and the design and development of an ancillary model to simulate neural and hormonal control during hemorrhagic shock. Both neural network and fuzzy logic approaches were studied to model neural and hormonal control. This combination of passive and control system models was referred to as the TPSIM. The TPSIM was developed with animal hemorrhagic shock data found in the literature. Additional animal data would be required for model refinement and validation.

Detailed summaries and results from this research may be found in the attached quarterly progress reports. In addition, SwRI presented the attached paper at the fall 1996 meeting of the IEEE Engineering and Medicine and Biology Society meeting. The software developed to implement the models was delivered on personal computer hardware to Dr. Frederick J. Pearce at the Walter Reed Army Institute of Research. The computer hardware was shipped on 15 October, 1996.

A Fuzzy Logic Model for Neural and Hormonal Compensation in Hemorrhagic Shock

Jian Ling and Brian L. Robey

Southwest Research Institute, San Antonio, Texas, 78238 U.S.A.

E-mail: jling@swri.edu, brobey@swri.edu

Abstract - Southwest Research Institute (SwRI) has developed a fuzzy logic model to simulate neural and hormonal compensation (NHC) mechanisms during hemorrhagic shock. This NHC model is a component in a larger trauma patient simulation model under development that predicts changes in hemodynamic parameters during and after hemorrhage. These predicted variables may then be used to determine and automate fluid resuscitation. To develop the fuzzy logic model, SwRI combined physiological knowledge about NHC with experimental hemorrhage data obtained from swine. Plausible predictions for physiological variables were obtained.

I. INTRODUCTION

Southwest Research Institute (SwRI) is developing an automated fluid resuscitation system for the Advanced Research Projects Agency (ARPA) and the U.S. Army. This system is composed of two components: a trauma patient simulation model for prediction of changes in hemodynamic parameters during and after a hemorrhage (with and without fluid resuscitation) and a decision-making system for selection of optimal fluid resuscitation strategies based on model predictions. This overall system is intended to enhance the quality of trauma care on the battlefield while conserving medical resources.

During hemorrhage, compensation mechanisms play an important role in maintaining blood pressure and cardiac output during hemorrhage. These mechanisms include baroreceptor feedback control, chemoreceptor control, central nervous system ischemic control, and hormonal regulation [1]. When arterial blood pressure decreases after severe hemorrhage, the baroreceptors in the walls of the great arteries elicit powerful stimulation to the sympathetic

vasoconstrictor system throughout the body. This increases peripheral resistance to maintain arterial blood pressure. The sympathetic constriction of the veins attempts to increase the venous return and restrict cardiac output. The sympathetic system also increases the heart rate and contractility of the heart. Chemoreceptors in the walls of blood vessels detect decreased oxygen content and then excite the vasomotor center to elevate blood pressure. The central nervous system invokes a strong sympathetic response as a final effort to prevent brain blood flow from decreasing to a lethal level.

Hormonal regulation includes the formation of angiotensin which constricts the peripheral arteries, thereby raising blood pressure. The hypothalamus secretes vasopressin which even further constricts the peripheral arteries and veins [1].

SwRI is developing a model for these neural and hormonal compensation (NHC) mechanisms during hemorrhage. This NHC model, in combination with a passive cardiovascular system model, forms the basis for the trauma patient simulator. This paper describes the use of fuzzy logic to simulate these complex and inter-related NHC mechanisms.

II. METHODS

The effects of NHC are adjustments of heart rate (HR), heart contractility (CT), peripheral resistance (PR), and venous compliance (VC) to return blood pressure and blood oxygen content to normal levels. To develop the fuzzy logic model, changes in mean arterial pressure (MAP) and oxygen debt (O2D) (the difference between oxygen consumption and oxygen delivery) were selected as NHC model inputs, and HR, CT, PR, and VC as model outputs (Fig. 1).

A. Fuzzy Logic System

A fuzzy logic system was chosen to model the NHC system. Fuzzy logic systems are able to handle nonlinear

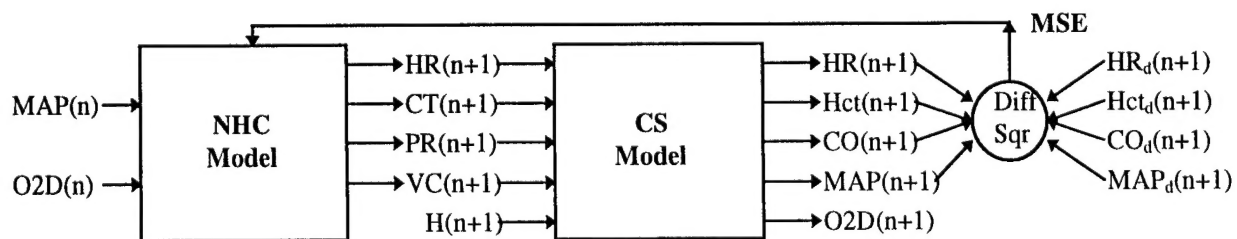


Fig. 1. Flow diagram for the trauma patient simulator comprised of both a neural and hormonal compensation (NHC) model and a cardiovascular system (CS) model [2]. The mean squared error (MSE) between the estimation and measurements (indicated by subscript d) for HR, Hct, CO, and MAP was used to optimize the NHC model.

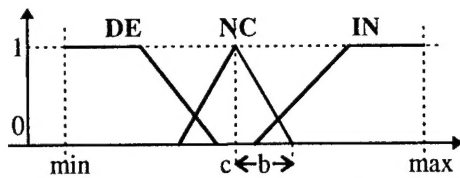


Fig. 2. Membership functions (MBFs) for "Decreased" (DE), "No Change" (NC), and "Increased" (IN). The variable c represents the center of the MBF; b is one-half of MBF's base width; min and max are the limits of the variable inputs and outputs.

Table 1. Four rules based on physiological compensation mechanisms.

IF (Inputs)		THEN (Outputs)			
MAP	O2D	HR	CT	PR	VC
DE	NC	IN	IN	IN	DE
DE	IN	IN	IN	IN	DE
NC	NC	NC	NC	NC	NC
IN	NC	DE	DE	DE	IN

relationships between inputs and outputs. Such systems can also incorporate domain-specific knowledge useful in problem solving. Previous attempts to model NHC with a neural network were less successful; predictions for PR and CT were unrealistic. To develop the NHC fuzzy logic model, three linguistic variables, *Decreased* (DE), *No Change* (NC), and *Increased* (IN), were used to describe the changes between inputs and outputs. The membership function (MBF) used to represent changes in inputs and outputs is illustrated in Fig. 2. Four fuzzy rules were developed to describe the physiological effects on HR, CT, PR, and VC based on changes in MAP and O2D (Table 1).

The fuzzy singleton approach was used to fuzzify the input values. Fuzzy MIN and MAX operators were adopted for the fuzzy inference engine [3]. The center-of-gravity defuzzifier was used to defuzzify the outputs from the NHC model.

B. Training the NHC Model

Optimal membership functions (i.e., the center and width of each MBF) were obtained by training the model with experimental data. Data was obtained from uncontrolled hemorrhage experiments on five swine performed by Bickell et al. [4]. The HR, MAP, CO, and Hct were measured at 0, 5, 15, 30, 60, 90, and 120 minutes after the start of each hemorrhage. The modified random search (MRS) optimization method [5] was used to train the model with averaged experiment data.

III. RESULTS AND DISCUSSION

Figs. 3 and 4 illustrate changes in HR, CT, PR, VC, MAP, CO, and O2D calculated by the trauma patient simulator with NHC for 33% blood loss in 5 minutes. Trends for PR, CT, and VC follow physiological expectations. In particular, PR doubled during hemorrhage. The results also show a decrease in CT after an initial increase. This may suggest

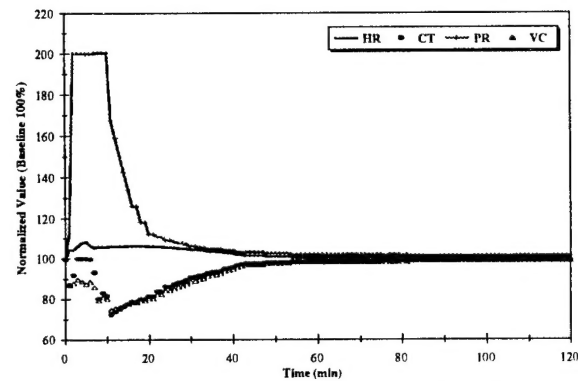


Fig. 3. Changes in heart rate (HR), heart contractility (CT), peripheral resistance (PR), and venous compliance (VC) during and after hemorrhage as predicted by the neural and hormonal compensation model.

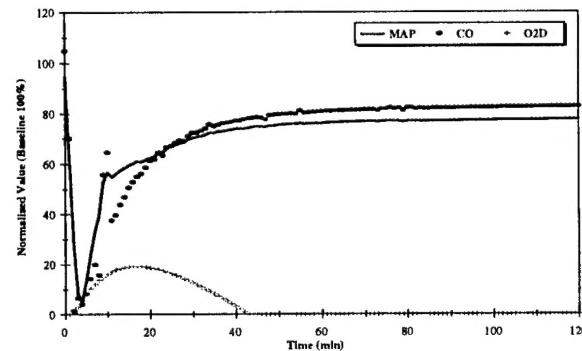


Fig. 4. Changes in mean arterial pressure (MAP), cardiac output (CO), and oxygen debt (O2D, in absolute value) during and after hemorrhage as predicted by the cardiovascular model with NHC.

that a reduction in heart muscle oxygen content prevents normal functioning. In conclusion, the fuzzy logic approach provides a means to include domain-specific knowledge required for solving many complex non-linear problems.

REFERENCES

- [1] A.C. Guyton, *Medical Physiology*. Philadelphia: W.B. Saunders Co., 1991.
- [2] T.J. Doherty, *A Mathematical Model of the Circulation for the Study of Hemorrhagic Shock and Fluid Resuscitation*. Ph.D. Dissertation, University of California at Berkeley, 1993.
- [3] L.X. Wang, *Adaptive Fuzzy Systems and Control*. Prentice Hall, Englewood Cliffs, 1994.
- [4] W.H. Bickell, J. O'Benar, S.P. Bruttig, C.E. Wade, J.P. Hannon, F. Tillman, W. Rodkey, "The hemodynamic response to aortotomy in the conscious chronically instrumented swine," *The Physiologist*, vol. 30, pp.228, 1987.
- [5] N. Baba, "A new approach for finding the global minimum of error function of neural networks," *Neural Networks*, Vol. 2, pp.367-373, 1989.

**Quarterly Progress Report
15 December 94**

2

**Quarterly Progress Report
15 March 95**

3

**Quarterly Progress Report
15 June 95**

4

**Quarterly Progress Report
15 September 95**

5

**Quarterly Progress Report
15 December 95**

6

**Quarterly Progress Report
15 March 96**

7

**Quarterly Progress Report
15 June 96**

8

Intentionally Left Blank

Quarterly Progress Report

1. Contract No. DAMD17-94-c4126 2. Report Date 15 December, 1994
- SwRI Project No. 12-6711
3. Reporting Period from 1 September, 1994 to 30 November, 1994.
4. PI Dr. Tammy J. Doherty 5. Phone (210) 522-2684
6. Institution Southwest Research Institute, San Antonio, Texas
7. Project Title Model for Trauma Patient Simulation and Automated Fluid Resuscitation
8. Current staff with percent effort of each on project

Tammy J. Doherty 38 %

Jian Ling 18 %

Jennifer Peacock 8 %

9. Contract expenditures to date (as applicable):

	this qtr/cumulative		this qtr/cumulative
Personnel	<u>4509.70 / 4509.70</u>	Travel	<u>0.00 / 0.00</u>
Fringe Benefits	<u>1970.73 / 1970.73</u>	Equipment/Supplies	<u>7569.95 / 7569.95</u>
Overhead	<u>7646.91 / 7646.91</u>	Facilities Capital	<u>673.96 / 673.96</u>

	this qtr/cumulative
subtotal	<u>22,371.25 / 22,371.25</u>
Indirect Costs	<u> / </u>
Fee	<u>1735.80 / 1735.80</u>
Total	<u>24,107.05 / 24,107.05</u>

10. Comments on administrative and logistical matters.

Start of project was delayed 9 days to obtain required signatures on contract. It also took longer than expected to acquire required programming software packages, and to implement these on the personal computer. The principal investigator did not commit expected effort during 1st

quarter due to prior commitments to ongoing projects. The PI will commit greater-than-scheduled effort during the second quarter.

11. Scientific Progress

Task 1: For reasons stated above, the "Passive system model development/refinement" task was not started until 10/2/94. Completion of this task required development of a model subsystem describing the exchange of fluid and solute among lung capillary interstitial and tissue cell spaces. A preliminary report of this effort is enclosed. In addition to the lung microvascular exchange subsystem model, equations were added to a previously-developed cardiovascular hemodynamics model for predicting kidney fluid output and oxygen transport. At this time, the passive system model is complete. Sensitivity analyses on this model will be conducted in the next week, with results to be included in the next quarterly report.

Task 2. Acquisition of existing data has been an ongoing effort since project startup. We currently have sufficient data for uncomplicated hemorrhage and resuscitation. We are currently attempting to obtain data for hemorrhage and resuscitation complicated by head injury, trauma, and pharmacological interventions.

Task 3. Several numerical optimization schemes were reviewed. Two have been implemented in C++ for use in identification of the deterministic control system. At this time, the mathematical model is implemented in Microsoft Quick BASIC. Methods have been established for calling these C++ optimization routines from Quick BASIC. However, because C++ and Fortran are both approximately 20 times faster than Quick BASIC, we have decided to initiate Task 10 by rewriting parts of the model that are computationally intensive in the C++ and Fortran languages. This will extend the time required to complete Task 3. However, this action will ultimately decrease time required for future tasks that require the model to be run over many iterations.

Task 4. Not started.

Task 5. NeuralWare is the neural network simulation package selected for use in development of the Neural Network Control System Model. At this time, we are attempting to write a NeuralWare User I/O program in C that would allow the NeuralWare networks to function as a control system model.

Tasks 6-9. Not started.

Task 10. Real time system development has been initiated by rewriting critical model components in Fortran and C++. This rewrite is expected to speed model execution by a factor of 10-20 times the current execution speed.

Tasks 11-12. Not started.

12. Plans and milestones for next quarter.

- a. Complete Task 1
- b. Continue to acquire data (Task 2)
- c. Complete Model Rewrite (part of Task 10)
- d. Complete Task 3 and initiate Task 4.
- e. Complete Task 5 and initiate Task 6.

Preliminary Report

**Model for Trauma Patient Simulation and Automated Fluid Resuscitation:
Exchange of Fluid and Solute Among Pulmonary Capillary, Interstitial, and
Tissue Cell Spaces**

December 15, 1994

SwRI Project No. 12-6711

Contract No. DAMD17-94-C4126

Prepared for:

**Director, U.S. Army Research Acquisition Activity
ATTN: SGRD-RMA-RC
Fort Detrick, MD 21702-5014
and
Deputy Director for Defense Healthcare Technologies
ARPA/Defense Sciences Office
3701 North Fairfax Drive
Arlington, VA 22203-1714**

Prepared by:

**Tammy J. Doherty and Jennifer L. Peacock
Southwest Research Institute
San Antonio, Texas**

MODEL FOR TRAUMA PATIENT SIMULATION AND AUTOMATED FLUID RESUSCITATION: EXCHANGE OF FLUID AND SOLUTE AMONG PULMONARY CAPILLARY, INTERSTITIAL, AND TISSUE CELL SPACES

FOREWORD

This report describes the development and initial testing of a pulmonary microvascular exchange model, a small portion of the work being performed under contract no. DAMD17-94-C4126. This model will be incorporated into a previously-developed, passive cardiovascular system model, for which similar reports are already available (Doherty 1993a, 1993b, 1993c, 1993d). The integrated passive system model will then form the basis for a mathematical model for Trauma patient simulation.

This is a preliminary report. It is expected that the pulmonary microvascular exchange model described here, will be further developed and refined during subsequent model integration and testing. A final version of this report will be incorporated into the final, project report, to be submitted at the conclusion of this contract.

INTRODUCTION

Previous reports (Doherty 1993a, 1993b, 1993c, 1993d) detail the development of a mathematical model that predicts the short-term (i.e., 1-3 hour) response of plasma volume, cardiac output, and arterial pressure to hemorrhage and fluid resuscitation. Because lung microvascular exchange does not significantly affect changes in cardiovascular hemodynamics, lung microvascular exchange was not included in that model. To simulate the trauma patient over longer time periods (i.e., 6-8 hours), however, factors such as pulmonary edema, filtration of fluid by the kidneys, and anaerobic as well as aerobic metabolism must also be considered. This report describes the preliminary development of a pulmonary microvascular exchange subsystem model for predicting pulmonary edema.

A 3-compartment (plasma, interstitial, and tissue cell) model provides the basis for model development and testing. The effects of different simplifying assumptions on model predictions were tested by creating alternate versions of this model and comparing predictions of plasma, pulmonary interstitial, and pulmonary tissue cell volumes over a wide range of simulation conditions and model parameter values. In this way, the required level of model complexity could be determined. The most appropriate model, based on results of these comparisons, was then used in sensitivity analyses, over the same range of simulation conditions and model parameter values. From these analyses, it was possible to identify the parameters that most greatly affect model predictions. Because there is little quantitative data of lung interstitial

volume for comparison with model predictions, direct comparisons of model predictions and observed data are not possible. Validation of the complete model for trauma patient simulation will be conducted as part of this contract, at a later time.

THE BASIC 3-COMPARTMENT MODEL

A three-compartment (plasma, pulmonary interstitial, and pulmonary tissue cell), lumped-parameter model was initially selected to describe lung microvascular exchange. This model is similar to the model described by Bert and Pinder (1982). Rates of compartment volume change (dV/dt) for blood plasma (subscript P), lung interstitial (subscript I_p) and lung tissue cell (subscript T_p) compartments are obtained by subtracting rates of fluid efflux from rates of fluid influx:

$$\frac{dV_P}{dt} = L_{v,p} - J_{v,Cplp} \quad 1)$$

$$\frac{dV_{Ip}}{dt} = J_{v,Cplp} - L_{v,p} - J_{v,IpTp} \quad 2)$$

$$\frac{dV_{Tp}}{dt} = J_{v,IpTp} \quad 3)$$

where $L_{v,p}$ is the rate of pulmonary lymph flow (interstitial to plasma), and $J_{v,ij}$ is the rate of fluid flux from compartment i to compartment j. Changes in plasma solute mass (dS/dt) for the three compartments may be obtained in a similar fashion, by subtracting rates of solute efflux from solute influx:

$$\frac{dS_P}{dt} = L_{s,p} - J_{s,Cplp} \quad 4)$$

$$\frac{dS_{Ip}}{dt} = J_{s,Cplp} - L_{s,p} \quad 5)$$

where $L_{s,p}$ is the rate of solute return to the vasculature via the pulmonary lymphatics, and $J_{s,ij}$ is the rate of solute flux from compartment i to compartment j. Solute transport between interstitial and tissue cell compartments is assumed to be negligible.

The Kedem-Katchalsky (1958) equations are used to describe the coupled flux of fluid ($J_{v,Cplp}$) and solute ($J_{s,Cplp}$) across the capillary wall:

$$J_{v,Cplp} = k_{v,Cplp} \left[(P_{Cp} - P_{Ip}) - \sum \sigma_{s,Cplp} (\Pi_{s,p} - \Pi_{s,Ip}) \right] \quad 6)$$

$$J_{s,Cplp} = k_{s,Cplp}(C_{s,p} - C_{s,lp}) + (1 - \sigma_{s,Cplp})\bar{C}_{s,Cplp}J_{v,Cplp} \quad 7)$$

It was verified in a previous report that these simple equations were as accurate for predicting gross movement of fluid and solute across the capillary wall as more complex equations given by Patlak (1963) and Katz (1985). Because the tissue cell membrane is considered to be impermeable to solutes, the Landis-Starling equation, extended to a solution of multiple solutes, may be used to describe fluid transport from the interstitial to the tissue cell compartment:

$$J_{v,lpTp} = k_{v,lpTp}[(P_{lp} - P_{Tp}) - \sum(\Pi_{s,lp} - \Pi_{s,Tp})] \quad 8)$$

A model for pulmonary lymph flow ($L_{v,p}$) as a function of interstitial hydrostatic pressure was obtained from Parker and coworkers (1981a, 1981b):

$$L_{v,p} = 0.002833(V_{lp} + V_{Tp}) - 0.0131784 \quad 9)$$

This relationship between lymph flow rate and interstitial fluid pressure assumes a normal value for lymph flow rate of $0.002 \text{ ml} \cdot \text{kg}^{-1} \cdot \text{min}^{-1}$ (see Appendix A). Transport of solutes in lymph is assumed to occur by bulk flow, i.e.:

$$L_{s,p} = C_{s,lp}L_{v,p} \quad 10)$$

Interstitial hydrostatic pressure is estimated using the following piece-wise linear relationship between P_{lp} and V_{lp} :

$$\begin{aligned} P_{lp} &= 26(V_{lp} + V_{Tp} - V_0) \quad \text{when } V_{lp} + V_{Tp} < V_0 \\ P_{lp} &= 2.08(V_{lp} + V_{Tp} - V_0) \quad \text{when } V_{lp} + V_{Tp} \geq V_0 \end{aligned} \quad 11)$$

For simplicity, three plasma solutes are considered: salts (subscript s), albumin (subscript a), and globulins (subscript g). Dextran of approximately 70 kD (subscript d), which are used in some artificial plasma volume expanders, are also considered. Because NaCl is the most abundant salt in plasma and interstitial fluid, the characteristics of NaCl are selected to represent all salt molecules. The osmotic pressure for NaCl is approximately (Harper 1969):

$$\Pi_s = (31.877)(19.33 \times 10^3)C_s \quad 12)$$

where C_s is salt concentration (g/ml), 31.877 converts grams of NaCl to milliosmoles, and 19.33×10^3 is the osmotic pressure (mm Hg) exerted by 1 mosm/ml of solute at normal body temperature. Cubic equations, presented by Landis and Pappenheimer (1963), are used to estimate partial osmotic pressures for albumin and globulin:

$$\Pi_a = 280C_a + 1800C_a^2 + 12000C_a^3 \quad 13)$$

$$\Pi_g = 210(C_a + C_g) + 1600(C_a + C_g)^2 + 9000(C_a + C_g)^3 - \Pi_a \quad 14)$$

where C_a and C_g are concentrations (g/ml) of albumin and globulin, respectively. Partial osmotic pressures of dextran-70 were estimated from the cubic relationship developed by Mazzoni et al. (1988) from experimental data provided by Thorén (1978):

$$\Pi_d = 620C_d + 9300C_d^2 + 5000C_d^3 \quad 15)$$

where C_d is dextran-70 concentration (g/ml).

The hyaluronic acid molecules, proteoglycans, and cross-linked collagen fibers of the interstitial gel restrict the total interstitial space available to macromolecules. Interstitial exclusion volumes for albumin are usually measured in the range of 40-50%, while those for globulin are measured in the 50-70% range (Parker et al. 1979). This exclusion volume affects the interstitial solute concentration. For example, the concentration of albumin in lymph, which is derived from "free" fluid in the interstitium is approximately 50% higher than the albumin concentration obtained from the entire interstitial space by homogenization. In this model, we assume that the exclusion volume for each macromolecule does not change size as fluid is added to, or depleted from, the interstitial space.

Solution of Equations

Model equations were solved numerically, using Euler's method, implemented in Microsoft Quick BASIC on an IBM-compatible PC.

SIMPLIFYING ASSUMPTIONS

Sixteen different models were created to test four different simplifying assumptions: 1) lumped interstitial and tissue cell compartments, 2) constant lymph flow rate, 3) constant interstitial pressure, and 4) ignore capillary-interstitial globulin flux:

Table 1. Simplifying assumptions.

model #	lumped I_p and T_p	constant L_v	constant P_i	ignore $J_{g,CpIp}$
1	yes	yes	yes	yes
2	yes	yes	yes	no

model #	lumped I_p and T_p	constant L_v	constant P_i	ignore $J_{g,Cplp}$
3	yes	yes	no	yes
4	yes	yes	no	no
5	yes	no	yes	yes
6	yes	no	yes	no
7	yes	no	no	yes
8	yes	no	no	no
9	no	yes	yes	yes
10	no	yes	yes	no
11	no	yes	no	yes
12	no	yes	no	no
13	no	no	yes	yes
14	no	no	yes	no
15	no	no	no	yes
16	no	no	no	no

Each model was used to predict results for each of 12 different simulated experiments:

Table 2. Simulated Experiments.

Experiment #	Description
1	No Perturbation (system remains in steady state)
2	50% increase in total blood volume
3	50% decrease in total blood volume
4	50% increase in pulmonary capillary pressure
5	50% decrease in pulmonary capillary pressure
6	50% increase in plasma NaCl
7	50% decrease in plasma NaCl

8	50% increase in plasma albumin
9	50% decrease in plasma albumin
10	Addition of 0.24 g of Dextran-70 to plasma (equivalent to 4 ml/kg of 6% Dextran-70)
11	25% decrease in plasma NaCl with a 25% decrease in plasma albumin
12	50% increase in plasma NaCl and addition of 0.24 g of Dextran-70 (equivalent to 4 ml/kg of 7.5% NaCl in 6% Dextran-70)

Normal parameter values (see Appendix A), as well as high and low values for each of the 10 flux parameters ($k_{v,CpIp}$, $k_{v,IpTp}$, $k_{s,CpIp}$, $k_{a,CpIp}$, $k_{g,CpIp}$, $k_{d,CpIp}$, $\sigma_{s,CpIp}$, $\sigma_{a,CpIp}$, $\sigma_{g,CpIp}$, $\sigma_{d,CpIp}$) were used, for a total of 21 different parameter value combinations. Thus, each of the 16 models was run a total of 252 times. Predicted percent changes in plasma volume, lung interstitial volume, and lung tissue volume at 1-minute, 5-minutes, and 30-minutes were saved to an array, and subsequently to a data file. Absolute differences (absolute values of calculated differences) between predictions generated by different models were then calculated. To test the effect of lumping the interstitial and tissue cell compartments, absolute differences between predictions generated by model 1 and 9, 2 and 10, 3 and 11, 4 and 12, 5 and 13, 6 and 14, 7 and 15, and 8 and 16 were computed. The maximum absolute difference over the 21 different parameter value combinations was then obtained, and plotted as stacked bar graphs (one bar for each model pair, each simulated experiment, at each time point) in Figures B1 through B3. The same procedure was used to test the other simplifying assumptions, by comparing other model pairs. These results are presented in figures B4 through B12.

lumped interstitial and tissue cell compartments

The basic three-compartment model includes both tissue cell and interstitial compartments. Because tissue cell membranes cannot support a hydrostatic pressure gradient, and because osmotic pressure gradients across the cell membranes are usually negligible, an argument may be made for lumping the tissue cell and interstitial compartments together. However, the capillary wall is normally more permeable to water and certain solutes (e.g., sodium) than are tissue cell membranes. Consequently, intravascular administration or depletion of solutes, and the subsequent alterations in interstitial solute concentration, may produce large osmotic gradients across the tissue cell membrane. In model studies of systemic microvascular exchange (Doherty et al 1993c), such gradients significantly affected predictions of plasma volume.

To test whether tissue cell and interstitial compartments could be lumped together, the interstitial-cellular fluid transport equation (Equation 8) was eliminated from corresponding three-compartment models. As expected, differences between interstitial volume predictions generated by 2-compartment and corresponding 3-compartment models (see Figure B2) were small (<5%) except for experiments in which plasma NaCl concentration was altered (Experiment # 6, 7, 11, 12). When plasma NaCl was altered, differences frequently exceeded 20%. Results were the same for the plasma and tissue cell compartments, although the magnitude of the absolute differences was different (see Figures B2-B3).

One problem in studying pulmonary microvascular exchange in isolation is that the systemic extravascular fluid compartment is not allowed to contribute to the restoration of capillary-interstitial hydrostatic and osmotic pressure balance. Except for the case of altered pulmonary capillary pressure, restoration of fluid balance is normally achieved by systemic microvascular exchange, and very little by pulmonary microvascular exchange. In this study, by attempting to restore fluid balance by among the pulmonary fluid compartments alone, pulmonary interstitial and tissue cell volume response to changes in plasma solute concentration changes are undoubtedly exaggerated. This over-prediction of pulmonary interstitial and tissue cell volumes could lead to overestimation of the absolute differences between predictions generated by different model pairs. However, in this case, absolute differences between model pairs for simulations in which dextran or albumin were altered were very small. Thus, it does not appear that differences between model predictions are affected by the over-prediction of interstitial and tissue cell volume changes. From these results, it may be concluded that both interstitial and tissue cell compartments are required when concentrations of small, highly permeable solutes are out of balance. This same effect was demonstrated in the systemic microvascular exchange model developed previously (Doherty 1993c).

constant lymph flow rate

Under normal circumstances, Starling forces favor a net flow of fluid out of the capillary, into the interstitial space. Fluid does not normally accumulate in the interstitium. Instead, excess interstitial fluid is returned to the circulation by the lymphatics. Lymph vessels originate as thin-walled, capillary-like, channels. At the origin, sequential endothelial cells overlap each other, forming valve-like structures. A positive interstitial-lymph pressure gradient causes the overlapping portion of the endothelial cells (i.e., the "flaps") to be pushed inward, admitting flow into the lymphatic capillary while prohibiting back flow. Thus, fluid enters the lymph capillary when interstitial volume and pressure are high, but fluid is not permitted to leave the lymph capillary when interstitial volume and pressure are low. Further from the origin, lymphatic endothelial cells are closer together, forming a true vessel capable of transporting both fluid and solute. Small lymph capillary vessels join together to form progressively larger lymph vessels. Lymph flow is achieved by rhythmic contraction of smooth muscle cells in large lymph vessels,

which tends to push flow from origin to circulation while valves present in prenatal lymph vessels prohibit back-flow (Guyton et al. 1975). The level of smooth muscle activity may be under sympathetic control (Dabney et al. 1988). From this conceptual model, it may be assumed that the rate of fluid transfer from the interstitium into the lymphatics, and from there to the vasculature depends on interstitial pressure and lymphatic smooth muscle activity. Equation 9 assumes that lymph flow rate is proportional to interstitial volume, which is related to interstitial pressure. Under conditions in which interstitial volume does not change markedly, this equation would add complexity to the model without affecting model predictions. On the other hand, when interstitial volume is much higher than normal, increased lymph flow rate may be an important mechanism for preventing edema.

To test whether the model may be simplified by ignoring variable lymph flow rate, the lymph flow rate - extravascular volume relationship of Equation 9 was discarded, and lymph flow rate was held at its initial value of $0.002 \text{ ml} \cdot \text{min}^{-1} \cdot \text{kg}^{-1}$. Differences between predictions of pulmonary interstitial volume generated by models assuming constant lymph flow rate and models using Equation 9 were very small for 1-minute prediction values, but were larger for the 5-minute, and 30-minute predictions (see Figure B4). Differences at 30-minutes frequently exceeded 2% and in one case exceeded 10%. Results were similar for plasma and pulmonary tissue cell volumes, although the magnitudes of the absolute differences were much smaller (see Figures B5 and B6). These results suggest that variable lymph flow rate may significantly effect model predictions under certain conditions, and that the assumption of constant lymph flow rate should not be used to simplify the model.

constant interstitial pressure

The interstitial matrix is made up of a network of hyaluronic acid molecules, proteoglycans, and cross-linked collagen fibers (Parker et al. 1979). The mechanical-elastic properties of the collagen molecules contribute to the development of a nonlinear interstitial pressure-volume relationship which differs from pressure-volume relationships typical of compartments filled with fluid. When the interstitium is dehydrated, the pressure-volume relationship is dominated by the mechanical elastic properties of the collagen fibers. At high interstitial volumes, the gelatin matrix breaks up (collagen fibers do not tolerate expansion) and the pressure-volume relationship assumes the characteristics of a fluid-filled compartment, dominated by the elastic effects of the boundaries of the compartment (Guyton et al. 1975), such as the cell membranes, capillary walls, and compartment boundaries within the body. The equations used to estimate interstitial hydrostatic pressure (Equation 11) corresponds to this physical description, consisting of a relatively steep pressure-volume relationship at negative interstitial pressures, and a more compliant region at positive interstitial pressures. In model studies of systemic microvascular exchange, however, it was shown that P_i did not change significantly during simulated experiments similar to those used in this study (Doherty 1993c). Therefore, such a detailed description of the interstitial compliance curve may be unnecessary.

On the other hand, the pulmonary interstitial space is much smaller than the systemic interstitial space, and relatively larger changes in interstitial pressure could occur for similar perturbations.

The assumption of constant interstitial pressure was tested by discarding the interstitial pressure - volume relationship of Equation 11. Instead, interstitial pressure was held at its initial value, which is calculated using Equation A1. Differences between predictions of interstitial volume generated by models assuming constant interstitial pressure and models that do not (see Figure B7) were highest at 30-minutes, frequently exceeding 20%. Results were similar for absolute differences in plasma volume (Figure B8), although the magnitudes of the absolute differences were much smaller. Absolute differences in pulmonary tissue cell volume were insignificant except for simulated experiments in which plasma NaCl was altered. In those cases, absolute differences were highest at 5-minutes and lowest at 30-minutes. These results suggest that the simplifying assumption of constant interstitial pressure should not be used to simplify the model.

Ignore capillary-interstitial globulin flux

Because globulin does not easily cross the capillary wall, capillary-interstitial globulin flux is frequently ignored in models of microvascular exchange. Based on Yoffey's work (1970), the basic three-compartment model assumes that the interstitial globulin concentration is 55% of the plasma concentration. The solute permeability coefficient for globulin was then calculated (Equation A3 in Appendix A) so that the system remained at steady state unless it was perturbed.

Except for Experiments 1 through 3, interstitial volume predictions generated by models that include capillary-interstitial globulin flux differ markedly from predictions generated by models that ignore globulin flux. Differences are larger at the 5- and 30-minute time periods than at the 1-minute time period. As mentioned previously, the response of pulmonary interstitial volume to changes in plasma solute concentration is undoubtedly greater than it would be if the systemic extravascular fluid compartments were allowed to participate. Absolute differences between predicted values might also be exaggerated. In this study, however, the effect of globulin flux on interstitial volume predictions was large not only for experiments in which plasma solute concentrations varied, but also for experiments in which pulmonary capillary pressure was altered even though changes in pulmonary capillary pressure would not be likely to affect systemic microvascular exchange. Thus, the predicted range of interstitial volume response to changes in capillary pressure is realistic. Because globulin flux affects pulmonary microvascular exchange under nearly all simulated conditions, including changes in pulmonary capillary pressure, inclusion of globulin flux appears to be warranted.

SENSITIVITY ANALYSES

Sensitivity analyses were performed to determine which model parameters had the greatest effect on model predictions. The basic, three-compartment pulmonary flux model was run over the 12 different simulated experiments, using 10 different values for each of the 10 flux parameters ($k_{v,CpIp}$, $k_{v,IpTp}$, $k_{s,CpIp}$, $k_{a,CpIp}$, $k_{g,CpIp}$, $k_{d,CpIp}$, $\sigma_{s,CpIp}$, $\sigma_{a,CpIp}$, $\sigma_{g,CpIp}$, $\sigma_{d,CpIp}$). Thus the model was run a total of 1200 times. Predicted percent changes in plasma volume, lung interstitial volume, and lung tissue volume at 1-minute, 5-minutes, and 30-minutes, were saved to an array, and subsequently to a data file. XY plots of plasma, interstitial, and tissue cell volumes versus each flux parameter, at each time point (one line per experiment), are presented in Appendix C.

sensitivity to $k_{v,CpIp}$

The rate at which fluid moves from the plasma to the interstitial space depends on the pulmonary capillary - interstitial fluid filtration coefficient, $k_{v,CpIp}$, as well as the plasma - interstitial hydrostatic and osmotic pressure differences (Equation 6). Figures C1 through C3 show the effect of changes in the parameter $k_{v,CpIp}$ on model predictions of interstitial, plasma and tissue cell volumes. The predicted response of pulmonary interstitial volume to large changes in plasma NaCl concentration (Experiments 6, 7, 11, and 12) was highly sensitive to changes in $k_{v,CpIp}$ at 1-minute (Figure C1). This effect is attenuated at 5-minutes (Figure C2), and nearly absent at 30-minutes (Figure C3). Because $k_{v,CpIp}$ affects the rate at which fluid balance is reestablished, but not the final volume distribution, the greatest effects of $k_{v,CpIp}$ are observed at 1-minute and 5-minutes, with relatively little sensitivity to $k_{v,CpIp}$ observed at 30-minutes. Pulmonary interstitial volume was relatively insensitive $k_{v,CpIp}$ for the other experiments. Plasma and tissue cell volumes were relatively insensitive to changes in $k_{v,CpIp}$ for the 12 simulated experiments (Figures C4 through C9).

One interesting feature observed in Figures C1 and C2 was the change in the response of pulmonary interstitial volume from the positive to the negative as $k_{v,CpIp}$ increased for Experiment 6, and from the negative to the positive as $k_{v,CpIp}$ increased for Experiment 7. According to Equation 6, interstitial volume would be expected to decrease as plasma solute concentration is increased (Experiment 6), and interstitial volume would be expected to increase as plasma solute concentration is decreased (Experiment 7). Figures C1 and C2, however, show that at low values of $k_{v,CpIp}$ the opposite occurs; interstitial volume initially increases as plasma NaCl concentration is increased (Experiment 6), and initially decreases when plasma NaCl concentration is decreased (Experiment 7). This apparent contradiction occurs because a three compartment model, rather than a two-compartment model was used. An increase in plasma NaCl causes water to move from the interstitial space to the blood plasma. This is true for all values of $k_{v,CpIp}$. The movement of NaCl in the opposite direction, as well as the loss of interstitial fluid causes interstitial plasma NaCl concentration to increase, creating an osmotic gradient across the tissue

cell membranes. In the three compartment model, this osmotic gradient causes water to move from the tissue cells, into the interstitial space. At very low values of $k_{v,CpIp}$, this results in a net loss of water in the tissue cell spaces (Figure D5), an initial gain of fluid in the interstitial space (Figure D1), and a net gain of fluid in the plasma space (Figure D3). In contrast, Figures D2, D3, and D4 show the percent change in interstitial, plasma, and tissue cell volumes when $k_{v,CpIp}$ is high. From these simulations, it is clear that the unexpected interstitial volume changes at low values of $k_{v,CpIp}$ result from interstitial-tissue cell fluid exchange, which is large relative to the interstitial-plasma fluid exchange.

Another interesting feature of Figures C1 through C3 is that, when plasma NaCl concentration is decreased, the magnitude of the percent change in interstitial volume at 1-minute is approximately double that when the plasma NaCl concentration is increased (at any value of $k_{v,CpIp}$). This appears to be the result of the nonlinear, pulmonary interstitial pressure - volume relationship (Equation 11). The interstitial compartment is less compliant at interstitial pressures less than zero, and more compliant at pressures greater than zero. Fluid loss from the interstitium results in a large decrease in interstitial hydrostatic pressure that acts to oppose further fluid loss. In contrast, when fluid is added to the interstitial space, hydrostatic pressure changes are small, and thus there is only a small force opposing further volume gain. The overall effect is that an increase in interstitial volume for a given perturbation (e.g. 50% decrease in plasma NaCl concentration) will be of greater magnitude than the decrease in interstitial volume for a corresponding perturbation in the opposite direction (e.g. 50% increase in plasma NaCl concentration).

sensitivity to $k_{v,IpTp}$

The rate at which fluid moves from the interstitial space to the lung tissue depends on the interstitial - lung tissue fluid filtration coefficient, $k_{v,IpTp}$ and interstitial - tissue hydrostatic and osmotic pressure differences (Equation 8). Figures C10 through C18 show the effect of changes in the parameter $k_{v,IpTp}$ on model predictions of pulmonary interstitial, plasma, and tissue cell volumes. Interstitial volume (Figure C4) shows little sensitivity to changes in $k_{v,IpTp}$. At 1-minute, decreasing the plasma NaCl concentration (Experiment 7) shows a slightly higher increase in interstitial volume for low values of $k_{v,IpTp}$ as compared to high values of $k_{v,IpTp}$. The 5-minute and 30-minute plots (Figures 11 and 12) show no effects of changes in $k_{v,IpTp}$. As with $k_{v,CpIp}$, plasma volume was not sensitive to changes in $k_{v,IpTp}$ for the 12 simulated experiments (Figures C13, C14, C15). Tissue volume showed a slight sensitivity to changes in $k_{v,IpTp}$ at 1-minute and 5-minutes (Figures C16, C17), but little or no sensitivity to $k_{v,IpTp}$ at 30-minutes.

sensitivity to $k_{s,CpIp}$

For experiments in which plasma NaCl was decreased (i.e., experiments 7 and 11) Interstitial volume predictions (% change from baseline) increased with decreasing values of

$k_{s,CpIp}$ (Figure C19). The effect was greater at 5-minutes (Figure C20), but nearly absent at 30-minutes (Figure C21), except for the lowest value of $k_{s,CpIp}$. For these simulated experiments, low values of $k_{s,CpIp}$ had a small effect of plasma volume which was completely absent at 30-minutes (Figures C22-C24). When plasma NaCl was decreased, predictions of tissue cell volume at 1-minute increased with increasing values of $k_{s,CpIp}$ (Figure C25). The effect was much smaller at 5-minutes (Figure C26), and absent at 30-minutes (Figure C27).

For experiments in which plasma NaCl was increased (i.e., Experiments 6 and 12), interstitial volume predictions increased with increasing values of $k_{s,CpIp}$ (Figure C19). The sensitivity of interstitial plasma volume predictions to $k_{s,CpIp}$ for these experiments was smaller, however, than sensitivity during experiments in which plasma NaCl was decreased. The effect was attenuated at 5-minutes (Figure C20), and nearly absent at 30-minutes (Figure C21), except for the lowest value of $k_{s,CpIp}$. For these simulated experiments, low values of $k_{s,CpIp}$ had a small effect on plasma volume (Figures C22-C24) which was, again, smaller than responses demonstrated during experiments in which NaCl was decreased. Predictions of pulmonary tissue cell volume demonstrate a significant degree of sensitivity to $k_{s,CpIp}$ at 1-minute (Figure C25), which is nearly absent at 5-minutes and 30 minutes (Figures C26-27).

sensitivity to $k_{a,CpIp}$

At 1-minute, pulmonary interstitial volume was insensitive to changes in $k_{a,CpIp}$, except for experiments in which plasma NaCl was altered (Figure C28). At 5- and 30-minutes, however, pulmonary interstitial volume was highly sensitive to changes in $k_{a,CpIp}$, except for simulated experiments 1 through 3, which did not show changes in pulmonary interstitial volume for any of the parameter values tested (Figures C29 and C30). Plasma volume was relatively insensitive to $k_{a,CpIp}$ at 1-minute (Figure C31) and only slightly sensitive at 5-minutes and 30-minutes (Figures C32 and C33). Pulmonary tissue cell volume appears to be insensitive to changes in $k_{a,CpIp}$ (Figures C34 through C36).

sensitivity to $k_{g,CpIp}$

Sensitivity of plasma volume, pulmonary interstitial volume, and pulmonary tissue cell volume to changes in $k_{g,CpIp}$ were qualitatively similar to, although much smaller in magnitude than sensitivities to $k_{a,CpIp}$. At 1-minute, pulmonary interstitial volume was insensitive to changes in $k_{g,CpIp}$, except for experiments in which plasma NaCl was increased (Figure C37). At 5- and 30-minutes, pulmonary interstitial volume was moderately sensitive to changes in $k_{g,CpIp}$, except for simulated experiments 1 through 3, which did not show changes in pulmonary interstitial volume for any of the parameter values tested (Figures C38 and C39). Plasma and pulmonary tissue cell volumes were insensitive to changes in $k_{g,CpIp}$ (Figures C40 through C45).

sensitivity to $k_{d,CpIp}$

Although the plasma and interstitial compartments responded significantly to the addition of Dextran-70 to the plasma compartment, these responses were unaffected by alterations in the Dextran-70 capillary-interstitial permeability coefficient (Figures C46 to C51). Tissue volume does not show an noticeable response to Dextran-70 administration for any of the parameter values tested (Figures C52 through C54).

sensitivity to $\sigma_{s,CpIp}$

At 1-minute, pulmonary interstitial volume was insensitive to changes in $\sigma_{s,CpIp}$, except for experiments in which plasma NaCl was altered (Figure C55). At 5-minutes, however, pulmonary interstitial volume was highly sensitive to changes in $\sigma_{s,CpIp}$, except for simulated experiments 1 through 3, which did not show changes in pulmonary interstitial volume for any of the parameter values tested (Figure C56). At 30-minutes, pulmonary interstitial volume was insensitive to changes in $\sigma_{s,CpIp}$ (Figure C57). Plasma volume was only slightly sensitive to $\sigma_{s,CpIp}$ at 1-minute (Figure C58) and was relatively insensitive at 5- and 30-minutes (Figures C59 and C60). Pulmonary tissue cell volume appears to be insensitive to changes in $\sigma_{s,CpIp}$ (Figures C61 through C63).

sensitivity to $\sigma_{a,CpIp}$

At 1-minute, pulmonary interstitial volume was insensitive to changes in $\sigma_{a,CpIp}$, except for experiments in which plasma NaCl was increased (Figure C64). At 5- and 30-minutes, pulmonary interstitial volume was moderately sensitive to changes in $\sigma_{a,CpIp}$ for all experiments except 1 through 3, which did not show changes in pulmonary interstitial volume for any of the parameter values tested (Figures C65 and C66). Plasma and pulmonary tissue cell volumes were relatively insensitive to changes in $\sigma_{a,CpIp}$ (Figures C67 through C72).

sensitivity to $\sigma_{g,CpIp}$

Both the qualitative and quantitative sensitivity of plasma, pulmonary interstitial, and pulmonary tissue cell volumes to changes in $\sigma_{g,CpIp}$ were similar to the sensitivity to $\sigma_{a,CpIp}$. At 1-minute, pulmonary interstitial volume was insensitive to changes in $\sigma_{a,CpIp}$, except for experiments in which plasma NaCl was increased (Figure C73). At 5- and 30-minutes, pulmonary interstitial volume was moderately sensitive to changes in $\sigma_{a,CpIp}$ for all experiments except 1 through 3, which did not show changes in pulmonary interstitial volume for any of the parameter values tested (Figures C74 and C75). Plasma and pulmonary tissue cell volumes were relatively insensitive to changes in $\sigma_{a,CpIp}$ (Figures C76 through C81).

sensitivity to $\sigma_{d,CpIp}$

At 1-minute, pulmonary interstitial volume was not noticeably sensitive to changes in the Dextran-70 capillary-interstitial solute reflection coefficient (Figures C82). At 5- and 30-minutes, however, some sensitivity was demonstrated for experiments 10 and 12, in which Dextran-70 was added to the plasma volume (Figures C83 and C84). Plasma and pulmonary tissue cell volumes did not demonstrate noticeable sensitivity to $\sigma_{d,CpIp}$ for any of the simulated experiments (Figures C85 through C90).

SUMMARY

Simplifying Assumptions

As in the previous study of systemic microvascular exchange (Doherty 1993c), it was found that two extravascular compartments (pulmonary interstitial and tissue cell) were required to accurately describe pulmonary microvascular exchange. It was also found that globulin flux affects model predictions for most of the simulation conditions tested, and that globulin flux should also be included. In contrast to previous studies of systemic microcirculatory exchange, the relationships between P_{Ip} and $(V_{Ip}+V_{Tp})$ of Equation 11, and between L_v and $(V_{Ip}+V_{Tp})$ of Equation 9, were found to have significant impact on model predictions. The most likely reason for the discrepancy between the two studies, is the difference in size between the systemic and pulmonary extravascular spaces. Because the pulmonary interstitial space is small, minor changes in interstitial volume and/or solute amount affect significant changes in interstitial pressure and solute concentration. In addition to the difference in compartment size, another consideration, is that during this model study, the systemic vasculature was not allowed to participate in restoring the hydrostatic/osmotic pressure balance after plasma solute concentrations were altered. While this factor was originally considered to be highly important, analyses of absolute differences between model pairs suggests that, although some absolute differences may be exaggerated, the results are qualitatively what one would expect if systemic microvascular exchange had been included.

Sensitivity Analyses

For the range of parameter values studied, the model predictions of pulmonary interstitial volume showed the greatest sensitivity to changes in the parameter $k_{v,CpIp}$. However, initial sensitivity (at 1-minute) was significant only for large changes in plasma NaCl concentration. At 5- and 30-minutes, pulmonary interstitial volume predictions were sensitive to $k_{v,CpIp}$ only for decreased plasma NaCl and albumin concentrations. Model predictions of pulmonary interstitial volume were also highly sensitive to changes in the parameters $\sigma_{s,CpIp}$, $\sigma_{a,CpIp}$, and $k_{a,CpIp}$. $\sigma_{s,CpIp}$ at

1-minute for experiments in which plasma NaCl was altered. This sensitivity to $\sigma_{s,CpIp}$ was attenuated at 5-minutes, and was nearly absent at 30-minutes. In contrast, sensitivity to $\sigma_{a,CpIp}$, and $k_{a,CpIp}$ was apparent for all experiments except Experiments 1-3, and was greatest at the later time points (5-minutes and 30-minutes). Sensitivity to $\sigma_{g,CpIp}$, and $k_{g,CpIp}$ was qualitatively similar to sensitivity to $\sigma_{a,CpIp}$, and $k_{a,CpIp}$, but was of smaller magnitude. Interstitial volume predictions were relatively insensitive to changes in $\sigma_{d,CpIp}$, and $k_{d,CpIp}$, even for experiments in which dextran was added to the plasma compartment.

Pulmonary tissue cell volume predictions were relatively insensitive to changes in model parameter values except when large quantities of NaCl were added to, or removed from the plasma compartment. Plasma volume was insensitive to changes in parameter values over all simulation conditions studied here.

CONCLUSIONS

This study demonstrated that the four simplifying assumptions (lumped interstitial and tissue cell compartments, constant lymph flow rate, constant interstitial pressure, and exclusion of capillary-interstitial globulin flux) were inappropriate for use over the range of simulation conditions tested here. This study did not demonstrate whether the basic 3-compartment model is of sufficient complexity to accurately predict pulmonary interstitial volume changes, and thus, pulmonary edema. This issue must be addressed in future studies.

This study also demonstrated the sensitivity of pulmonary interstitial volume to changes in certain parameter values. This is disconcerting due to the wide range of reported values for these parameters in the literature. This issue must also be addressed in future studies.

REFERENCES

- Bert J.L., Pinder K.L. Pulmonary microvascular exchange: an analog computer simulation. *Microvasc. Res.* 27: 51-70, 1984.
- Brigham K.L. Lung lymph composition in experimental pulmonary edema. In: *Pulmonary Edema*. A.P. Fishman and E.M. Renkin, eds. Bethesda: American Physiological Society, 1979, pp. 161-173.
- Brigham K.L., Staub N.C. Lung interstitial protein: studies of lung lymph. In: J.T. Sgouris and A. Rene (eds.), *Proceedings of the Workshop on Albumin*. Bethesda, MD: National Institutes of Health, 1975.
- Brody J.S., Stemmler E.J., du Bois A. Longitudinal distribution of vascular resistance in the pulmonary arteries, capillaries, and veins. *J. Clin. Invest.* 47: 783, 1968.
- Casley-Smith J.R. Lymph and lymphatics. In: *Microcirculation*. G. Kaley and B.M. Altura eds. Baltimore: University Park Press, pp 423-502, 1977.
- Chinard F.P., Enns T. Transcapillary pulmonary exchange of water in the dog. *Am. J. Physiol.* 178: 197, 1954.
- Dabney J.M., Buehn M.J., Dobbins D.E. Constriction of lymphatics by catecholamines, carotid occlusion, or hemorrhage. *Am. J. Physiol.* 255: H514-H524, 1988.
- Doherty T.J. A mathematical model for the study of hemorrhagic shock and fluid resuscitation: the isolated left heart. Institute Report # 476, Letterman Army Institute of Research, Presidio of San Francisco, CA, 1993a.
- Doherty T.J. A mathematical model for the study of hemorrhagic shock and fluid resuscitation: transcapillary exchange. Institute Report # 477, Letterman Army Institute of Research, Presidio of San Francisco, CA, 1993b.
- Doherty T.J. A mathematical model for the study of hemorrhage and fluid resuscitation: fluid and solute exchange between vascular, interstitial, and tissue cell compartments. Institute Report # 478, Letterman Army Institute of Research, Presidio of San Francisco, CA, 1993c.
- Doherty T.J. A mathematical model for the study of hemorrhage and fluid resuscitation: the systemic and pulmonary vasculature. Institute Report # 479, Letterman Army Institute of Research, Presidio of San Francisco, CA, 1993d.

Erdmann A.J., Vaughan T.R., Brigham K.L., Woolverton W.C., and Staub N.C. Effect of increased vascular pressure on lung fluid balance in unanesthetized sheep. *Circ Res.* 37: 271-284, 1975.

Gaar K.A., Jr., Taylor A.E., Owen L.J. Pulmonary capillary pressure and filtration coefficient in the isolated perfused lung. *Am. J. Physiol.* 213: 910-914, 1967.

Granger H.J., Dhar J., Chen H.I. Structure and function of the interstitium. In: J.T. Sgouris and A. Rene (eds.), *Proceedings of the Workshop on Albumin*. Bethesda, MD: National Institutes of Health, 1975.

Gump F.E. Lung fluid and solute compartments. In: *Lung Water and Solute Exchange*. N.C. Staub ed. Dekker, New York: pp 75-95, 1978.

Guyton A.C. *Basic Human Physiology: Normal Function and Mechanisms of Disease*, 2nd Edition. Philadelphia: WB Saunders Co., 1977.

Guyton A.C., Lindsey A.W. Effect of elevated left atrial pressure and decrease in plasma protein concentration on the development of pulmonary edema. *Circ. Res.* 7: 649, 1959.

Guyton A.C., Taylor A.E., Granger H.J. *Circulatory Physiology II: Dynamics and Control of the Body Fluids*. New York: W.B. Saunders Co., 1975.

Haraldsson B., Moxham B.J., Rippe B. Capillary permeability to sulfate-substituted dextran fractions in the rat hindquarter vascular bed. *Acta Physiol. Scand.* 115: 397-404, 1982.

Harper H.A. *Review of Physiological Chemistry*. Los Altos, CA: Lange Med Pub, 1969, pp. 533-535.

Katz M.A. New formulation of water and macromolecular flux which corrects for non-ideality: theory and derivation, predictions, and experimental results. *J. Theor. Biol.* 112: 369-401, 1985.

Kedem O., Katchalsky A. Thermodynamic analysis of the permeability of biological membranes to non-electrolytes. *Acta Biochem Biophys* 27: 229-246, 1958.

Landis E.M., Pappenheimer J.R. Exchange of substances through capillary walls. In: *Handbook of Physiology*, Section 2, Volume 2. Bethesda, MD: American Physiological Society, 1963, pp. 961-1034.

Laurent, T.C. The interaction between polysaccharides and other macromolecules. II. The exclusion from hyaluronic acid gels and solutions. *Biochem. J.* 93:106-112, 1964.

Levine O.R., Mellins, R.B., Fishman A.P. Quantitative assessment of pulmonary edema. *Circ. Res.* 17: 414-426, 1965.

Levine O.R., Mellins, R.B., Senior R.M., Fishman A.P. The application of Starling's law of capillary exchange to the lungs. *J. Clin. Invest.* 46: 934-944, 1967.

Mazzoni M.C., Borgstrom P., Arfors K.E., Intaglietta M. Dynamic fluid redistribution in hyperosmotic resuscitation of hypovolemic hemorrhage. *Am. J. Physiol.* 255: H629-H637, 1988.

Mellins R.B., Levine O.R., Skalak R., Fishman A.P. Interstitial pressure of the lung. *Circ Res.* 24: 197-212, 1969

Parker J.C., Crain M., Grimbert F., Rutili G., Taylor A.E. Total lung lymph flow and fluid compartmentation in edematous dogs. *J. Appl. Physiol.: Resp. Environ. Exercise Physiol.* 51(5): 1268-1277, 1981a.

Parker J.C., Roselli R.J., Harris T.R., Brigham K.L. Effects of graded increases in pulmonary vascular pressures on lung fluid balance in unanesthetized sheep. *Circ. Res.* 49: 1164-1172, 1981b.

Parker J.C., Guyton A.C., Taylor A.E. Pulmonary transcapillary exchange and pulmonary edema. In: A.C. Guyton and D.B. Young (eds.), *International Review of Physiology, Cardiovascular Physiology III*; Vol. 18. Baltimore: University Park Press, 1979, pp. 261-315.

Patlak C.S., Goldstein D.A., Hoffman J.F. The flow of solute and solvent across a two-membrane system. *J. Theor. Biol.* 5: 426-442, 1963.

Perl W., Silverman F., Delea A.C., Chinard F.P. Permeability of dog lung endothelium to dodium, diols, amides, and water. *Am. J. Physiol.* 230: 1708-1721, 1976.

Shepherd J.T., Vanhoutte P.M. *The Human Cardiovascular System: Facts and Concepts*. New York: Raven Press, 1979.

Snashall P.D., Hughes J.M.B. Lung water balance. *Rev. Physiol. Biochem. Pharmacol.* 89:5-62, 1981.

Snashall P.D., Nakahara K., Staub N.C. Estimation of perivascular fluid pressure in isolated perfused dog lung lobes. *J. Appl. Physiol. (Respirat. Environ. Exercise Physiol.)* 46(5): 1003-1010, 1979.

Staub N.C. Pulmonary edema: physiologic approaches to management. *Chest* 74(5): 559-564, 1978.

Staub N.C. Pulmonary edema. *Physiol. Rev.* 54: 674-811, 1974.

Staub N.C. Steady state pulmonary transvascular water filtration in unanesthetized sheep. *Circ. res.* 28-28(Suppl I): 135-139, 1971.

Taylor A.E. and Drake R.E. Fluid and protein movement across the pulmonary microcirculation. In: N.C. Staub (ed.), *Lung Biology in Health and Disease*, Vol. 9, Lung Solute Exchange. New York: Marcel Dekker, 1977

Thorén L. Dextran as a plasma volume substitute. In: G.A. Jamieson and T.J. Greenwalt (eds), *Blood Substitutes and Plasma Volume Expanders*. New York: Liss, 1978, pp. 265-282.

Wangensteen D.O., Lysaker E., Savaryn P. Pulmonary capillary and reflection coefficients in the adult rabbit. *Microvasc. Res.* 14: 81-97, 1977.

Winn R., Nadir B., Gleisner J., Stothert J., Hildebrandt J. Deficiencies in premembrane model of microvascular fluid and solute transudation. *J. Appl. Physiol.: Resp. Environ. Exercise Physiol.* 51(6): 1574-1580, 1981.

Yipintosoi T. Single passage extraction and permeability estimation of sodium in normal dog lungs. *Circ. Res.* 39: 523-531, 1976.

Yoffey J.M., Courtice F.C. Lymphatics, lymph, and the lymphomyeloid complex. New York: Academic Press, pp. 160-205, 1970.

APPENDIX A

Initial Conditions and Normal Parameter Values

Table A1. Initial Conditions

Variable	symbol	Value used in Simulation	Literature	
			Value	Reference
Total Blood Volume	V_B	70 ml/kg	5-6 liters	Guyton 1977
Blood Hematocrit	HCT	45%	0.45	Shepherd and Vanhoutte 1979
Total Plasma Volume	V_P	38.5 ml/kg		
Pulmonary Extravascular Volume	$V_{ev,p}$	5.35 ml/kg	331-406 ml	Snashall et al 1979
			383 ml	Staub 1974
Pulmonary Interstitial Volume	V_{ip}	3.2 ml/kg		
Pulmonary Tissue Volume	V_{Tp}	2.15 ml/kg	150 ml	Gump 1978
Plasma NaCl Concentration	$C_{s,p}$	0.0093 g/ml	0.0093 g/ml	Guyton 1977
Plasma Albumin Concentration	$C_{a,p}$	0.045	0.045 g/ml	"
Plasma Globulin Concentration	$C_{g,p}$	0.025	0.025 g/ml	"
Interstitial NaCl Concentration ¹	$C_{s,ip}$	0.0093 g/ml		
Interstitial Albumin Concentration ¹	$C_{a,ip}$	0.036 g/ml	$0.8 \cdot C_{a,p}$	Yoffrey and Courtice 1970
Interstitial Globulin Concentration ¹	$C_{g,ip}$	0.0 g/ml	$0.55 \cdot C_{a,p}$	
Tissue Osmotic Pressure	Π_{Tp}	$\Pi_{Tp,init} = \Pi_{s,ip} + \Pi_{a,ip} + \Pi_{g,ip}$		
NaCl Interstitial Volume	$V_{s,ip}$	100 % of "normal" interstitial volume		
Albumin Interstitial Volume	$V_{a,ip}$	56 % of "normal" interstitial volume	25%	Laurent 1964 (in gel)
			50%	Granger, Dhar, and Chen 1975
			50%	Brigham and Staub 1975
Globulin Interstitial Volume	$V_{g,ip}$	45 % of "normal" interstitial volume	16%	Laurent 1964 (in gel)
Dextran-70 Interstitial Volume	$V_{d,ip}$	65 % of "normal" interstitial volume		

¹ "Interstitial" concentrations are concentration in free fluid (corresponding to lymph concentration)

Table A1. Initial Conditions

Variable	symbol	Value used in Simulation	Literature	
			Value	Reference
Pulmonary Capillary Pressure	P_{Cp}	9 mm Hg	9.0	Parker et al 1979
			9.0	Snashall and Hughes 1981
			7.0	Gaar et al 1967
			9.8	Brody et al 1968
Pulmonary Interstitial/Tissue Cell Pressure	P_{lp}	calculated (Equation A1)	0.0	
Volumetric Lymph Flow Rate	L_v	0.002 ml/kg·min	0.002-0.004	Staub 1978
			0.002-0.0038	Staub 1971
			0.001-0.002	Casley-Smith 1977
Pulmonary Capillary - Interstitial Volumetric Flux	$J_{v,Cp-lp}$	same as L_v		
Pulmonary Interstitial - Tissue Cell Volumetric Flux	$J_{v,lp-tp}$	0.0 ml/kg·min		
Rate of NaCl Transport in Lymph	L_s	$C_{s,lp} \cdot L_v$		
Rate of Albumin Transport in Lymph	L_a	$C_{a,lp} \cdot L_v$		
Rate of Globulin Transport in Lymph	L_g	$C_{g,lp} \cdot L_v$		
Pulmonary Capillary - Interstitial NaCl Flux	$J_{s,Cp-lp}$	same as L_s		
Pulmonary Capillary - Interstitial Albumin Flux	$J_{a,Cp-lp}$	same as L_a		
Pulmonary Capillary - Interstitial Globulin Flux	$J_{g,Cp-lp}$	same as L_g		

Table A2. "Normal" Parameter Values

Parameter	symbol	Value used in Simulation	Literature	
			Value	Reference
Pulmonary Capillary Fluid Filtration Coefficient	k_{p-lp}	0.02	0.7 ml/min-mm Hg-g (wet tissue)	Guyton and Lindsey 1959, Levine et al. 1967, Mellins et al. 1969, Levine et al. 1965
			0.1 ml/min-mm Hg-g (wet tissue)	Erdmann et al. 1975, Staub 1971
			0.083×10^{-4} ml/s-cm H_2O -g (wet tissue)	Chinard and Enns 1954
Tissue Cell Membrane Fluid Filtration Coefficient	k_{lp-tp}	0.00105		
Pulmonary Capillary NaCl Permeability Coefficient	$k_{s,CP-lp}$	11.67	2.14 ml/kg-min	Yipintosoi 1976
Pulmonary Capillary Albumin Permeability Coefficient	$k_{a,CP-lp}$	calculated (Equation A2)	2.76×10^{-3} ml/min	Erdmann et al. 1975 (assuming capillary surface area is 500 cm^2)
			9.0×10^{-7} ml/min	Taylor and Drake 1977 (dog)
			2.04×10^{-6} ml/min	Staub 1974 (conscious sheep)
			2.76×10^{-7} ml/min	Staub 1974 (mathematical model)
Pulmonary Capillary Globulin Permeability Coefficient	$k_{g,CP-lp}$	calculated (Equation A3)	1-10 ml/hr	Winn et al 1981, Brigham et al 1979
			4.44×10^{-6} ml/min	Erdmann et al. 1975 (assuming capillary surface area is 500 cm^2)
			6.0×10^{-8} ml/min	Staub 1974 (mathematical model)
Pulmonary Capillary Dextran-70 Permeability Coefficient	$k_{d,CP-lp}$	0.000952 (1/3 of systemic value)		
Pulmonary Capillary NaCl reflection coefficient	$\sigma_{s,CP-lp}$	0.10	0.30	Perl et al 1976
			0.048	Wangensteen et al 1977 (rabbit)
Pulmonary Capillary Albumin reflection coefficient	$\sigma_{a,CP-lp}$	0.75	0.8	Staub 1974 (mathematical model)

Table A2. "Normal" Parameter Values

Parameter	symbol	Value used in Simulation	Literature	
			Value	Reference
Pulmonary Capillary Globulin reflection coefficient	$\sigma_{g,Cplp}$	0.90	0.40	Wangensteen et al 1977 (rabbit)
Pulmonary Capillary Dextran-70 reflection coefficient	$\sigma_{d,Cplp}$	0.75	0.9	Staub 1974 (mathematical model)
			0.75	Mazzoni et al. 1988 (systemic microvasculature)
			0.547	Haraldsson et al 1982 (rat hindquarter)

A.3 Calculation of P_{Ip} and Certain Parameter Values

Initial values for P_{Ip} , and "normal" values of $k_{a,CpIp}$ and $k_{g,CpIp}$ were calculated to require the non-perturbed system to remain in steady state. These values were recalculated after set parameter values changes. Because of the dependence between $k_{a,CpIp}$ and $\sigma_{a,CpIp}$, and between $k_{g,CpIp}$ and $\sigma_{g,CpIp}$, $\sigma_{a,CpIp}$ and $\sigma_{g,CpIp}$ were also recalculated after set changes in $\sigma_{a,CpIp}$ and $\sigma_{g,CpIp}$, respectively. The following equations were used:

$$P_{Ip} = \frac{-L_{v,p}}{k_{v,CpIp}} + \left(P_C - \sigma_{a,CpIp} \left(\Pi_{a,p} - \Pi_{a,Ip} \right) - \sigma_{g,CpIp} \left(\Pi_{g,p} - \Pi_{g,Ip} \right) \right) \quad A1)$$

$$k_{a,CpIp} = \frac{L_{v,p} \left(C_{a,Ip} - \bar{C}_{a,Plp} (1 - \sigma_{a,CpIp}) \right)}{(C_{a,p} - C_{a,Ip})} \quad A2)$$

$$k_{g,CpIp} = \frac{L_{v,p} \left(C_{g,Ip} - \bar{C}_{g,Plp} (1 - \sigma_{g,CpIp}) \right)}{(C_{g,p} - C_{g,Ip})} \quad A3)$$

$$\sigma_{a,CpIp} = 1 - \frac{(C_{a,Ip} \cdot L_{v,p} - k_{a,CpIp} (C_{a,p} - C_{a,Ip}))}{\bar{C}_{a,Plp} \cdot L_{v,p}} \quad A4)$$

$$\sigma_{g,CpIp} = 1 - \frac{(C_{g,Ip} \cdot L_{v,p} - k_{g,CpIp} (C_{g,p} - C_{g,Ip}))}{\bar{C}_{g,Plp} \cdot L_{v,p}} \quad A5)$$

APPENDIX B

Tests of Simplifying Assumptions

Preliminary Report 12/15/94
Contract # DAMD17-94-C4126

Maximum Absolute Difference in Lung Interstitial Volume (% change) (2- vs. 3- Compartment Models)

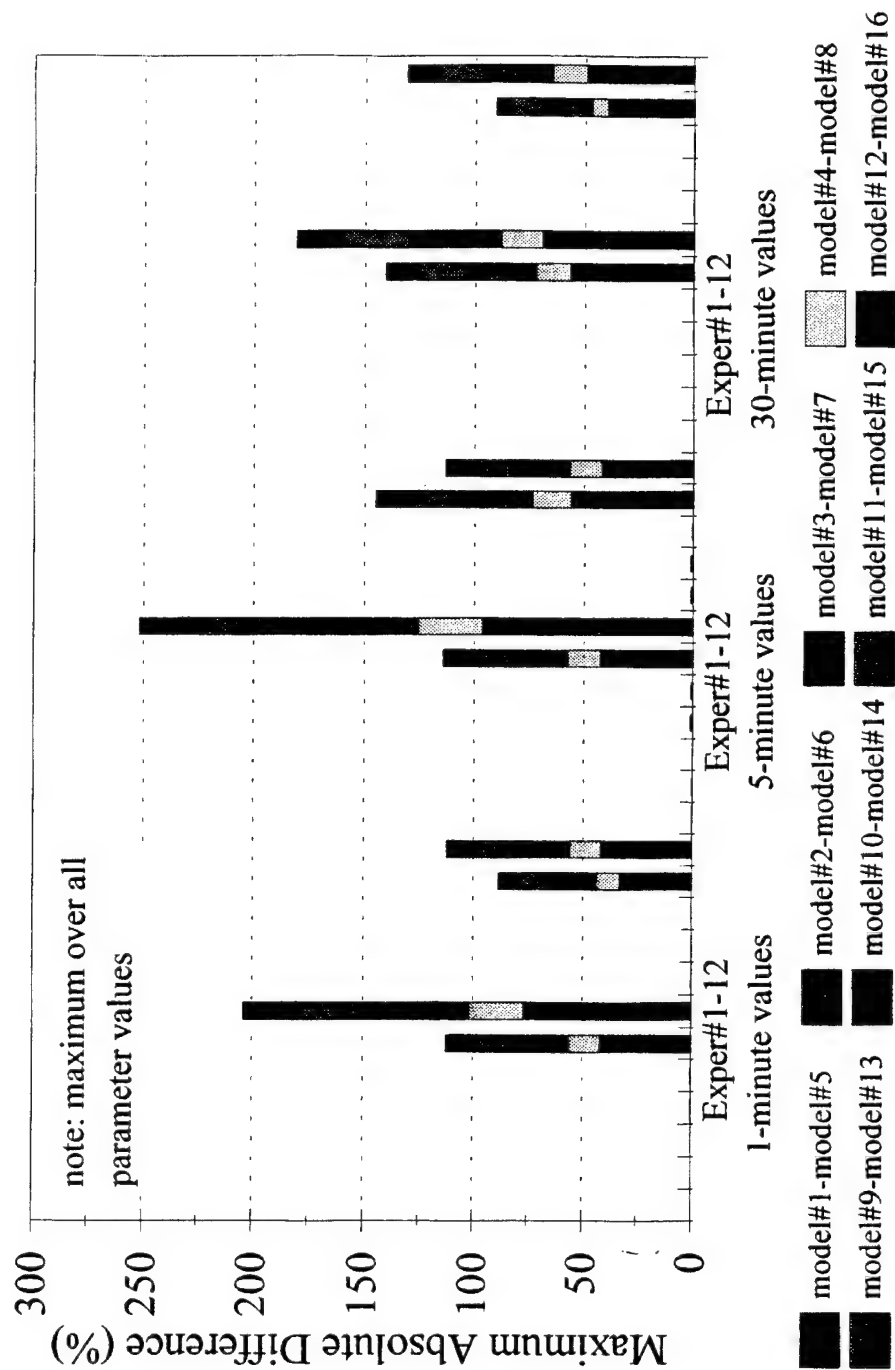


Figure B1

Maximum Absolute Difference in Total Plasma Volume (% change) (2- vs. 3- Compartment Models)

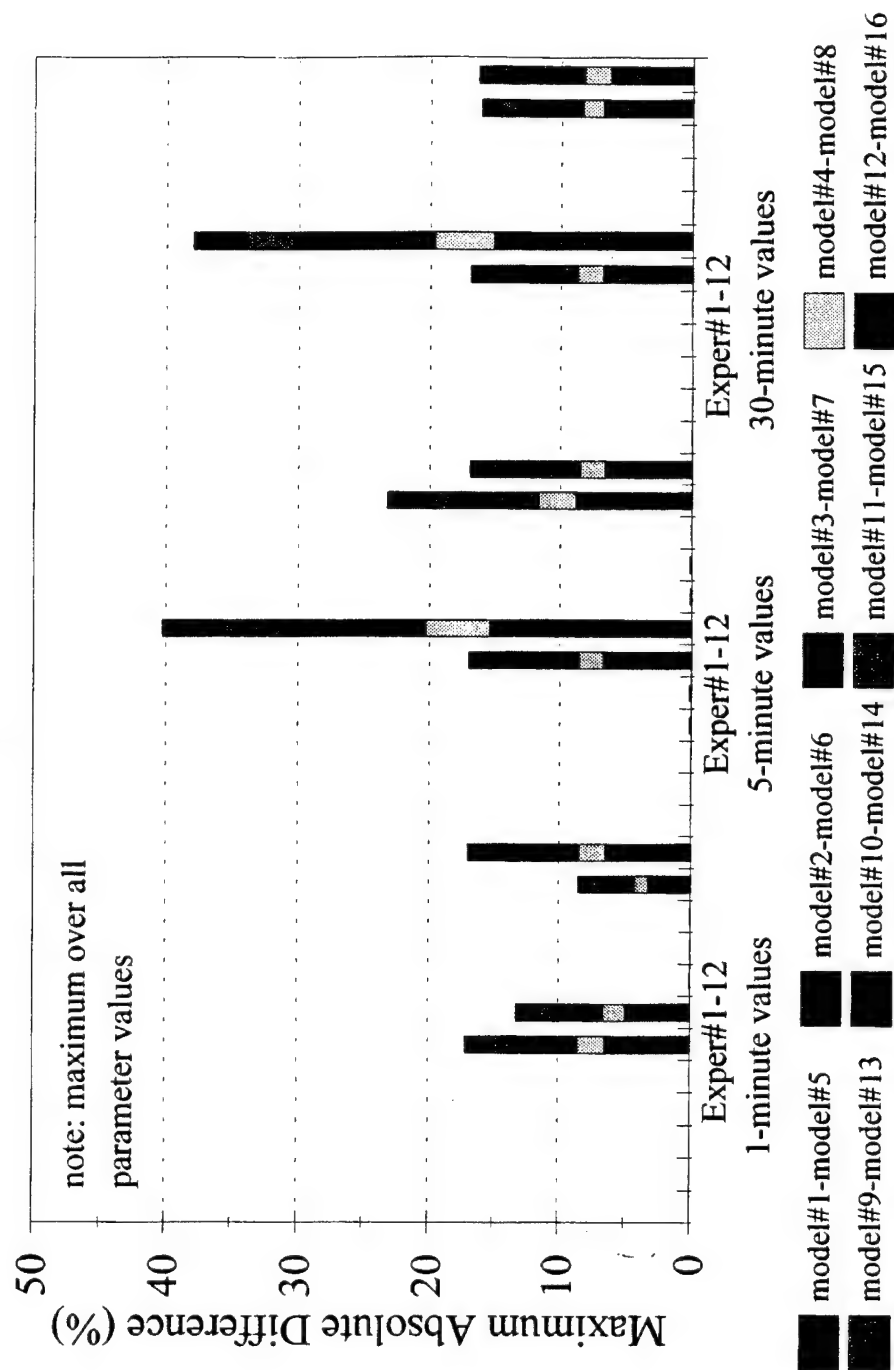


Figure B2

Maximum Absolute Difference in Lung Tissue Cell Volume (% change) (2- vs. 3- Compartment Models)

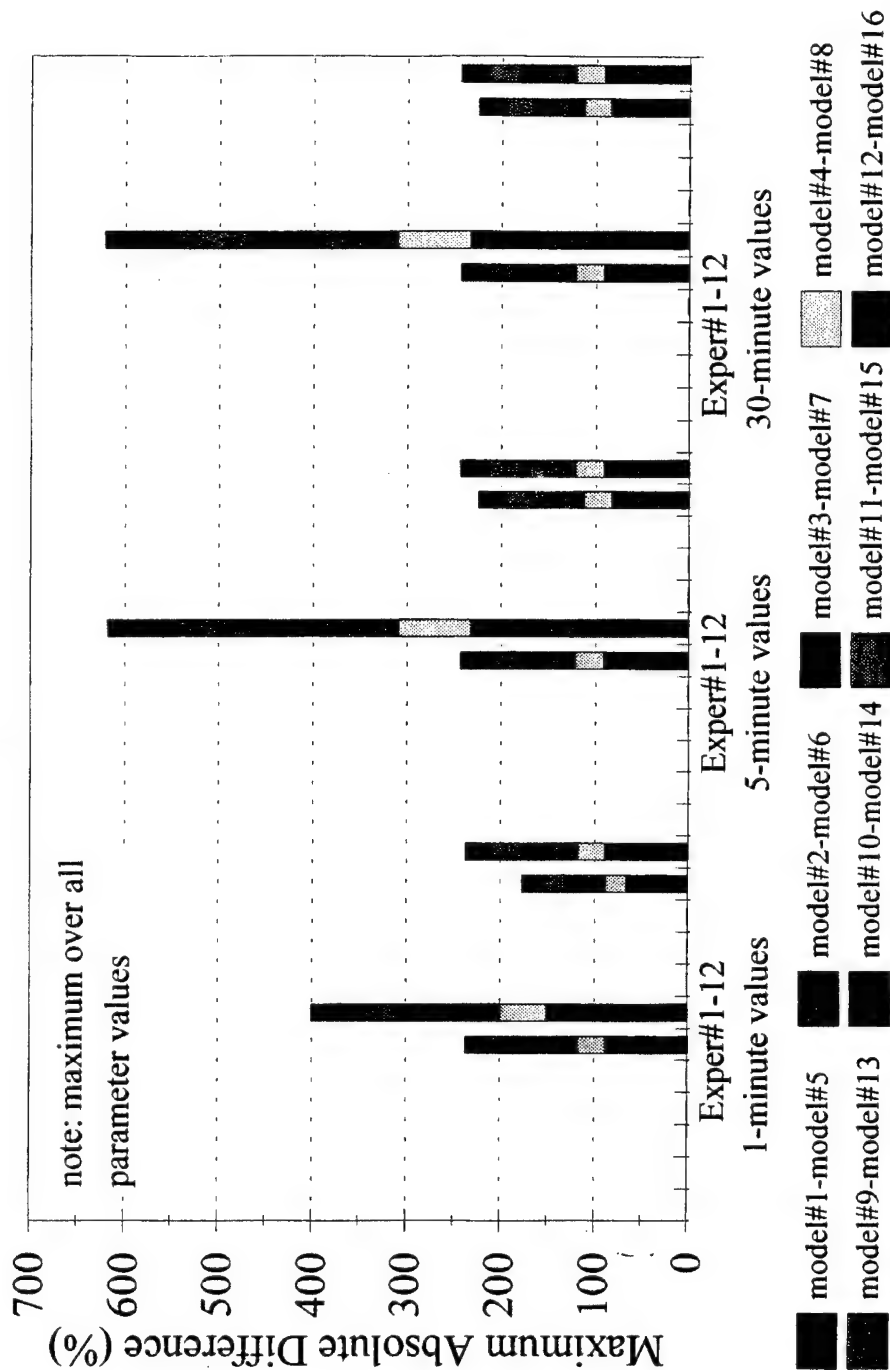


Figure B3

Maximum Absolute Difference in Lung Interstitial Volume (% change) (Constant vs. Variable Lymph Flow)

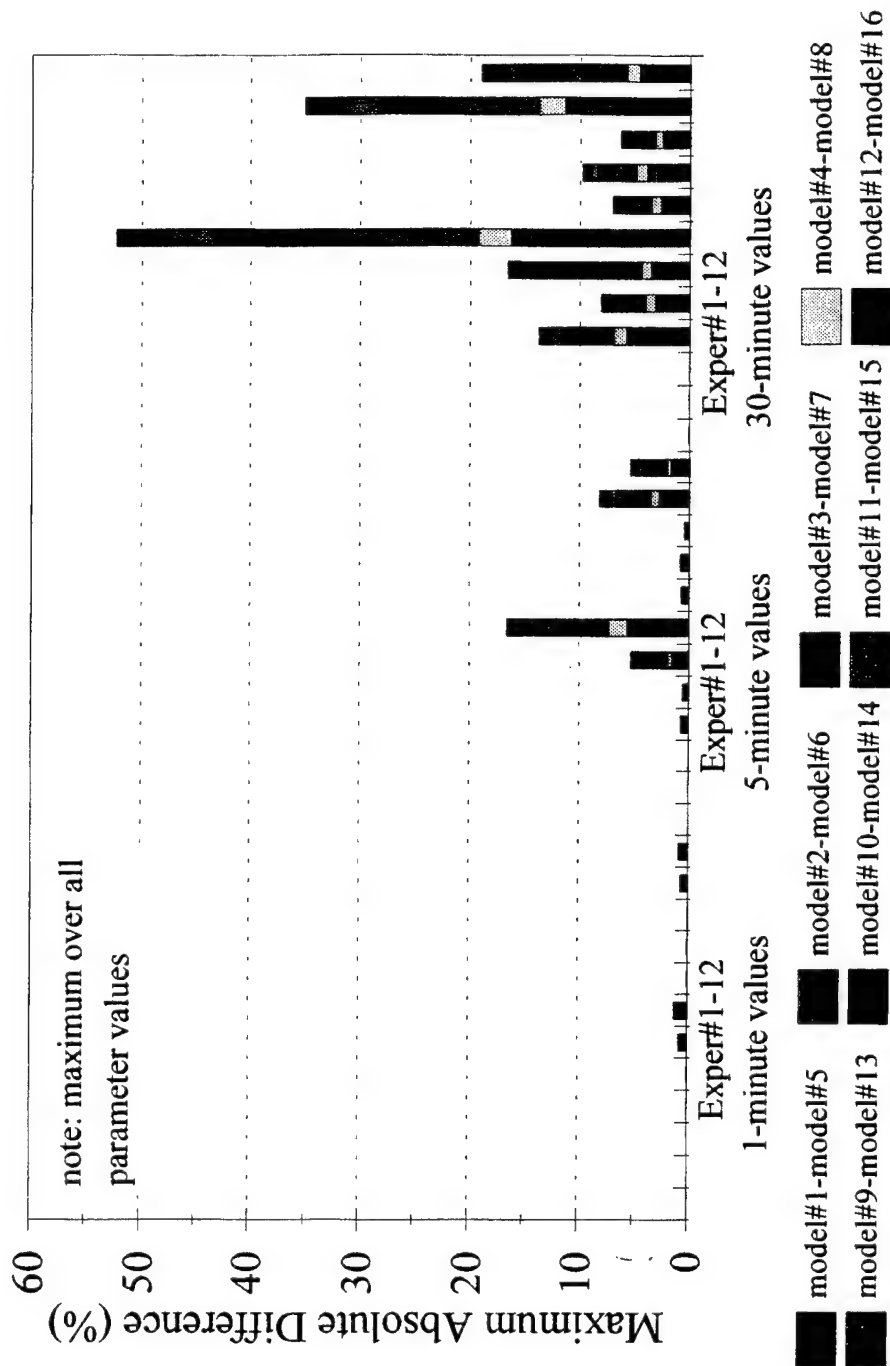


Figure B4

Maximum Absolute Difference in Total Plasma Volume (% change) (Constant vs. Variable Lymph Flow)

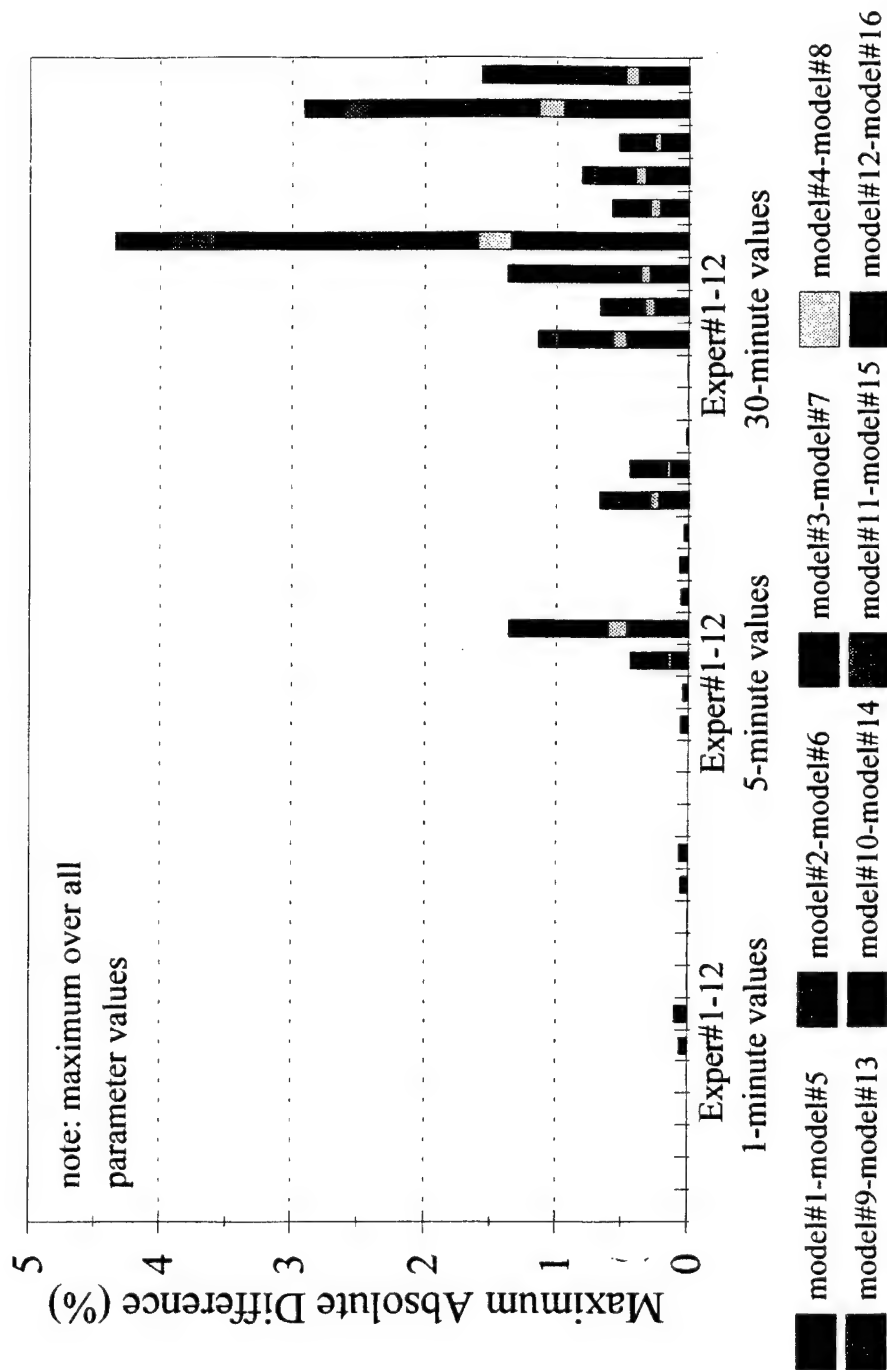


Figure B5

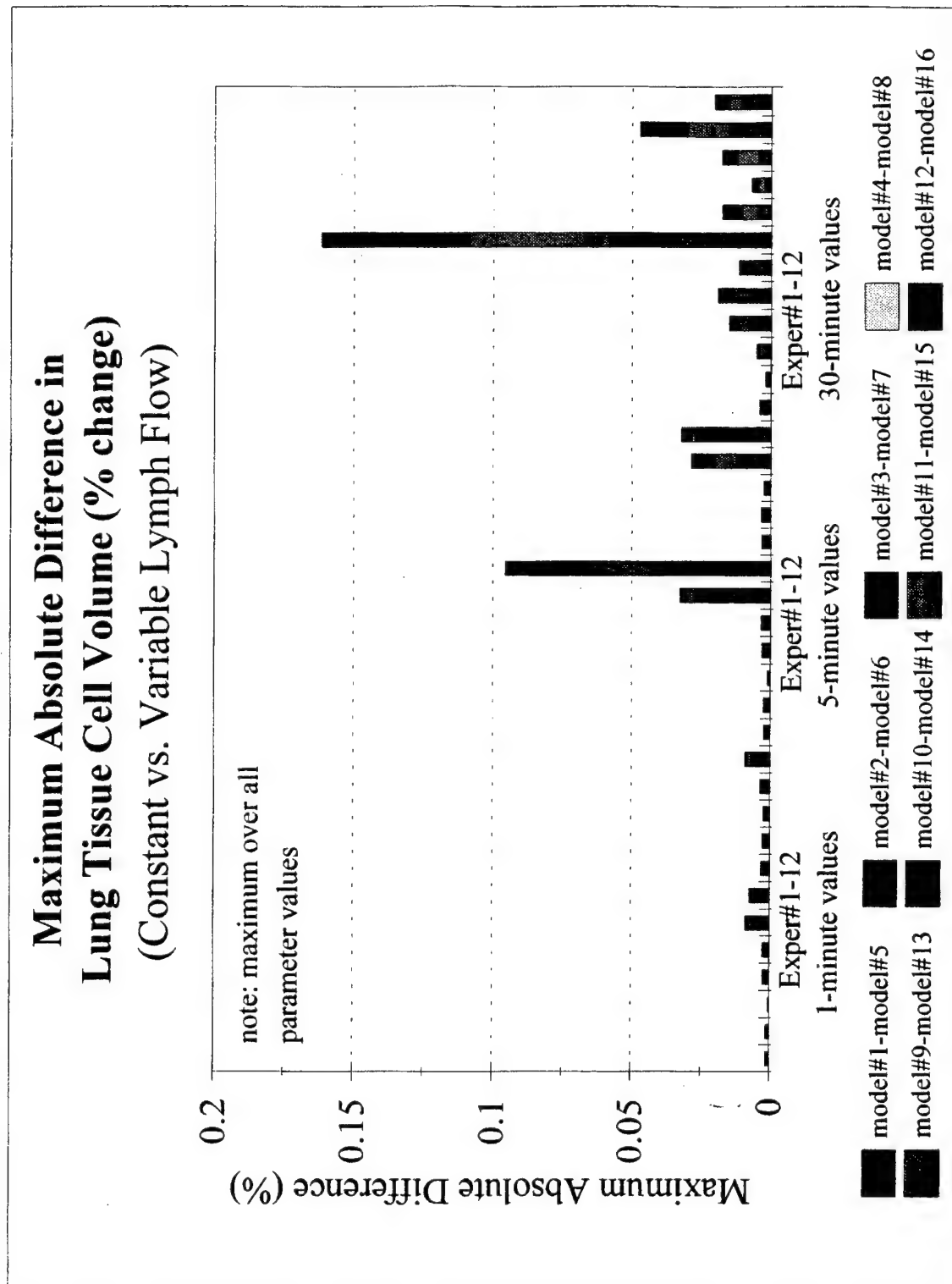


Figure B6

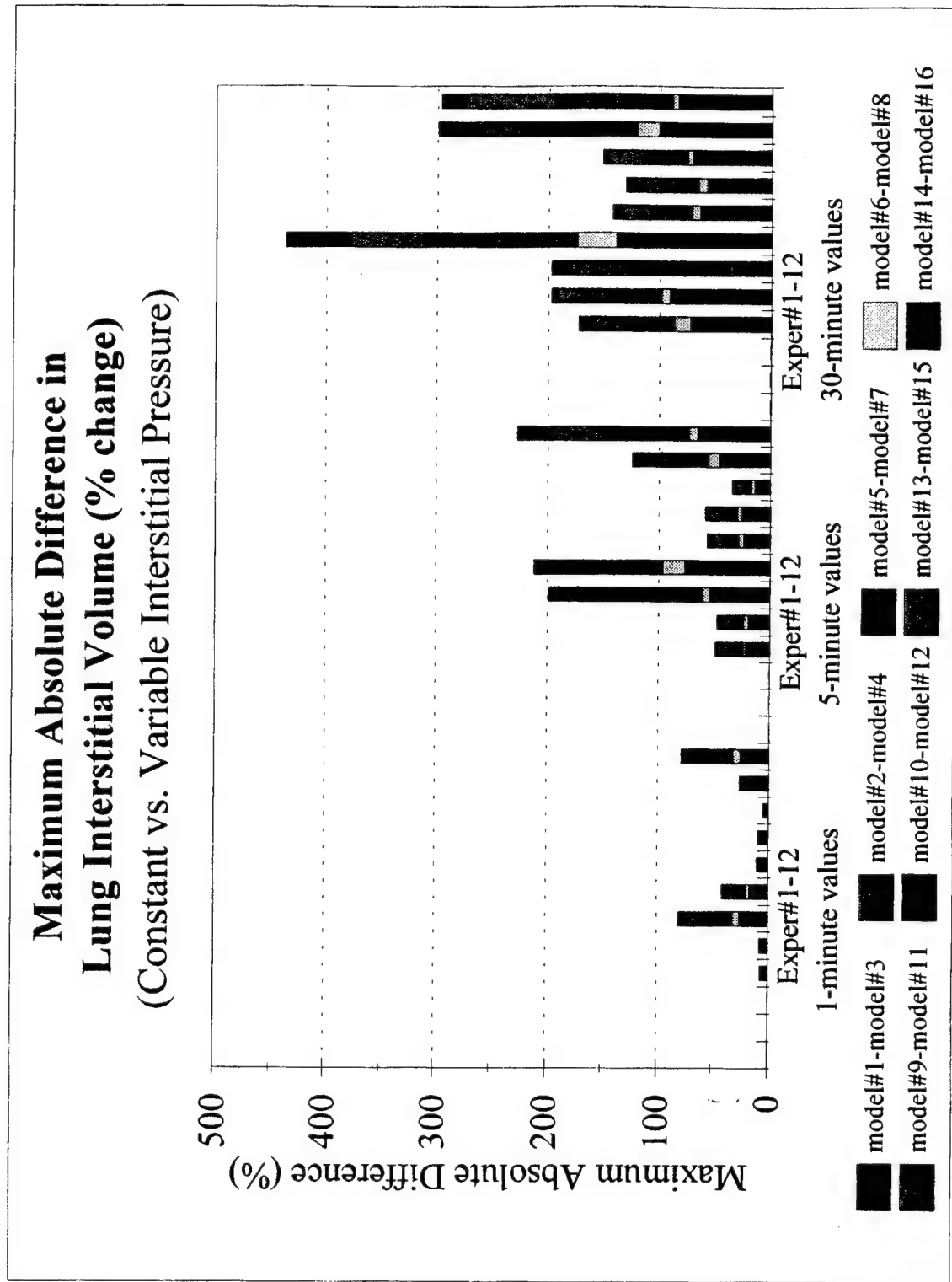


Figure B7

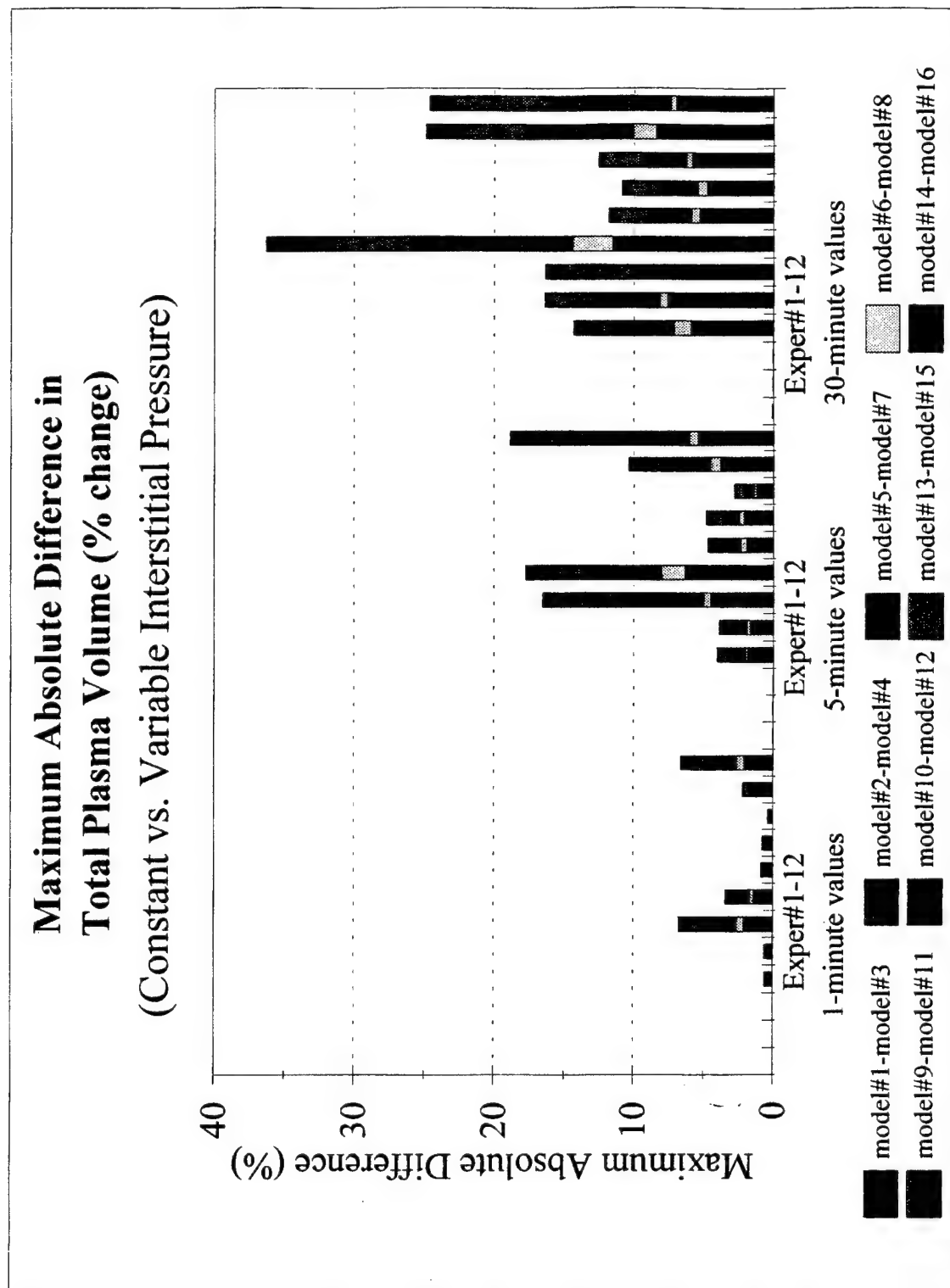


Figure B8

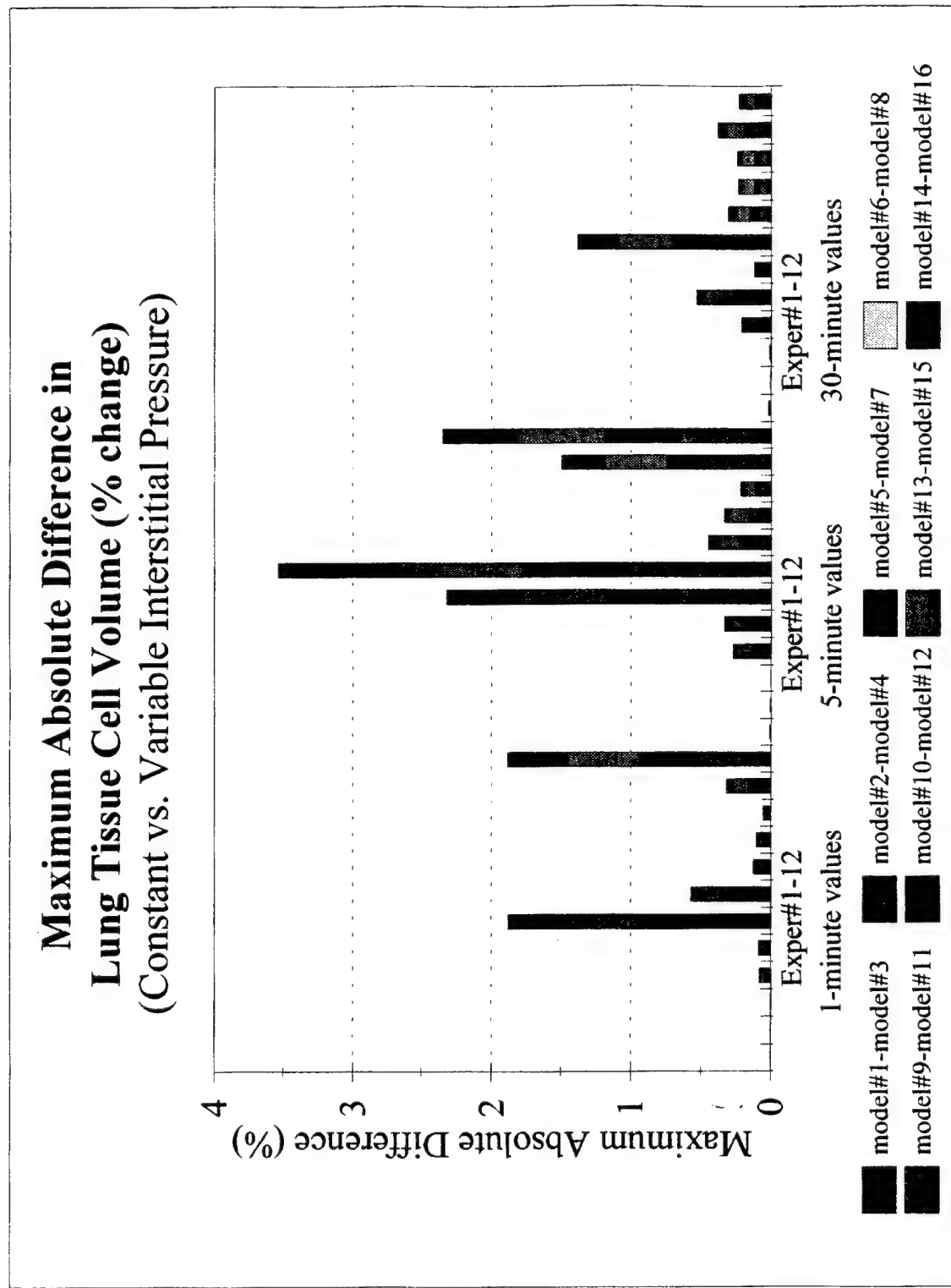


Figure B9

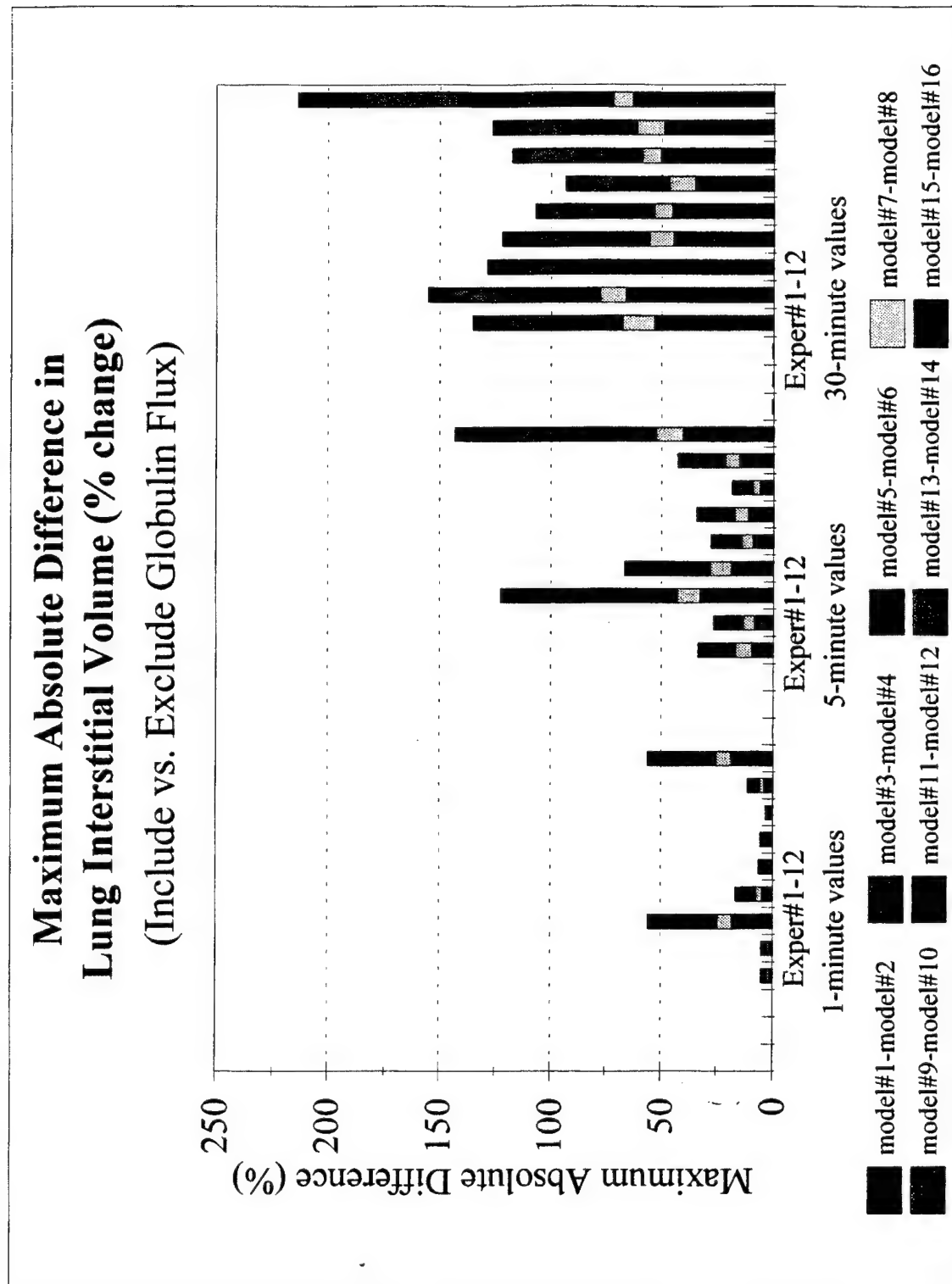


Figure B10

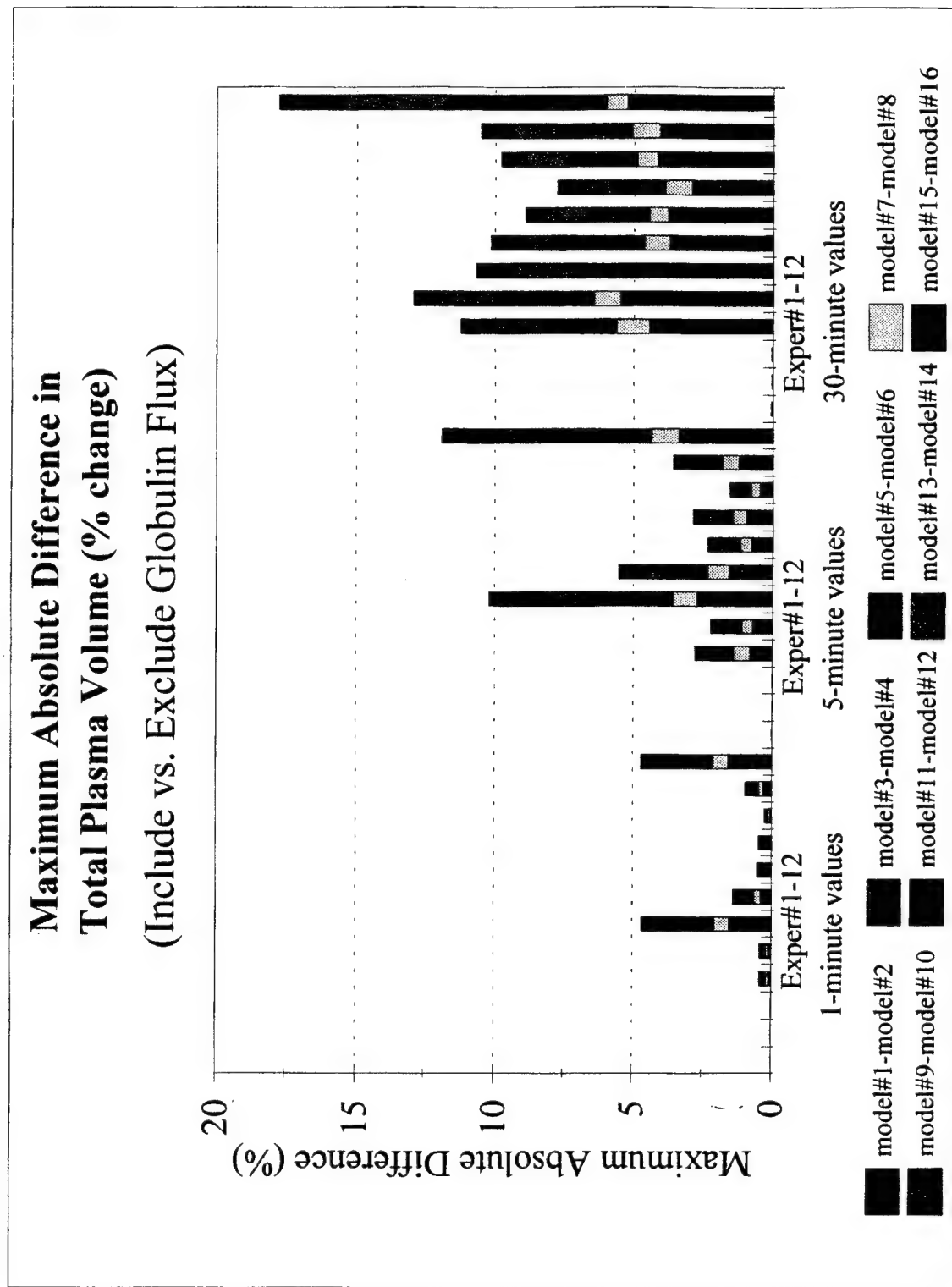


Figure B11

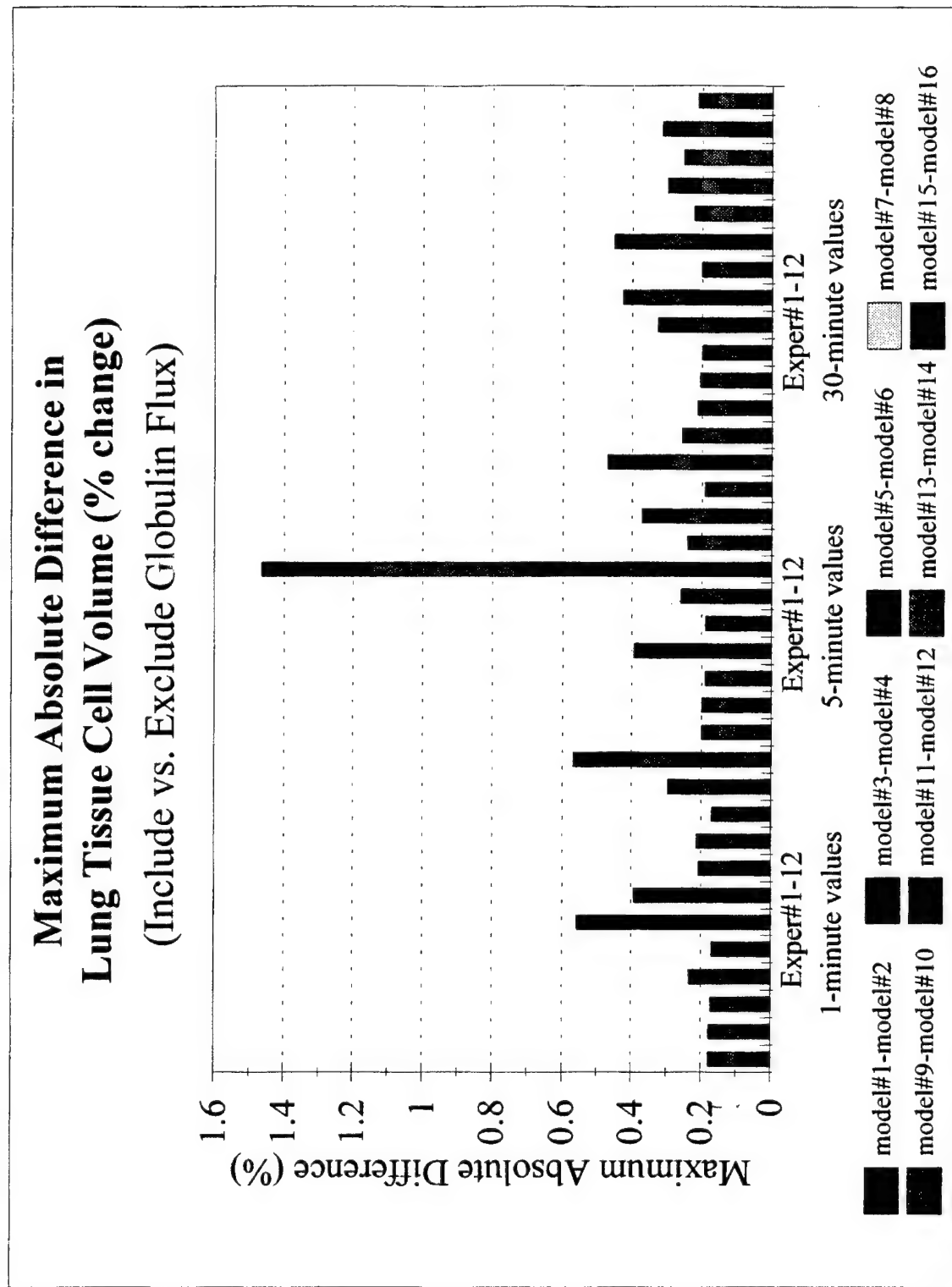


Figure B12

APPENDIX C

Sensitivity Analyses

Abbreviations Used In This Section:

IV Pulmonary Interstitial Volume (V_{ip})
PV Plasma Volume (V_P)
IV Pulmonary Tissue Cell Volume (V_{Tp})
k.p2i Pulmonary Capillary-Interstitial Fluid Filtration Coefficient ($k_{v,CpIp}$)

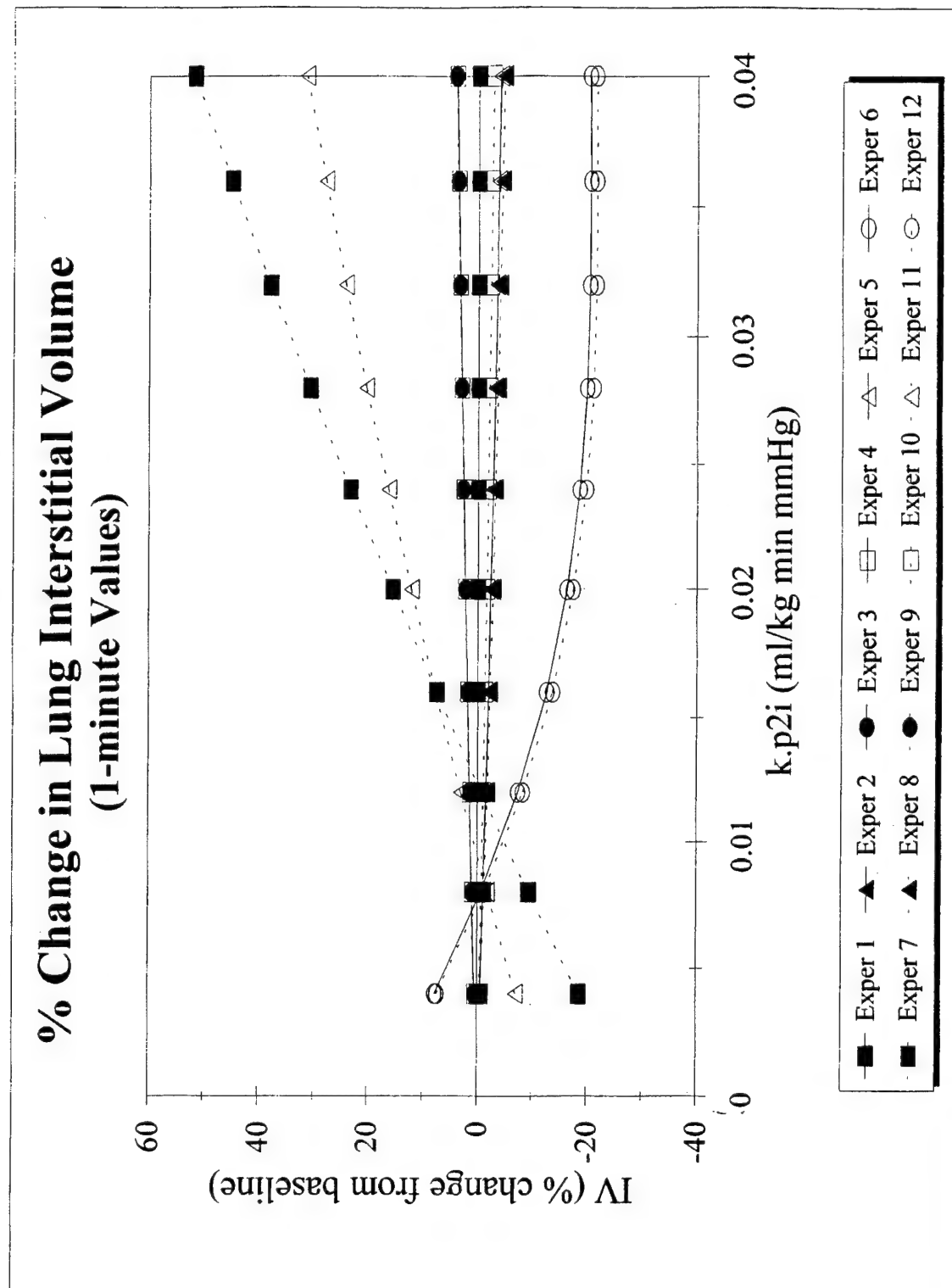


Figure C1

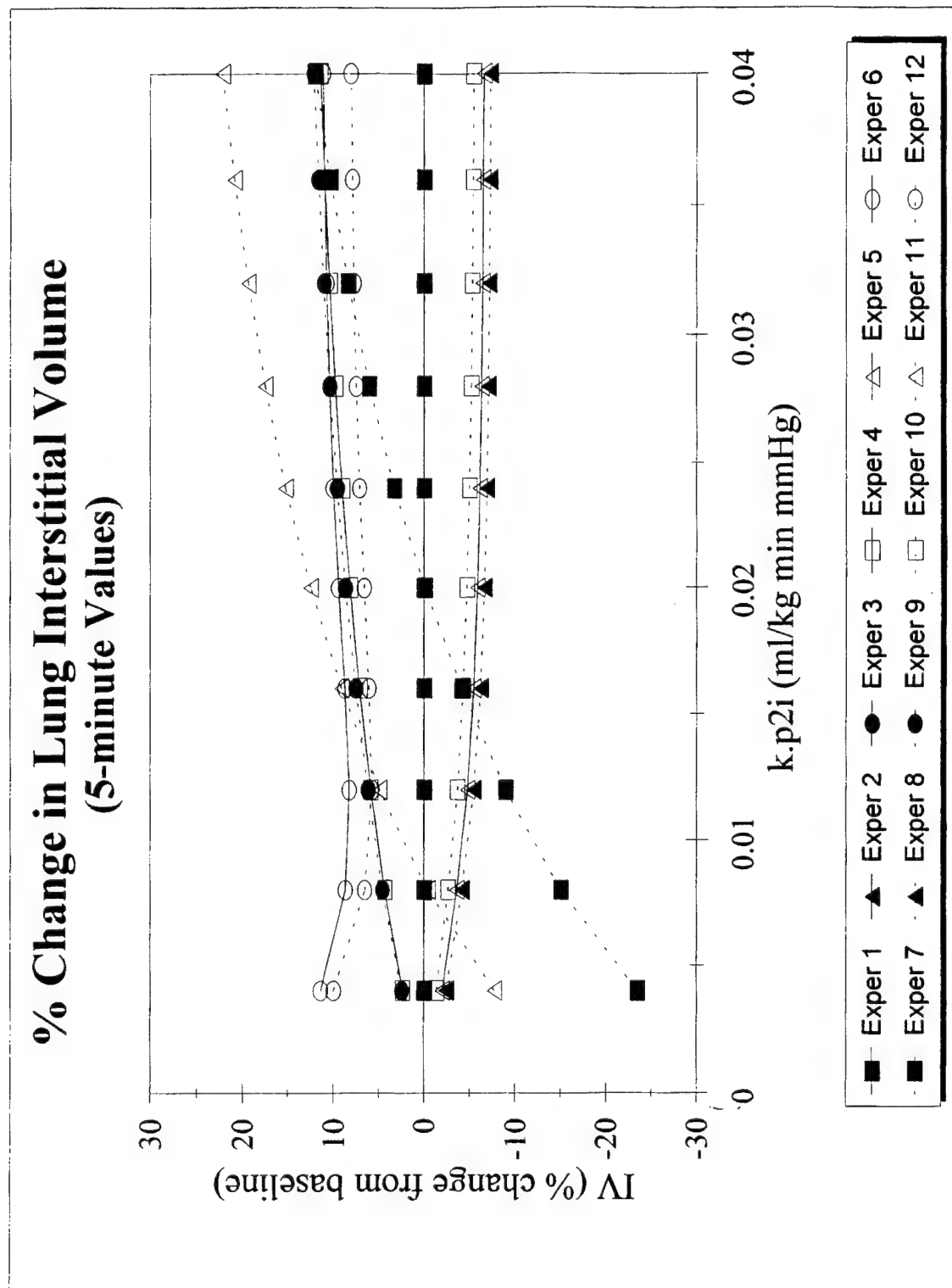


Figure C2

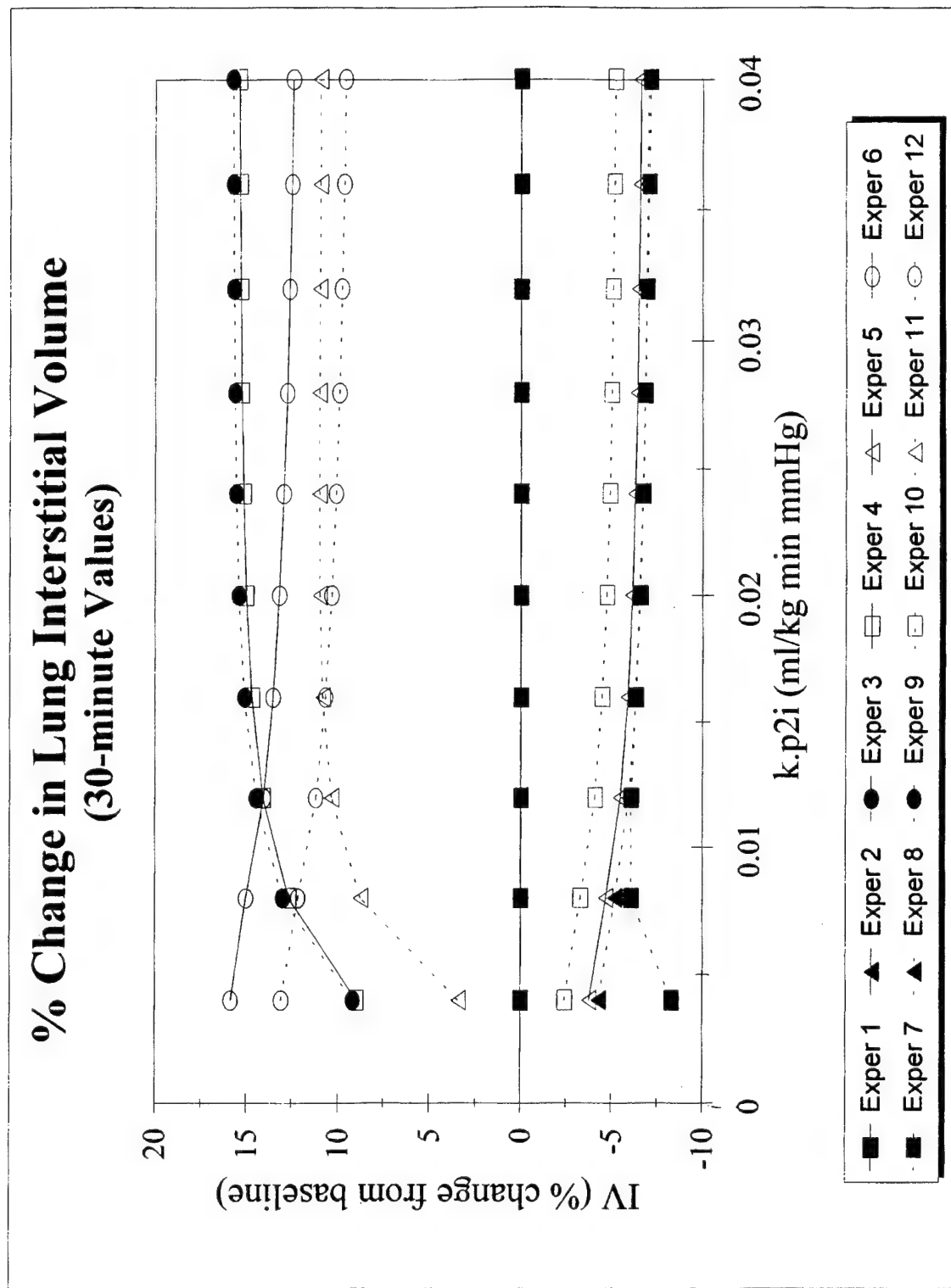


Figure C3

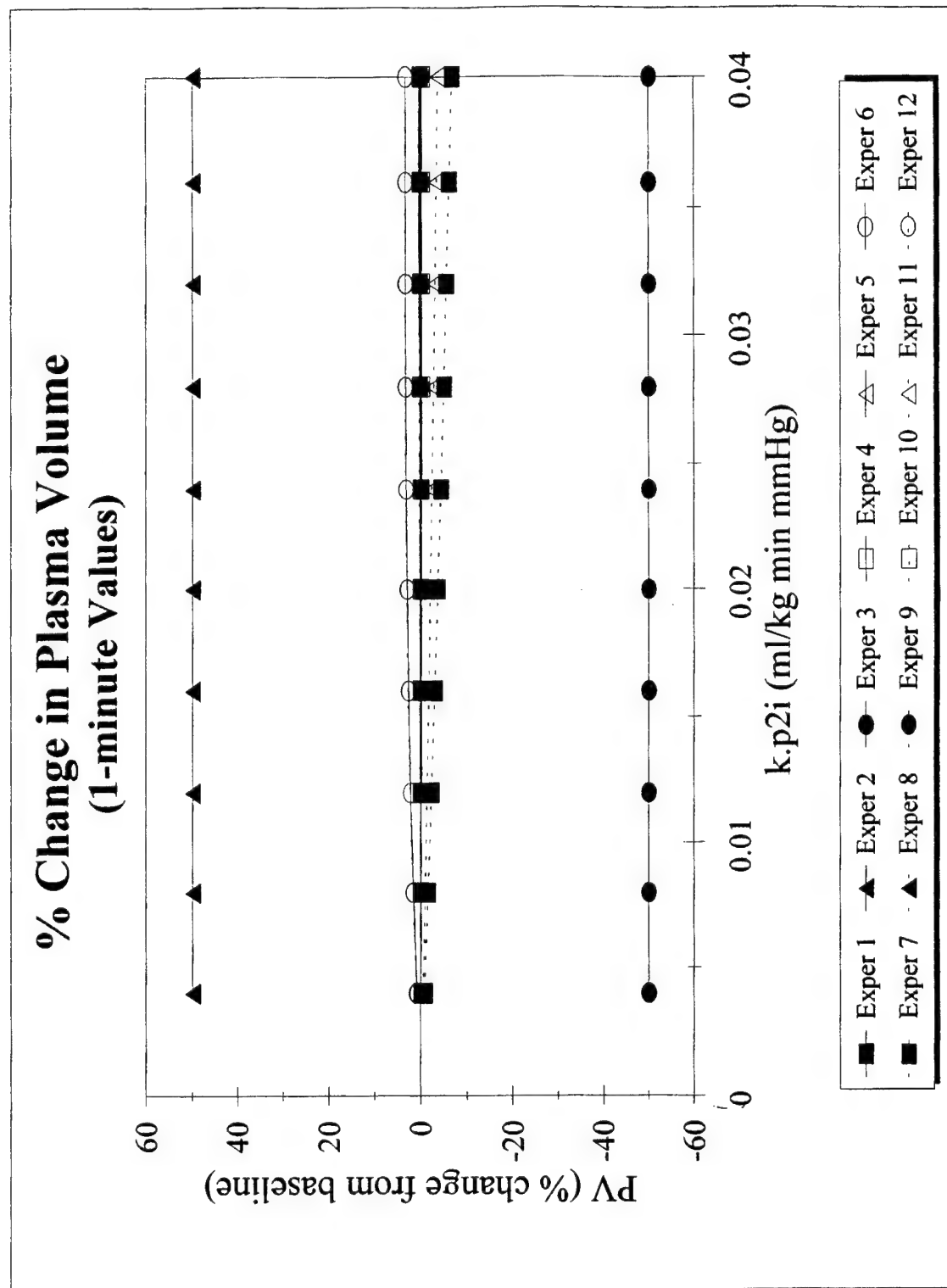


Figure C4

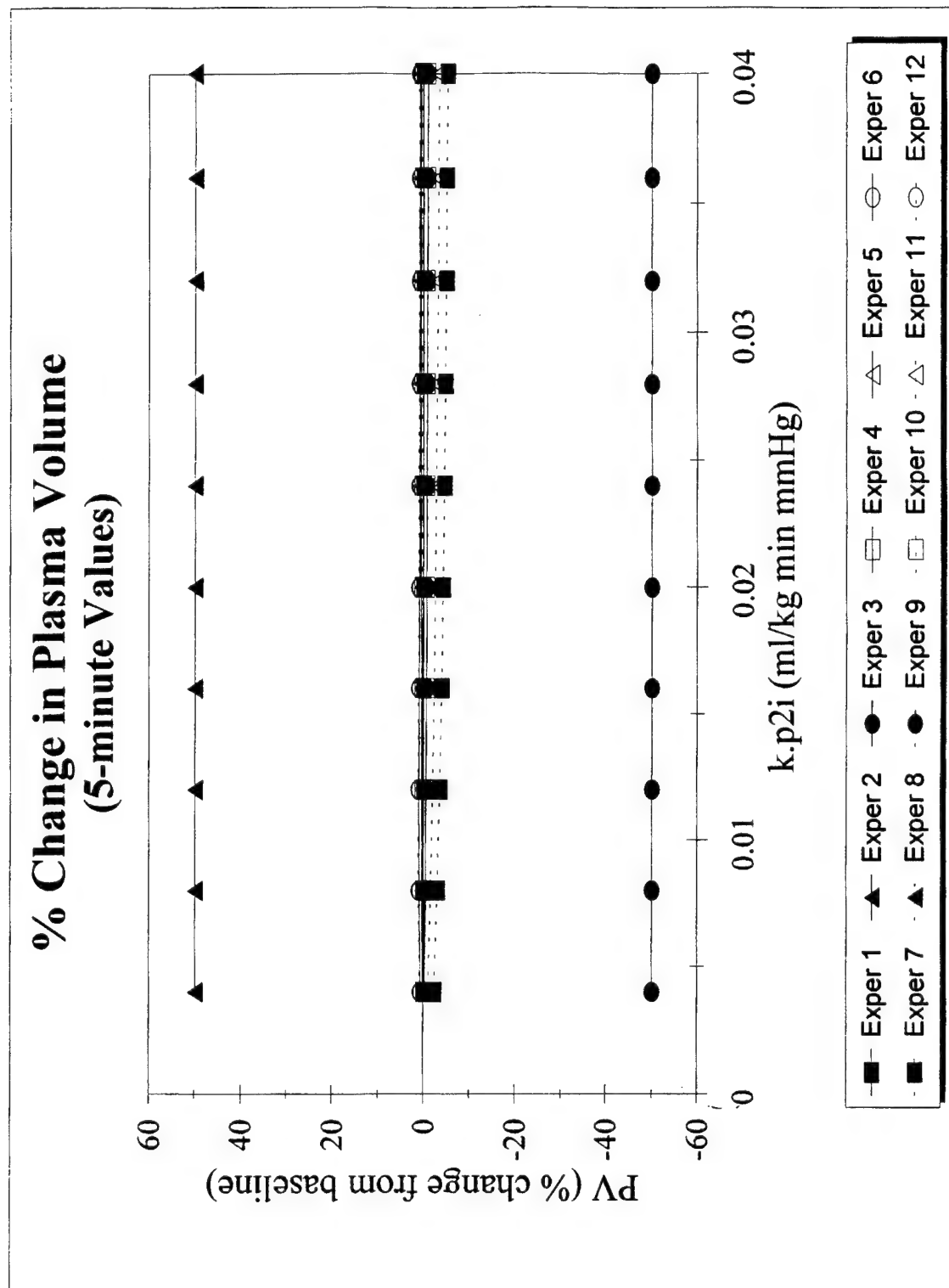


Figure C5

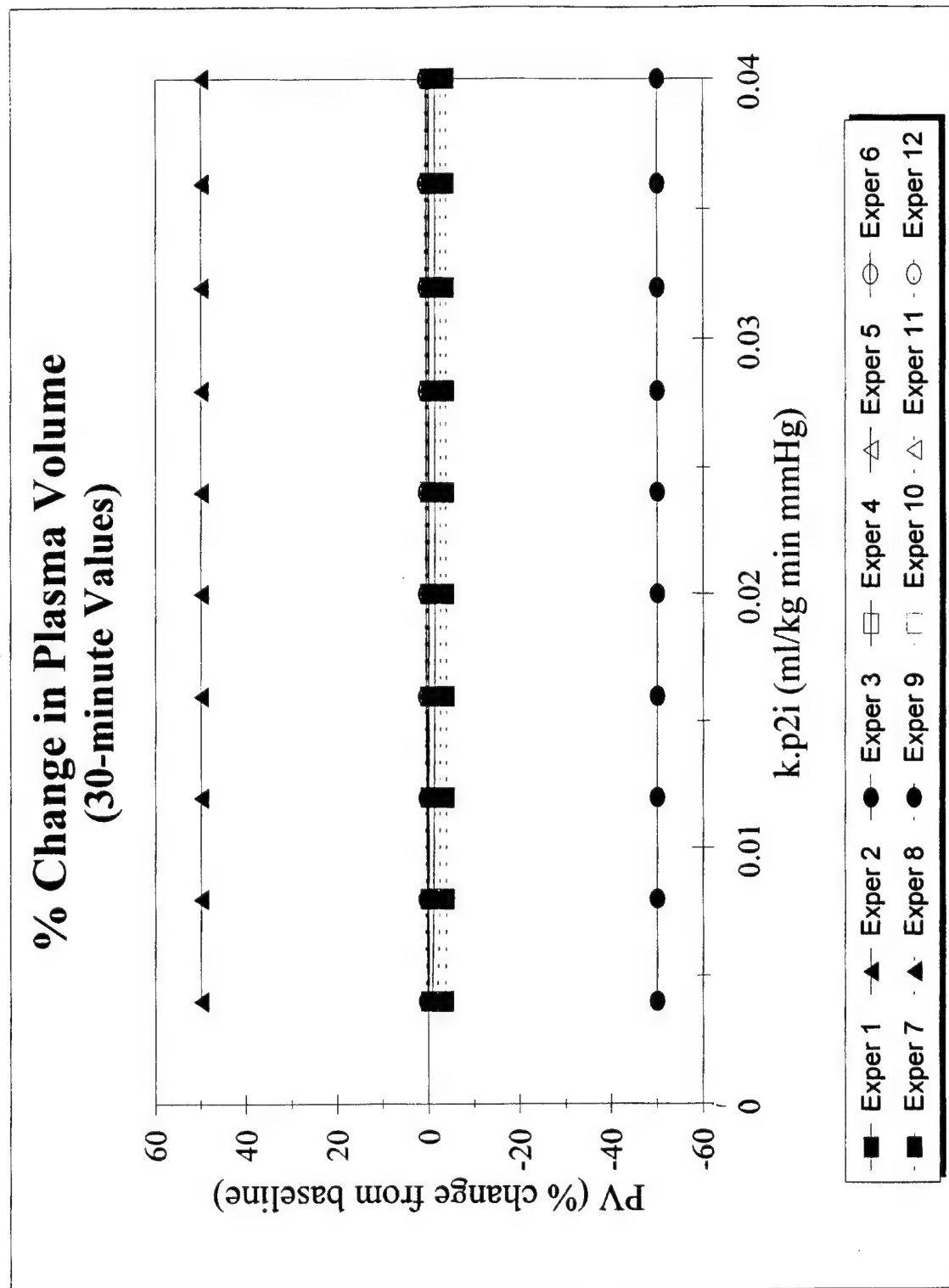


Figure C6

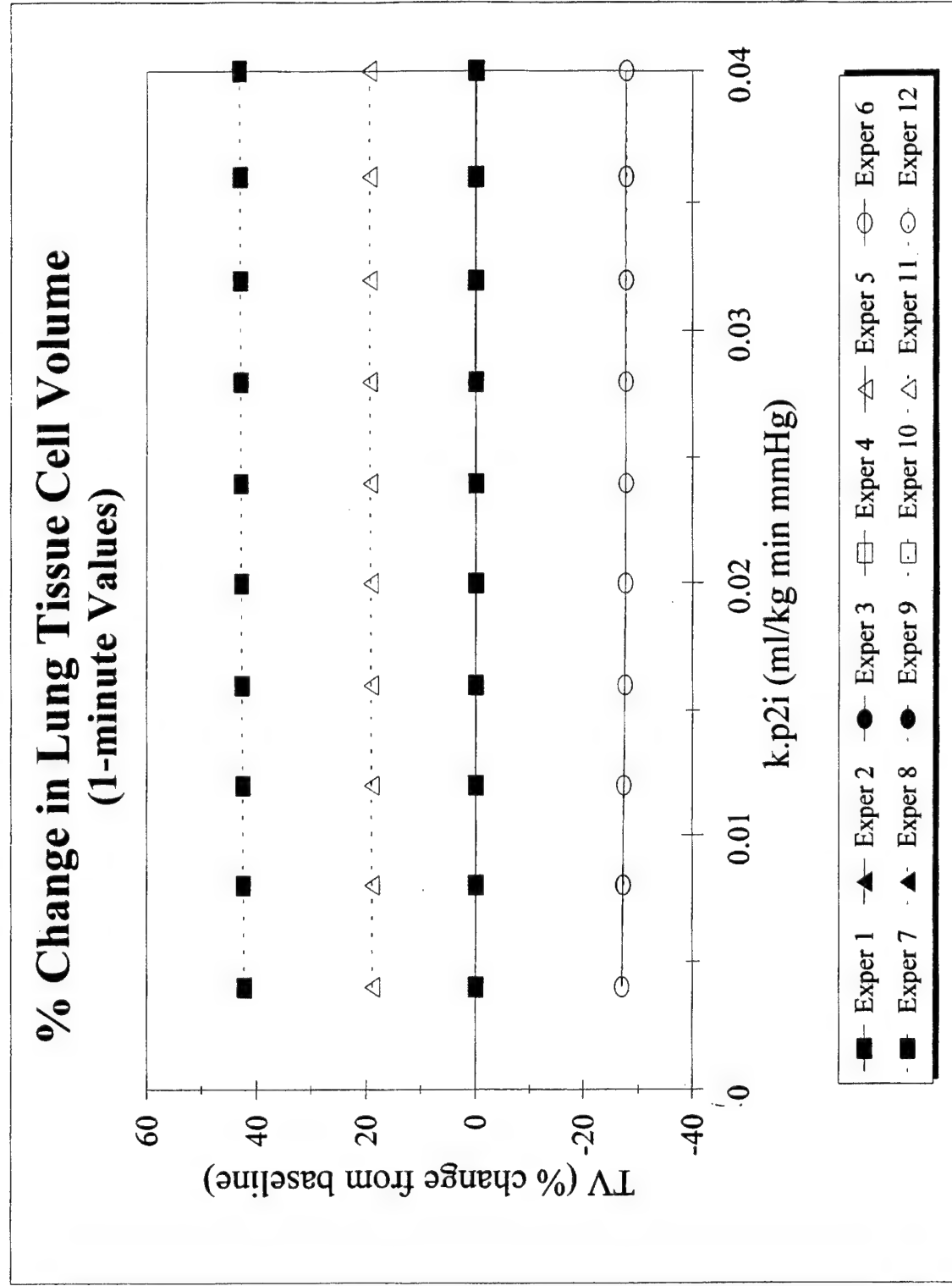


Figure C7

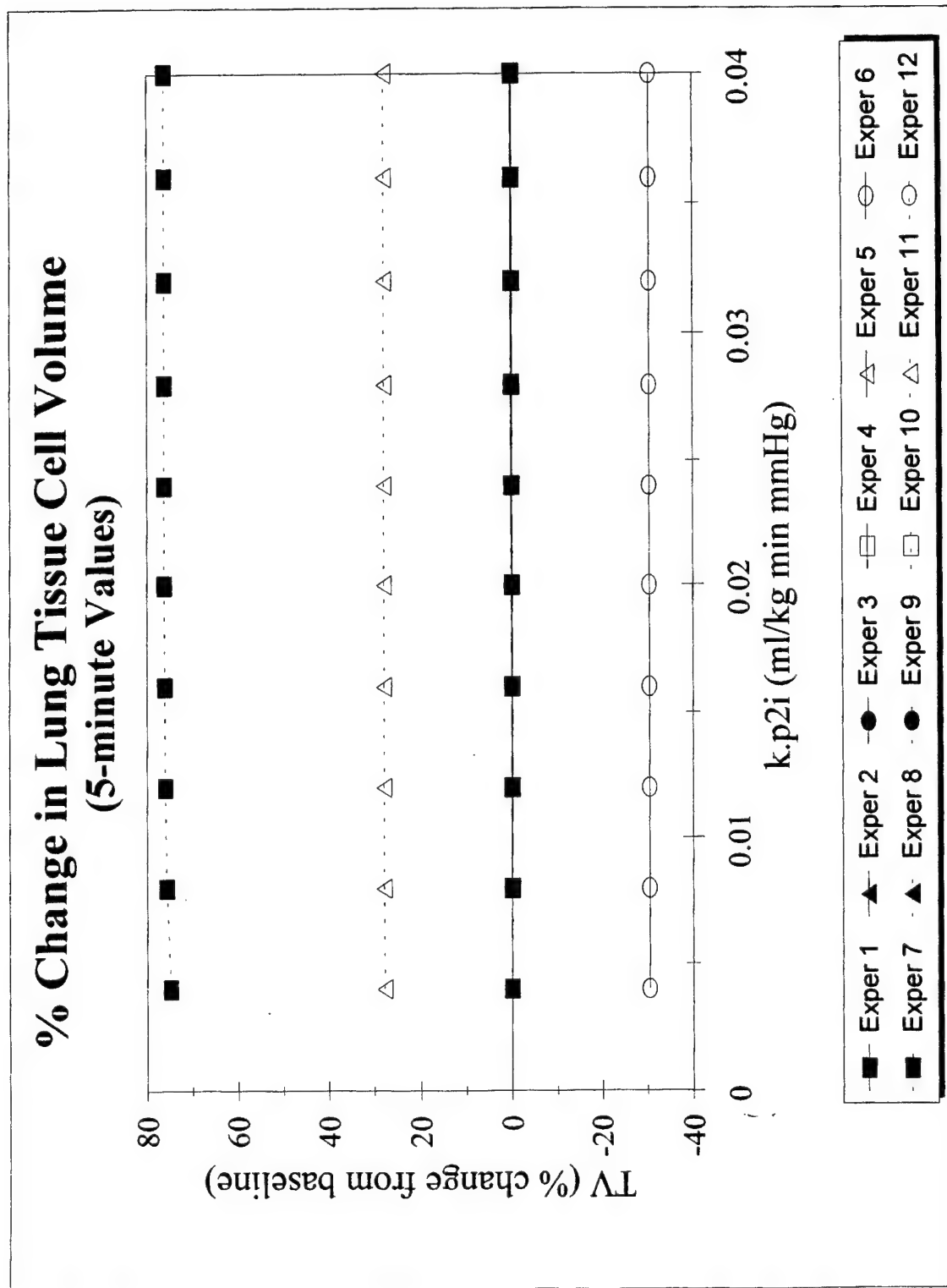


Figure C8

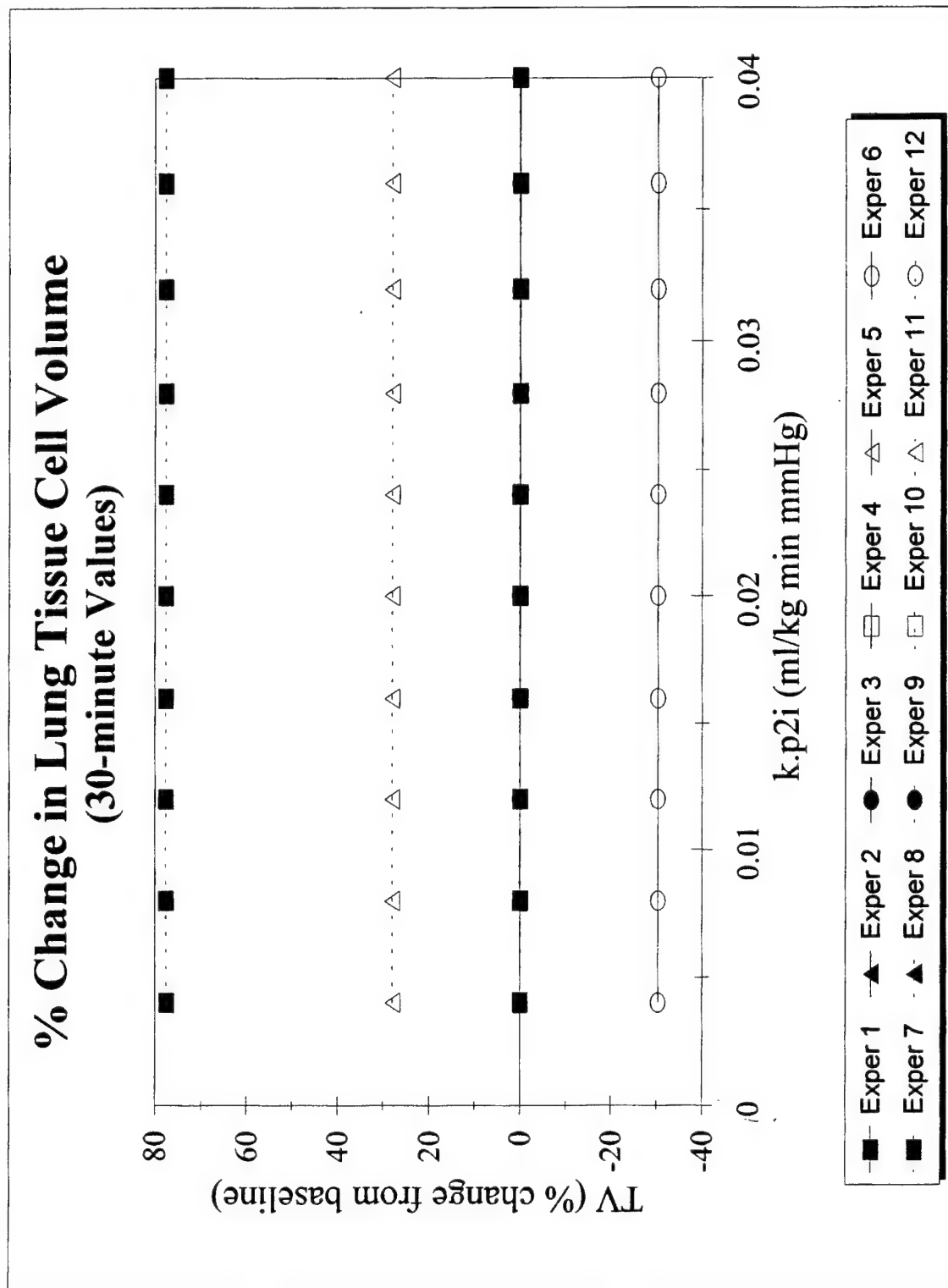


Figure C9

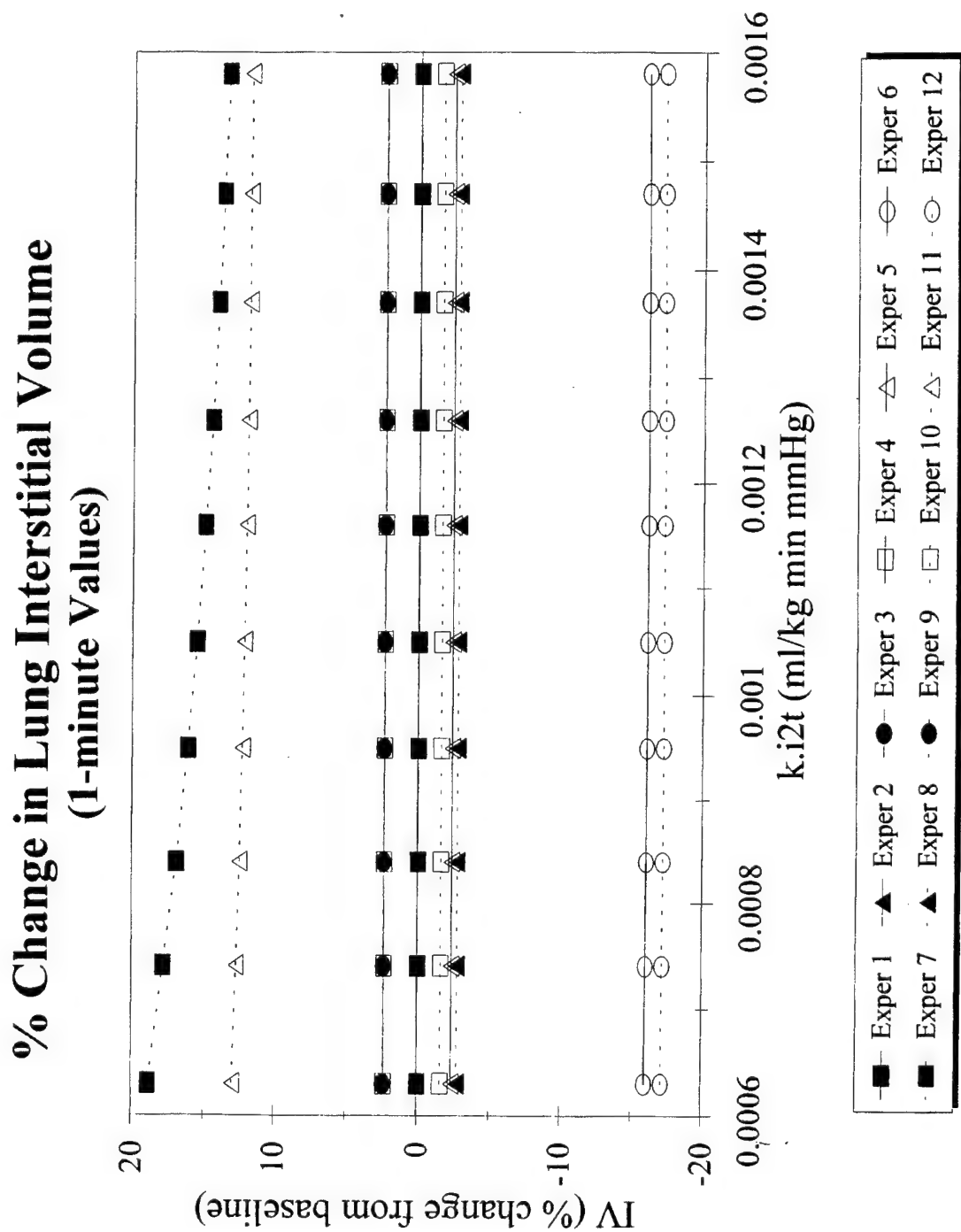


Figure C10

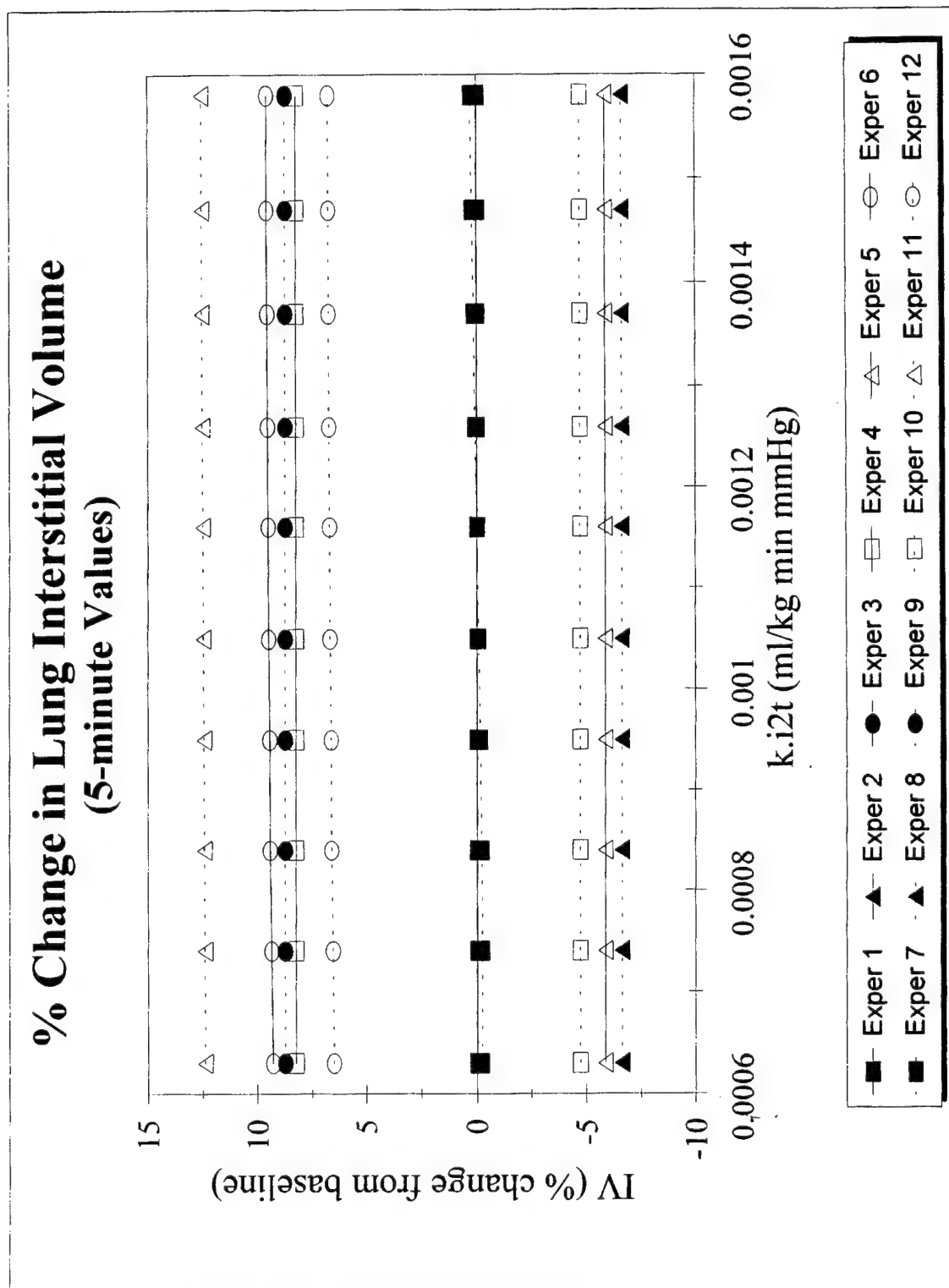


Figure C11

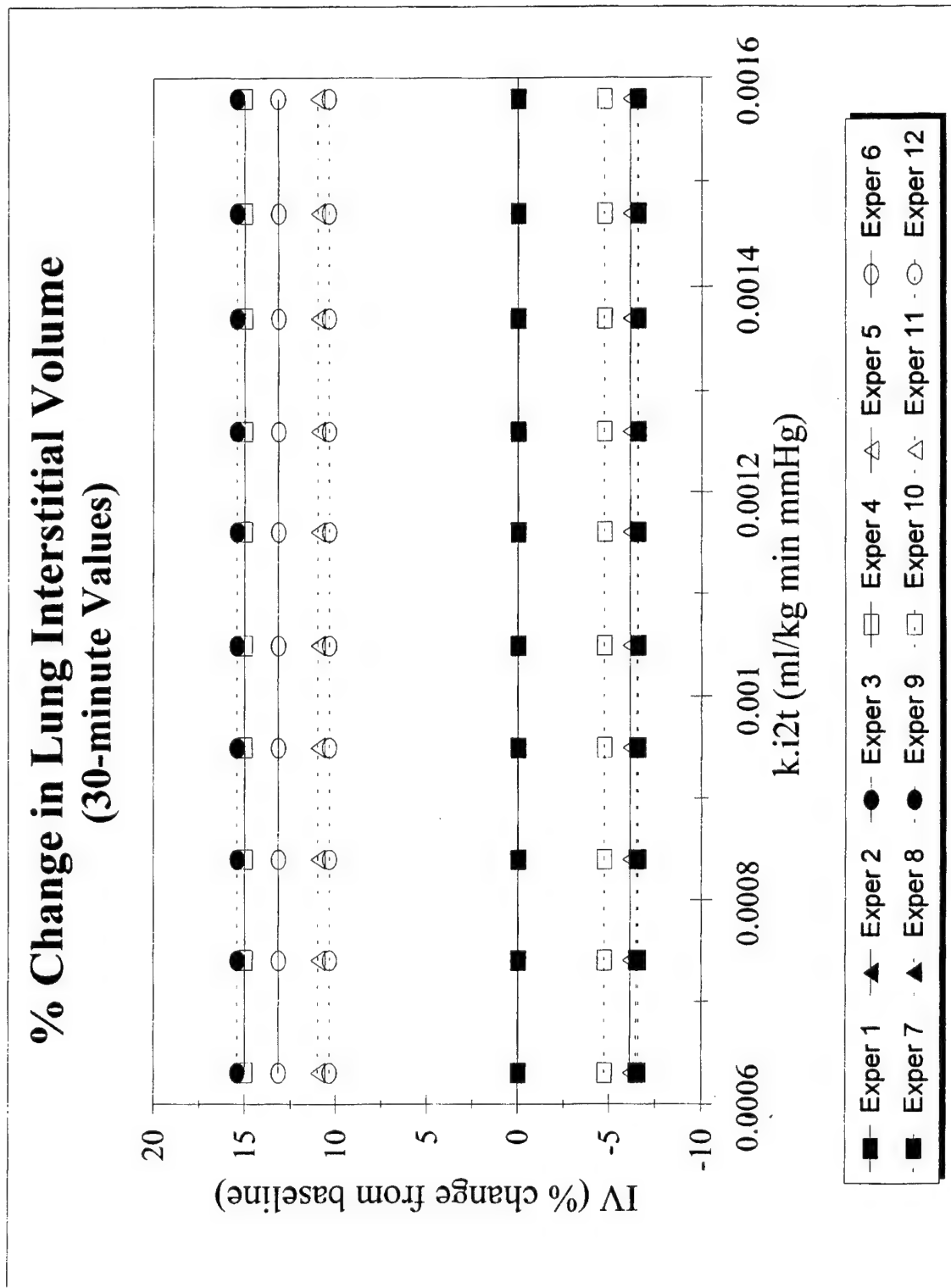


Figure C12

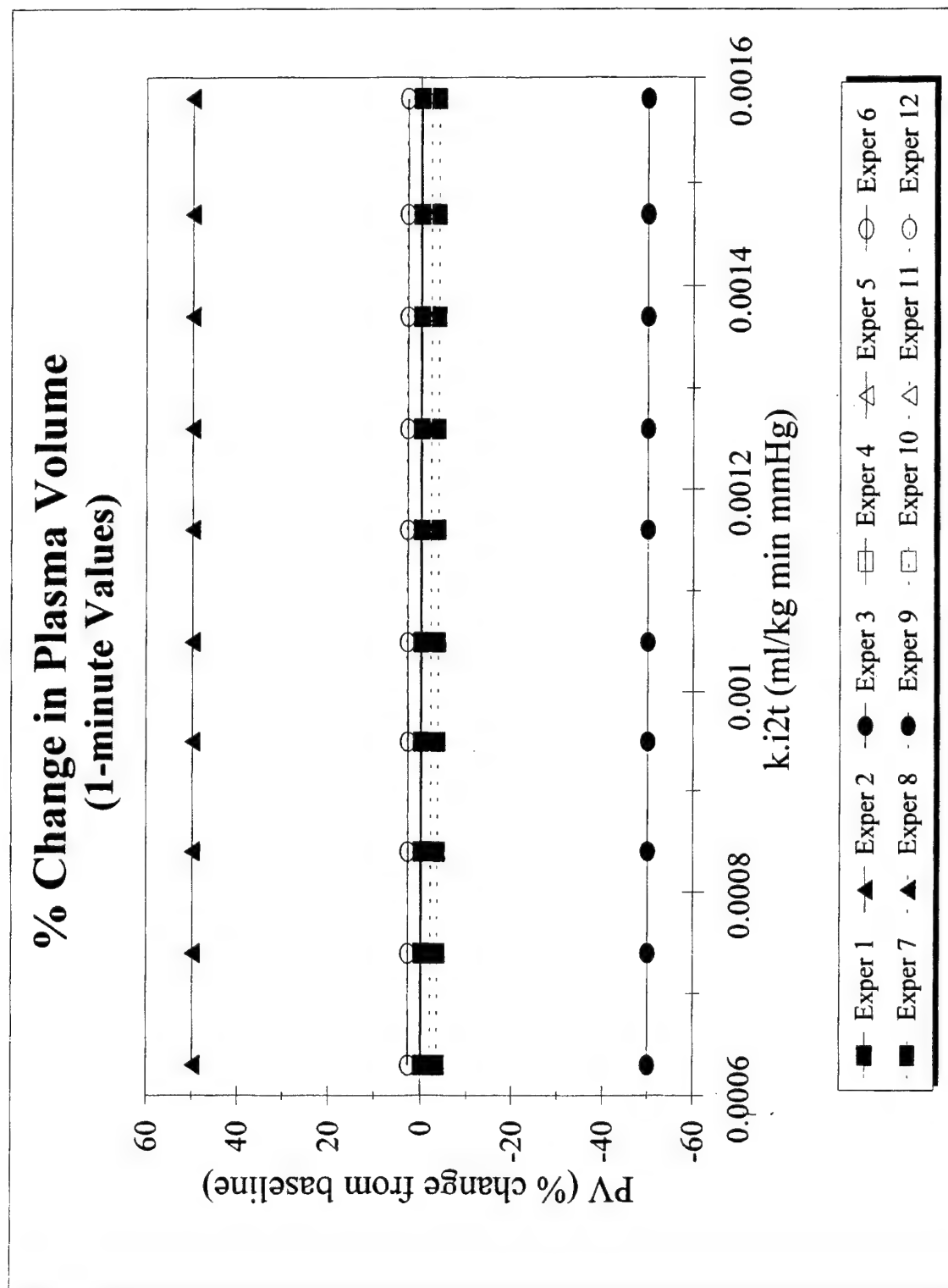


Figure C13

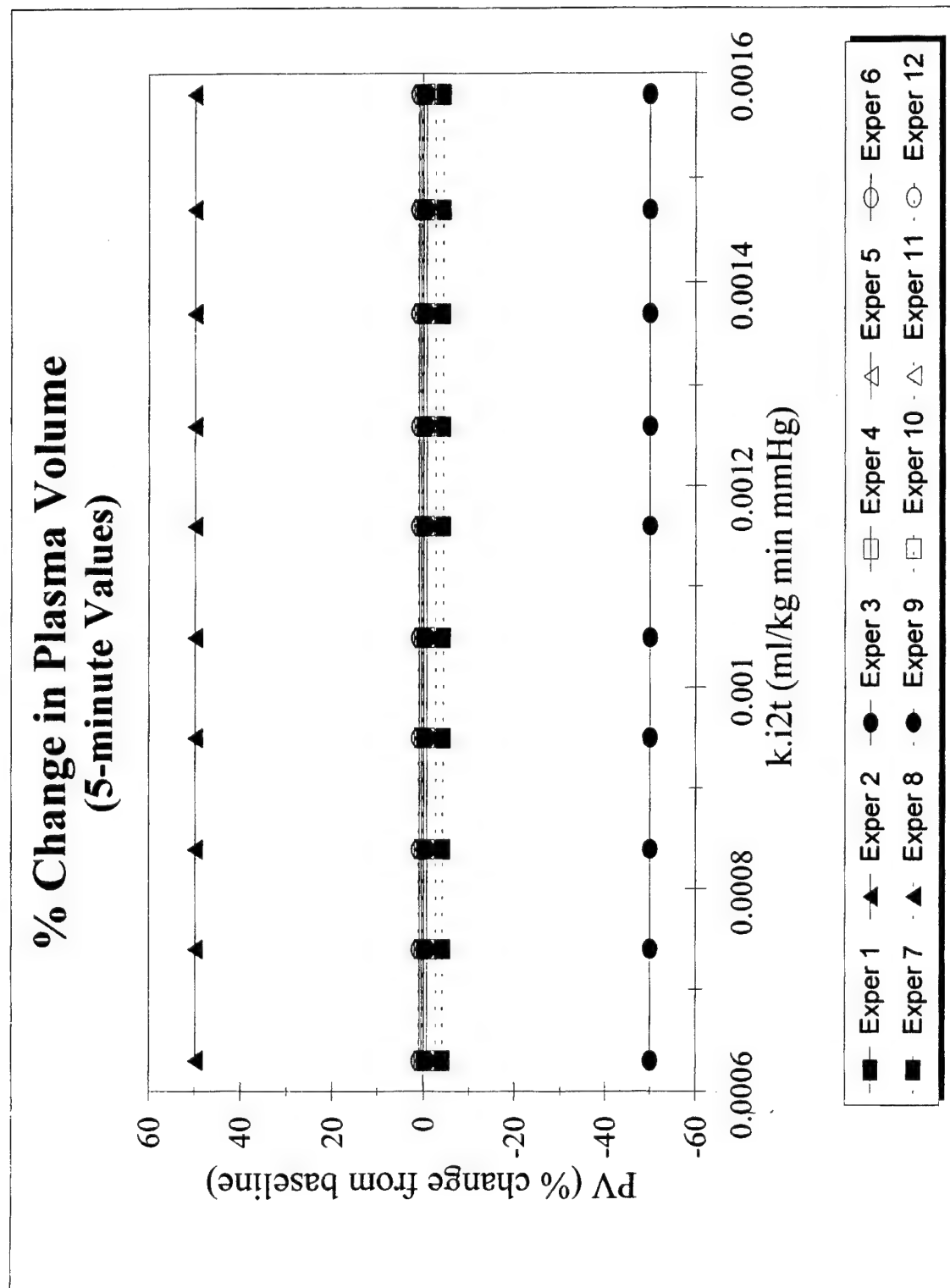


Figure C14

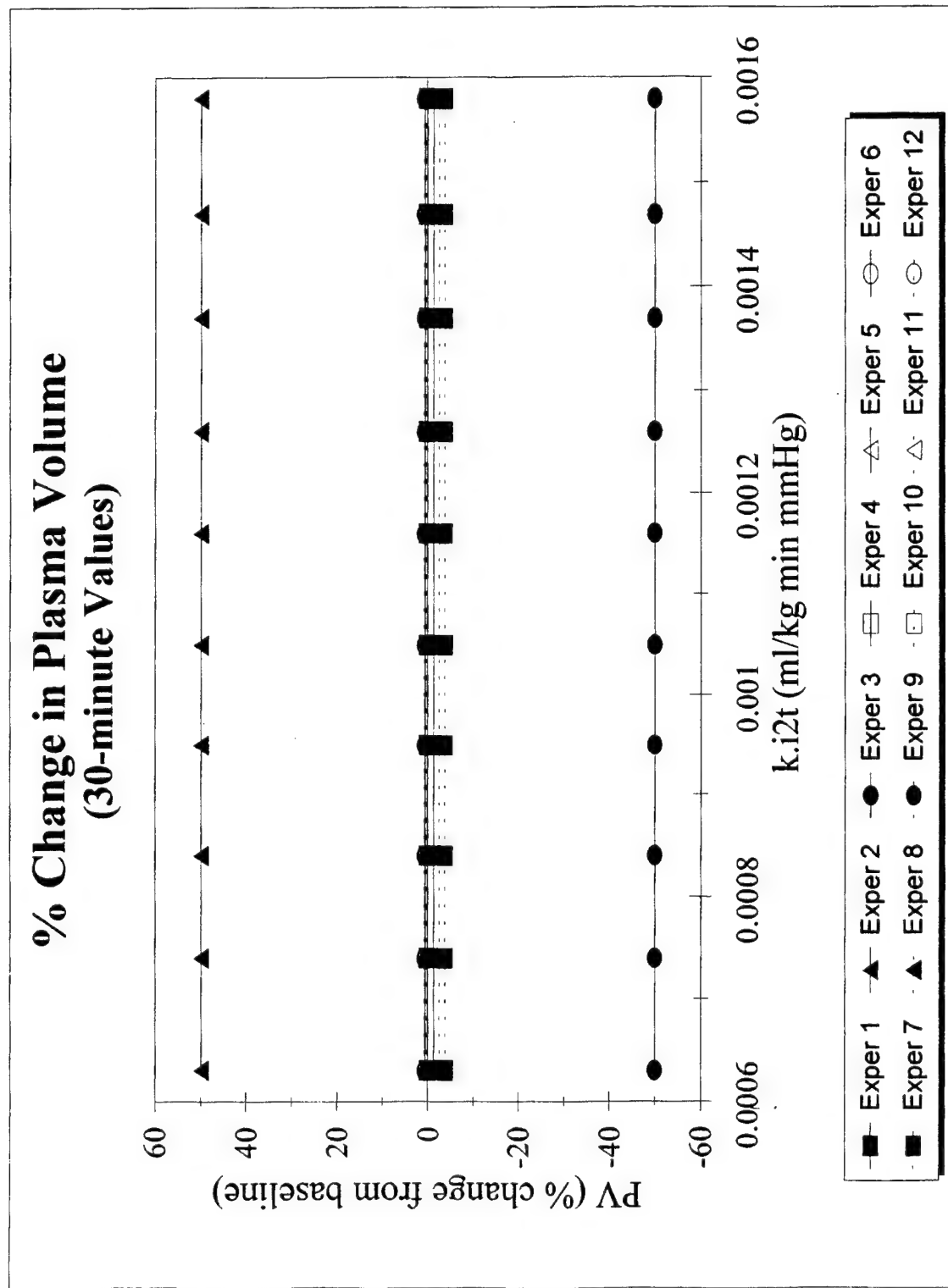


Figure C15

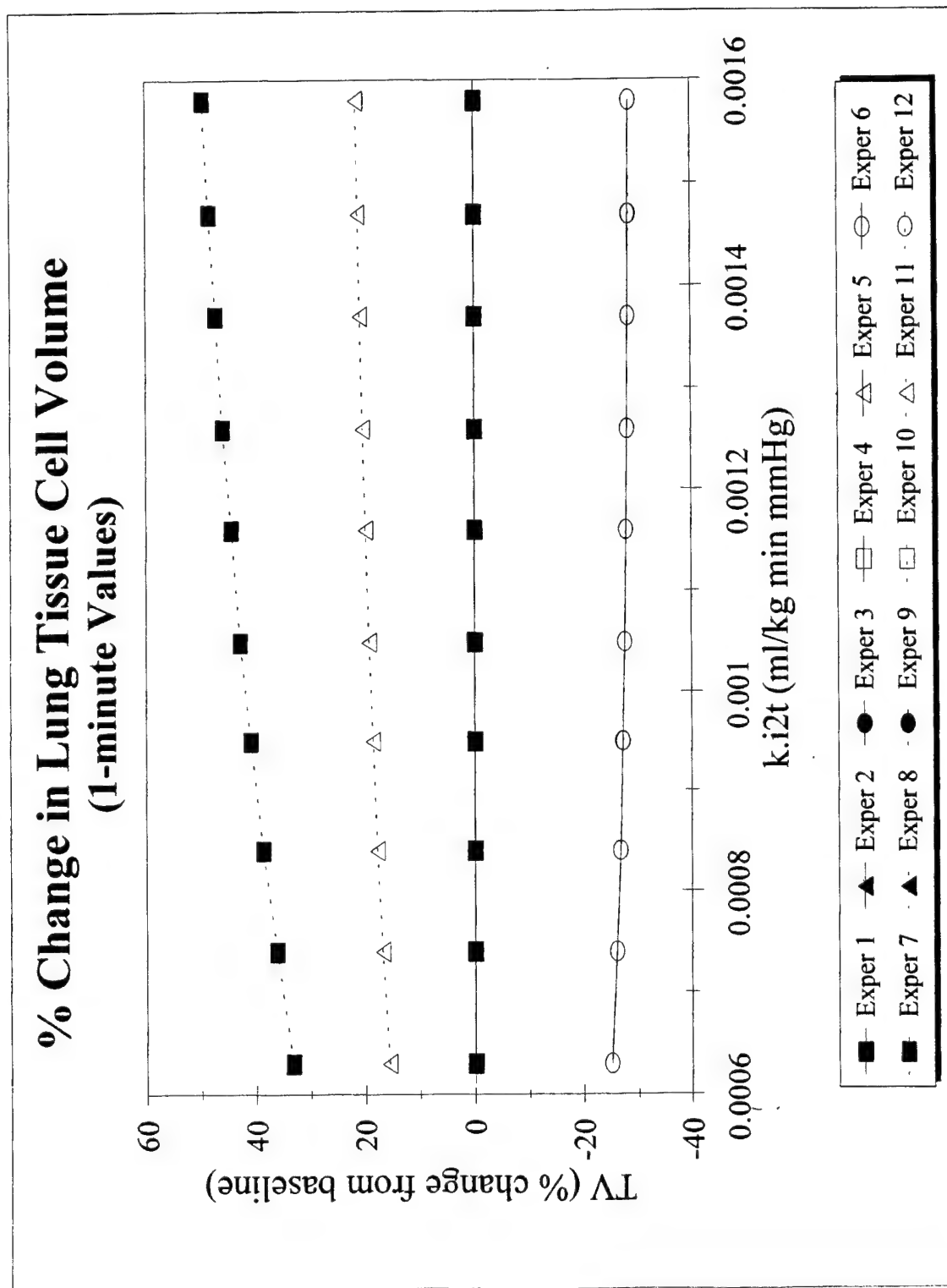


Figure C16

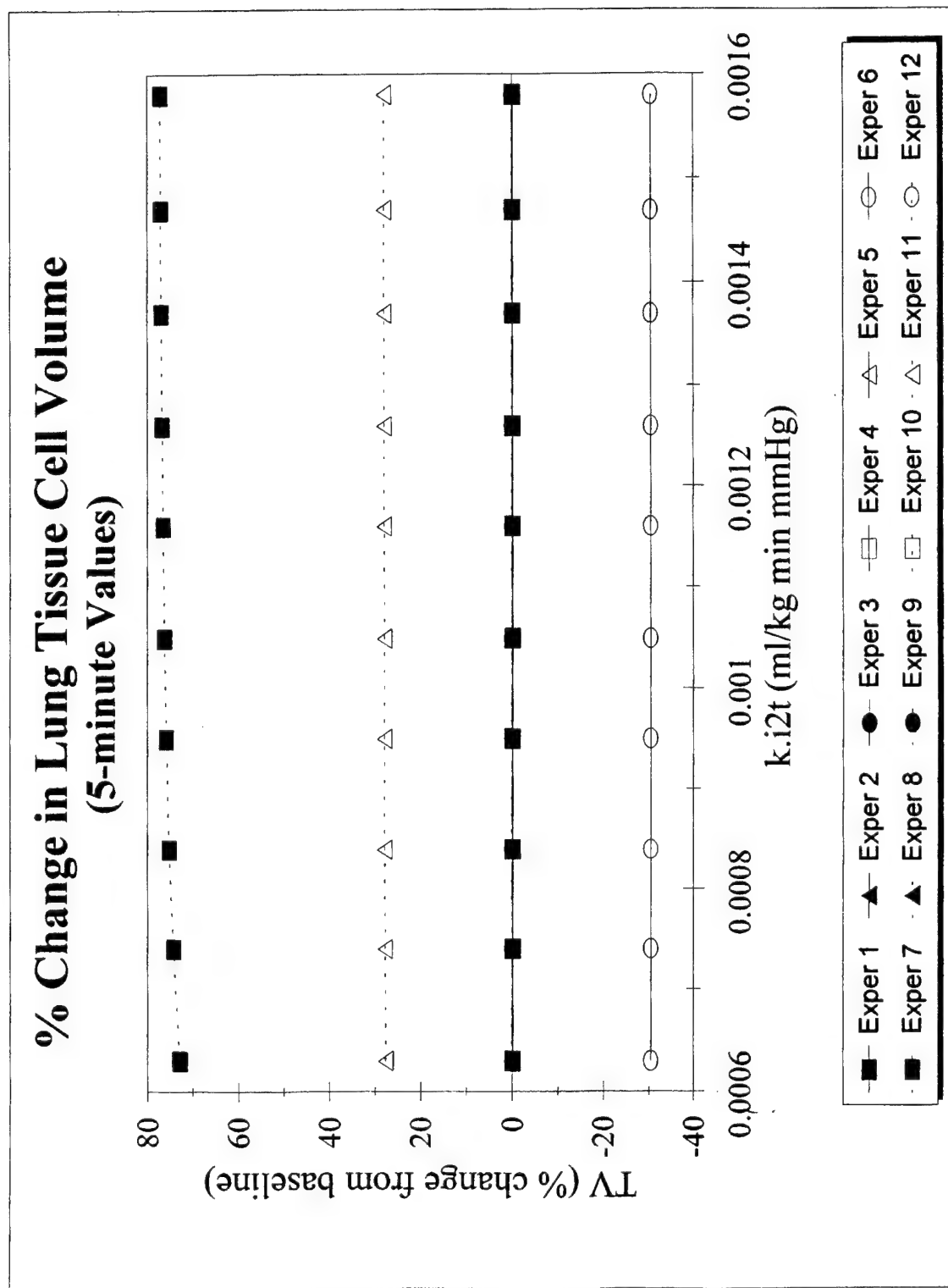


Figure C17

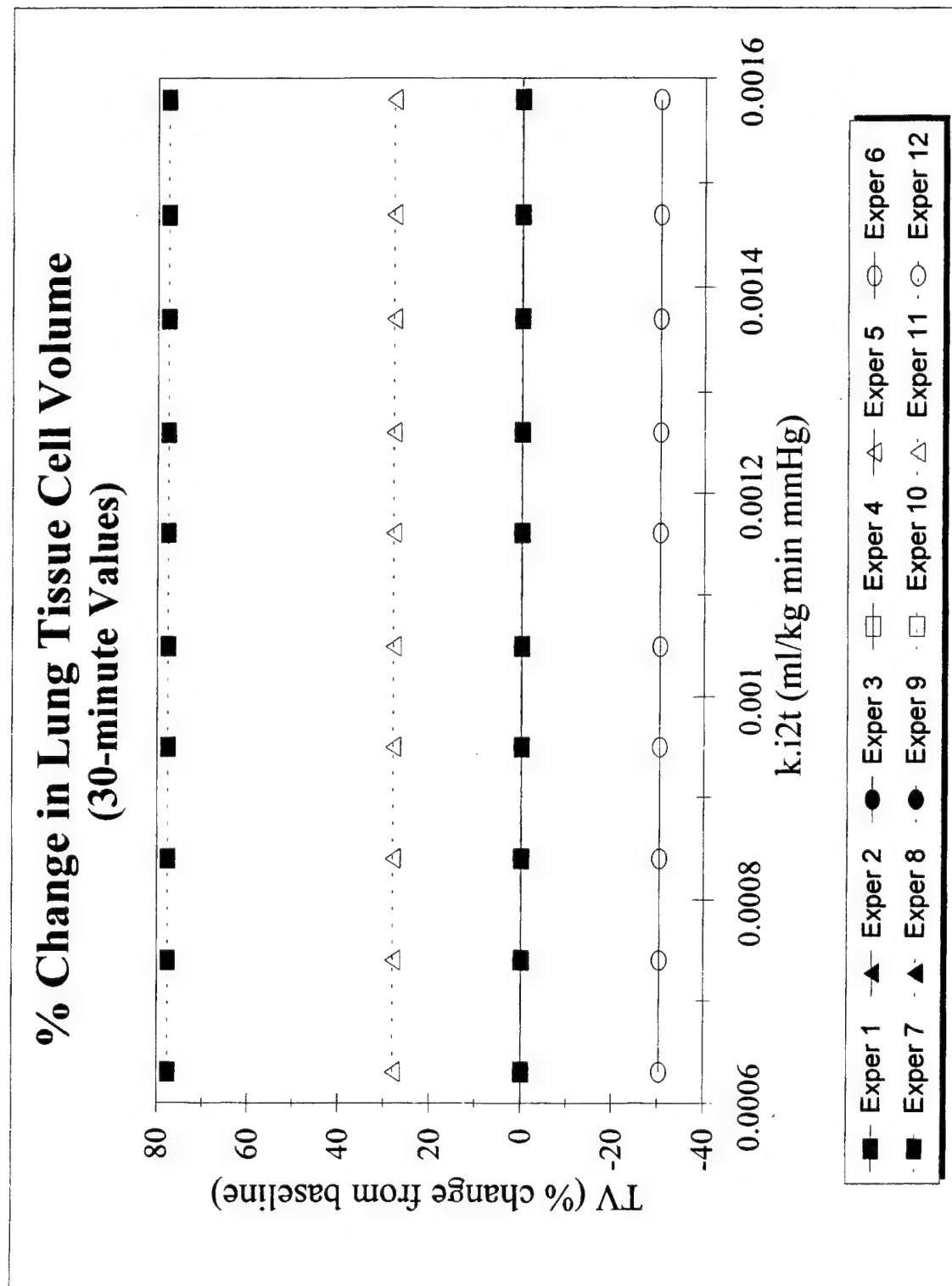


Figure C18

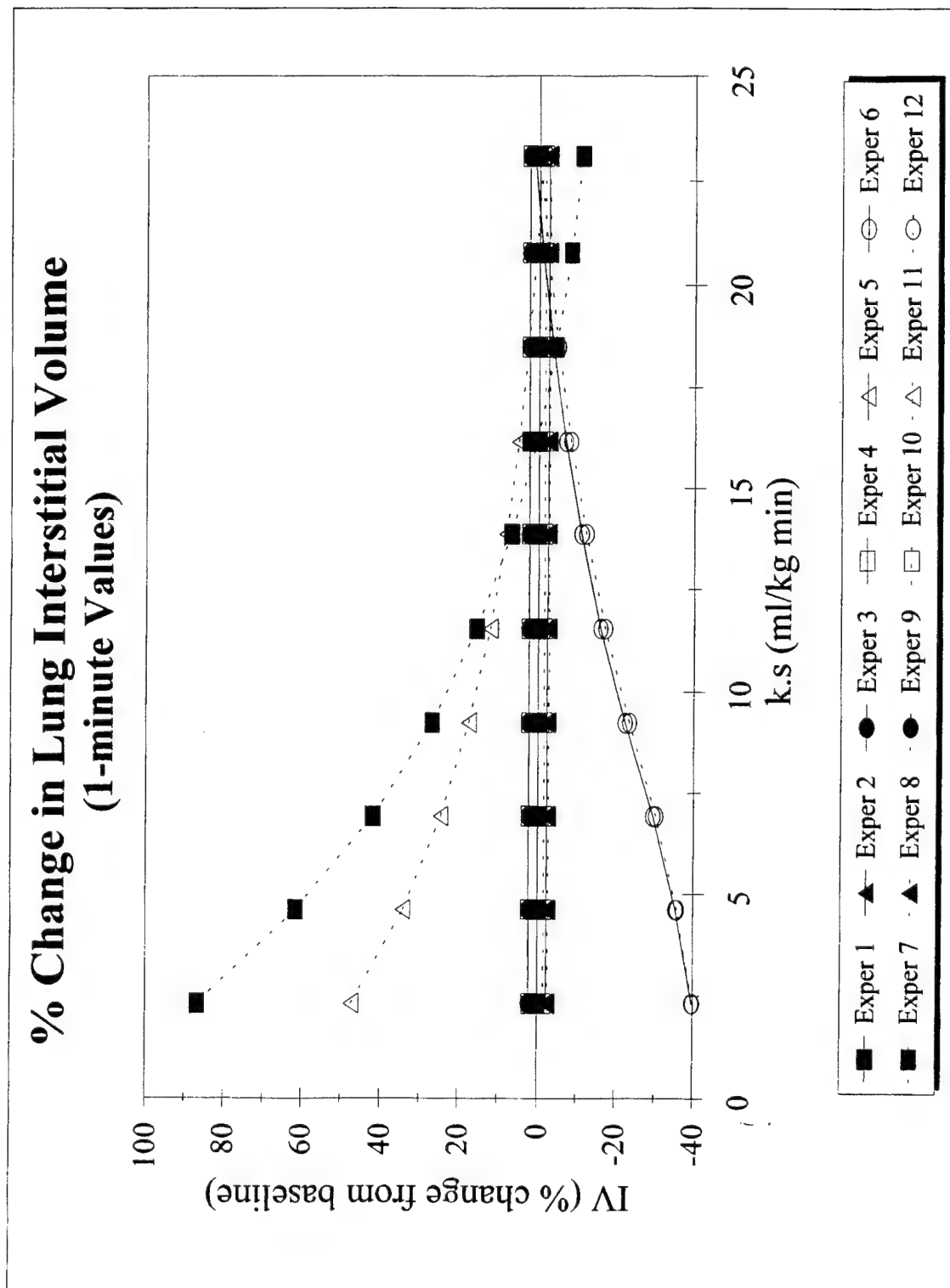


Figure C19

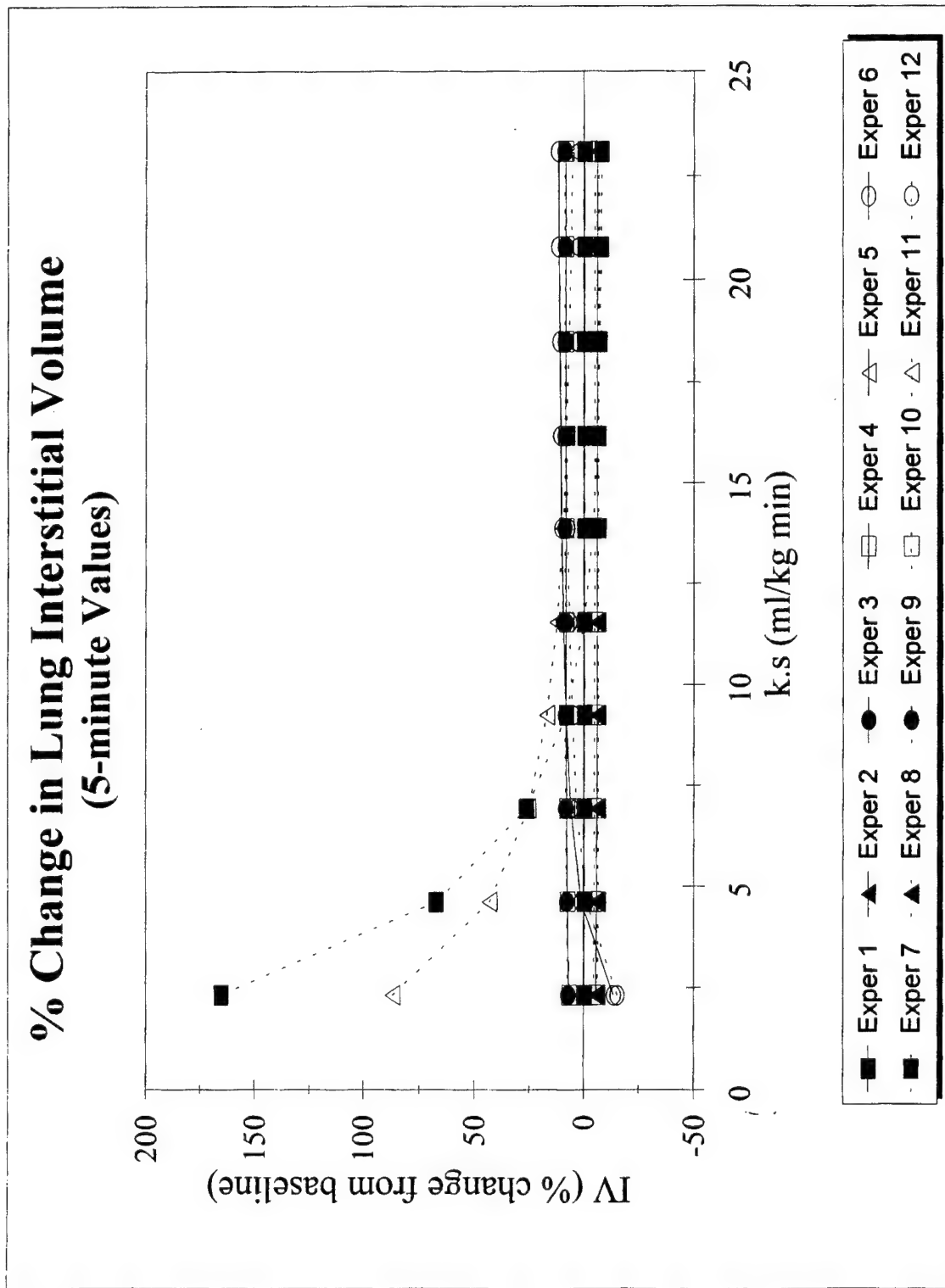


Figure C20

% Change in Lung Interstitial Volume (30-minute Values)

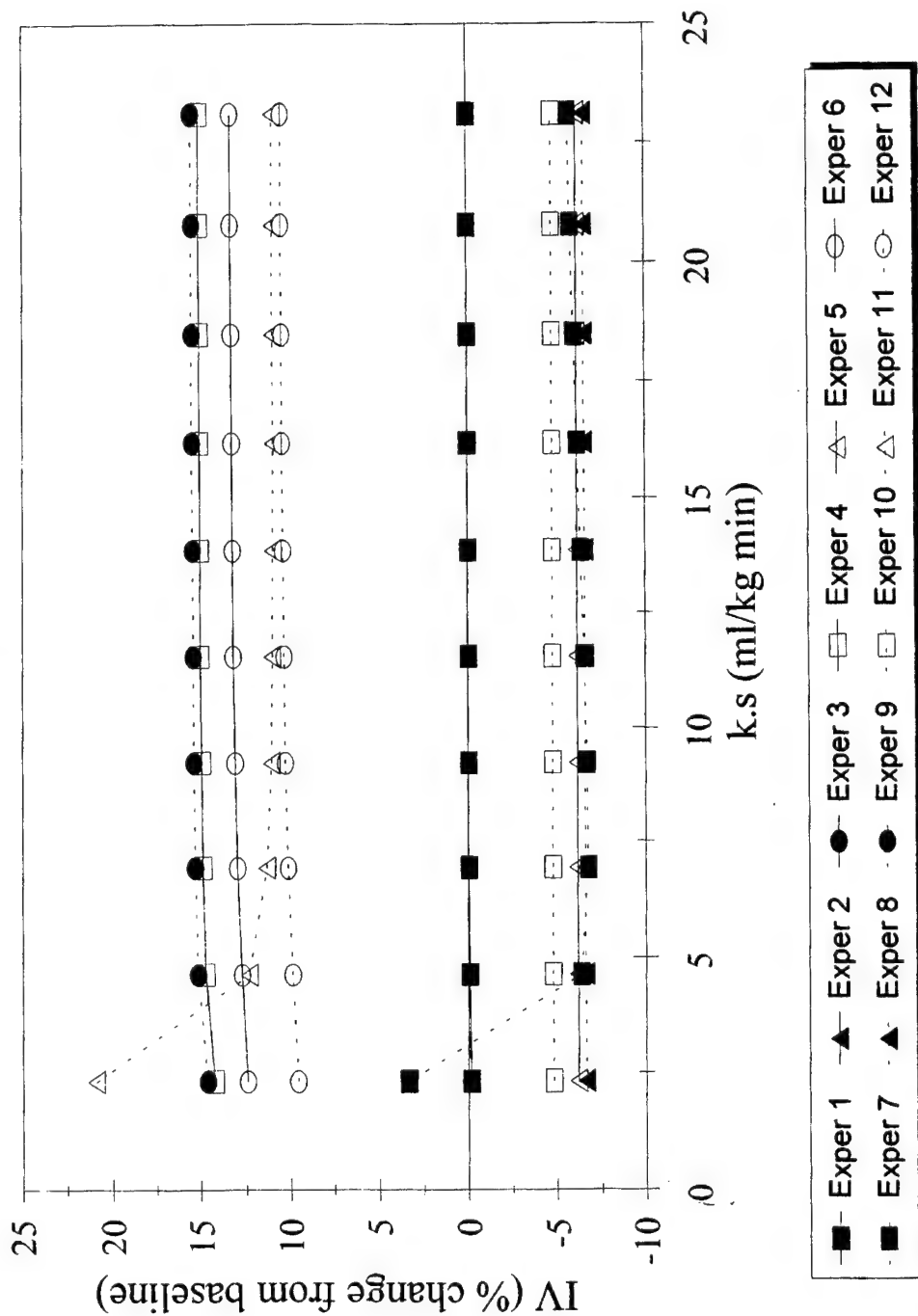


Figure C21

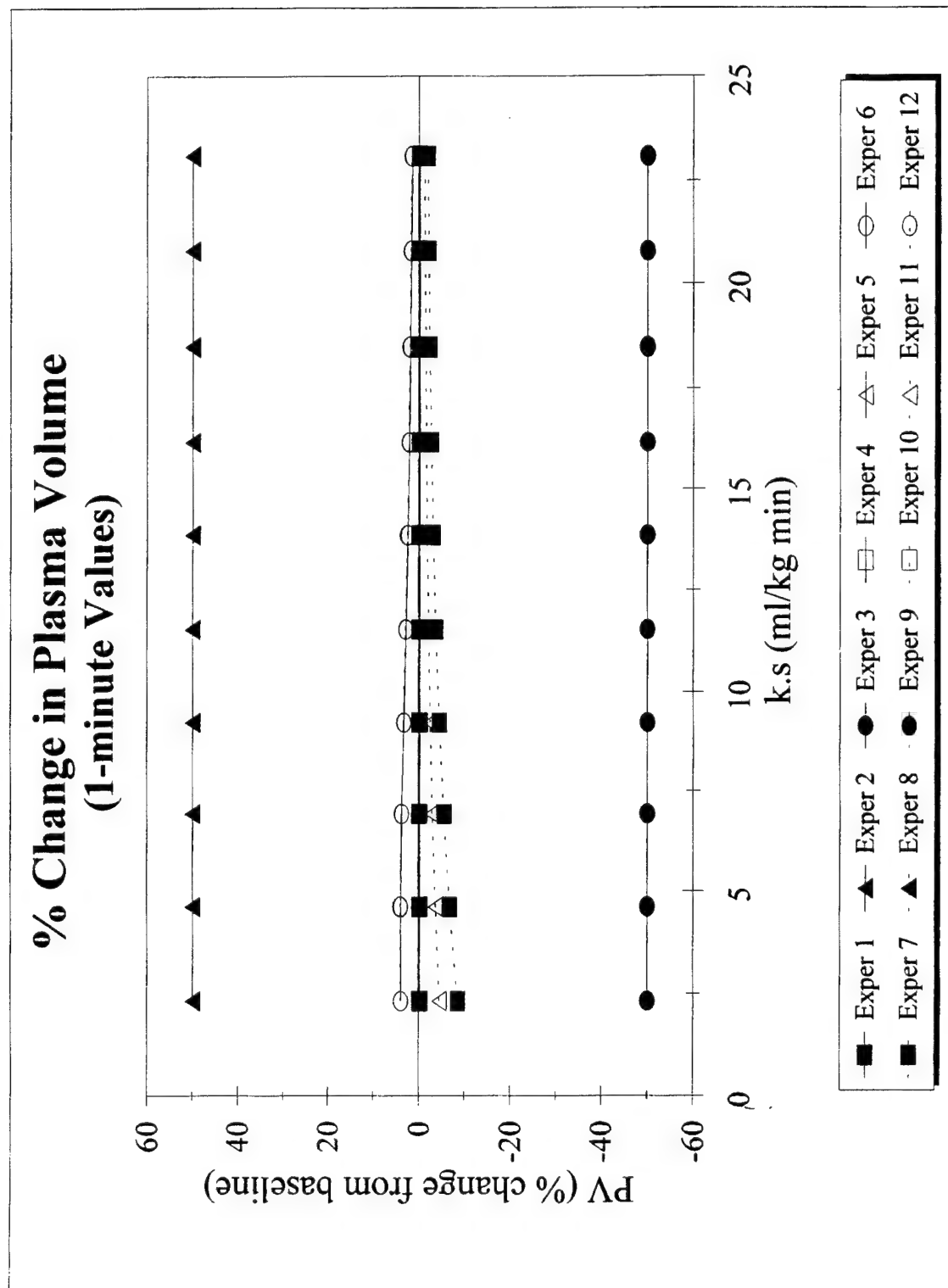


Figure C22

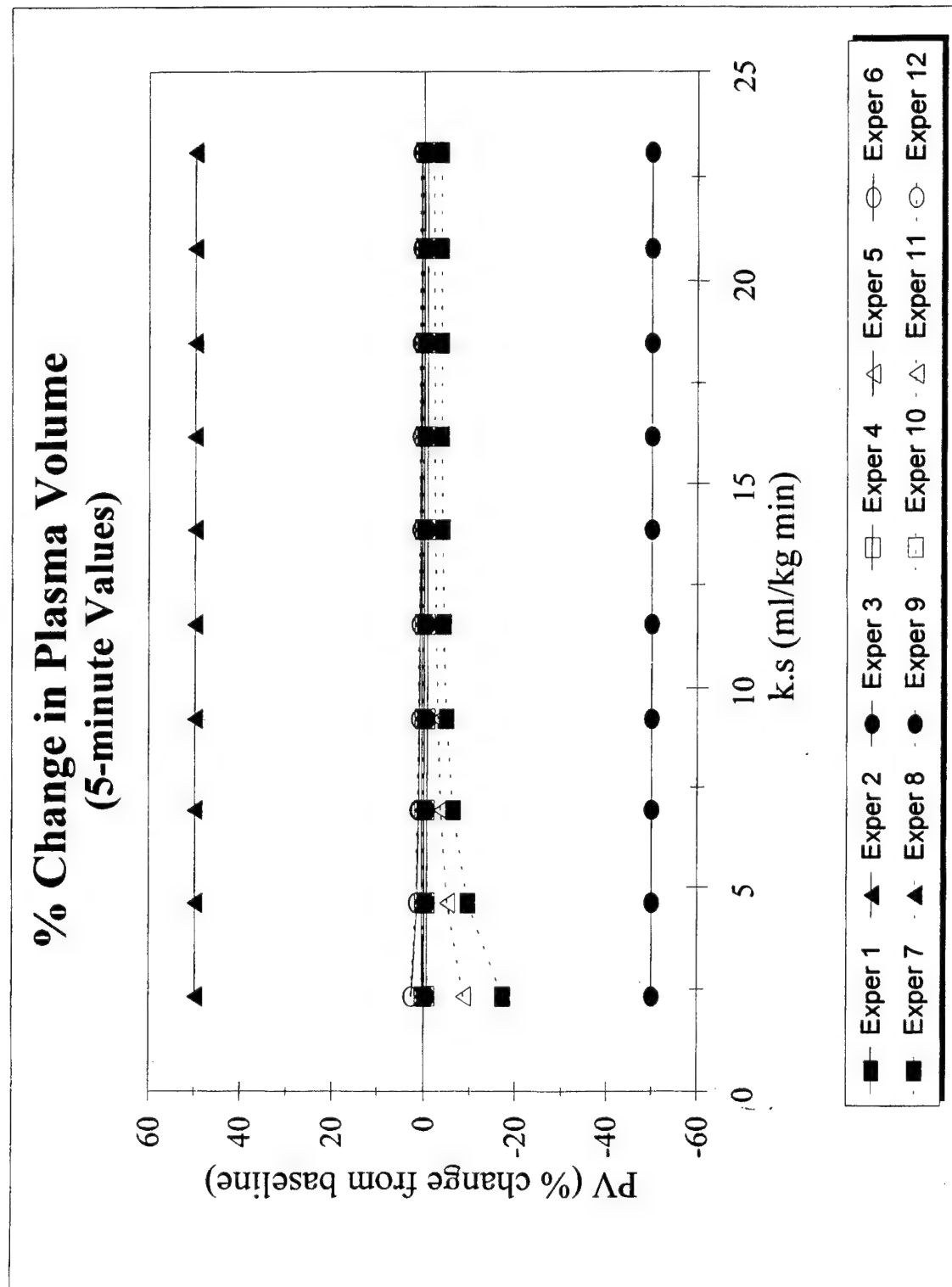


Figure C23

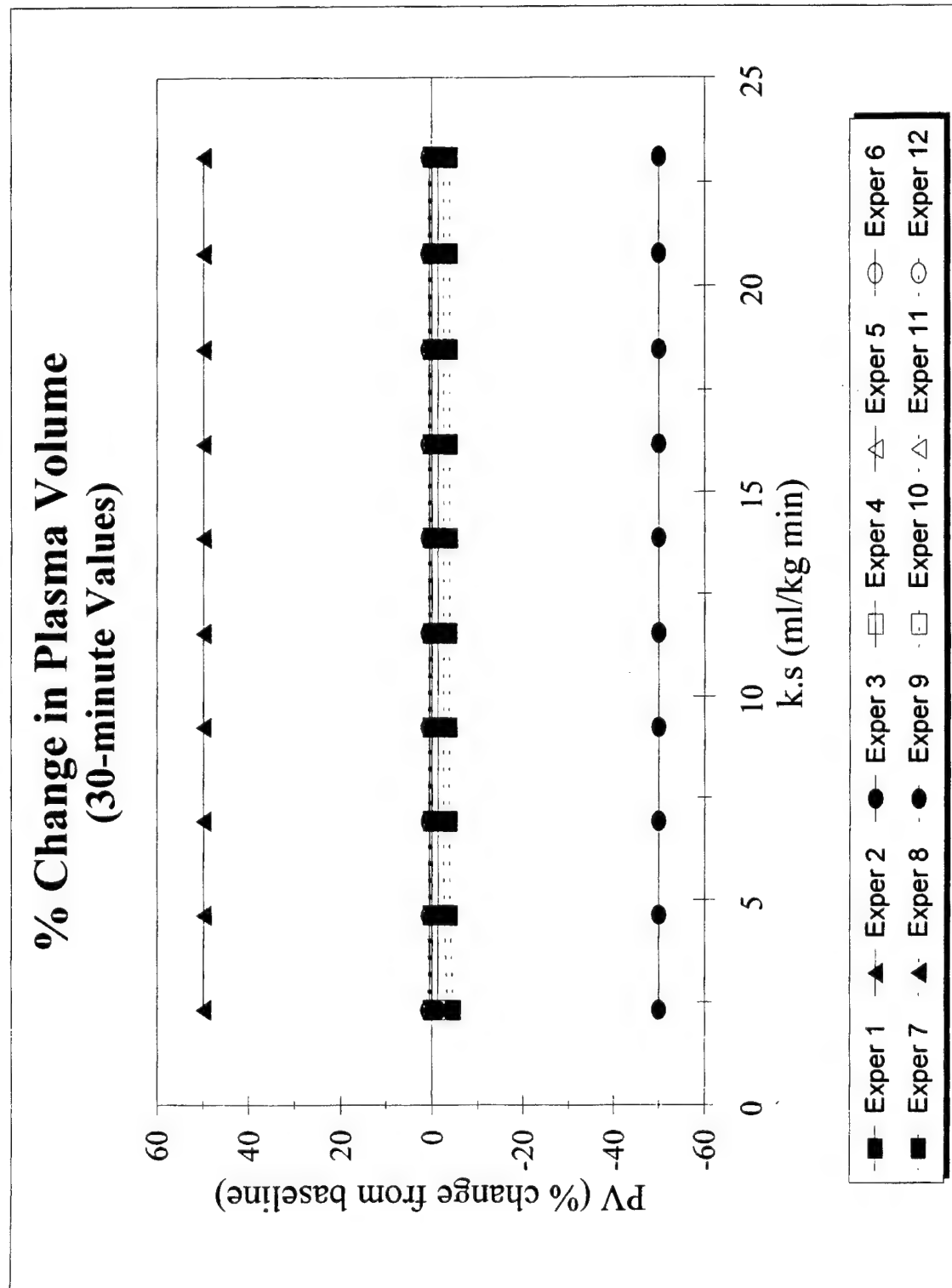


Figure C24

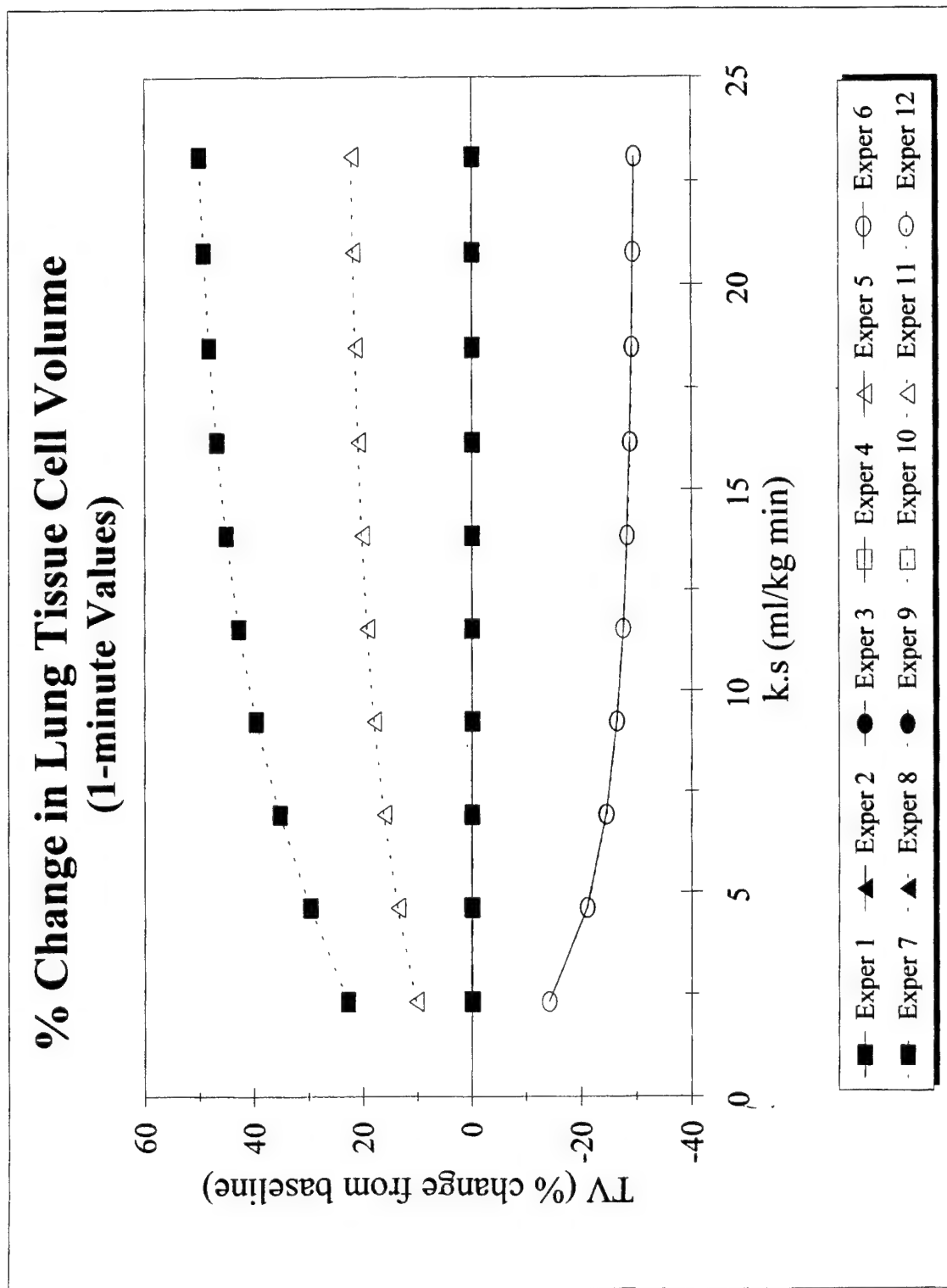


Figure C25

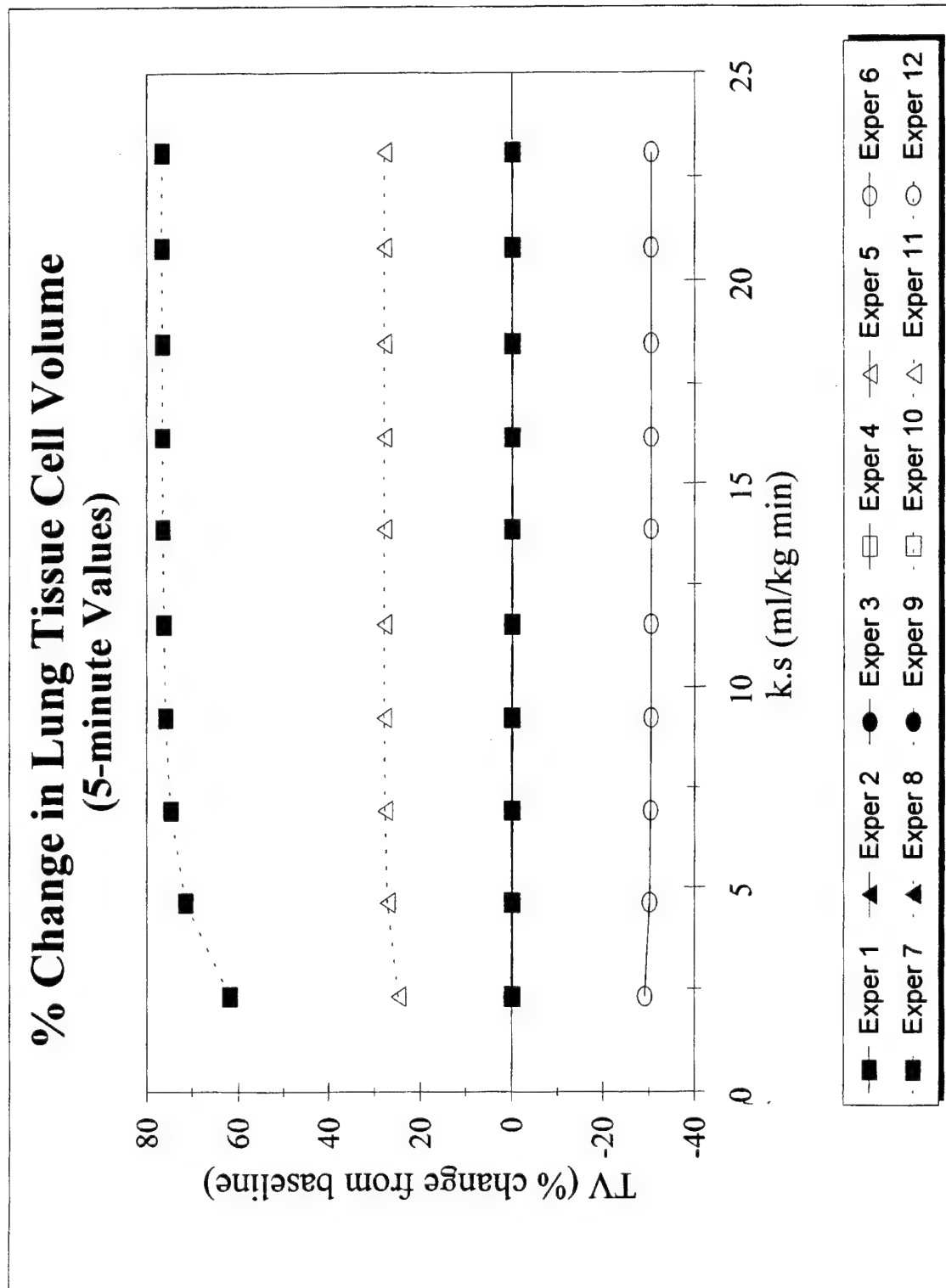


Figure C26

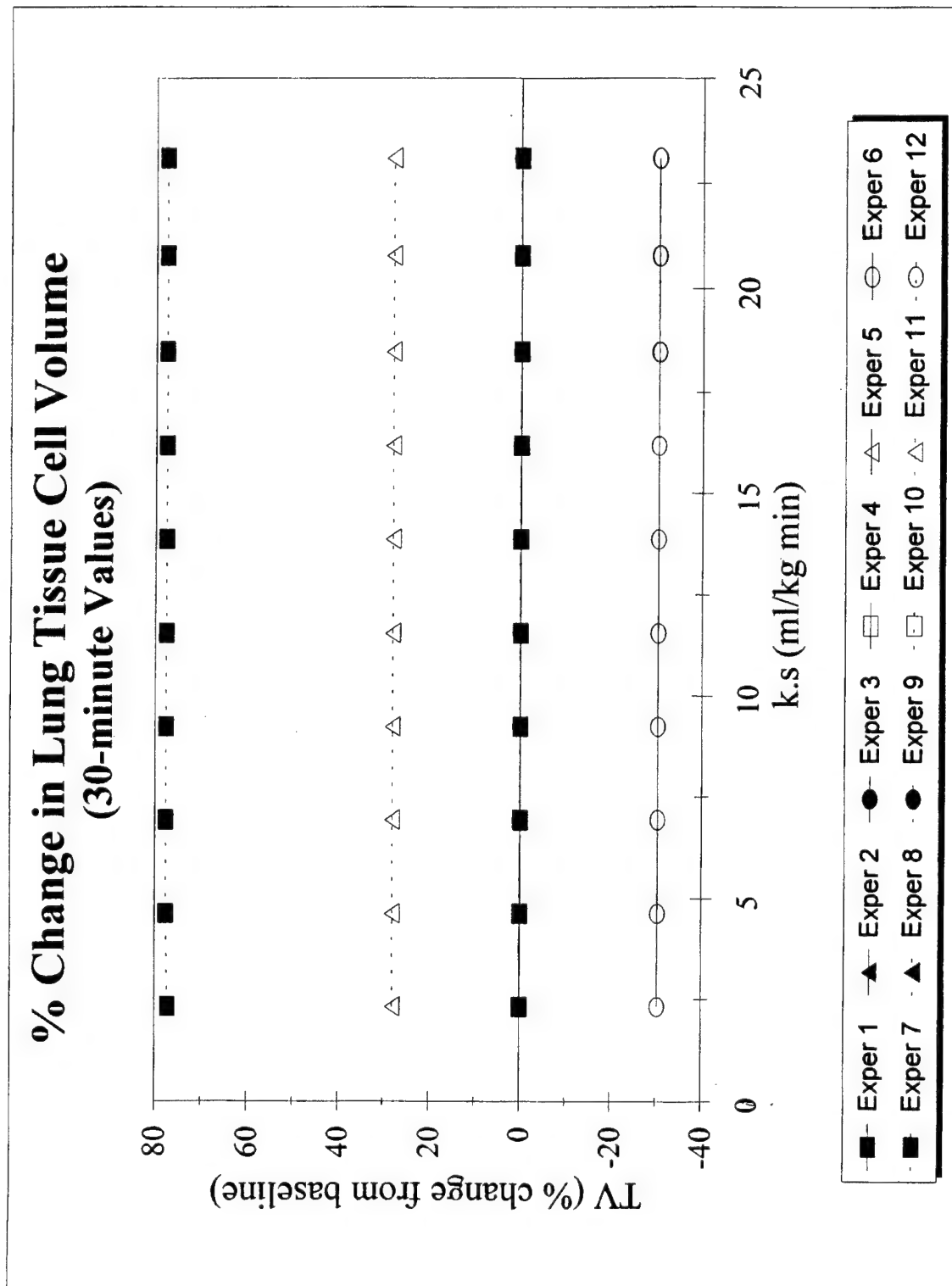


Figure C27

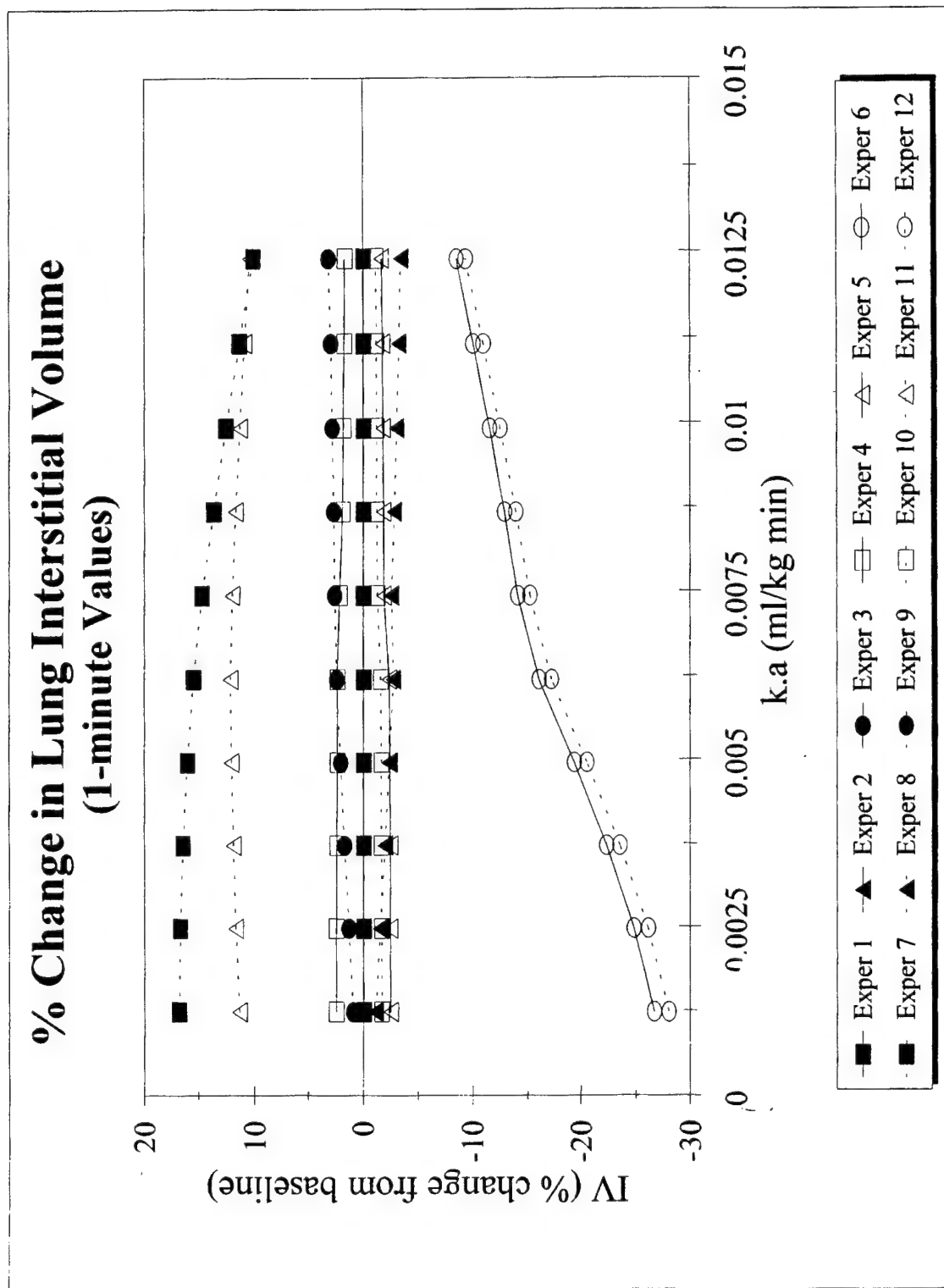


Figure C28

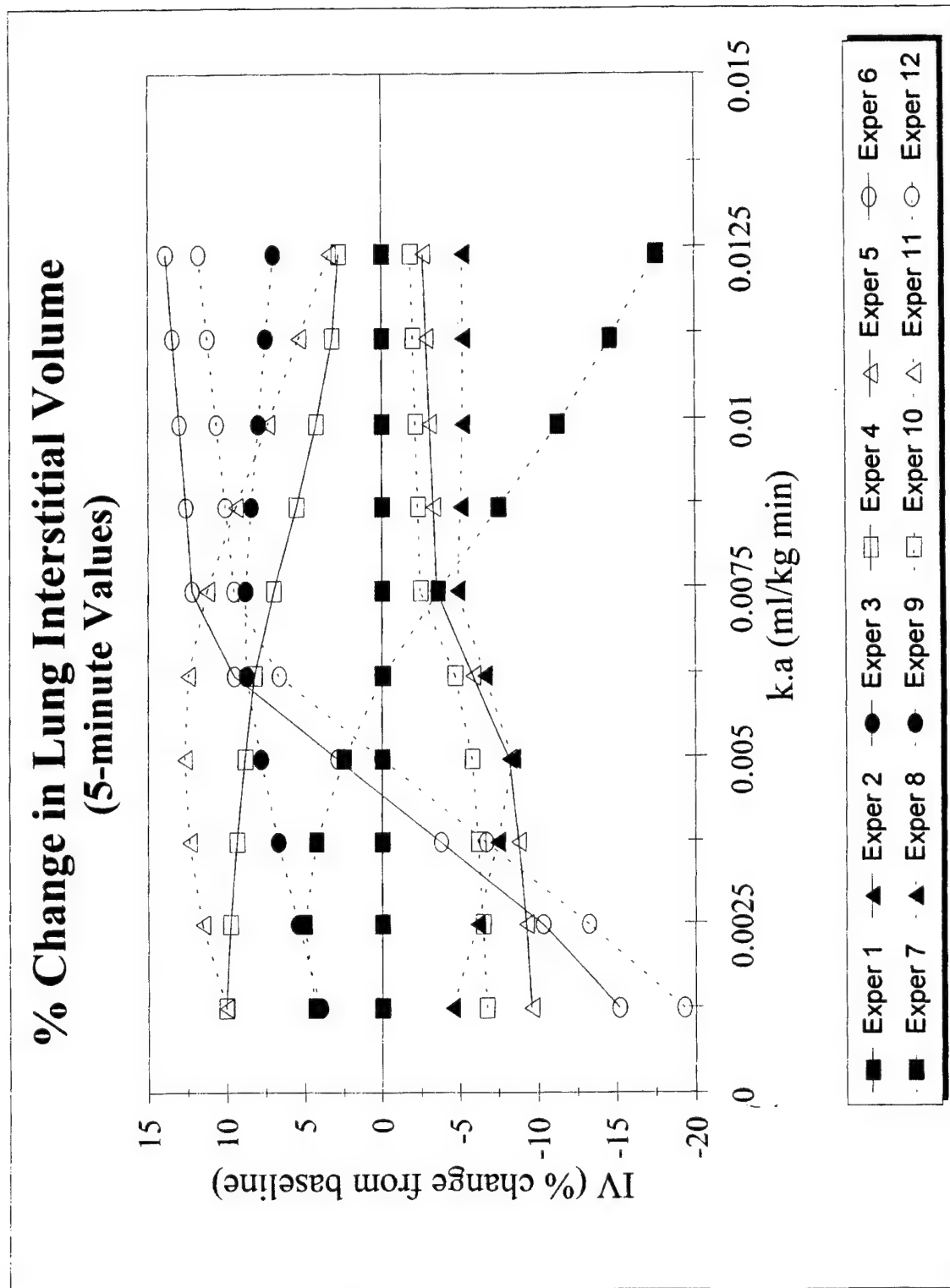


Figure C29

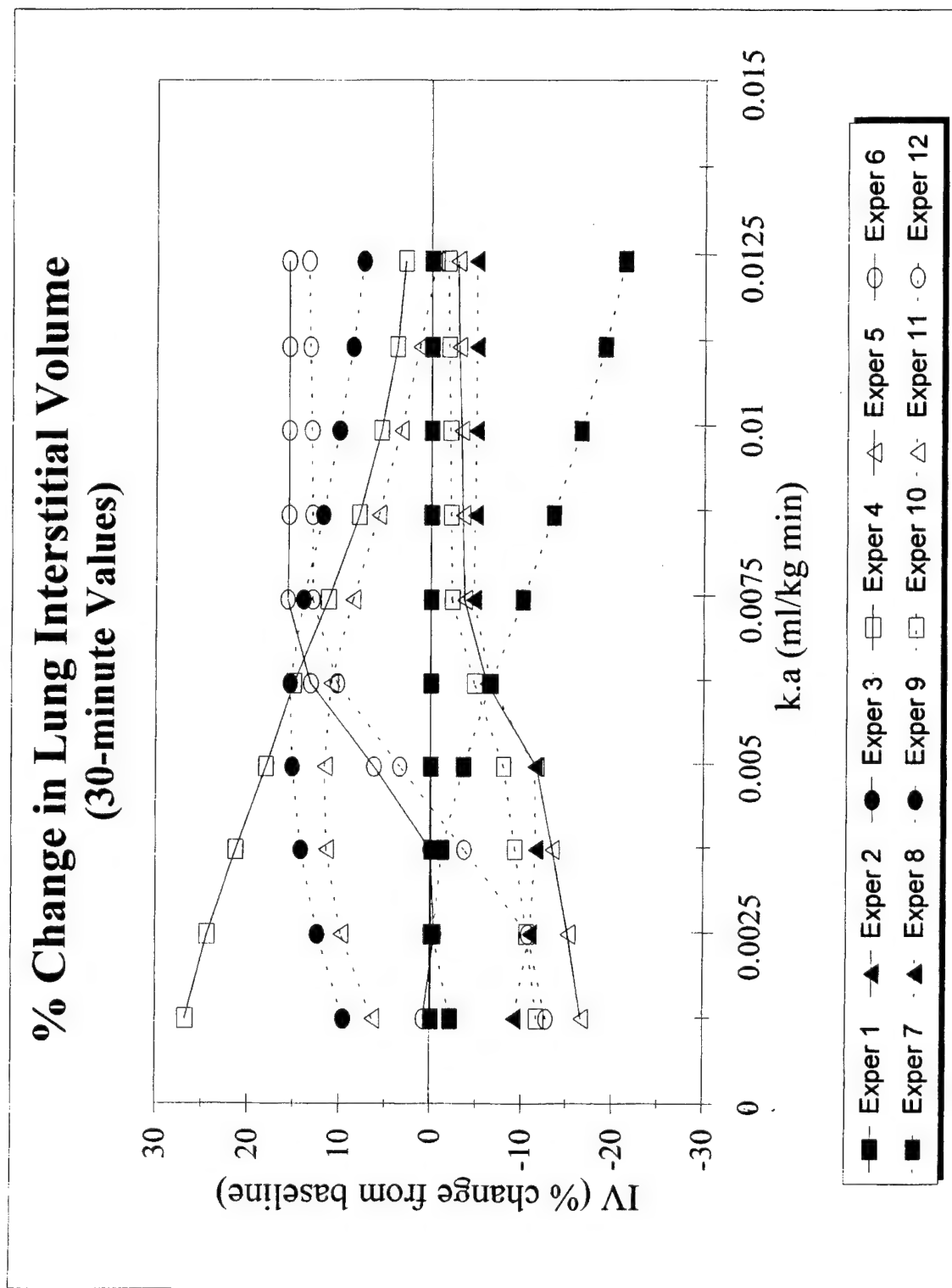


Figure C30

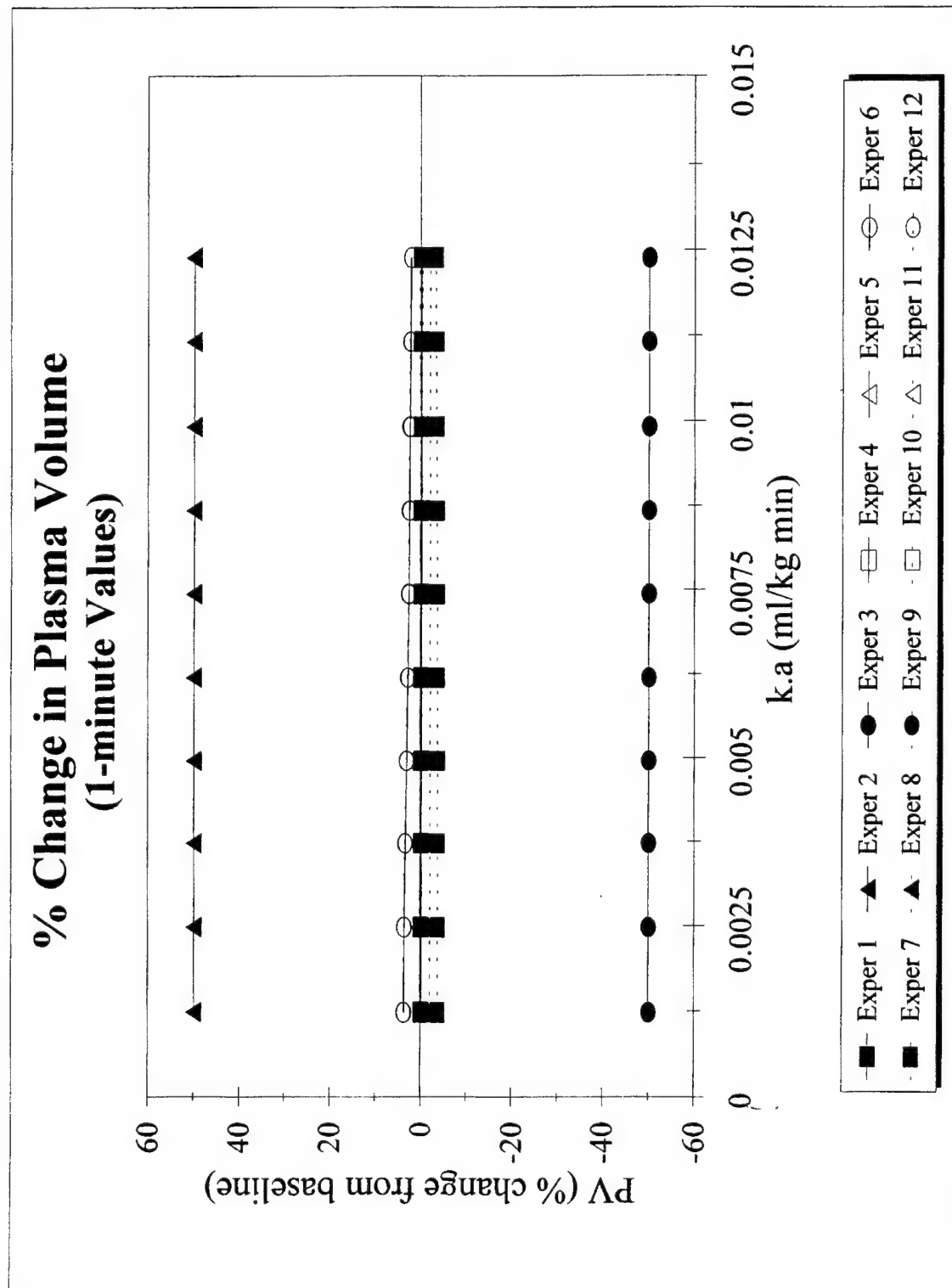


Figure C31

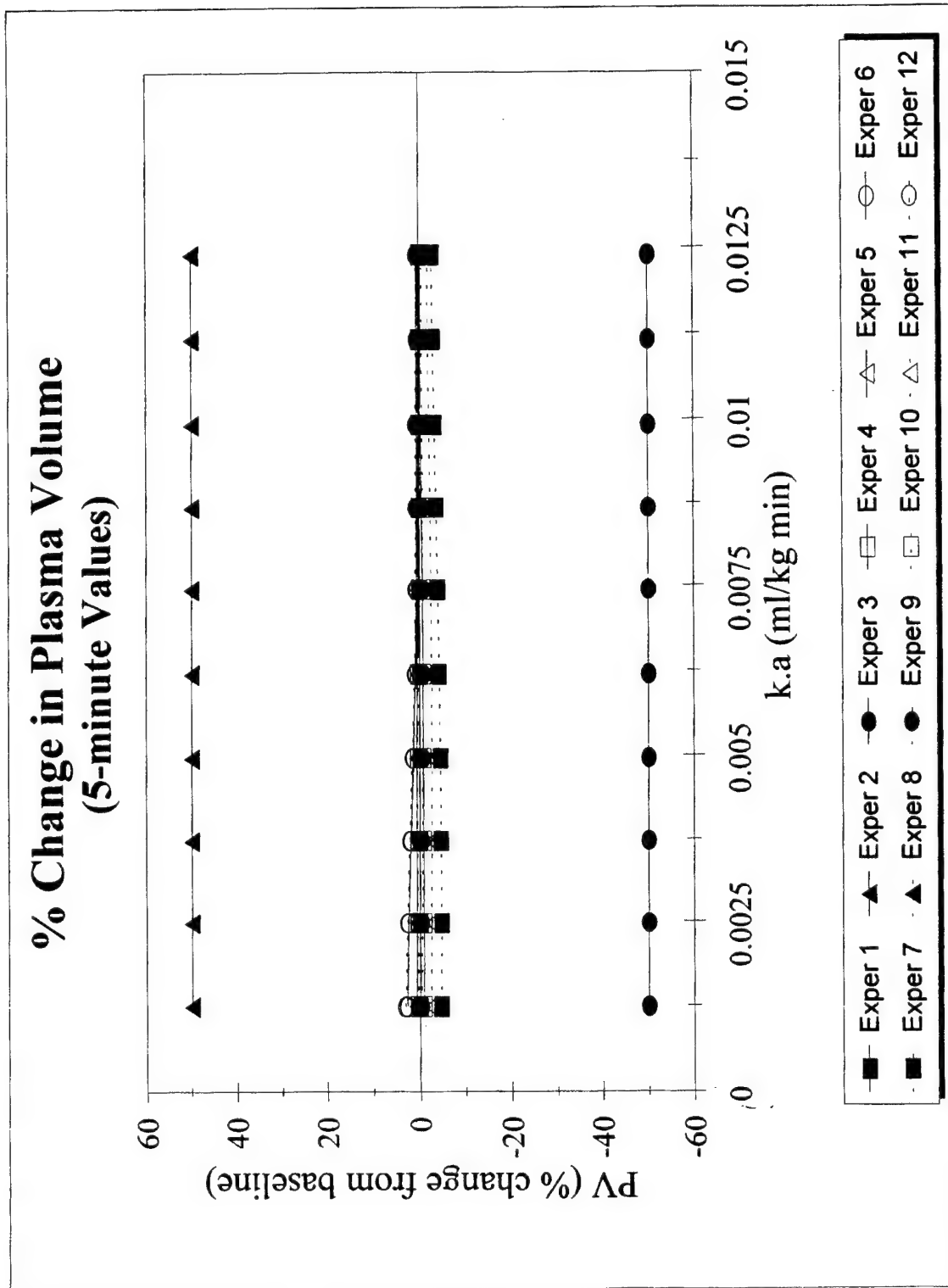


Figure C32

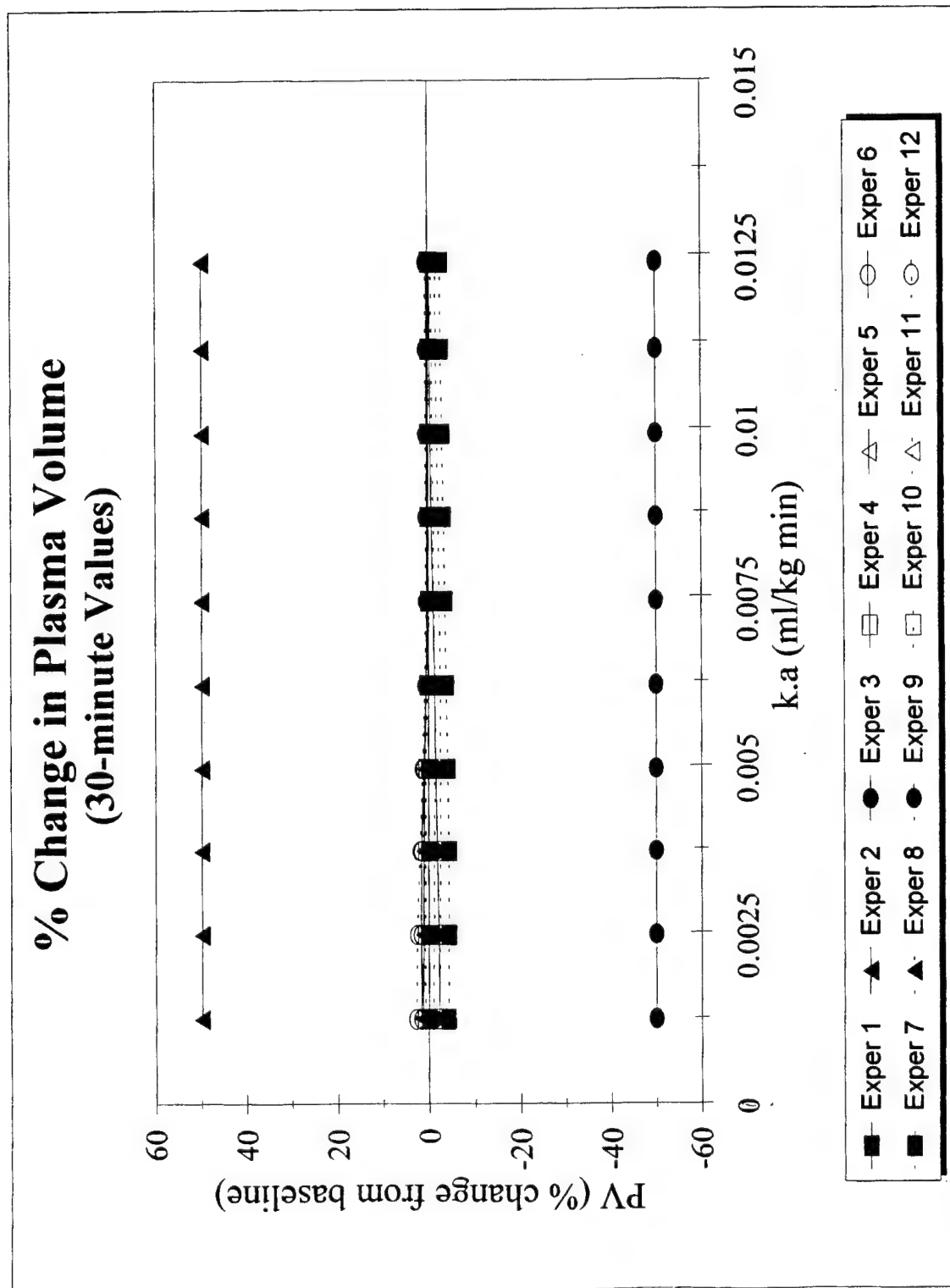


Figure C33

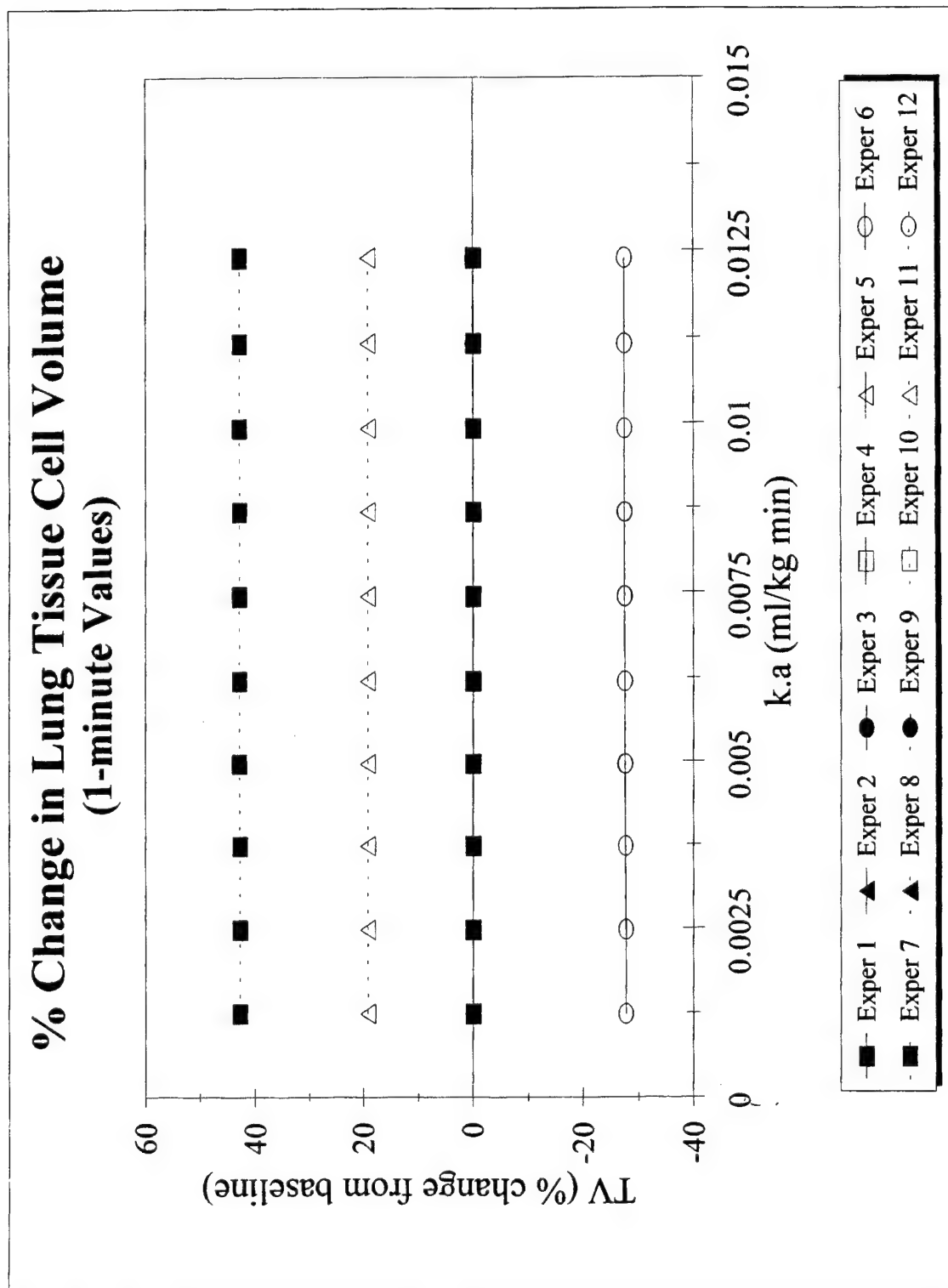


Figure C34

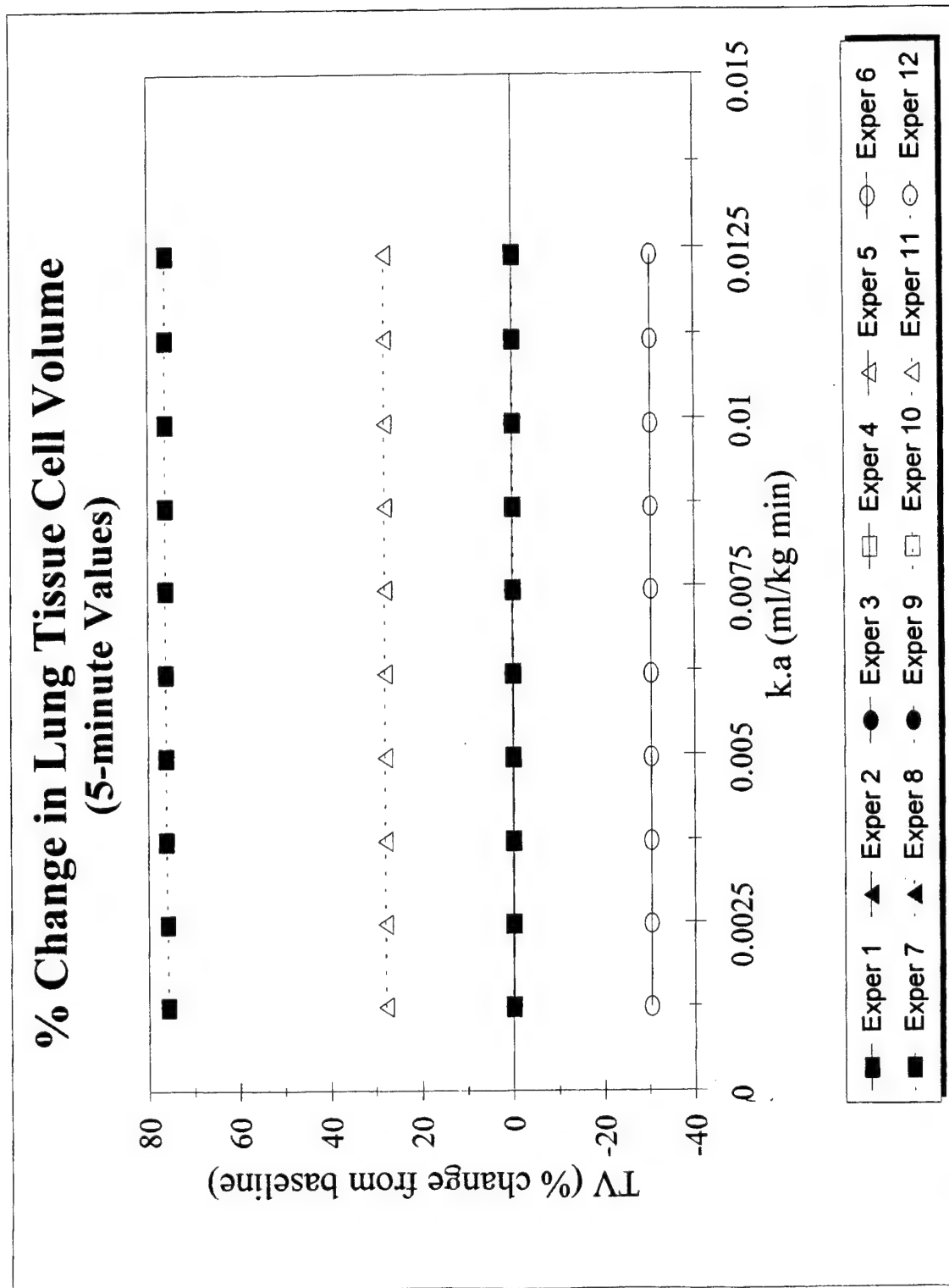


Figure C35

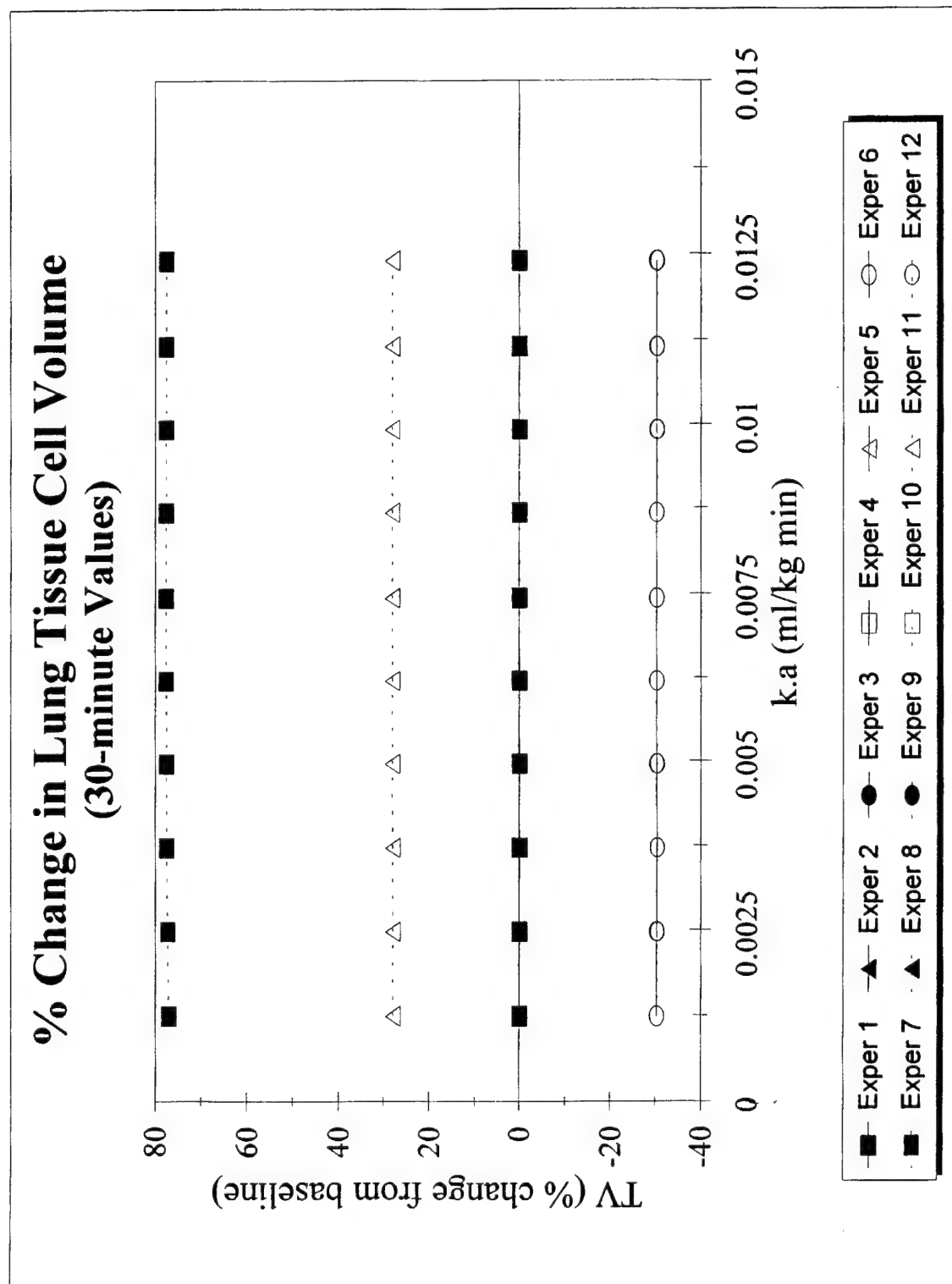


Figure C36

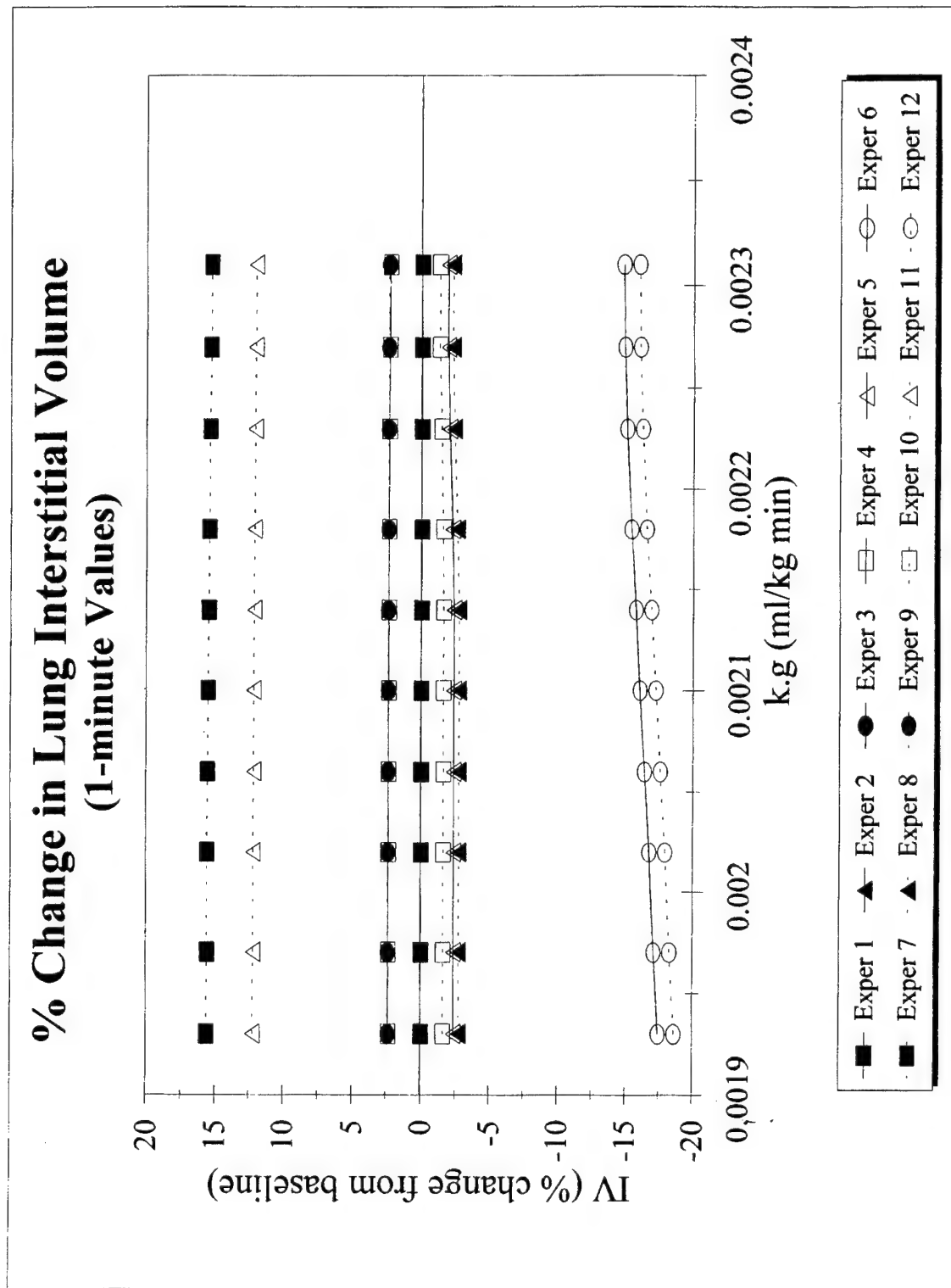


Figure C37

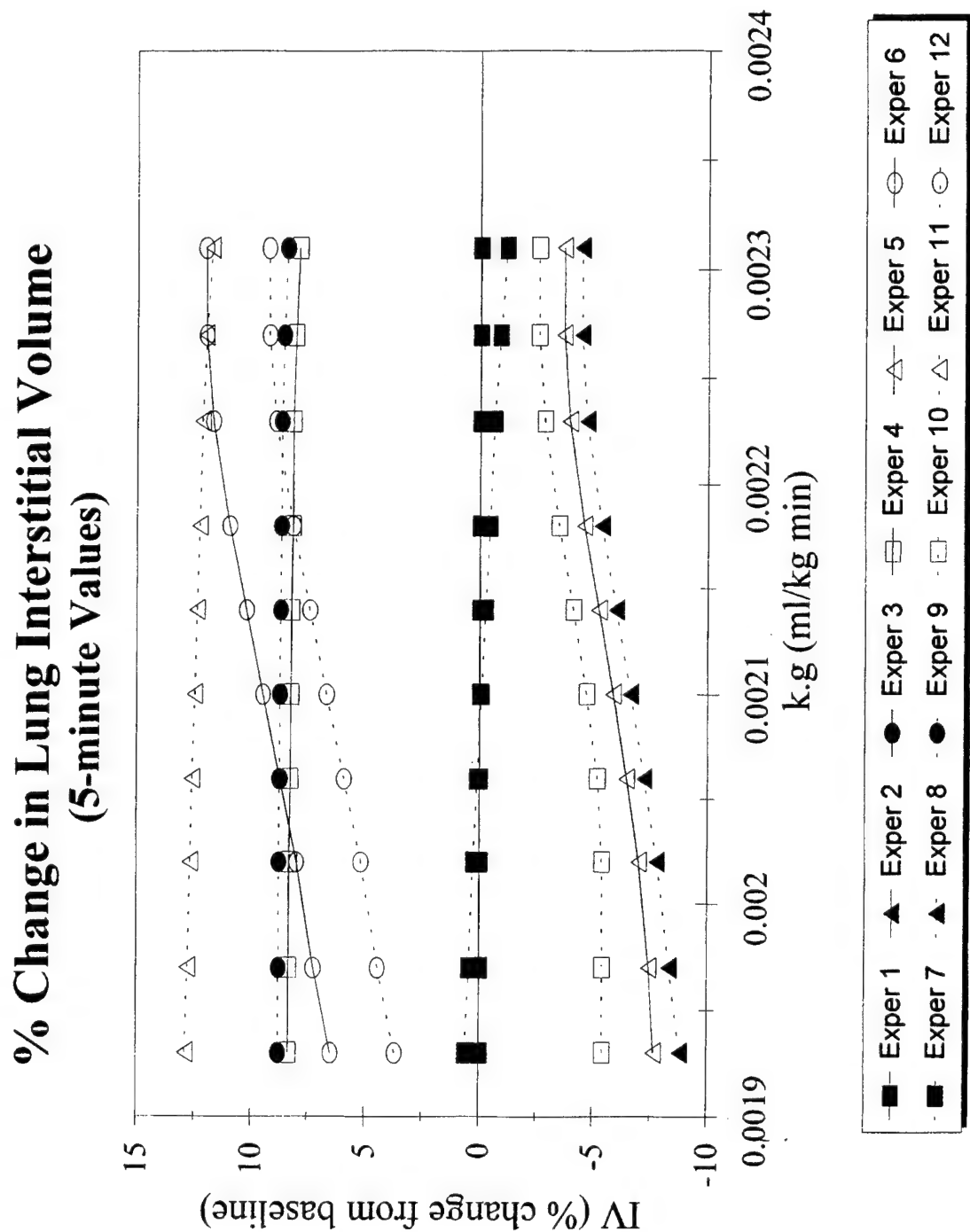


Figure C38

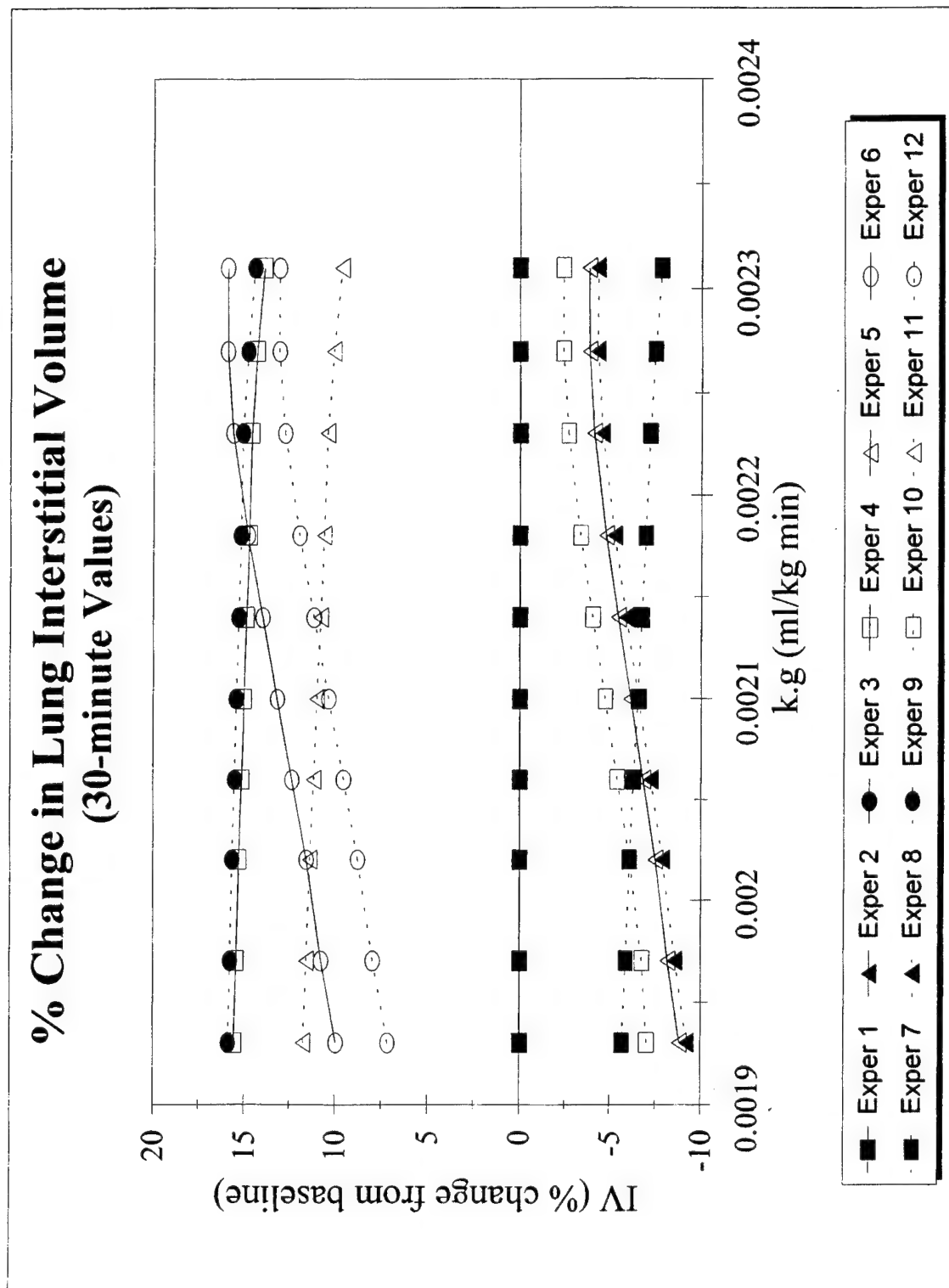


Figure C39

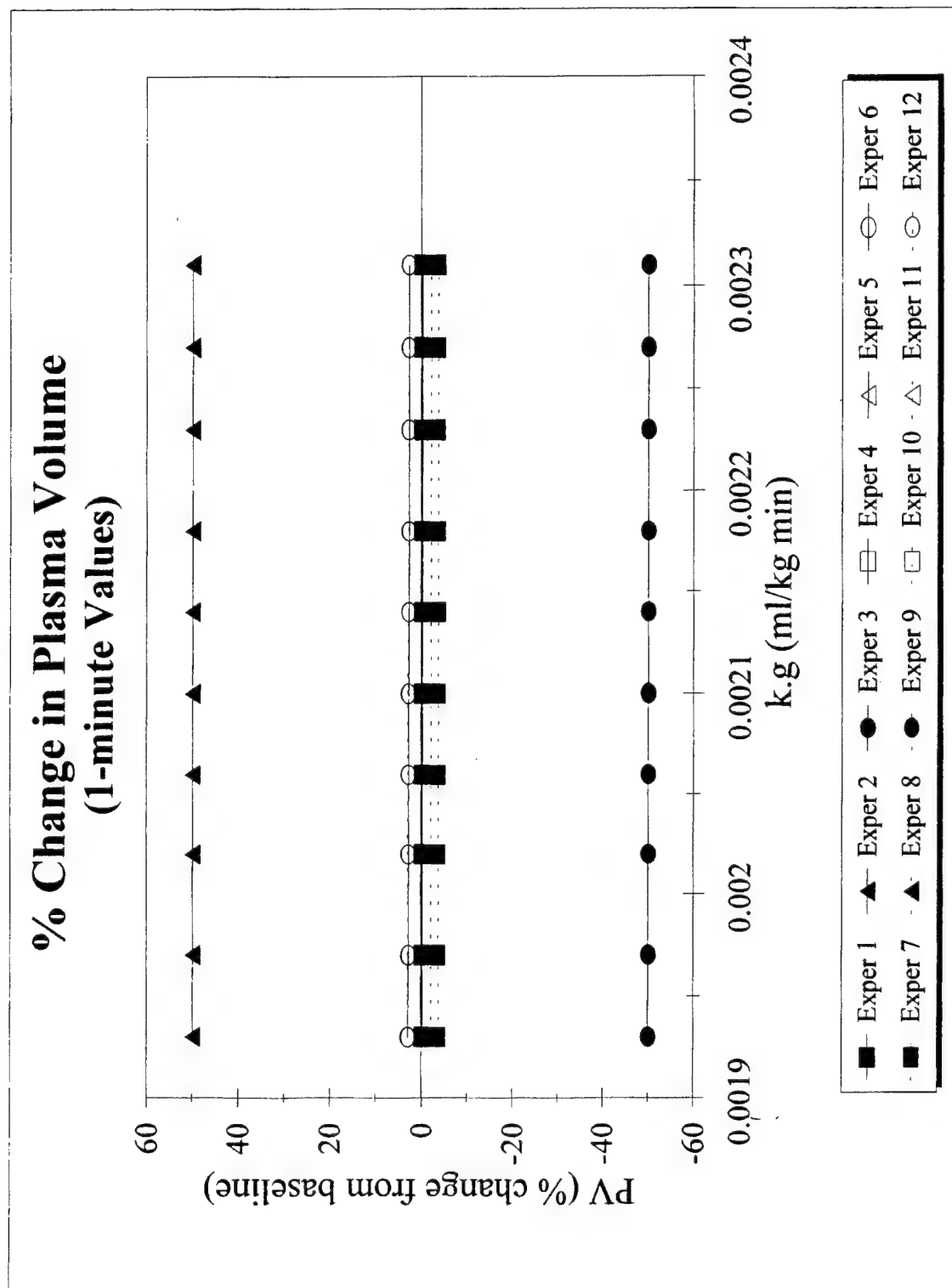


Figure C40

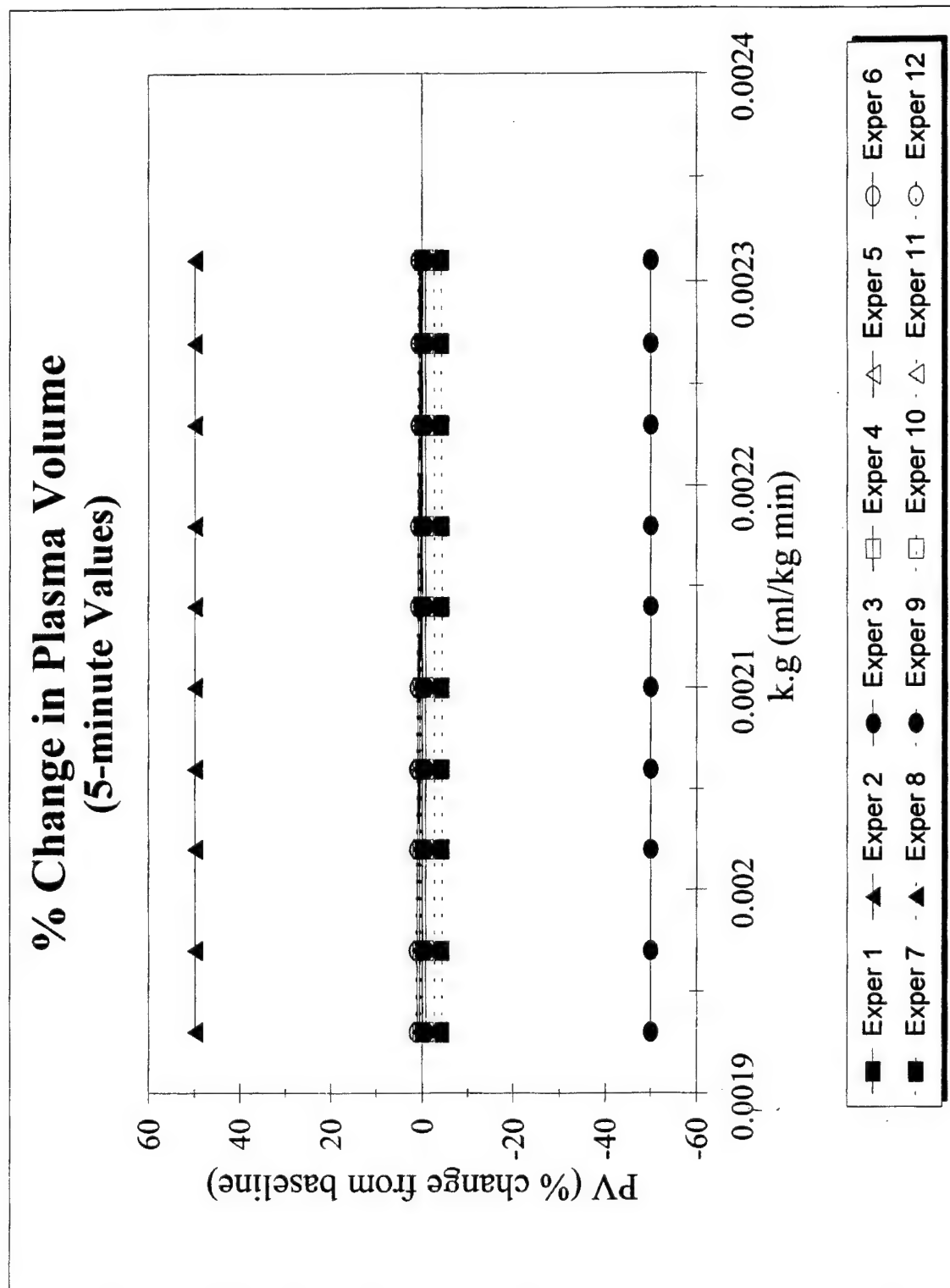


Figure C41

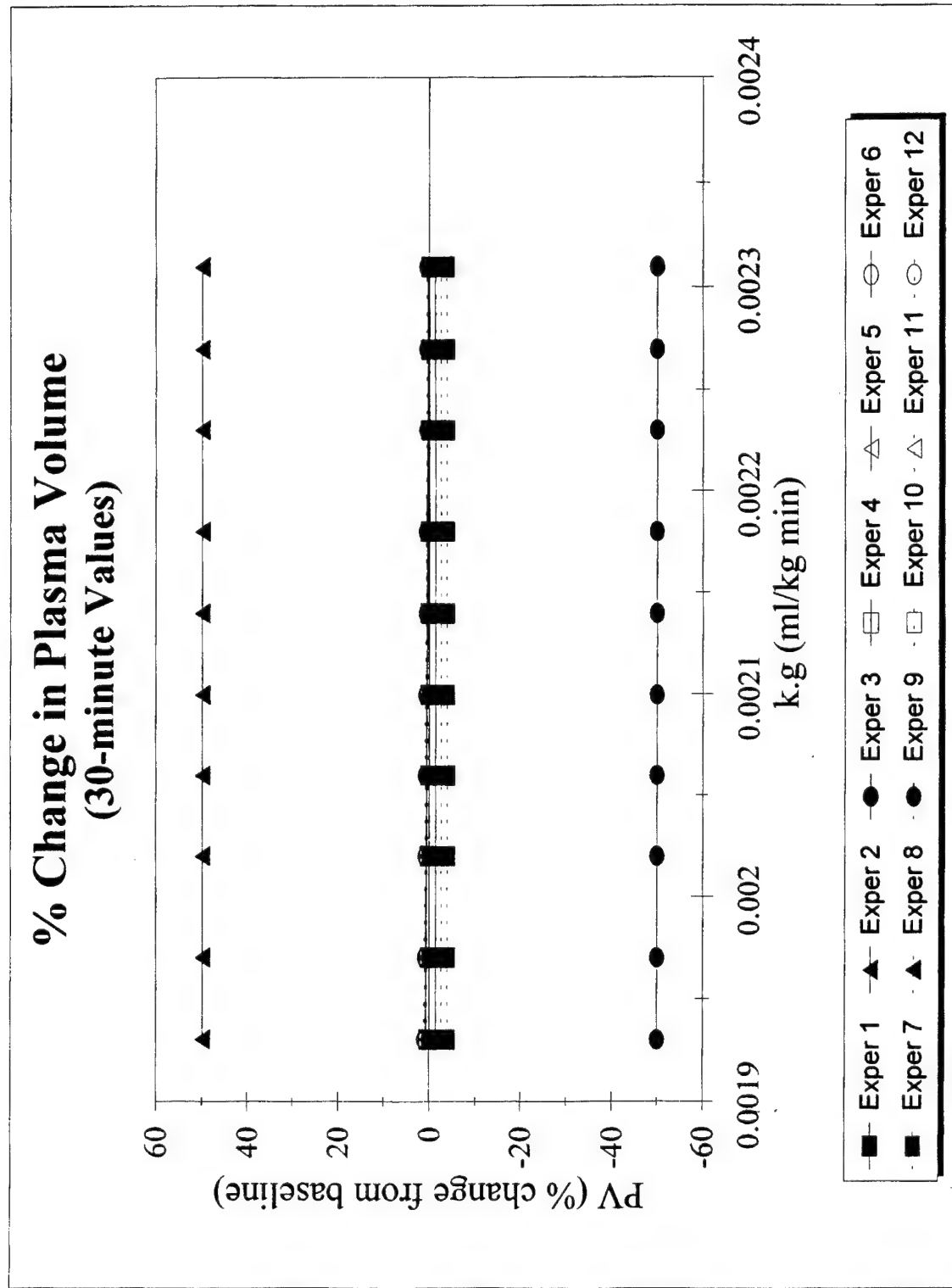


Figure C42

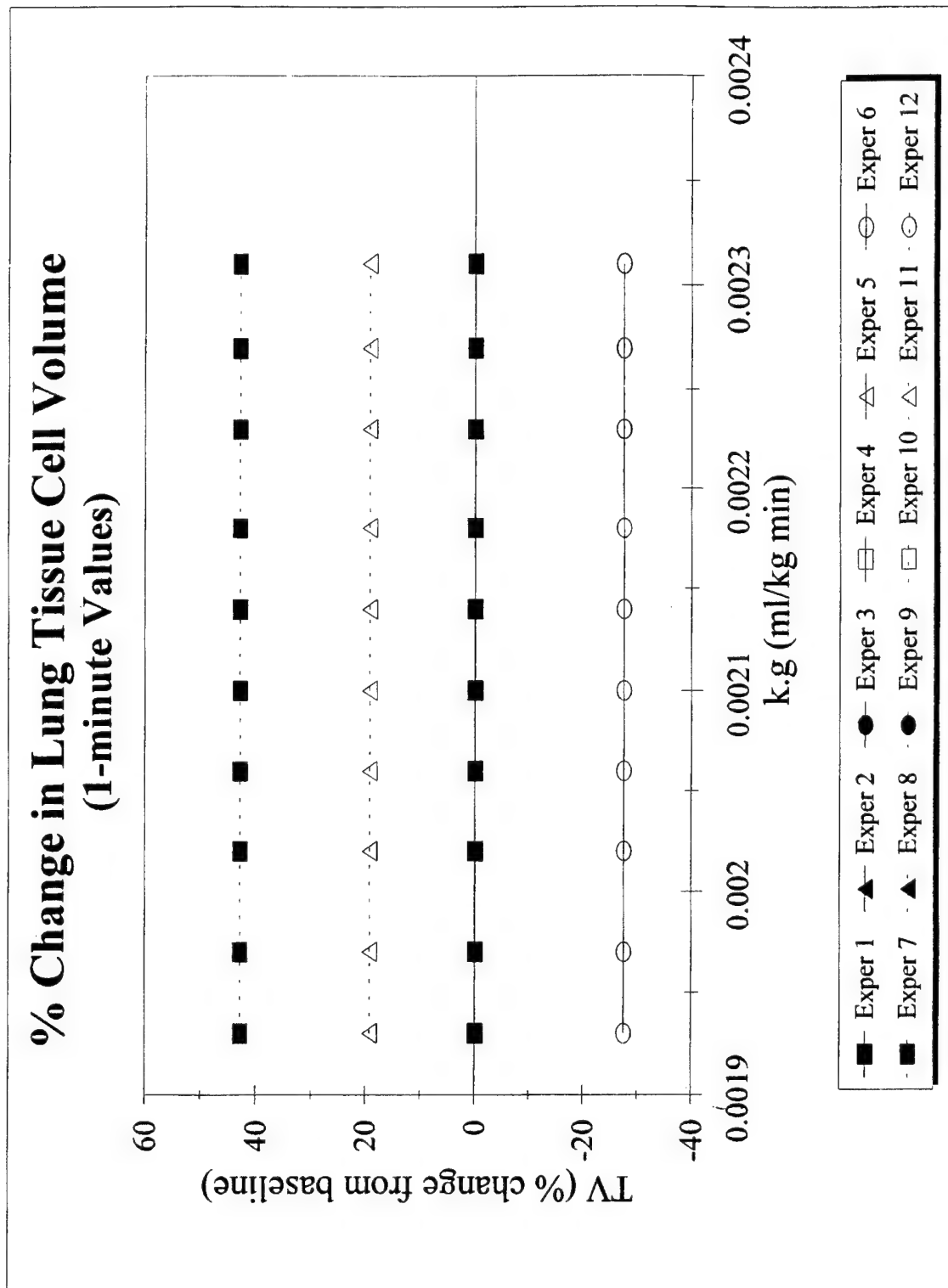


Figure C43

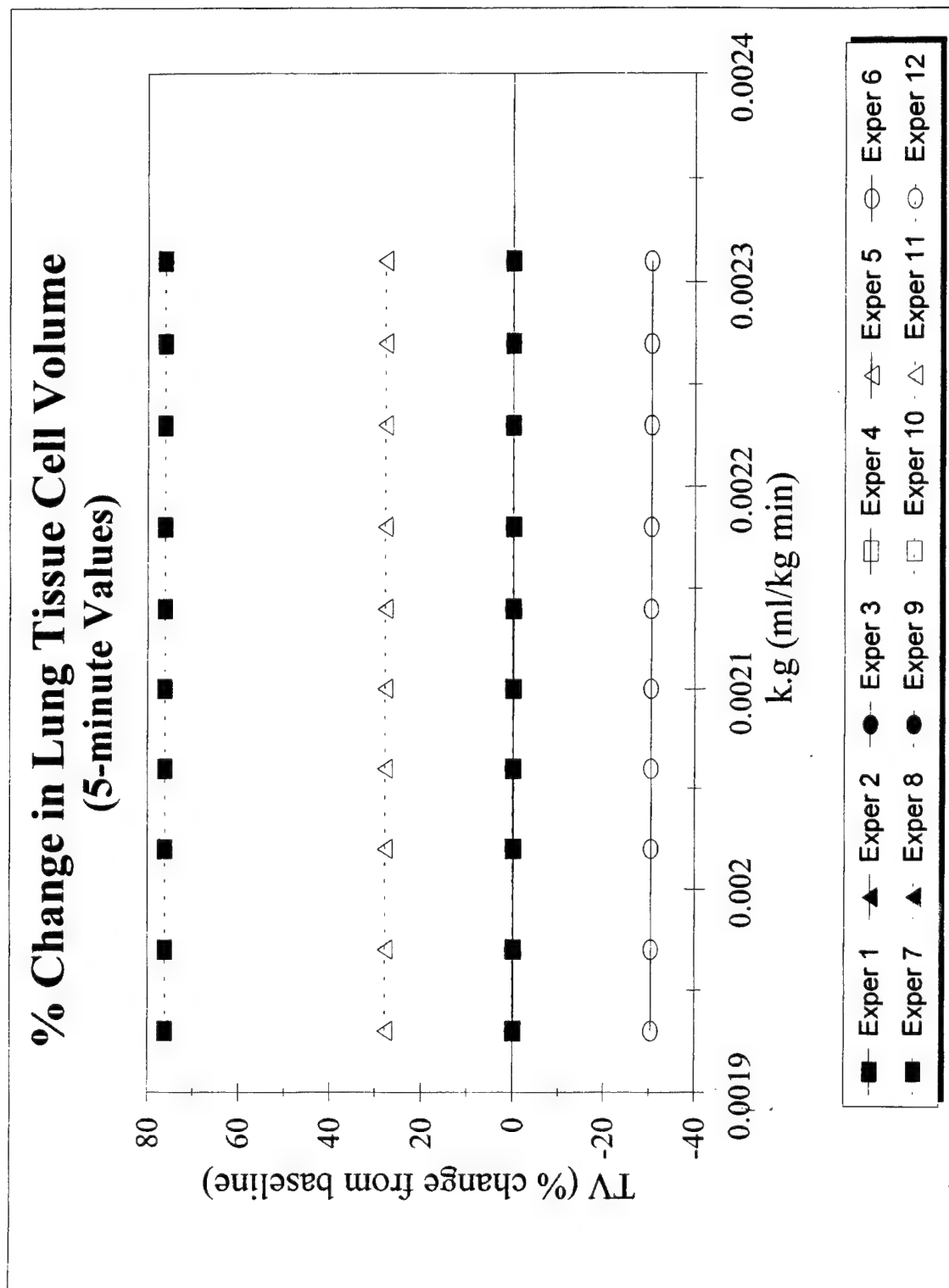


Figure C44

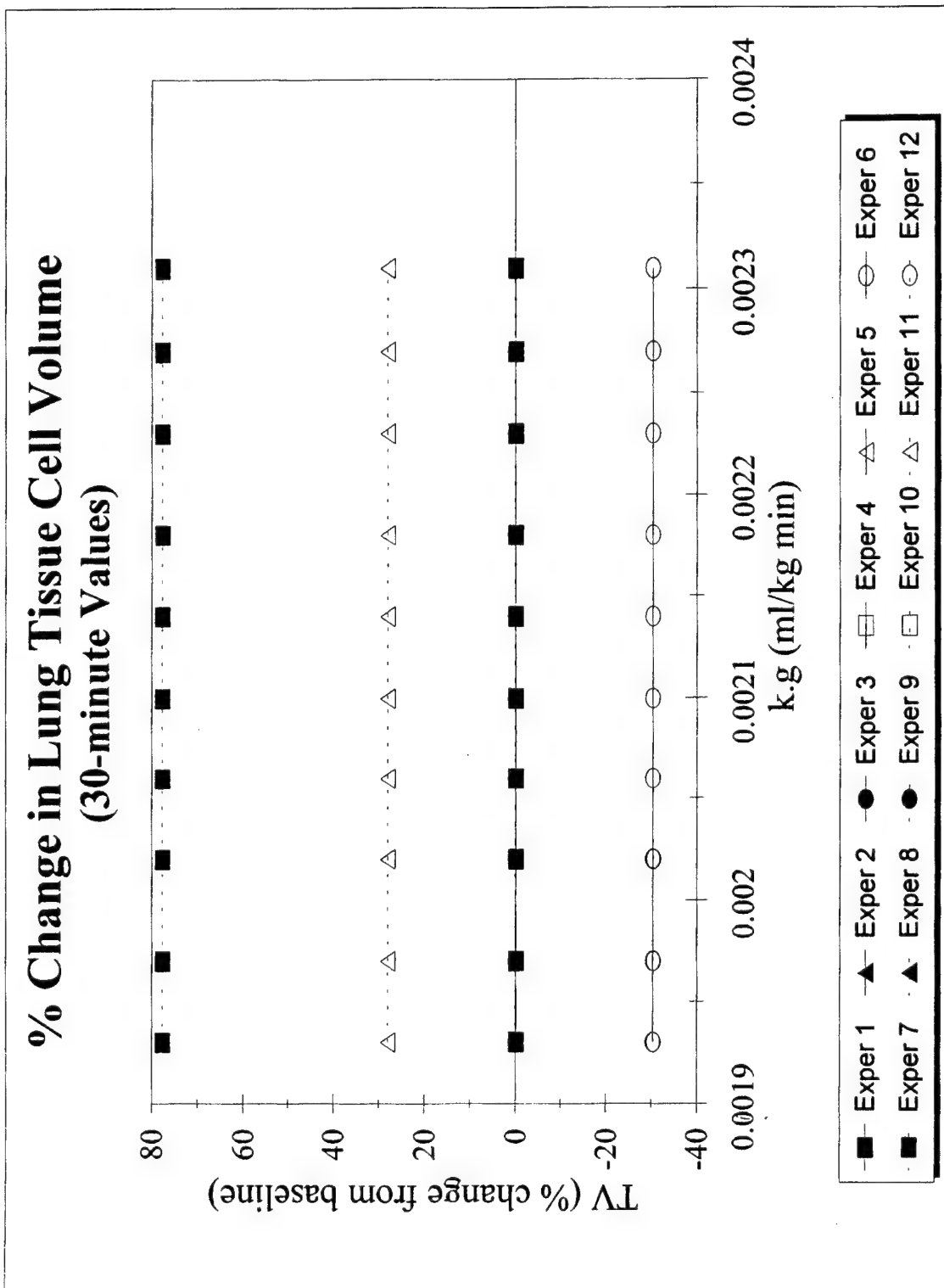


Figure C45

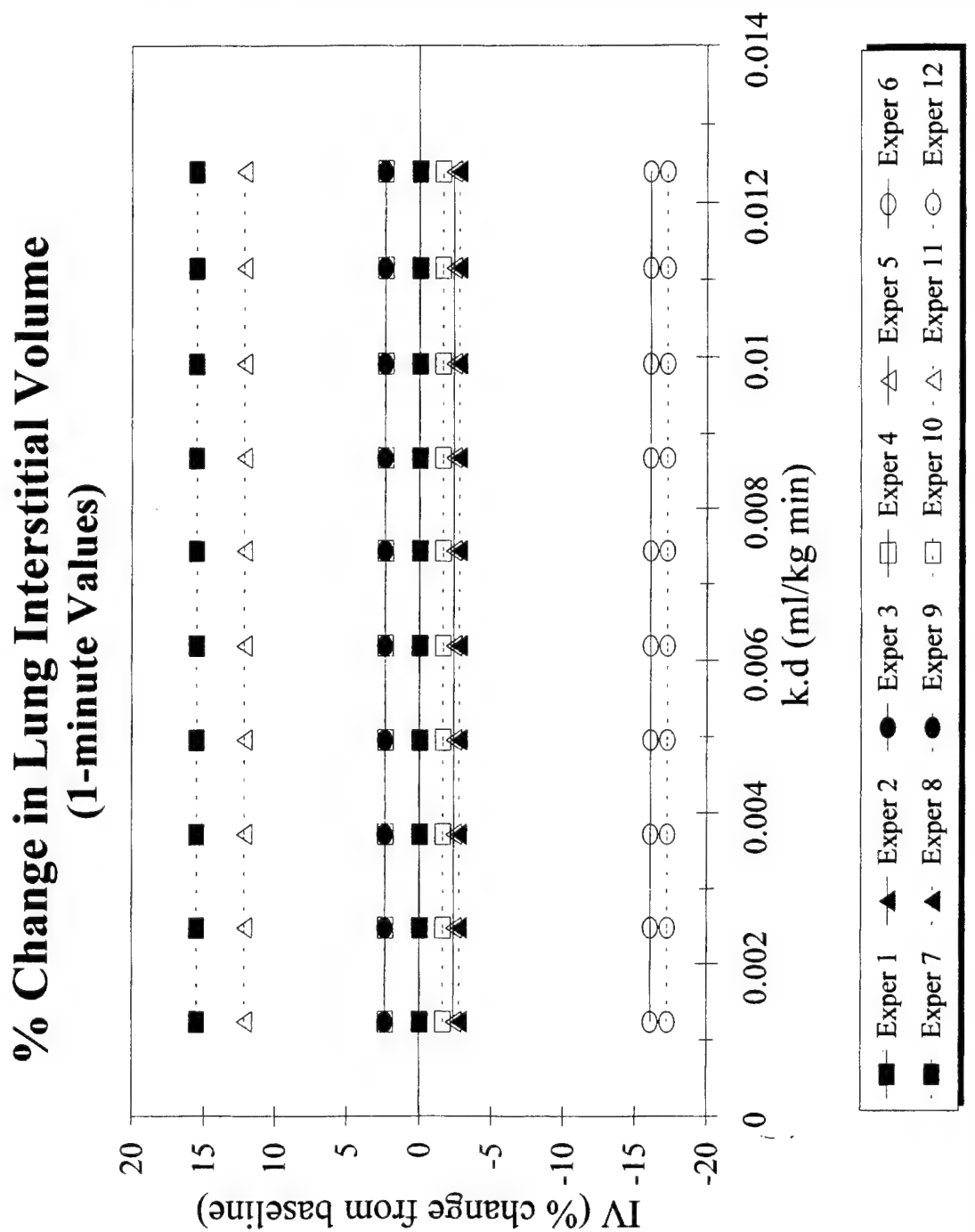


Figure C46

% Change in Lung Interstitial Volume (5-minute Values)

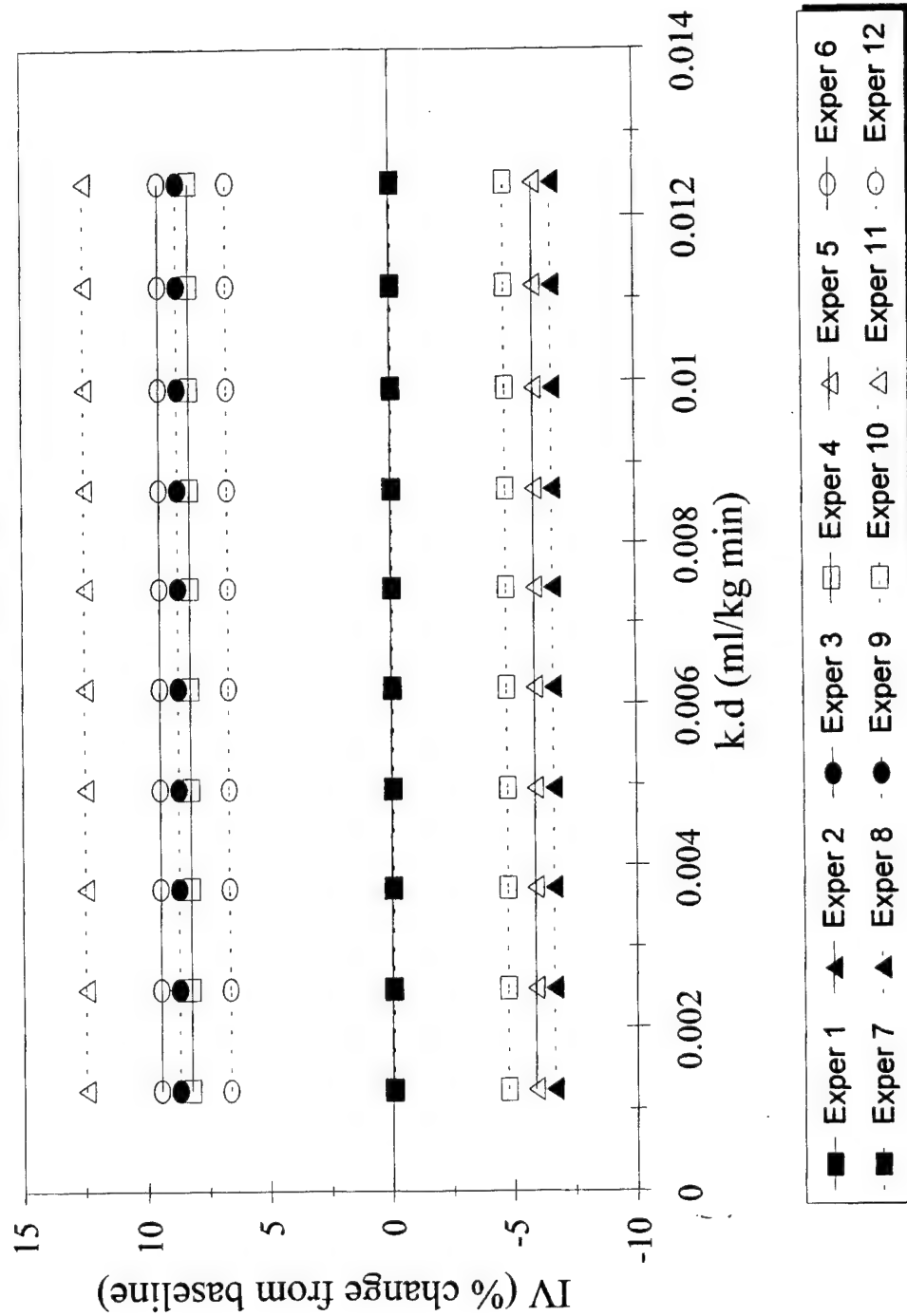


Figure C47

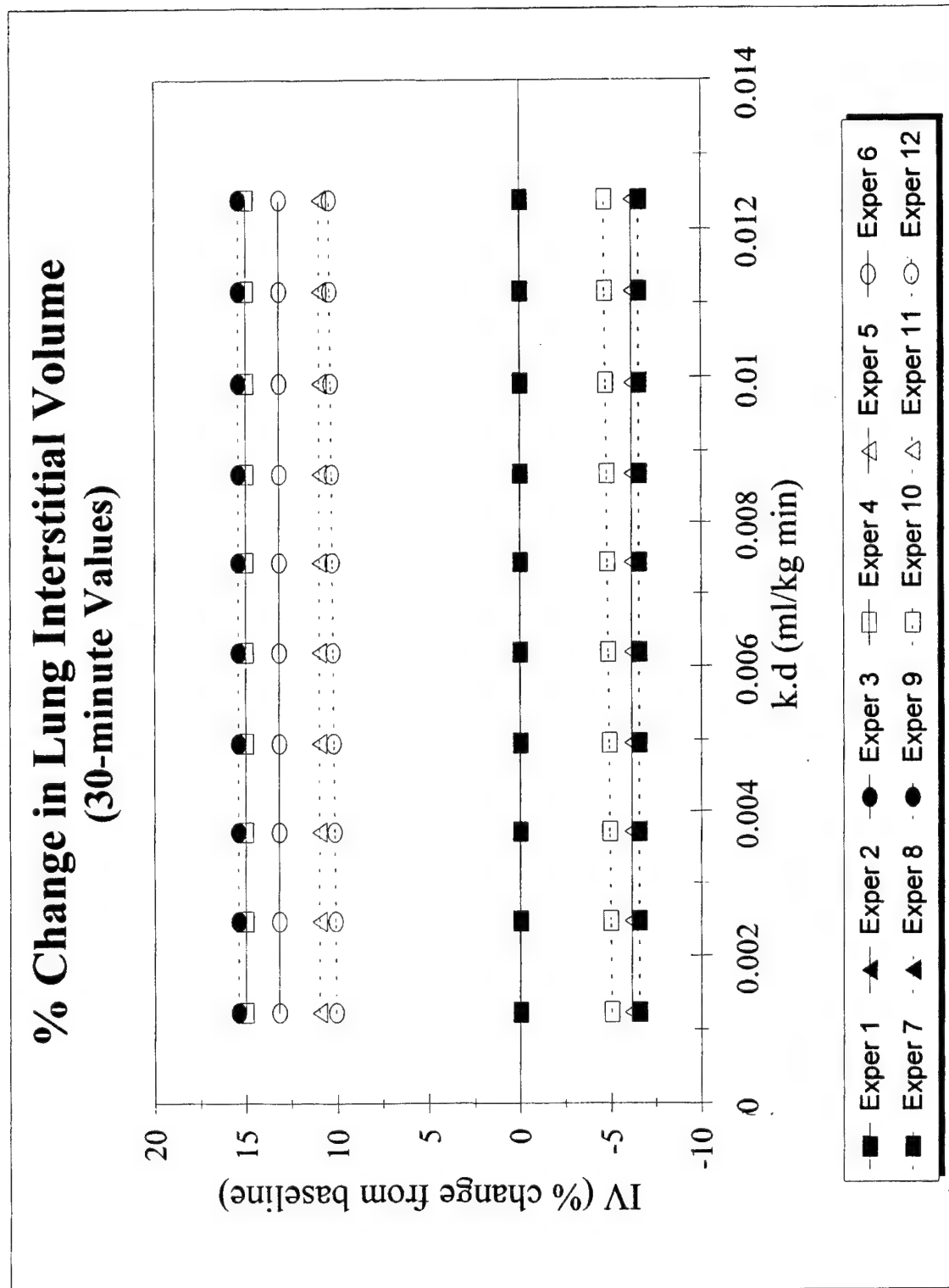


Figure C48

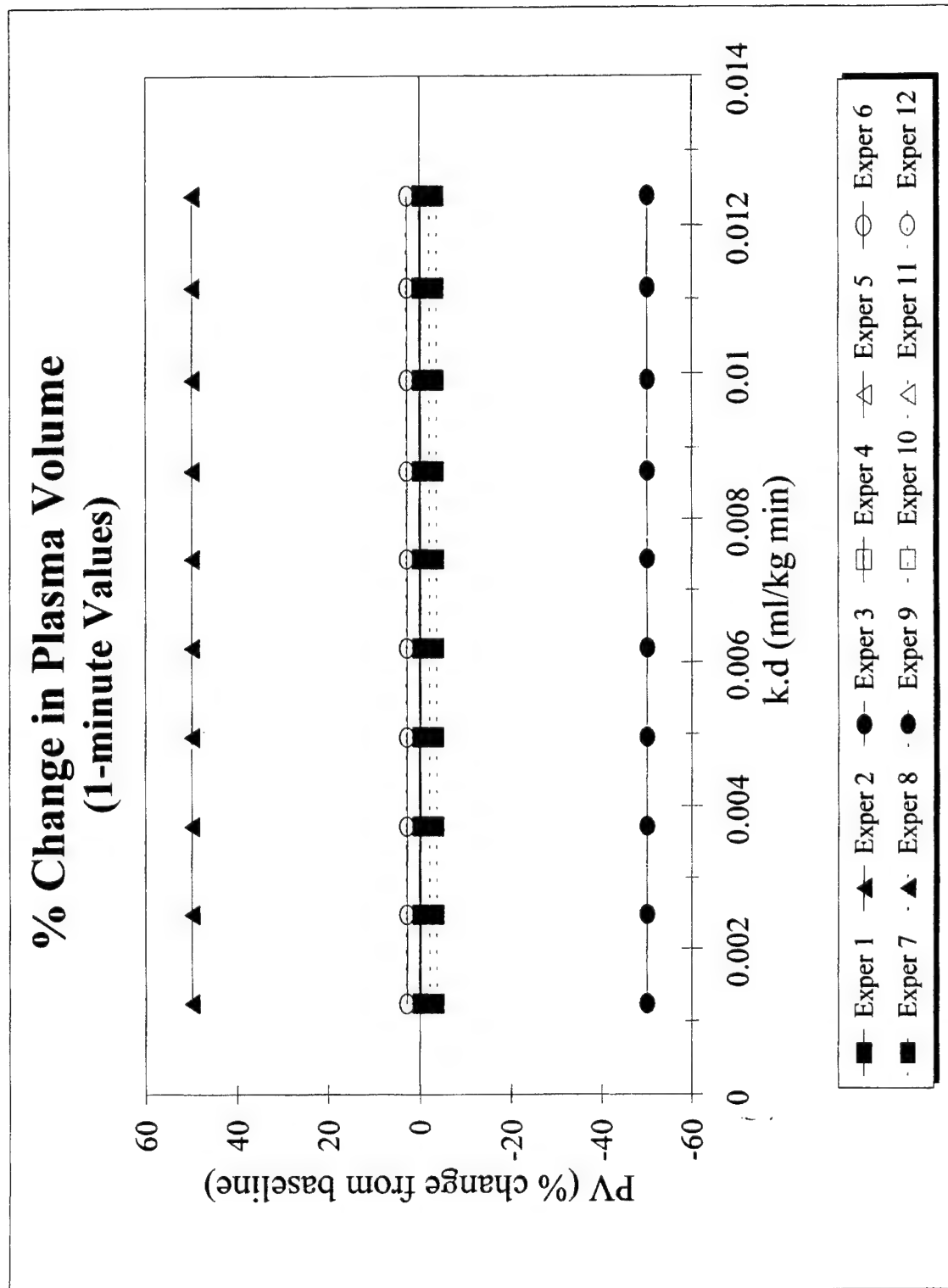


Figure C49

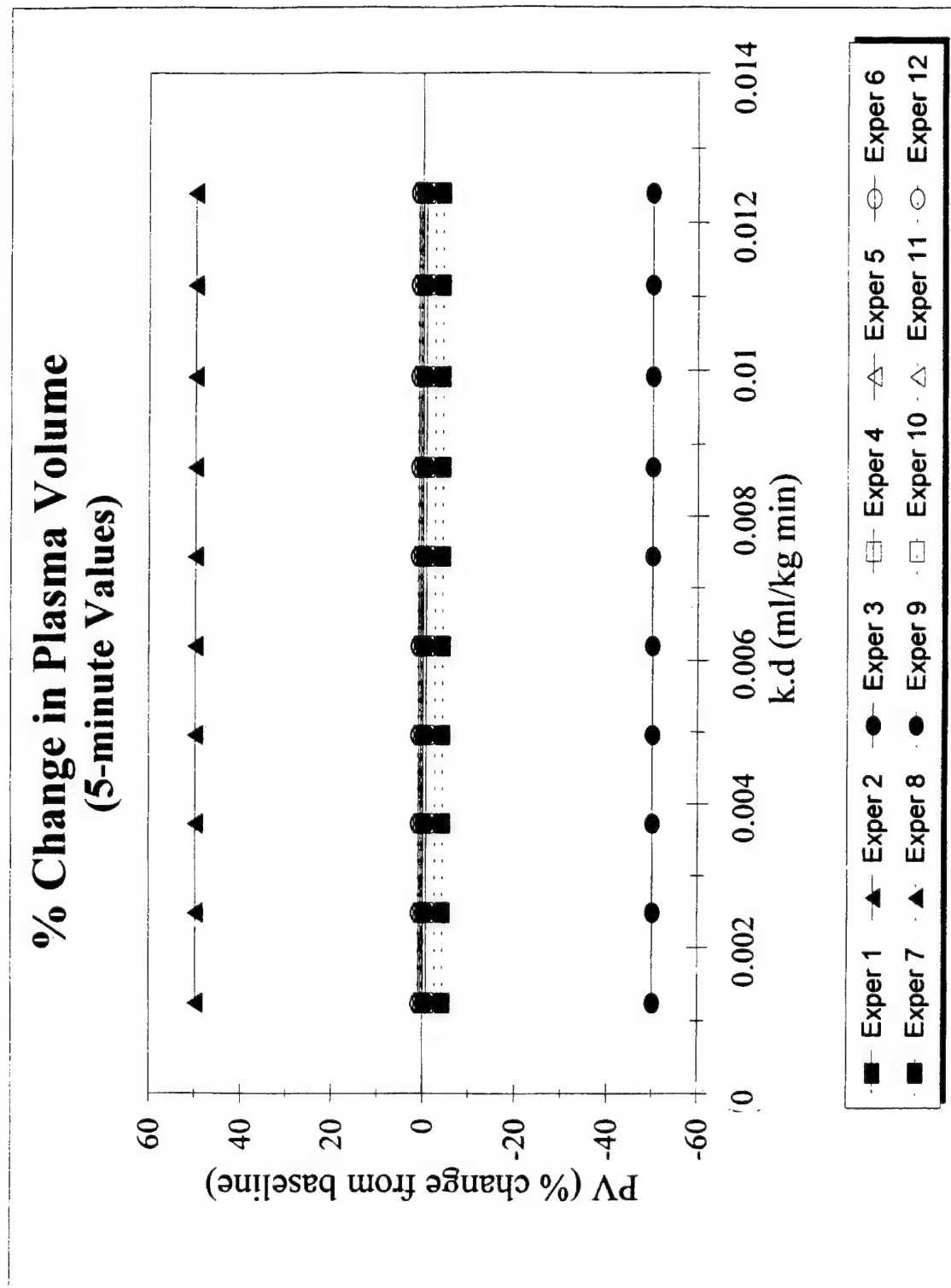


Figure C50

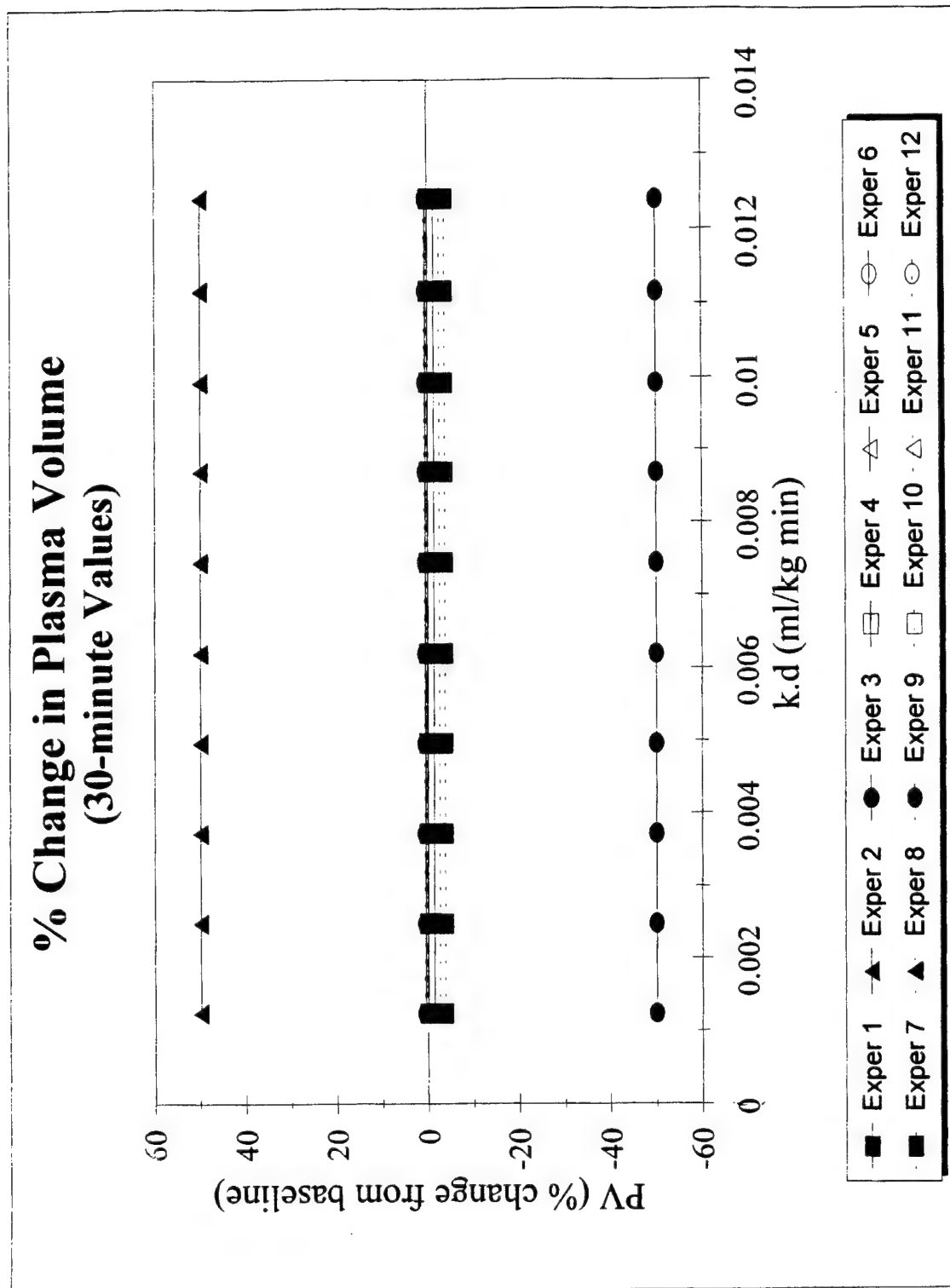


Figure C51

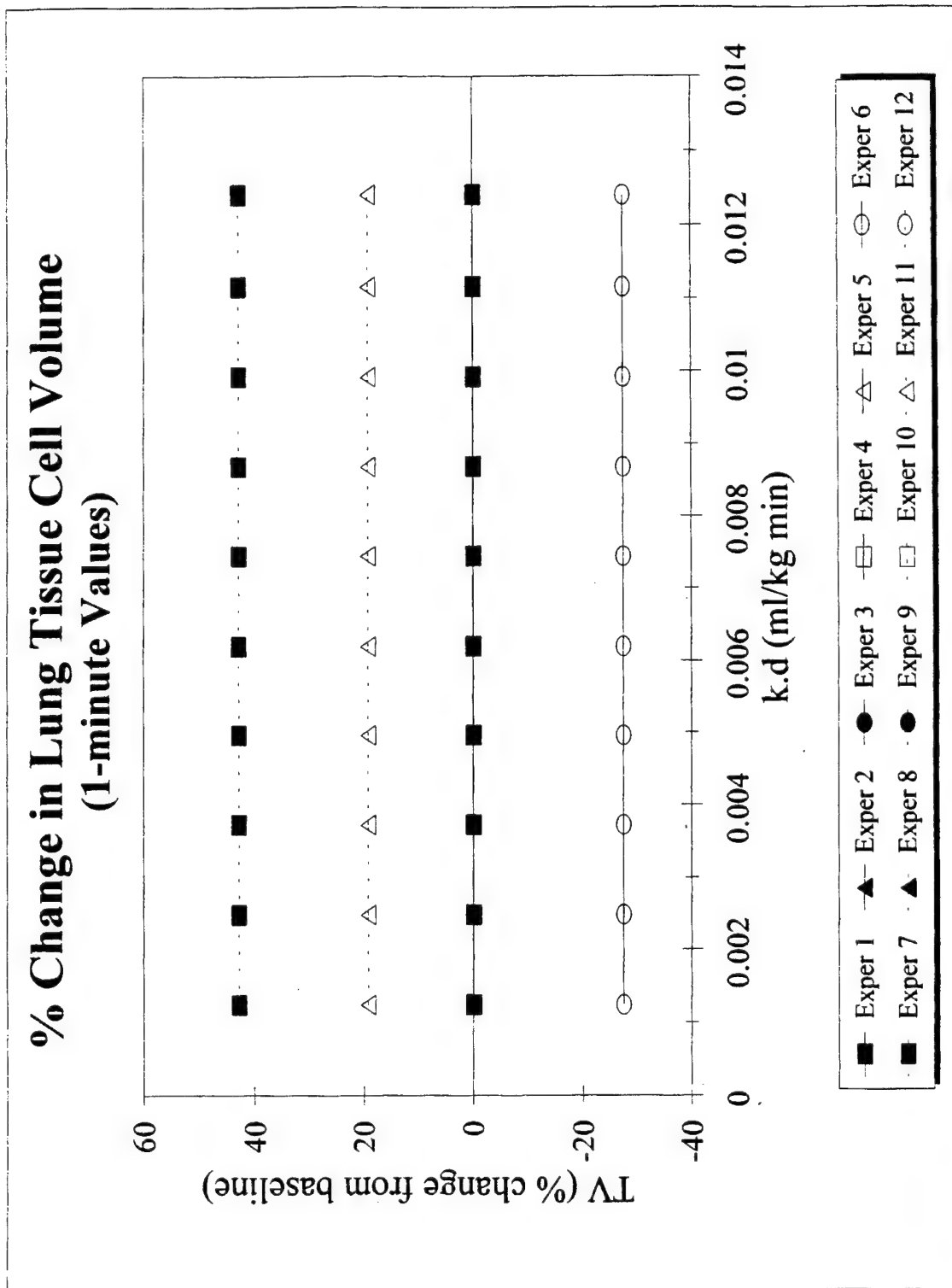


Figure C52

% Change in Lung Tissue Cell Volume (5-minute Values)

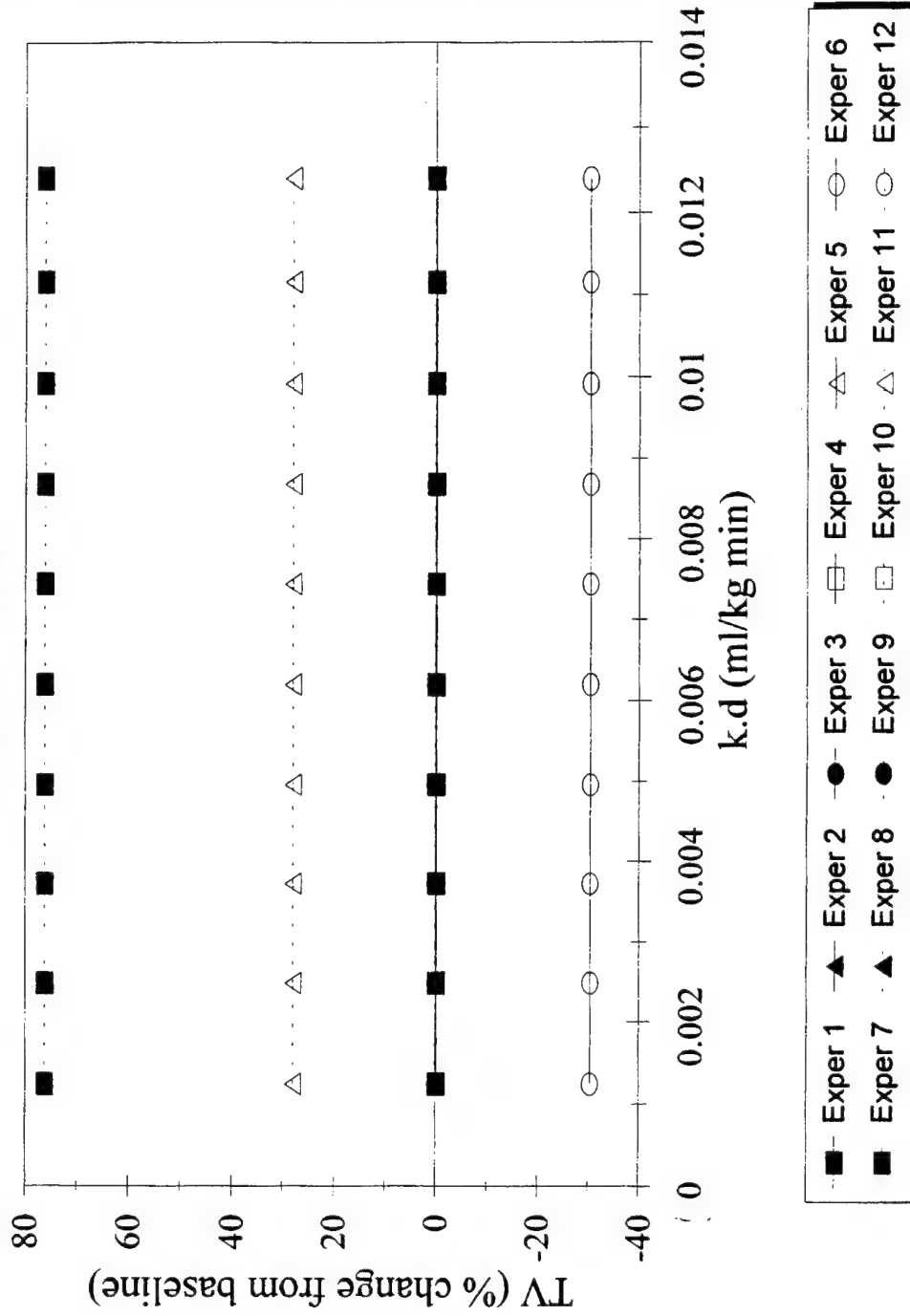


Figure C53

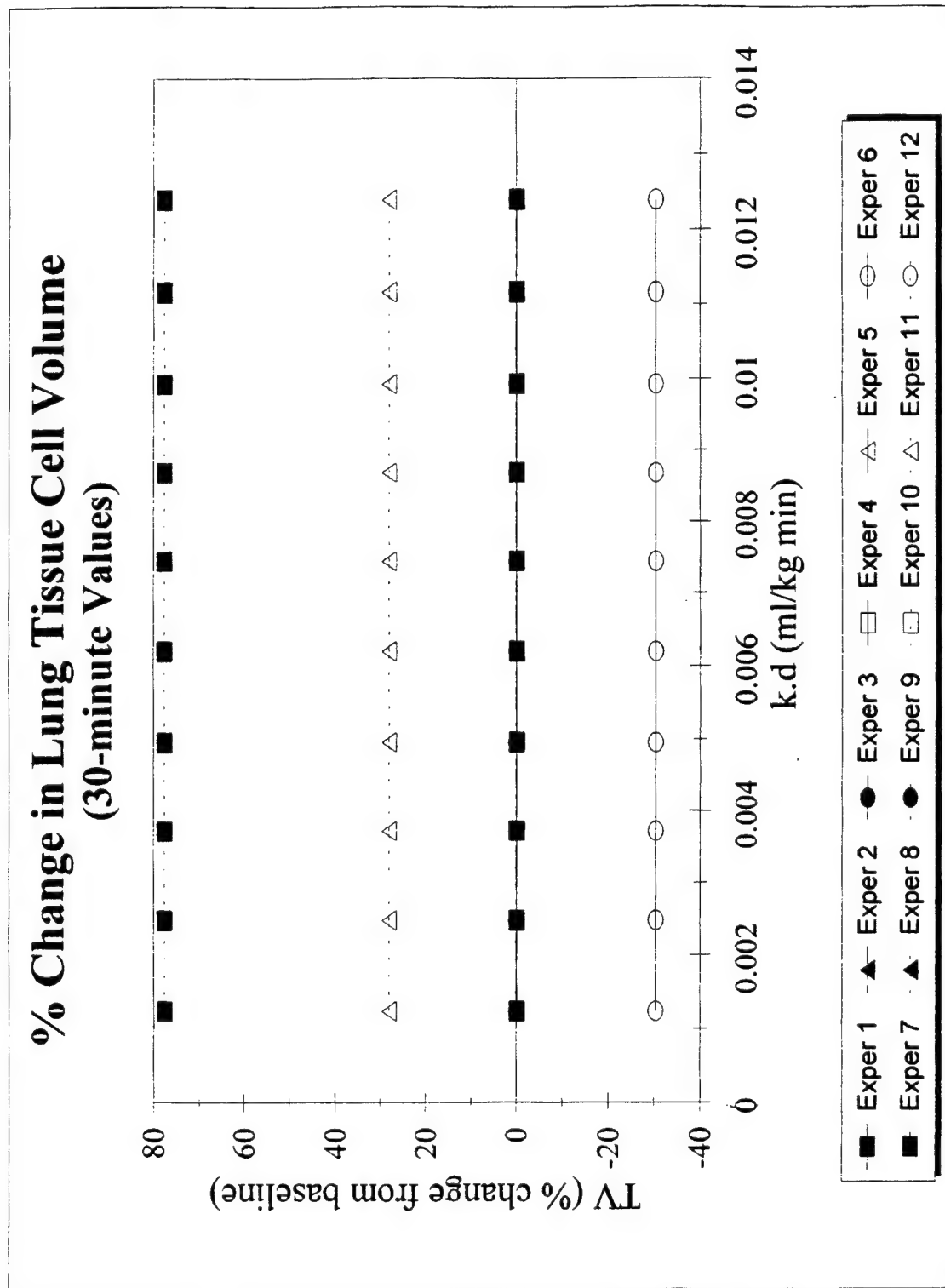


Figure C54

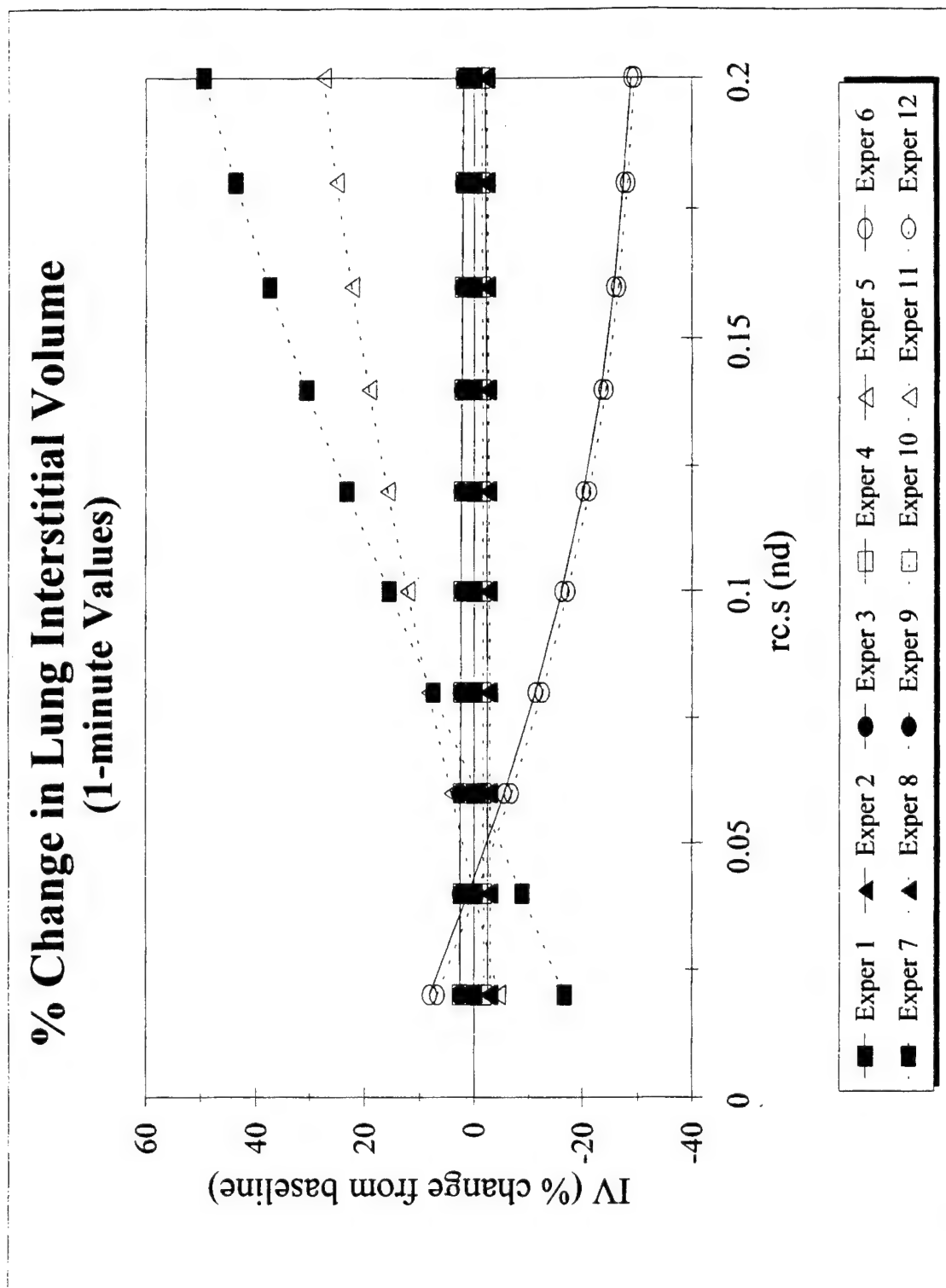


Figure C55

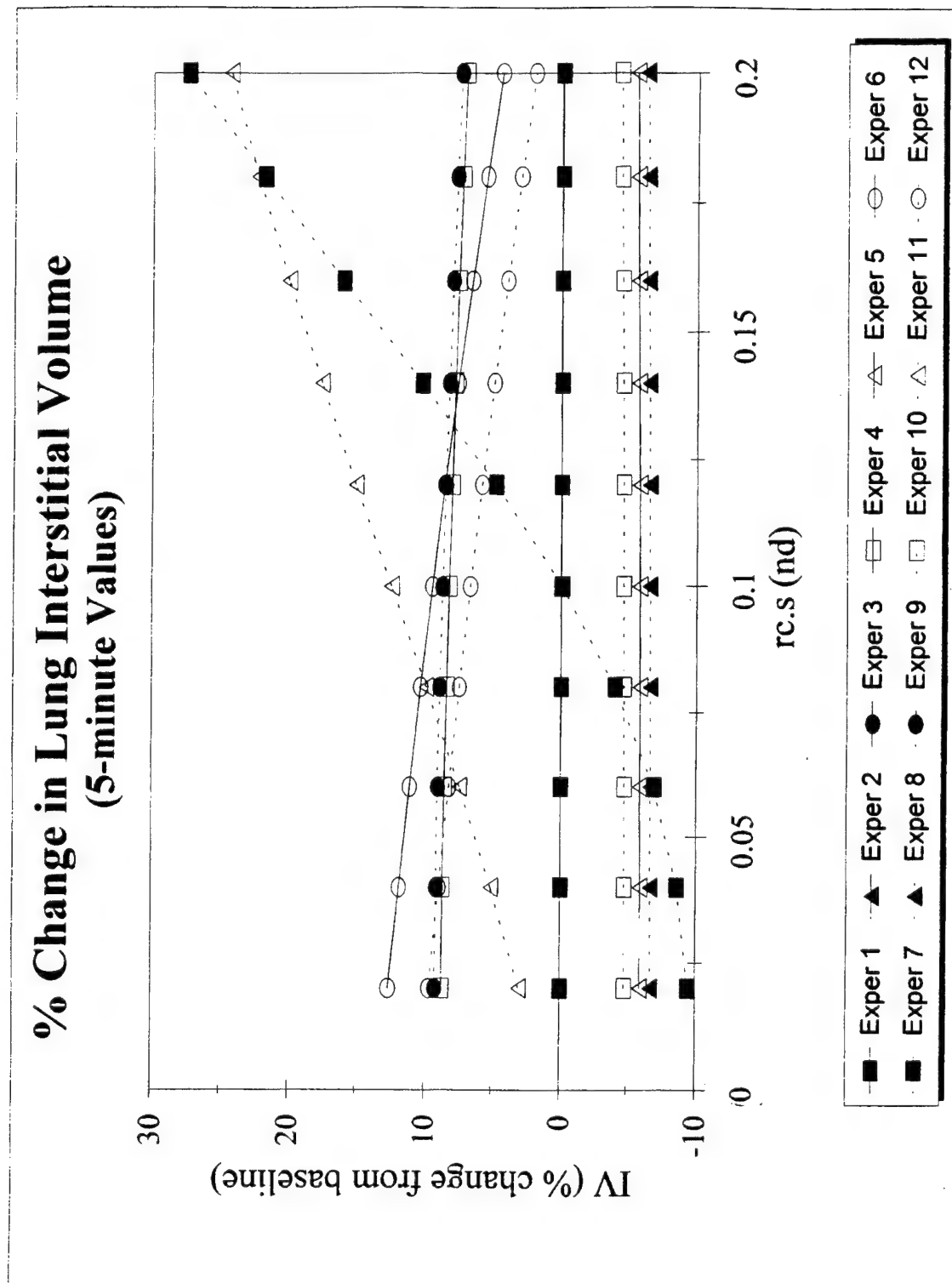


Figure C56

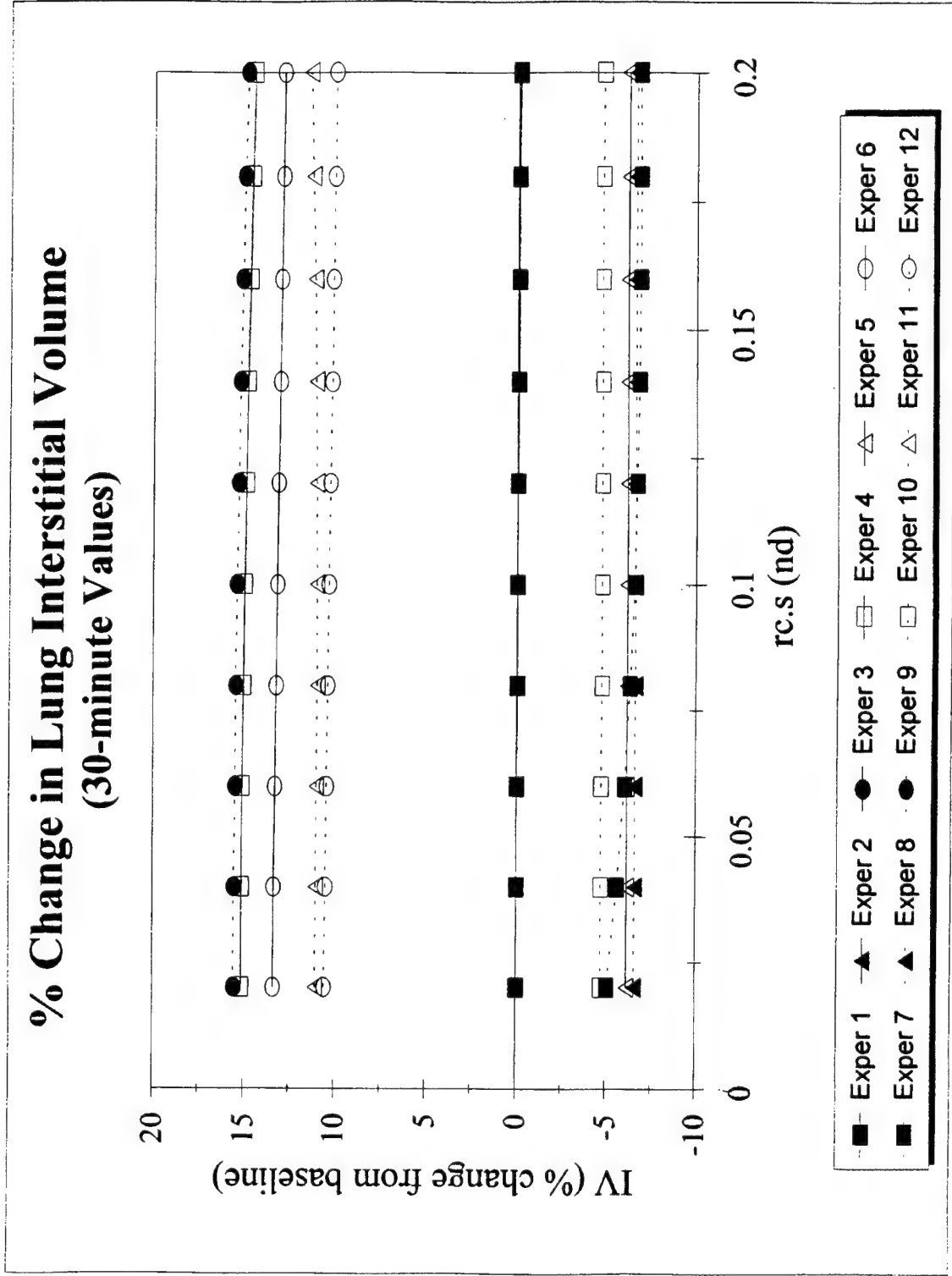


Figure C57

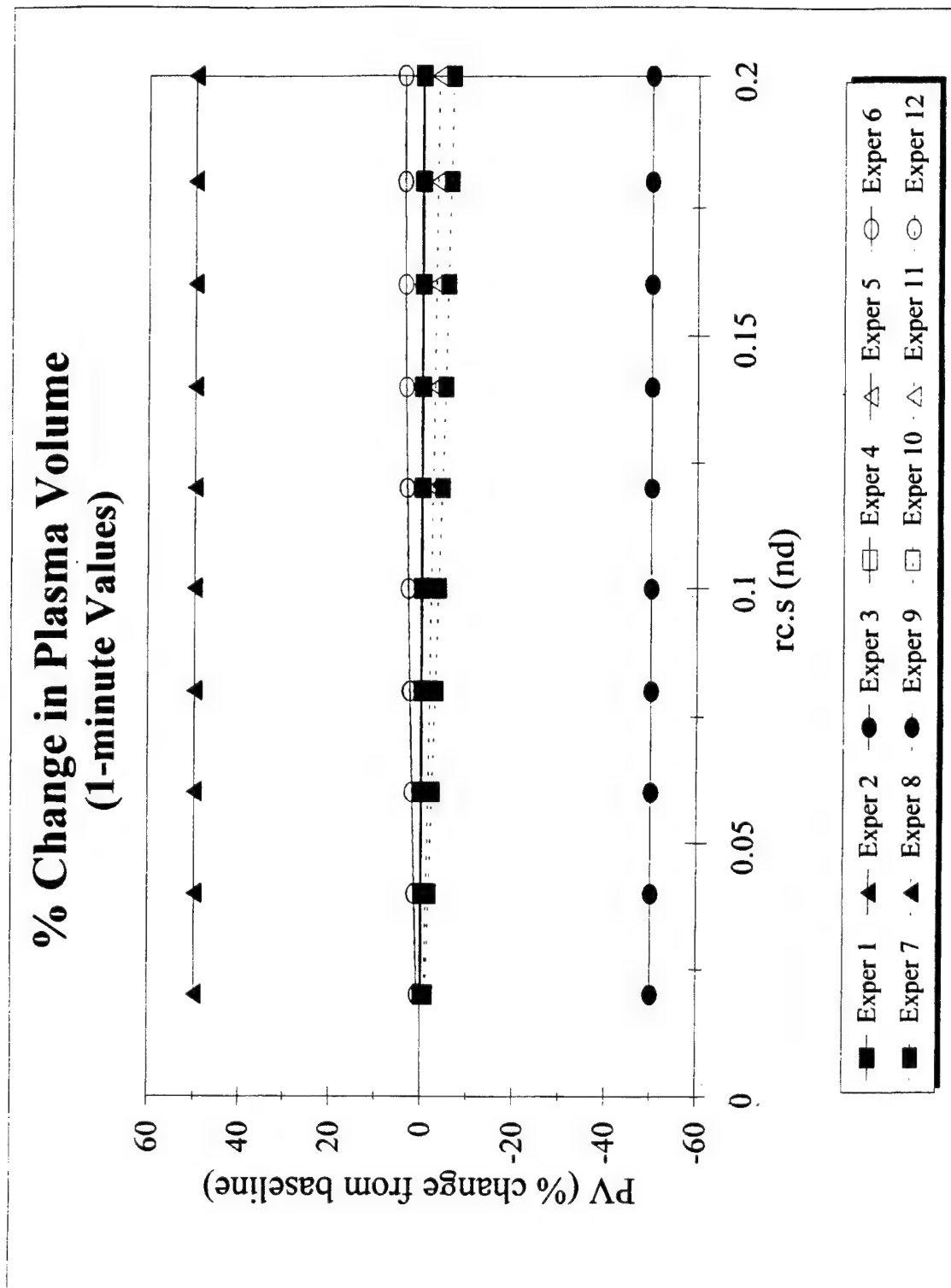


Figure C58

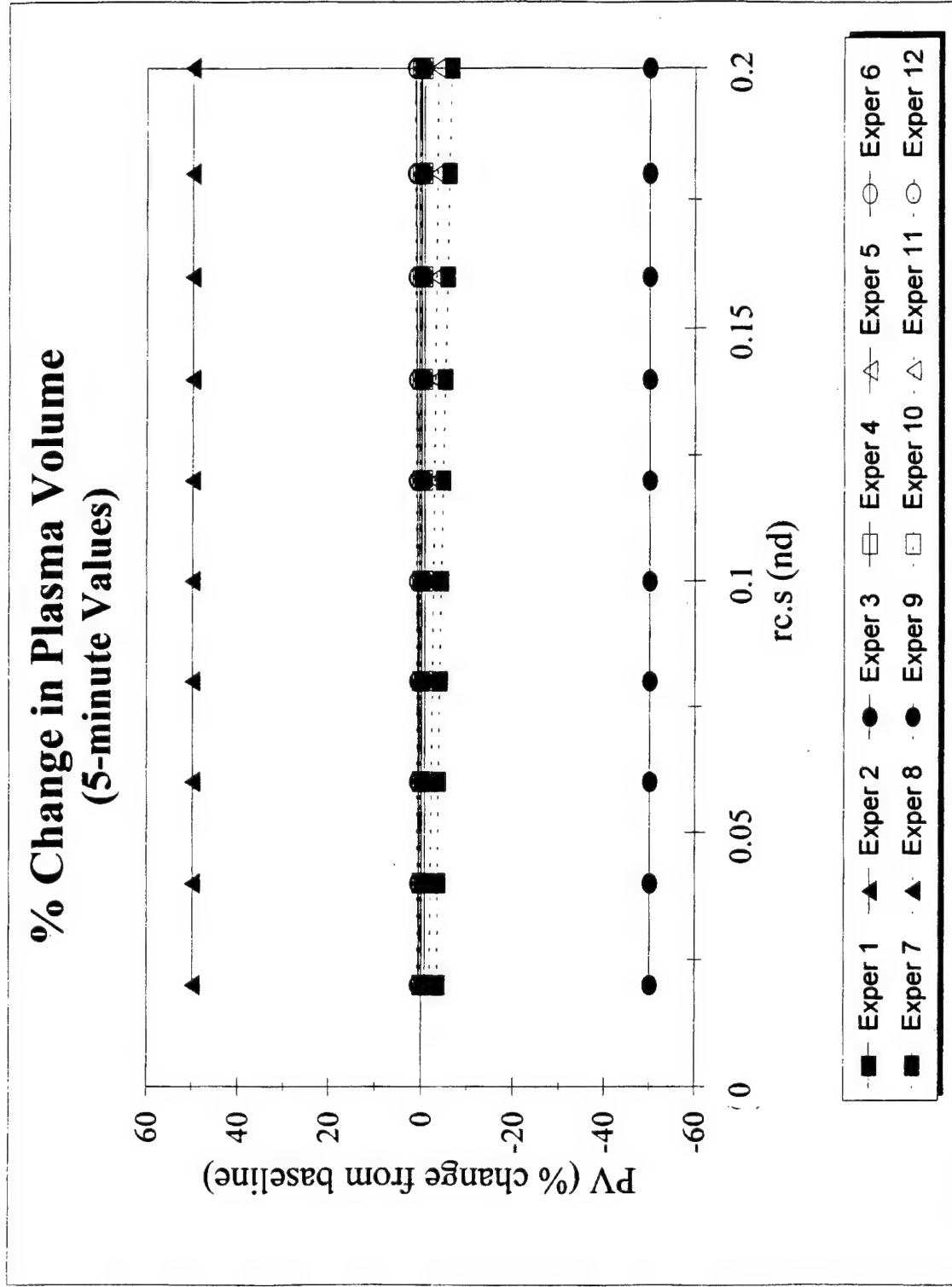


Figure C59

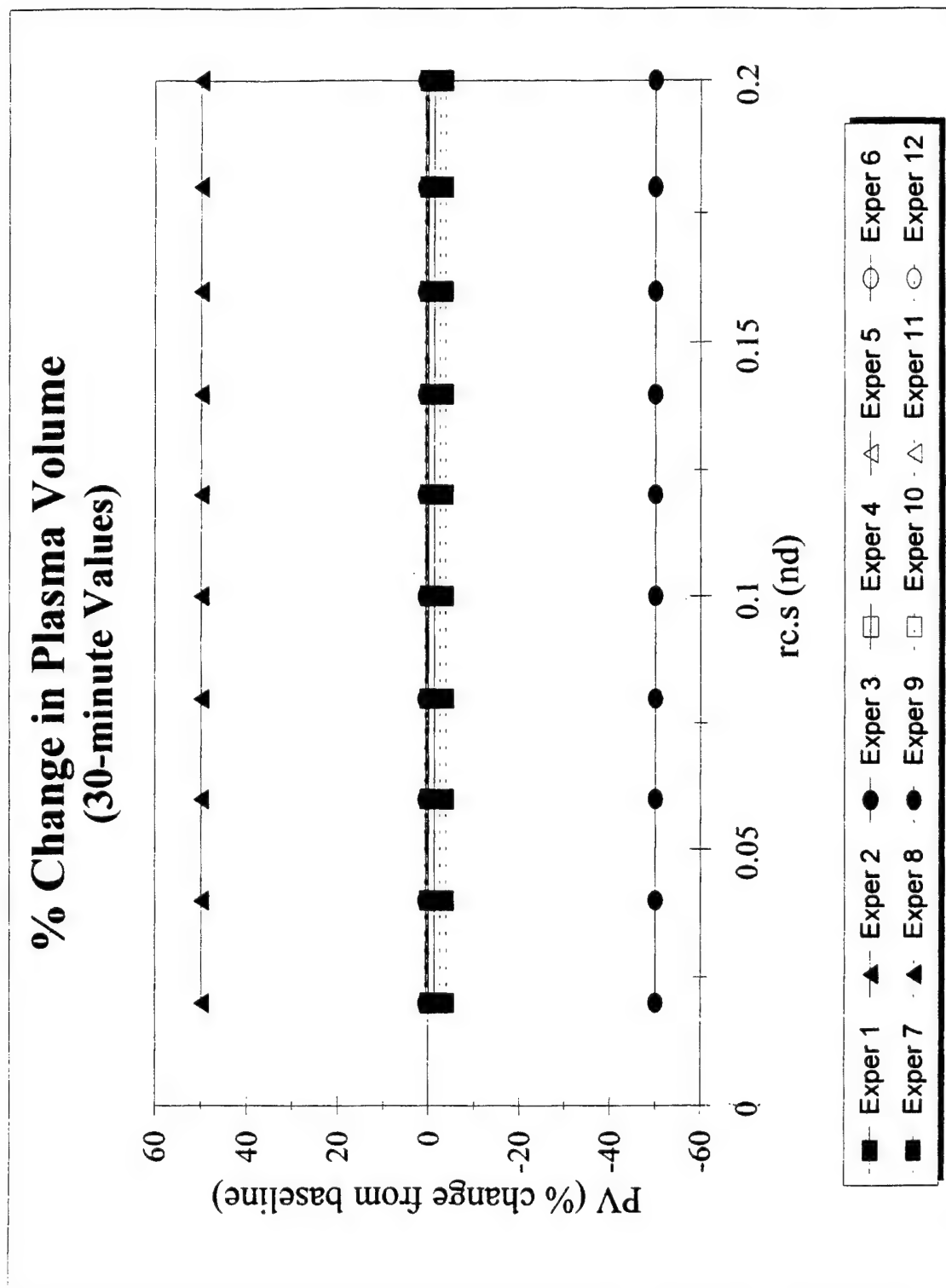


Figure C60

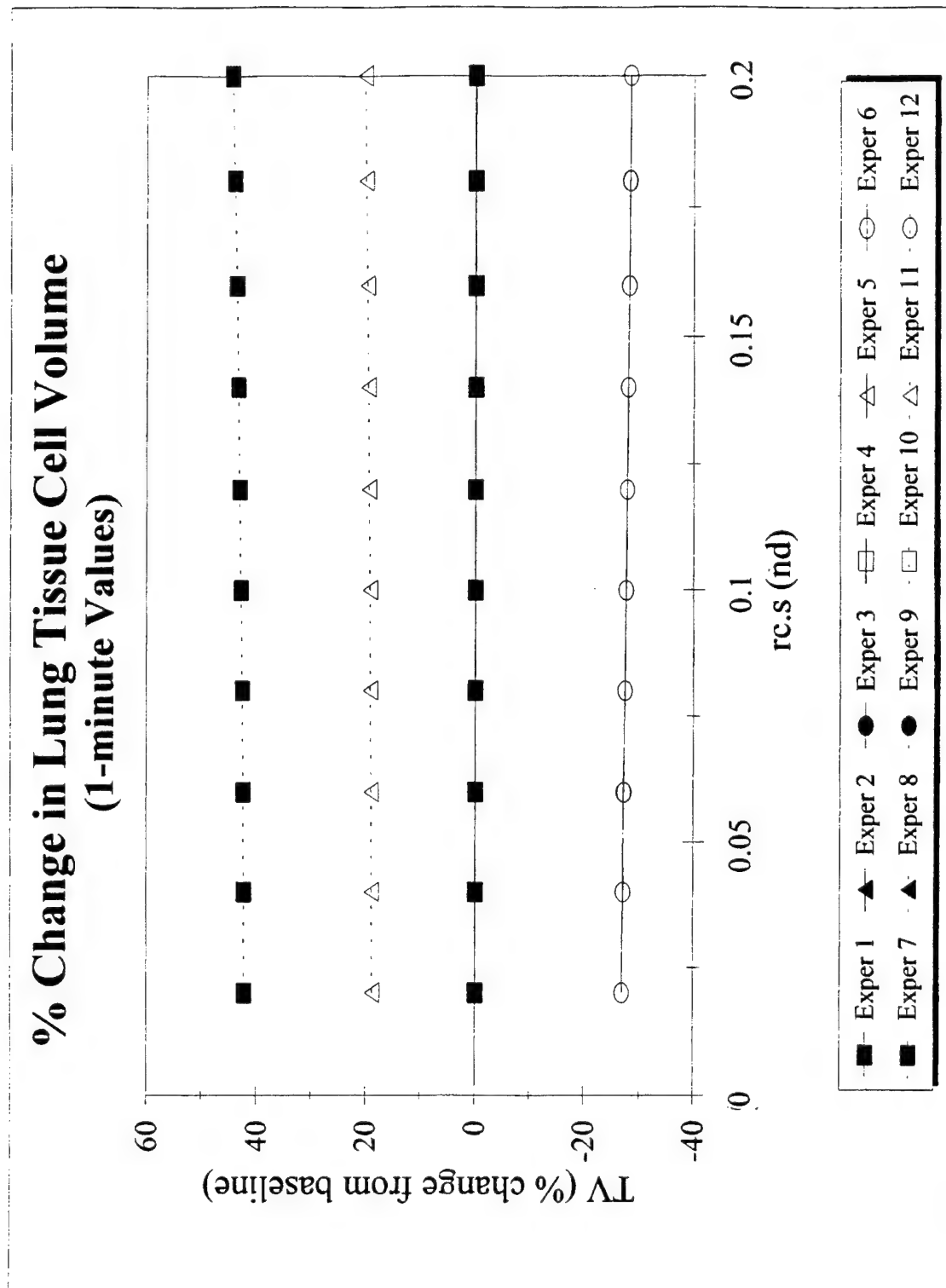


Figure C61

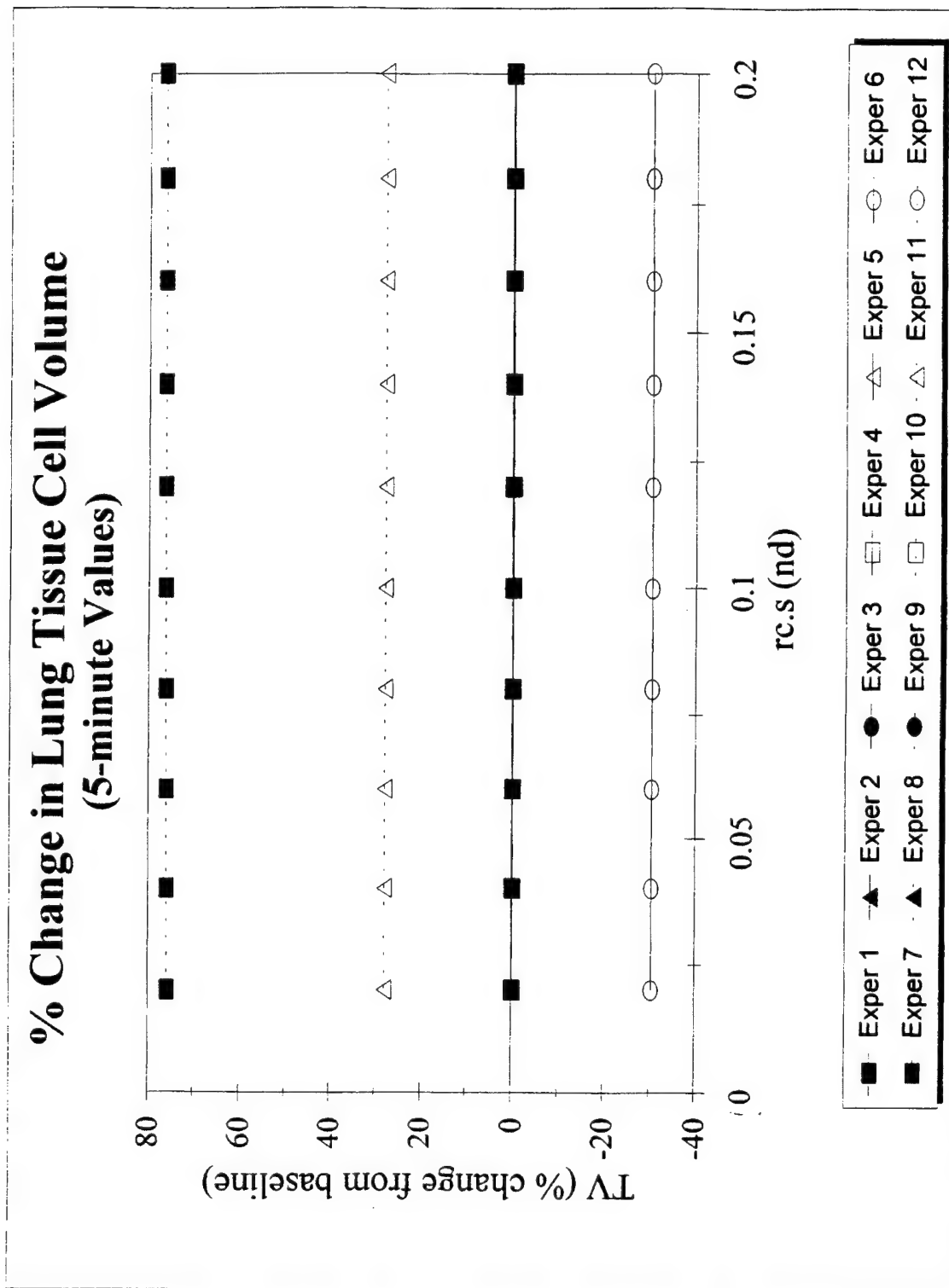


Figure C62

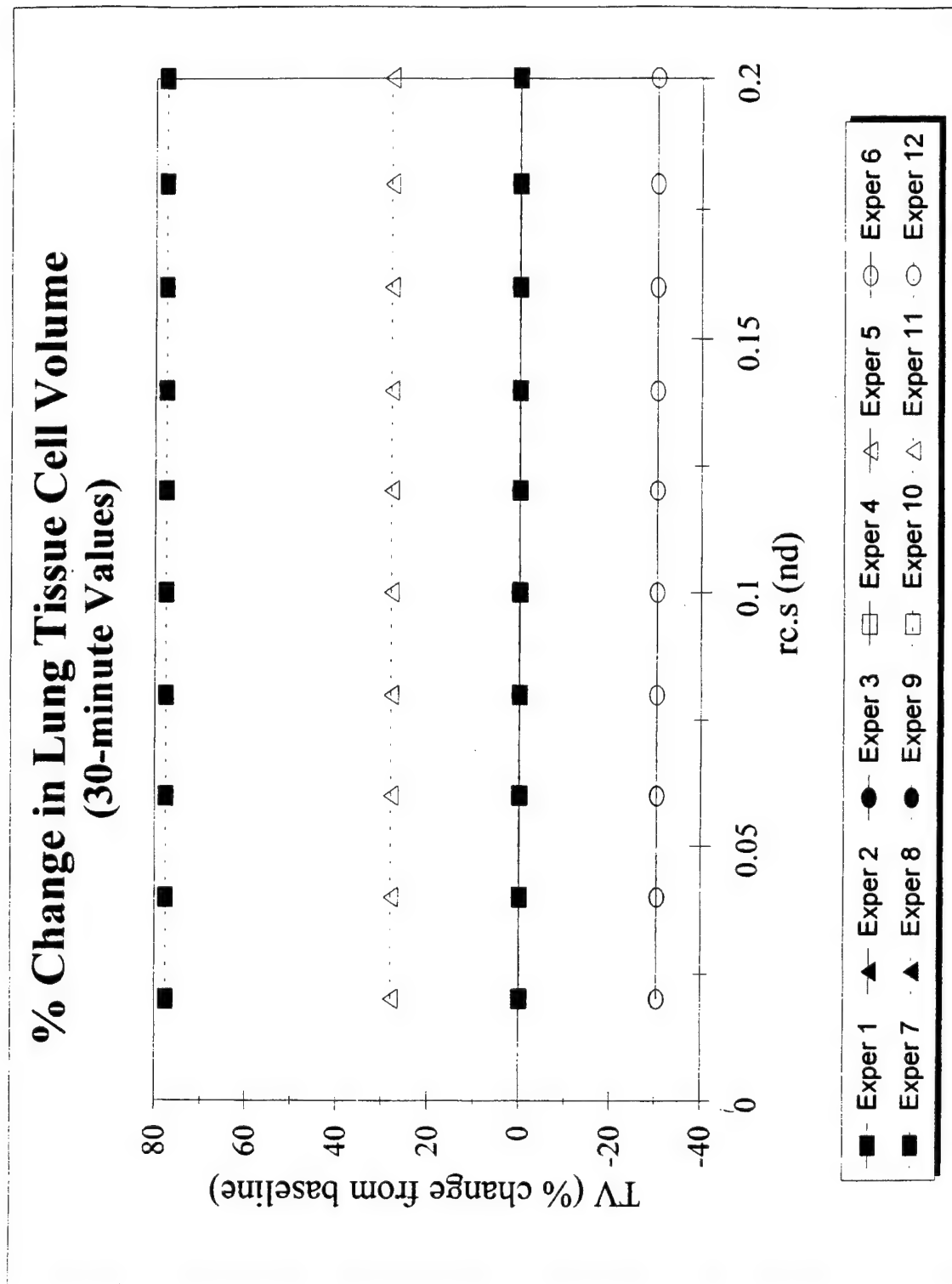


Figure C63

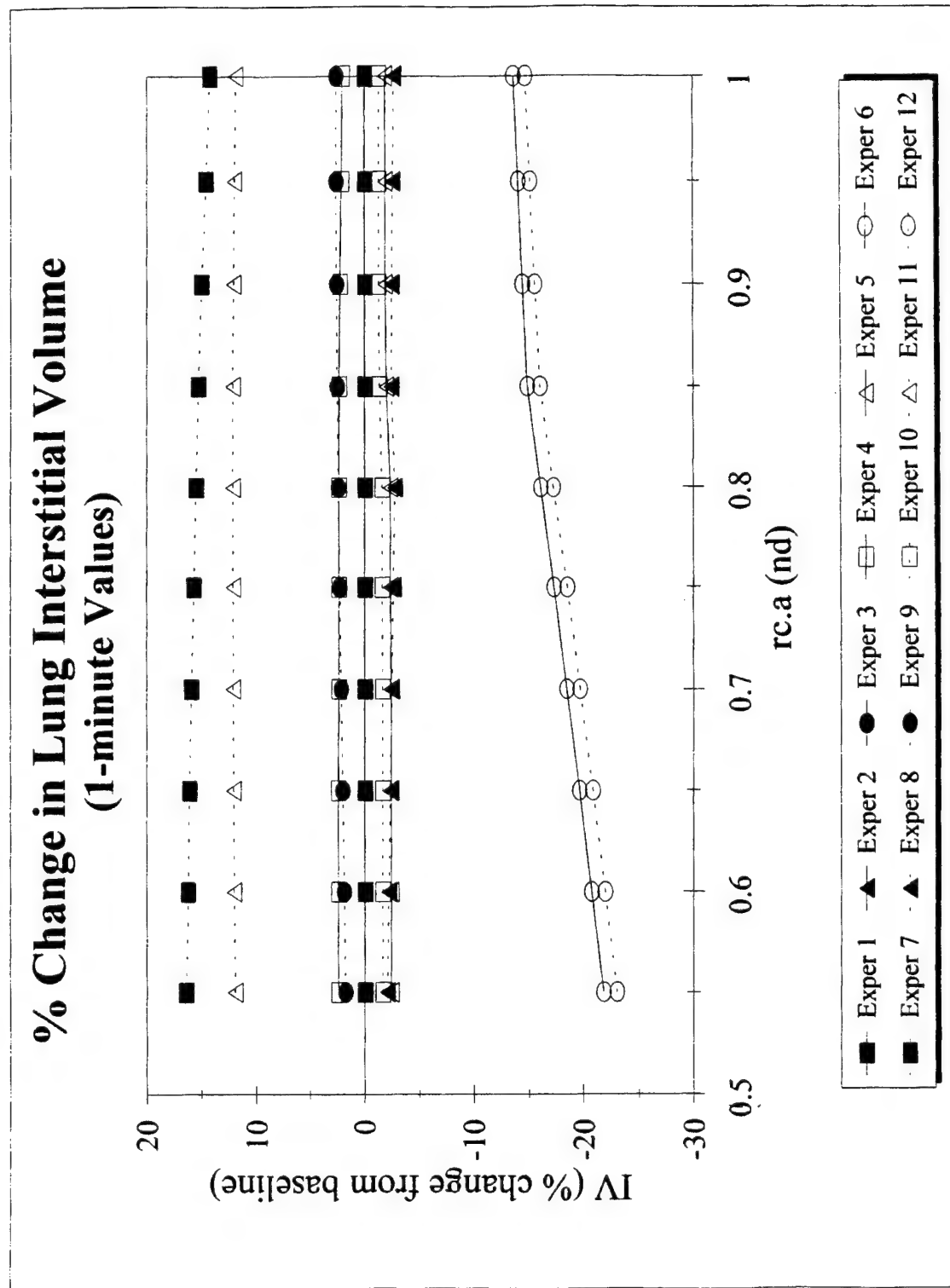


Figure C64

% Change in Lung Interstitial Volume (5-minute Values)

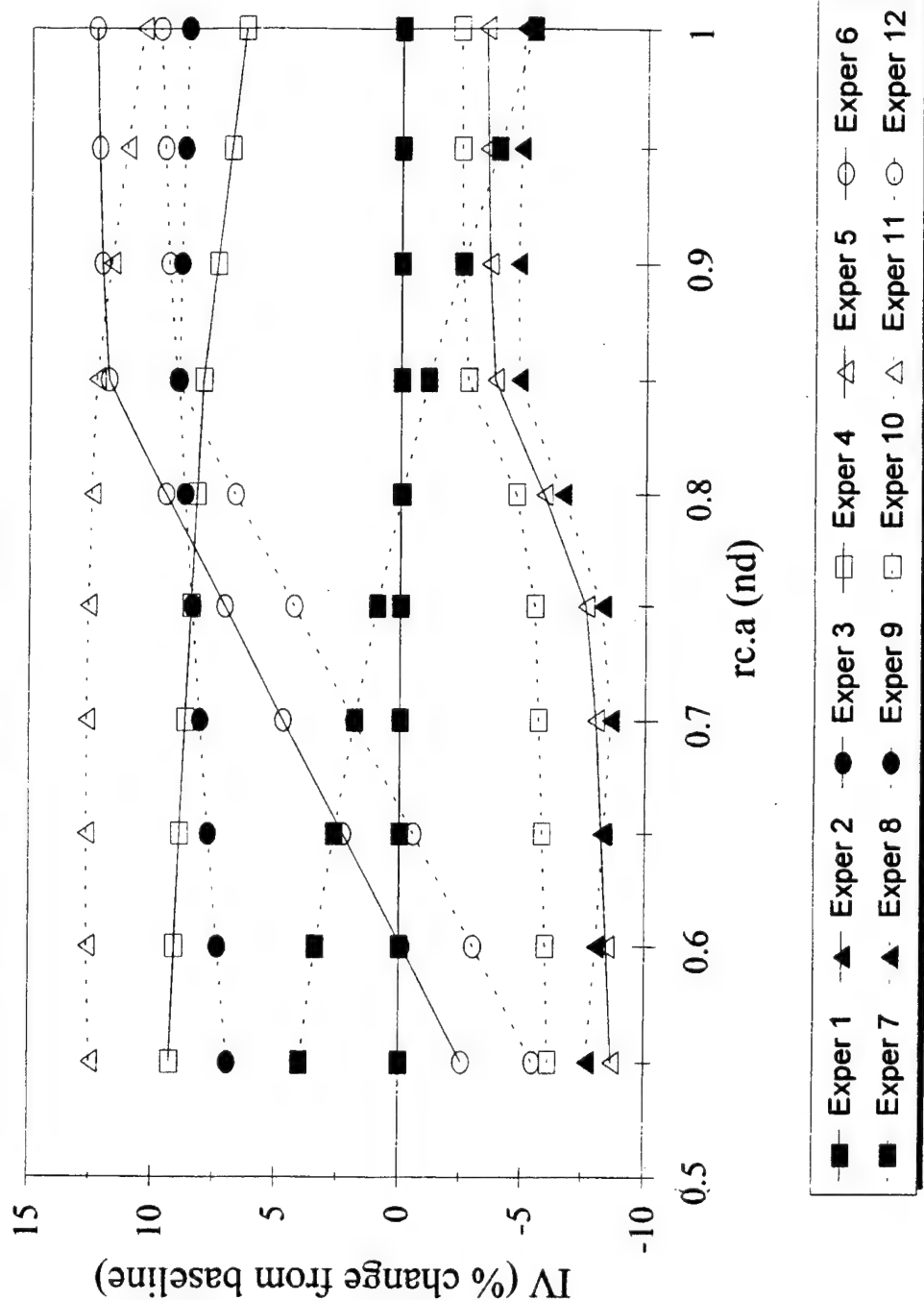


Figure C65

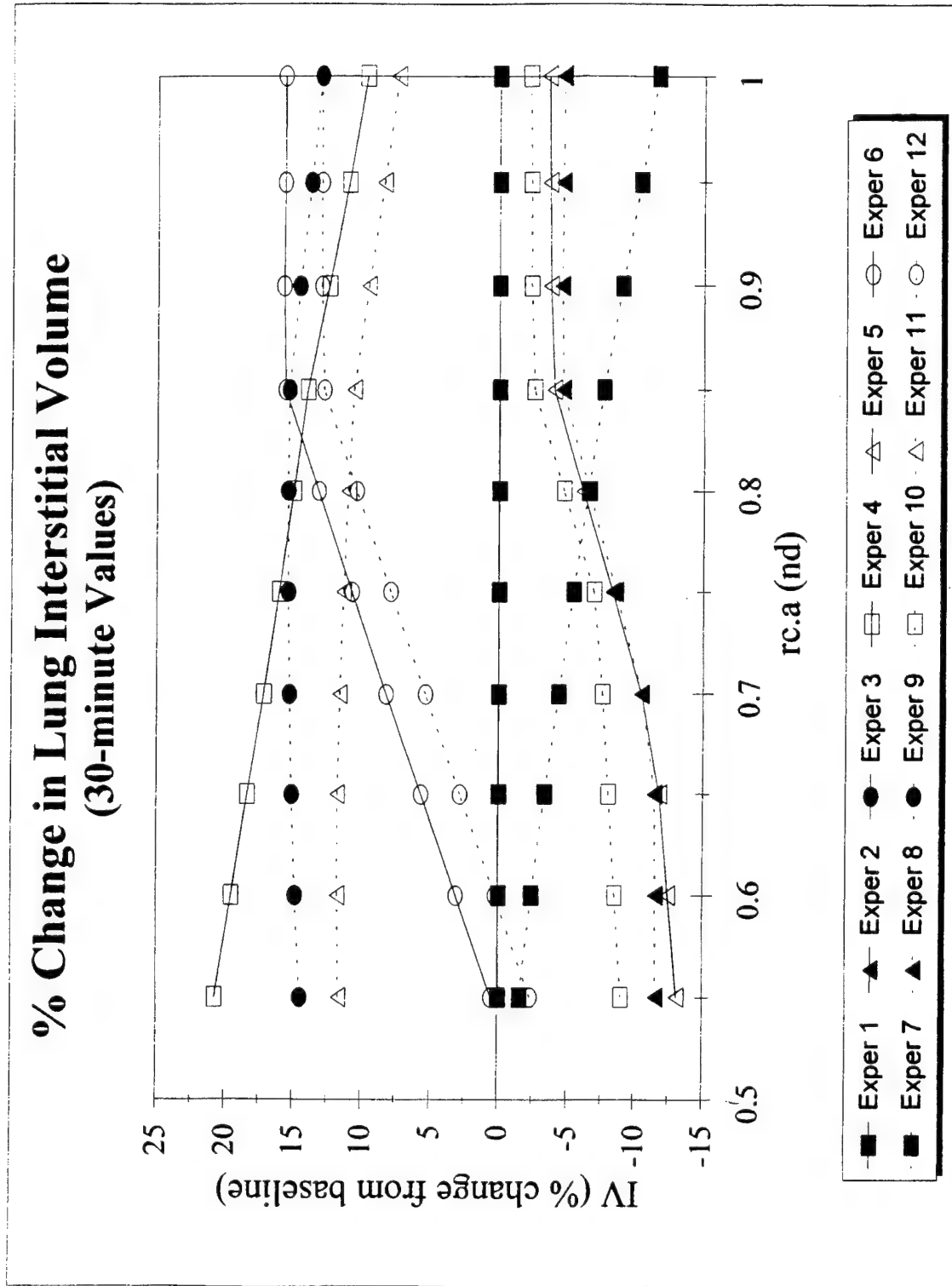


Figure C66

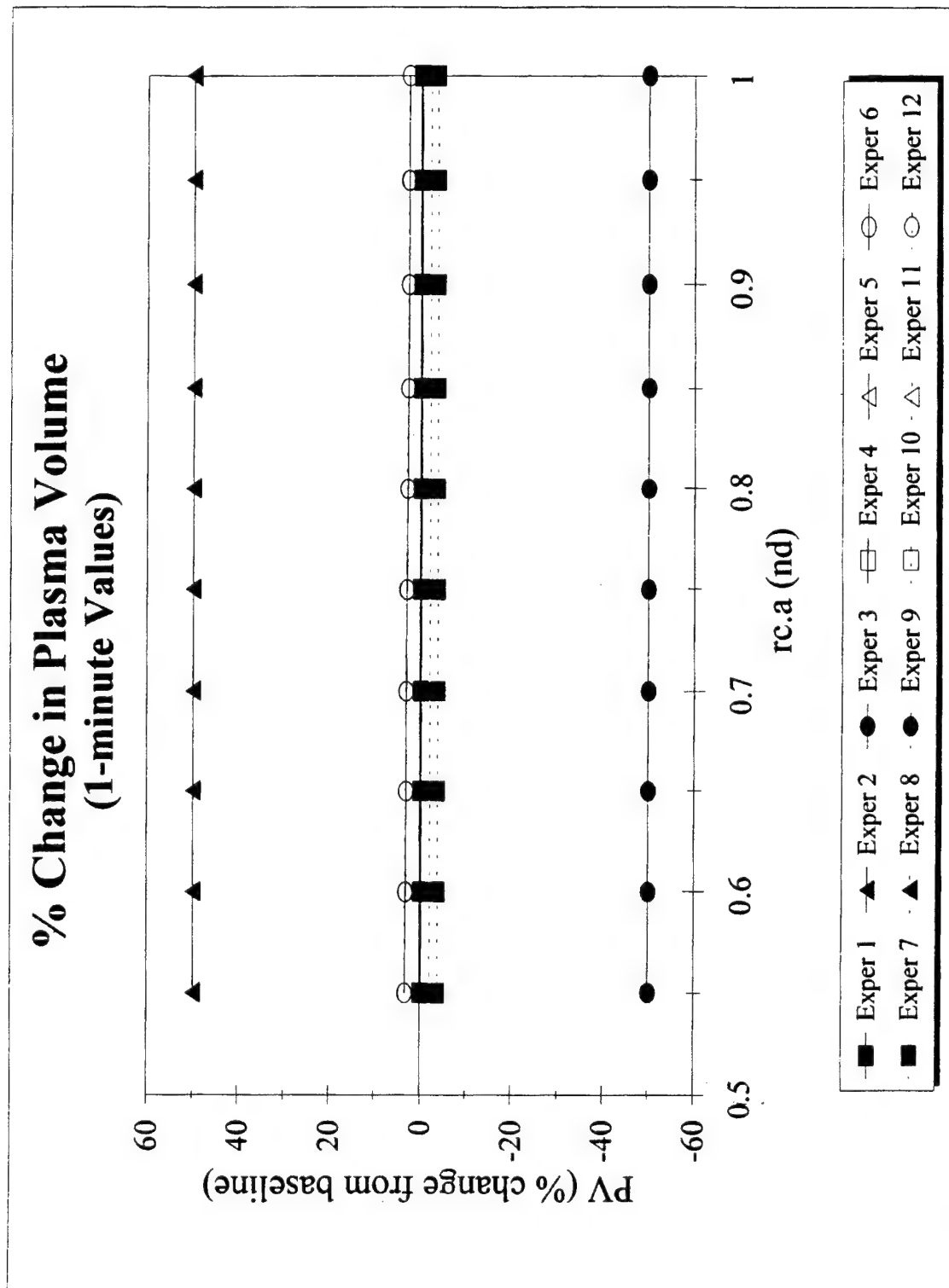


Figure C67

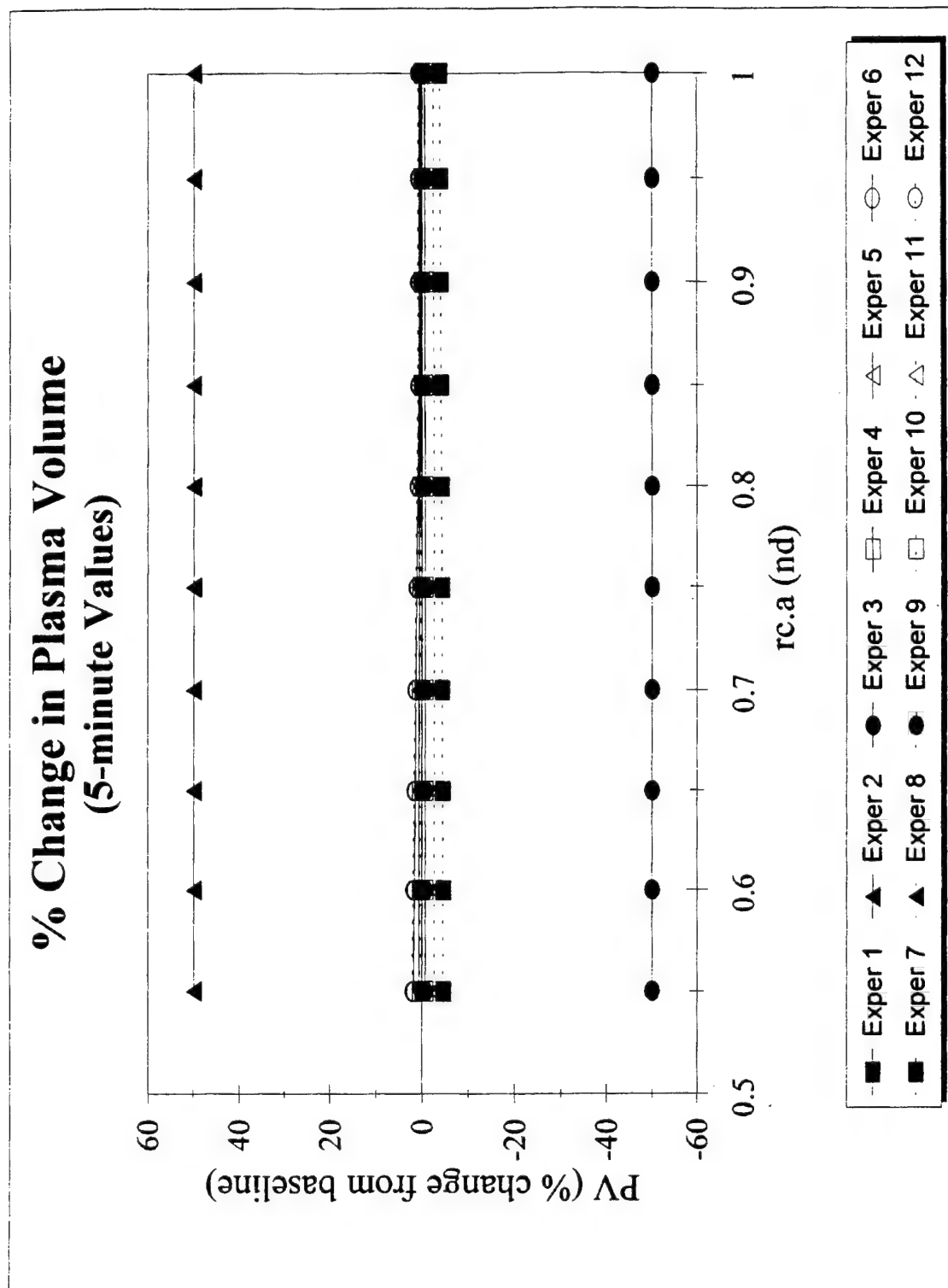


Figure C68

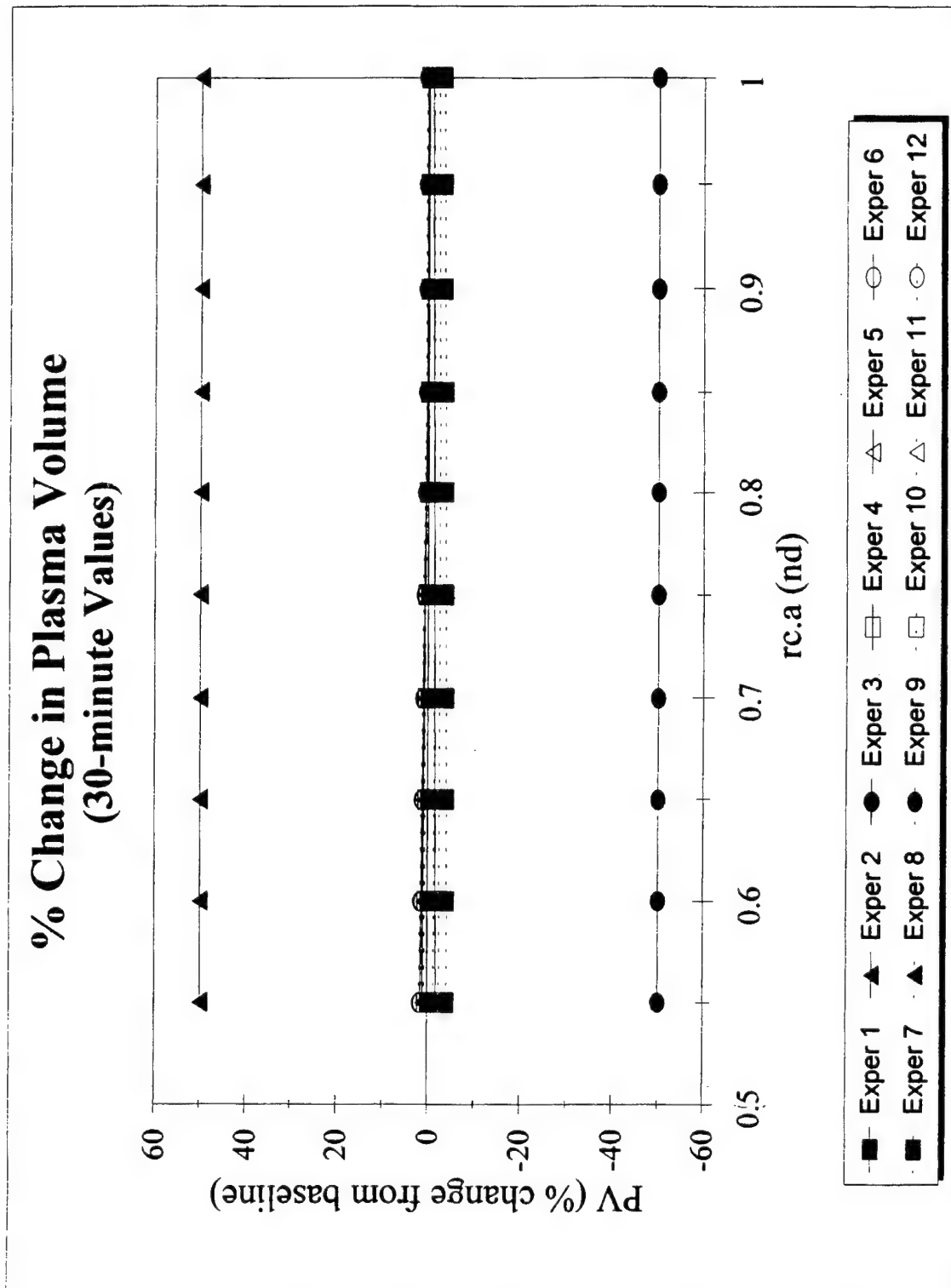


Figure C69

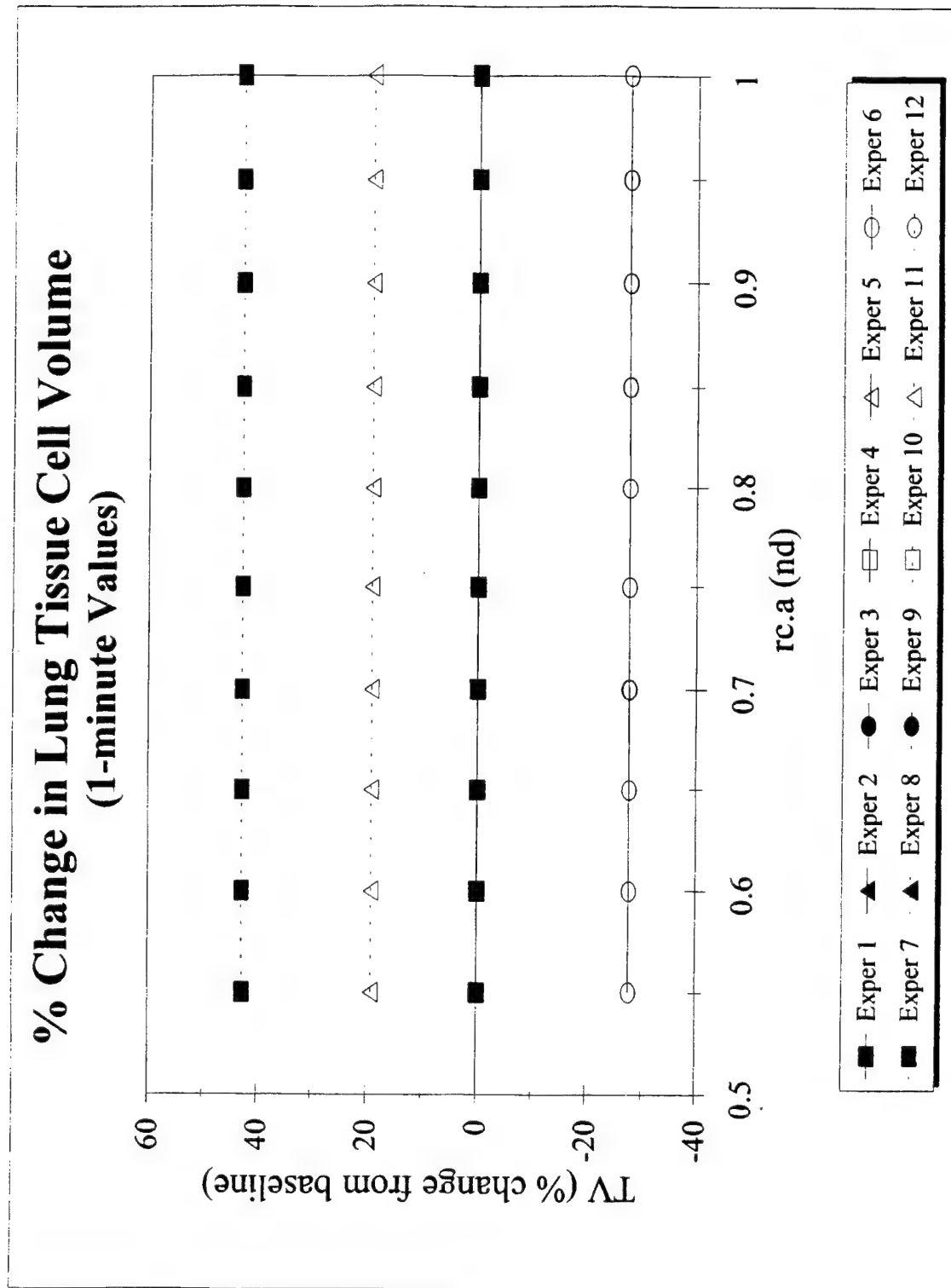


Figure C70

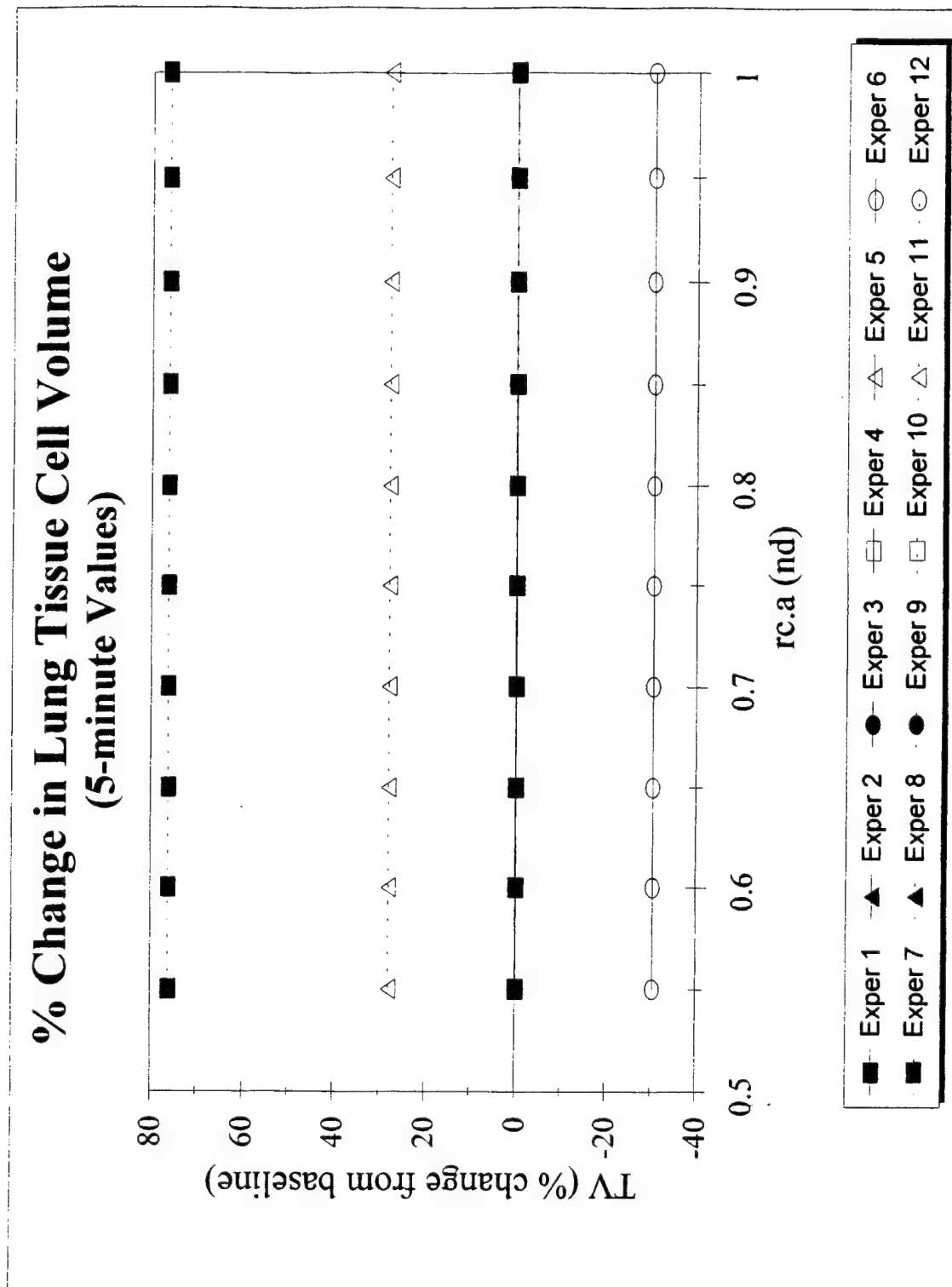


Figure C71

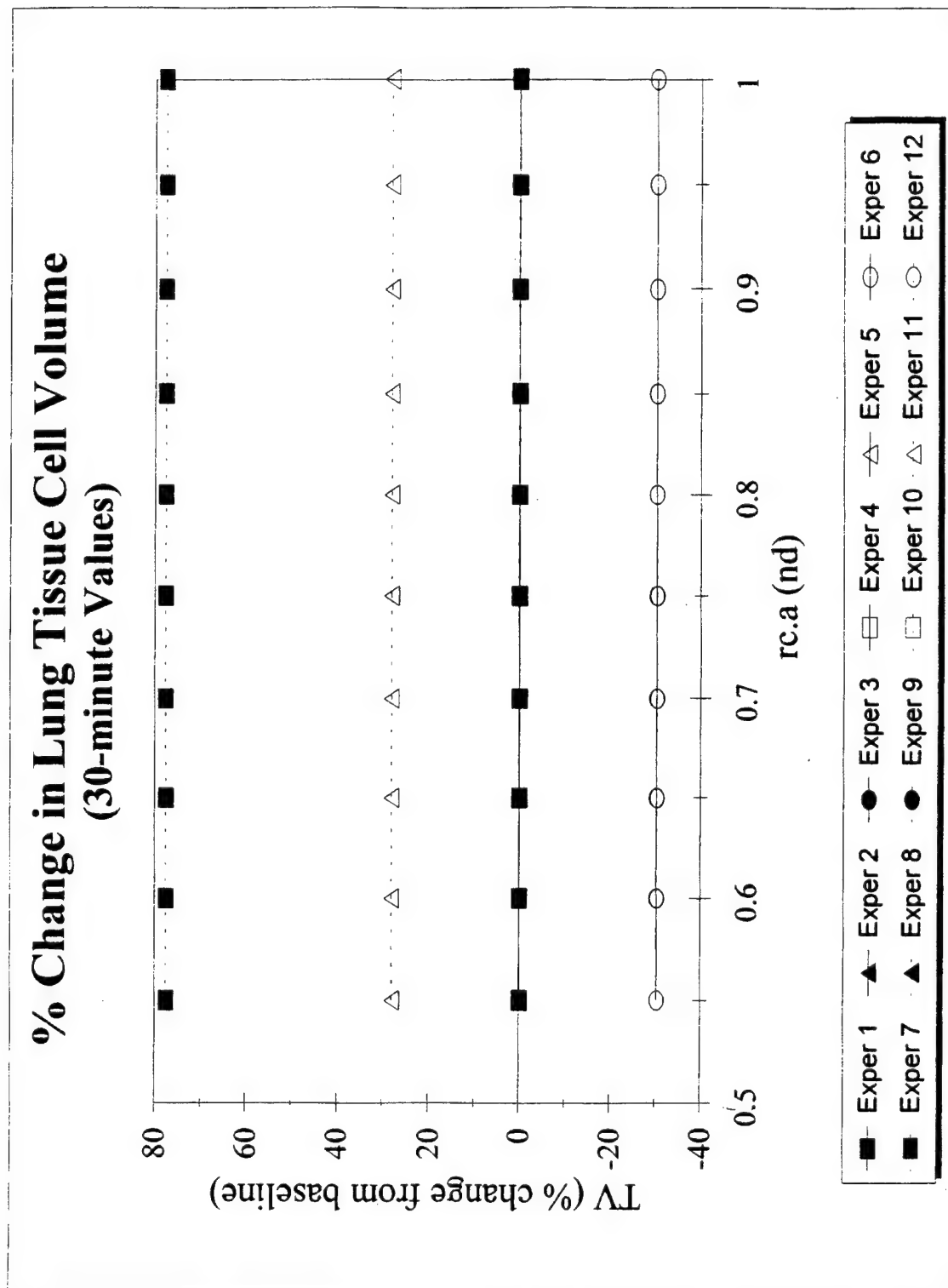


Figure C72

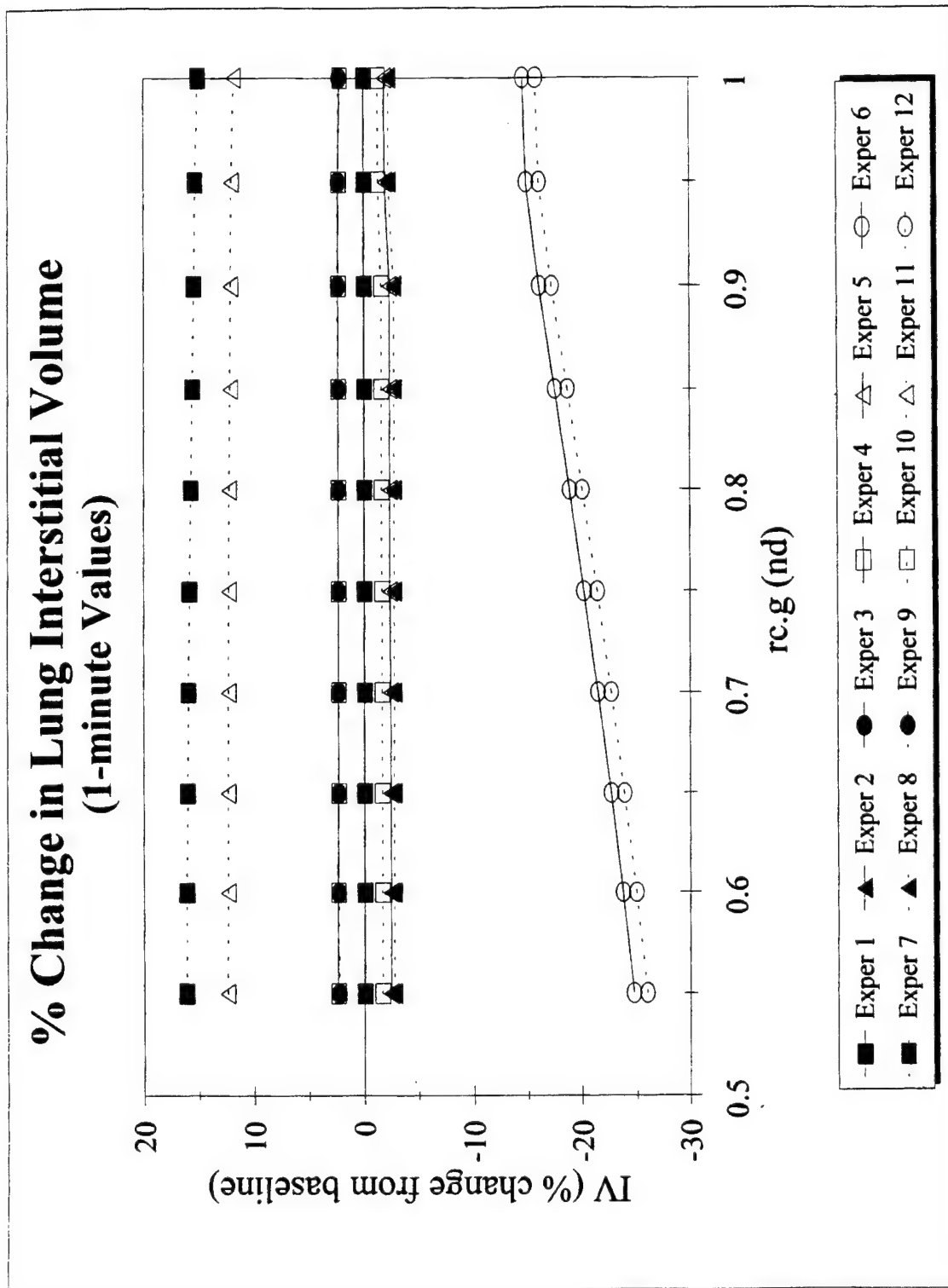


Figure C73

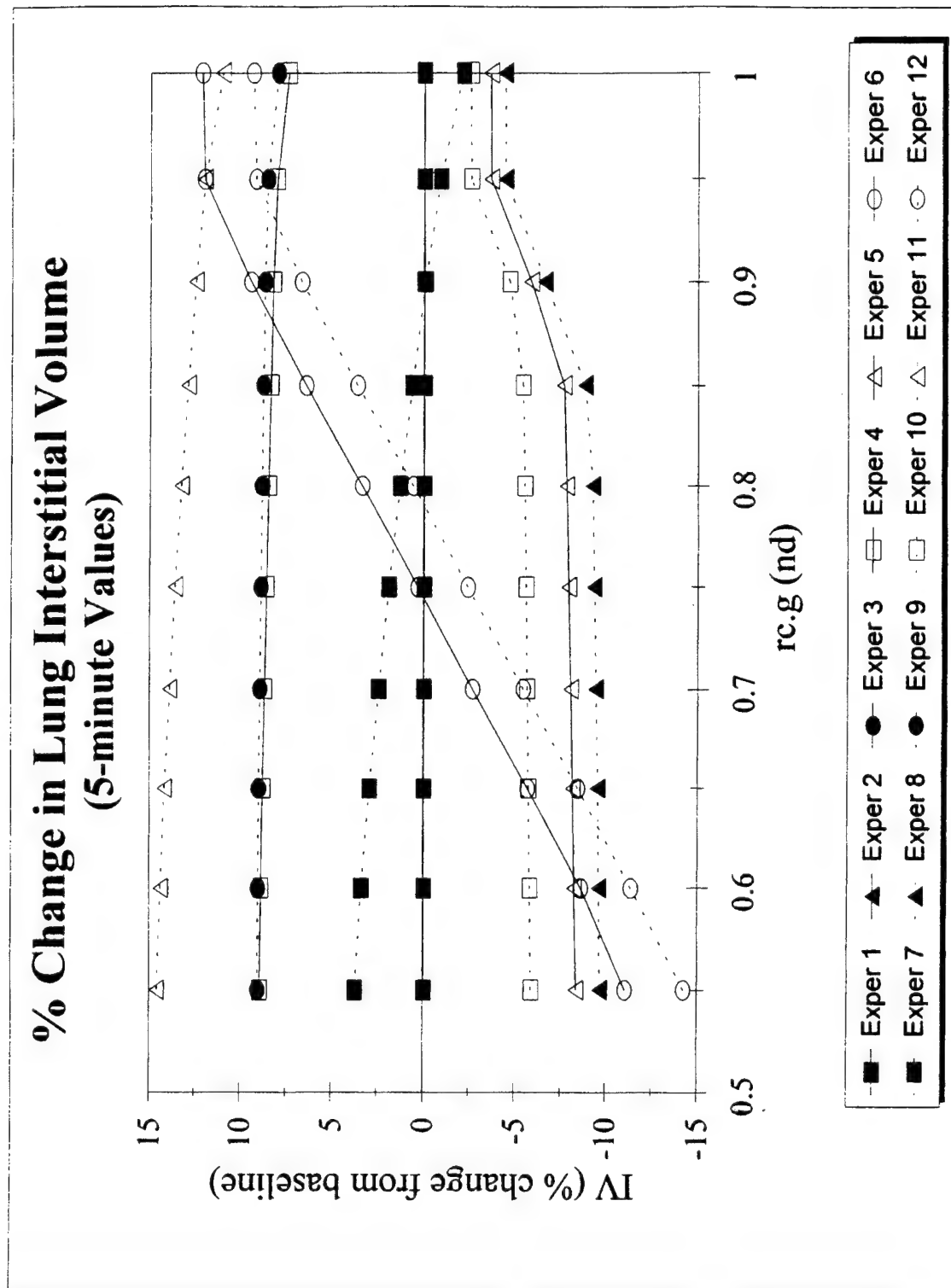


Figure C74

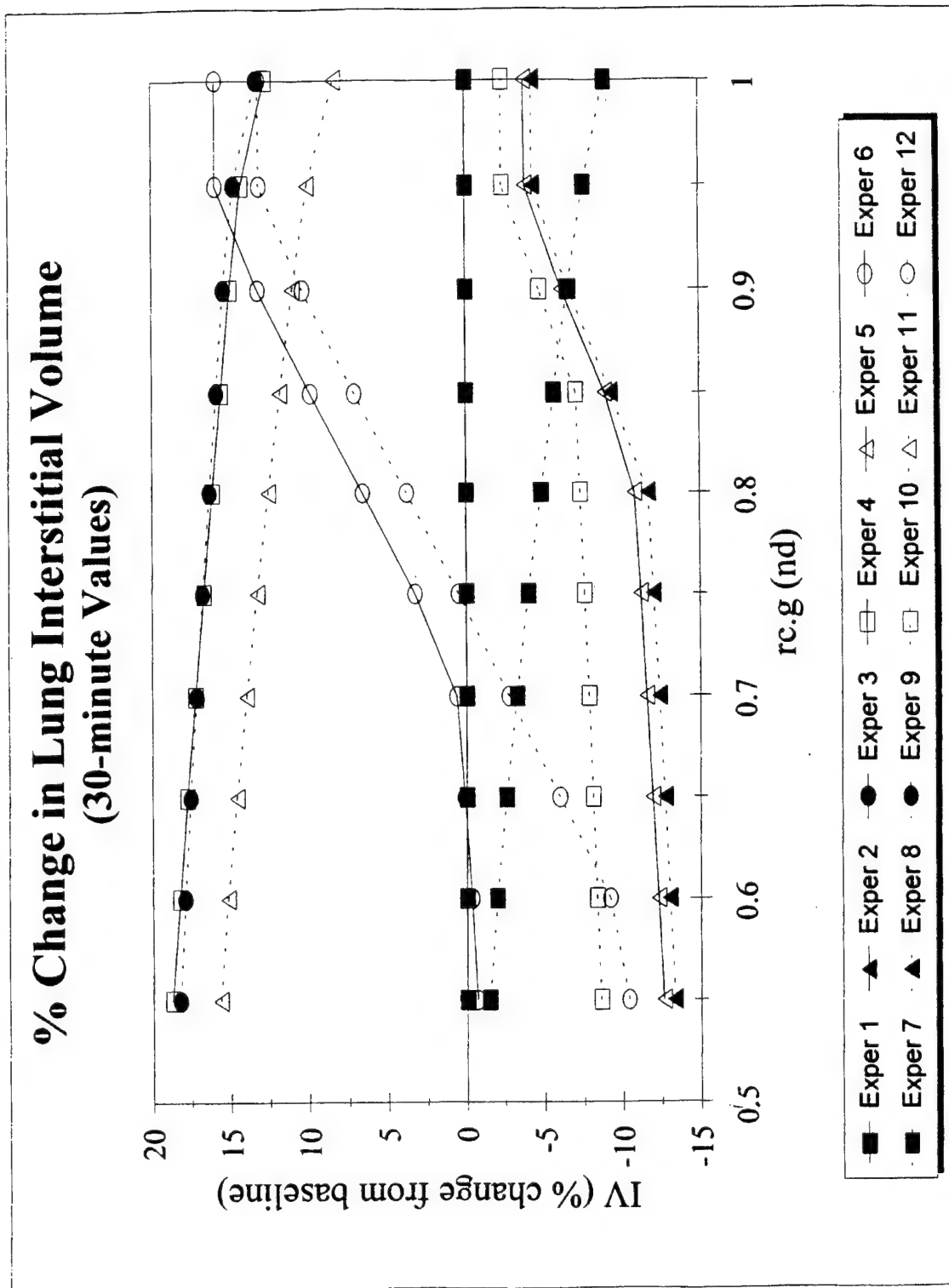


Figure C75

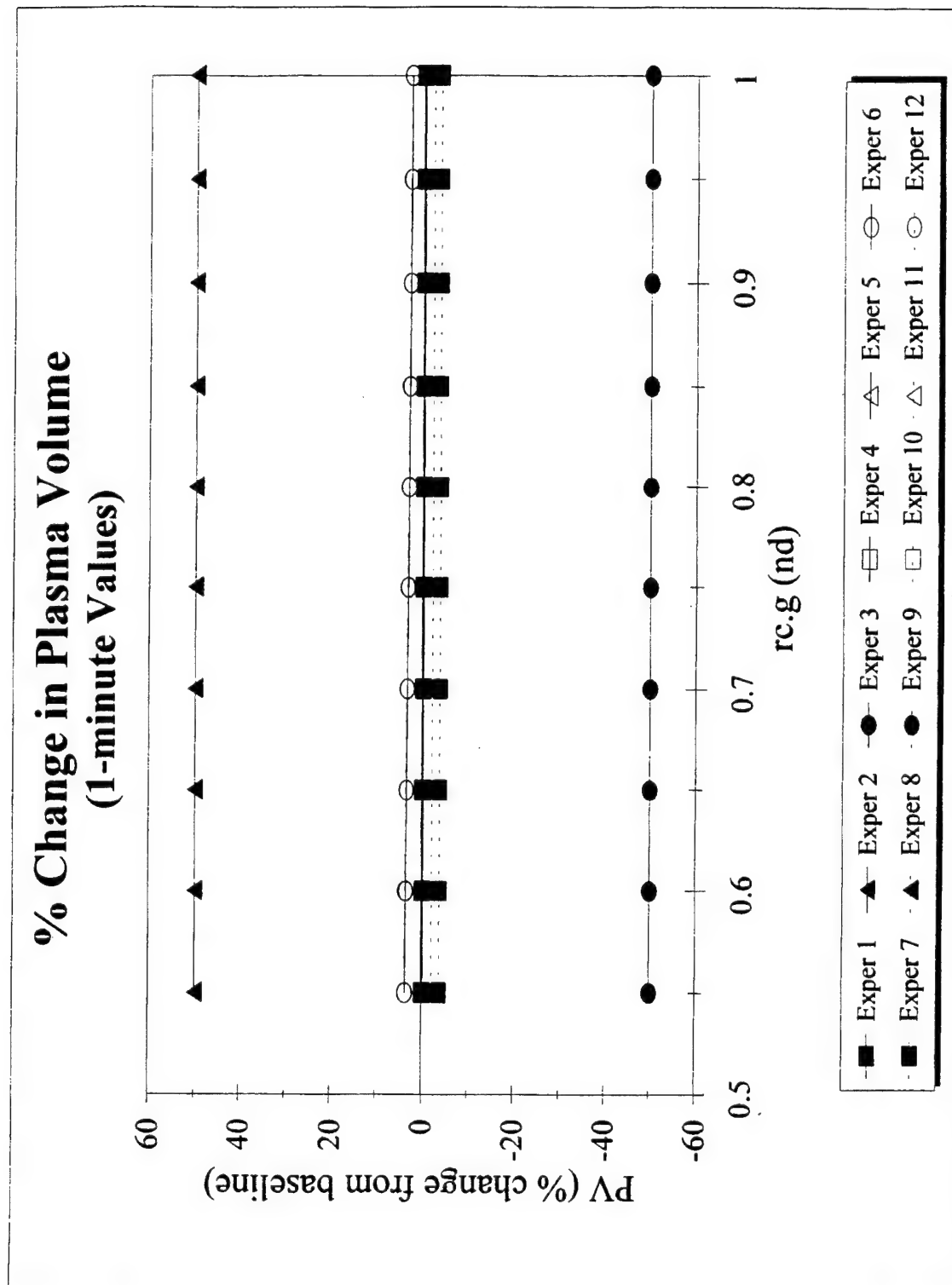


Figure C76

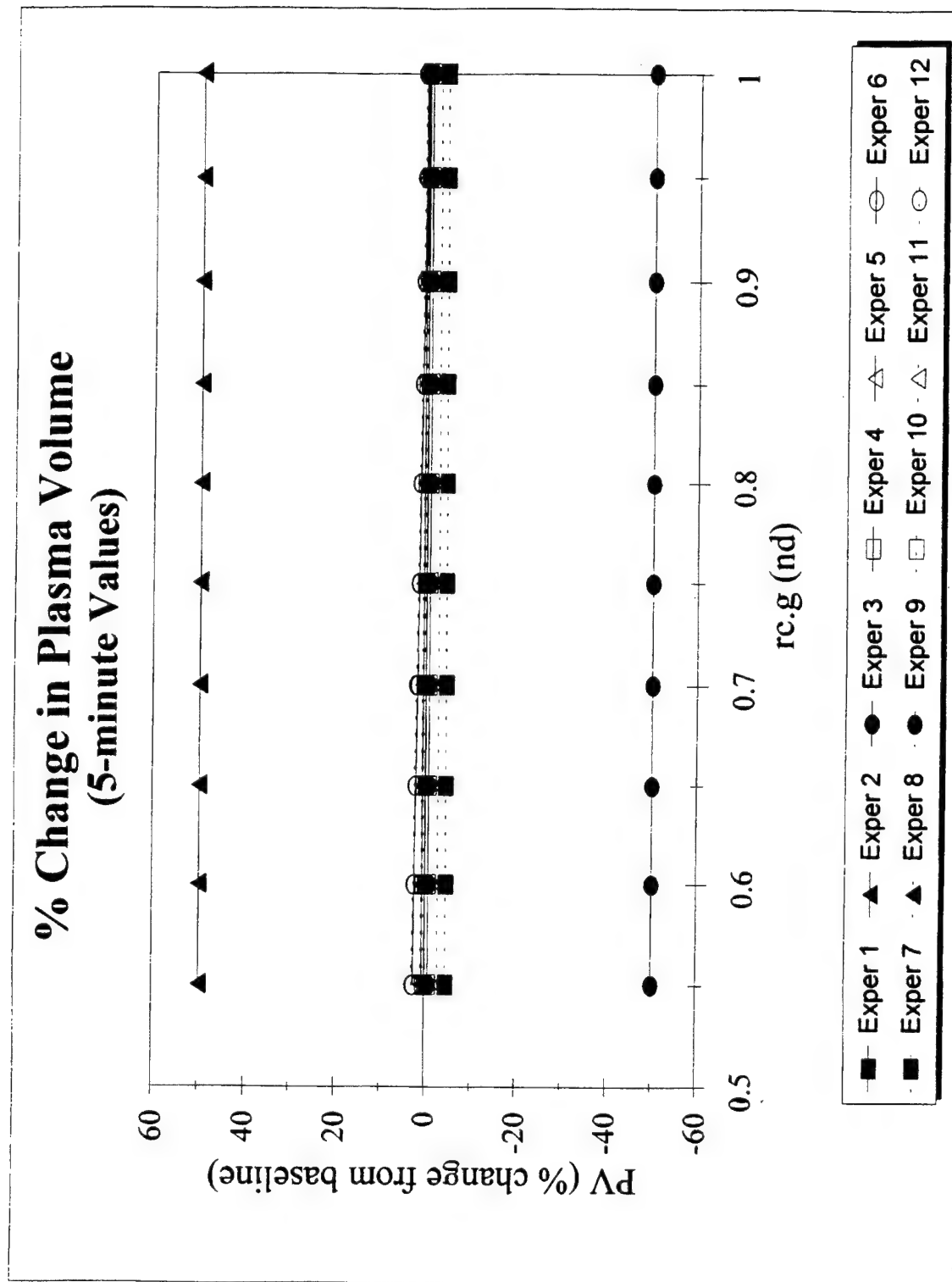


Figure C77

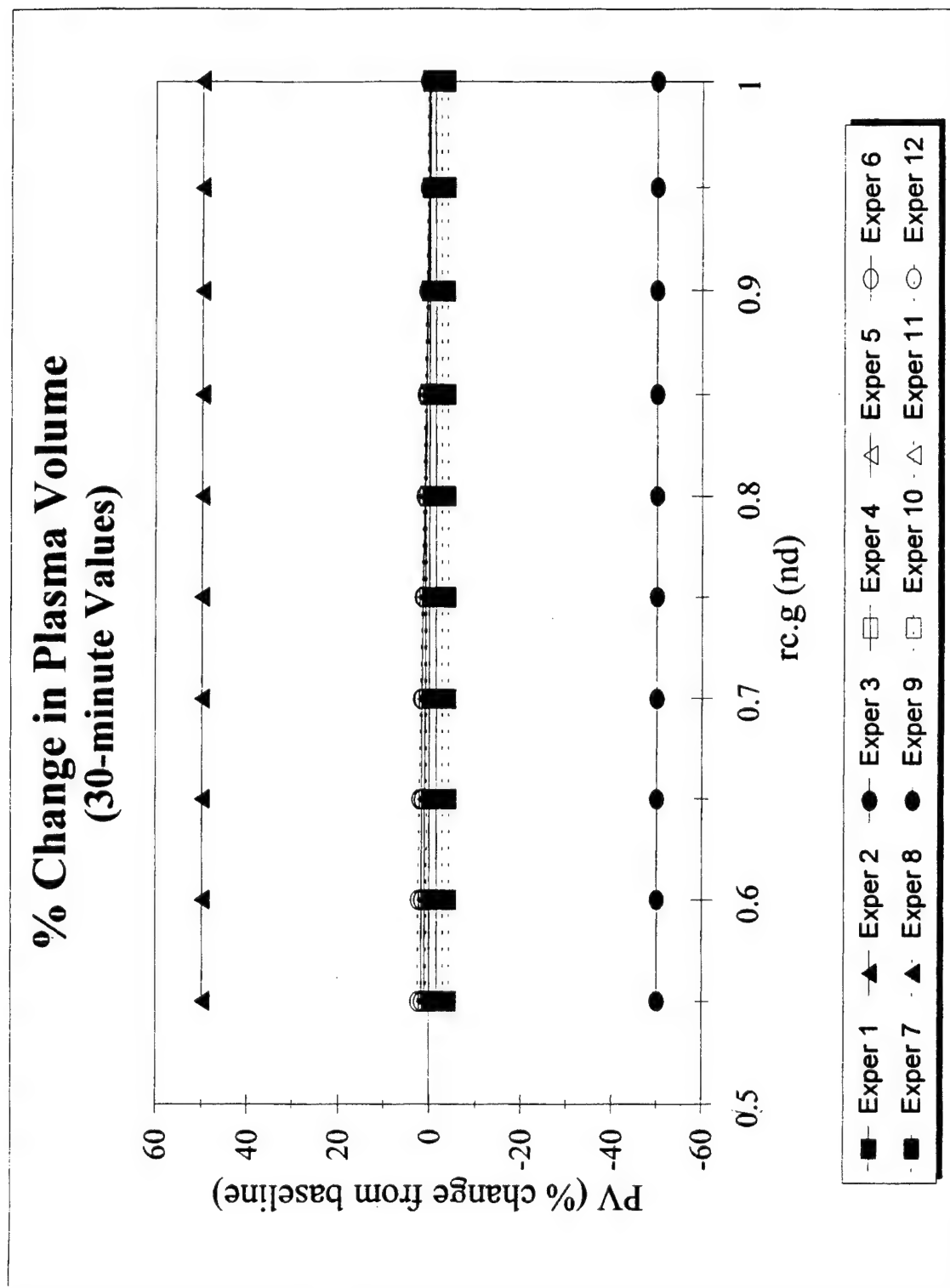


Figure C78

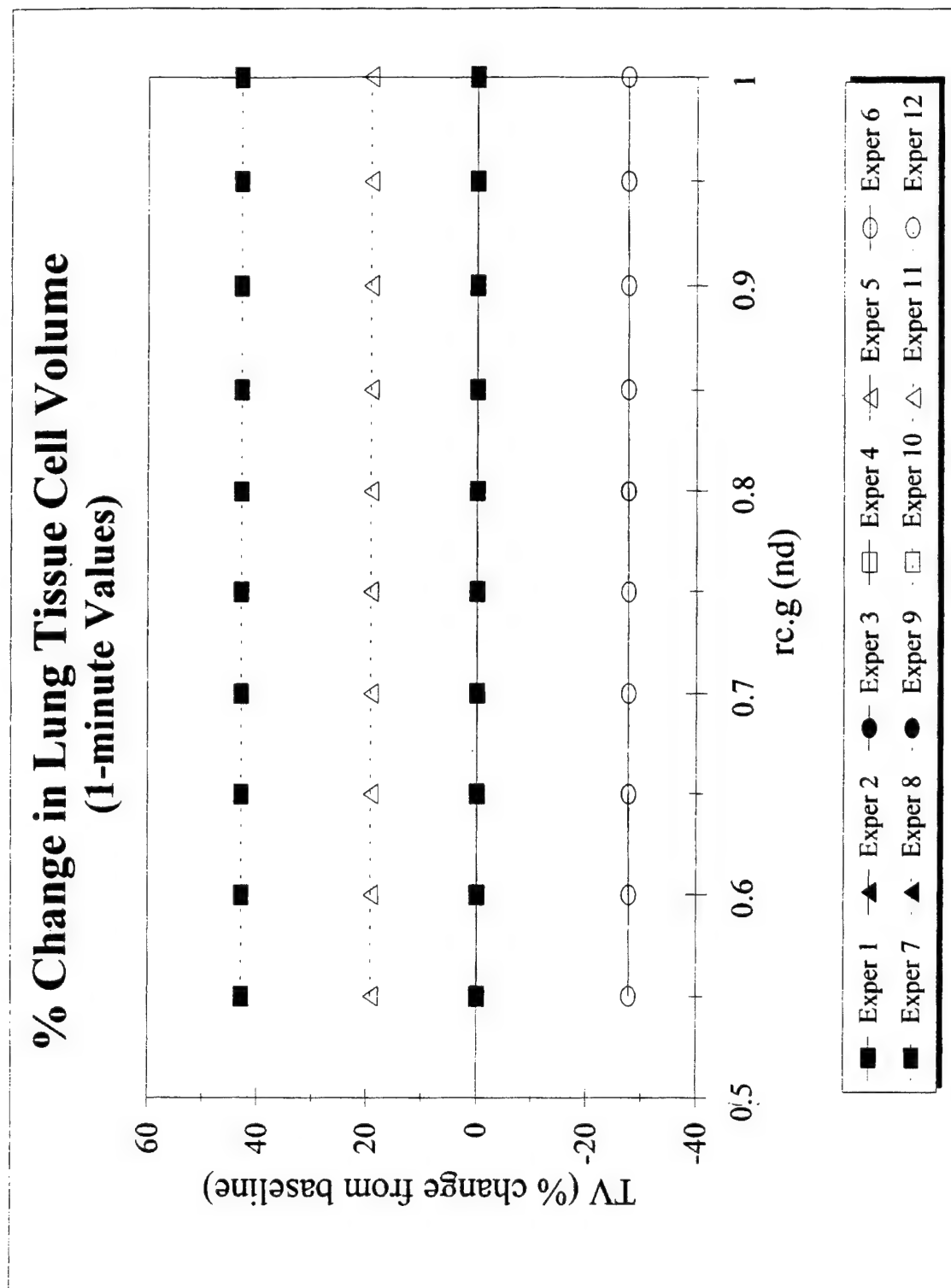


Figure C79

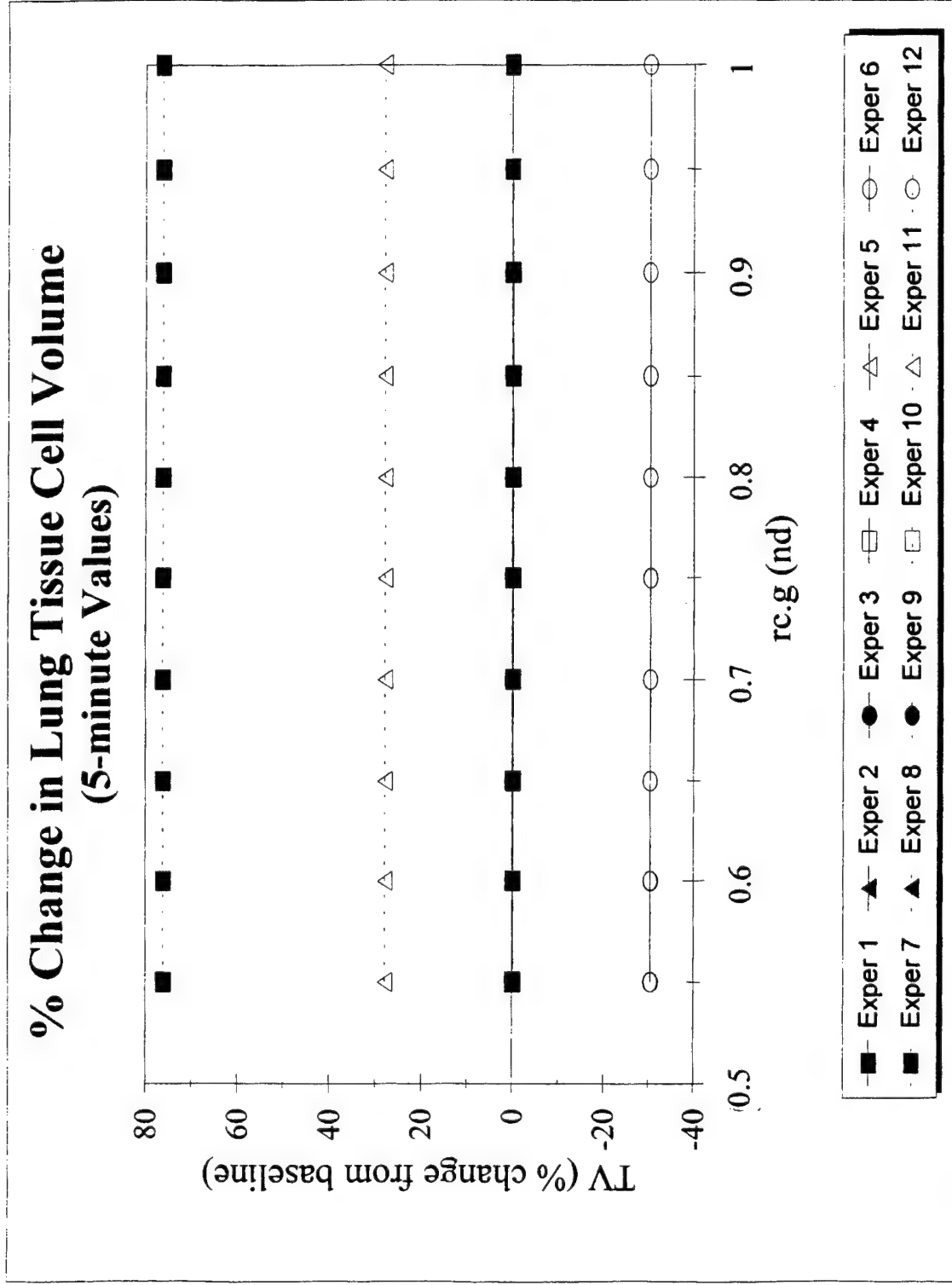


Figure C80

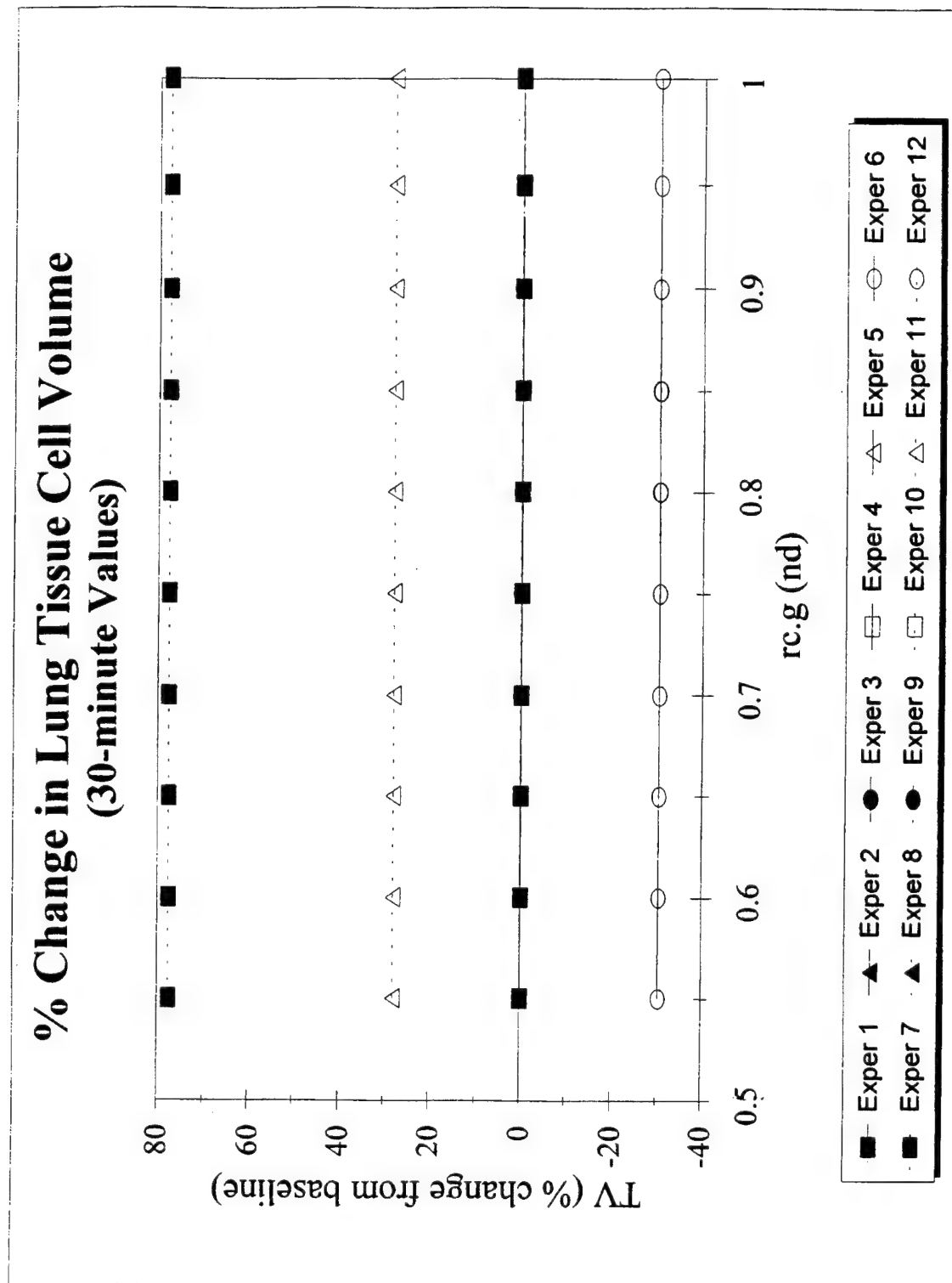


Figure C81

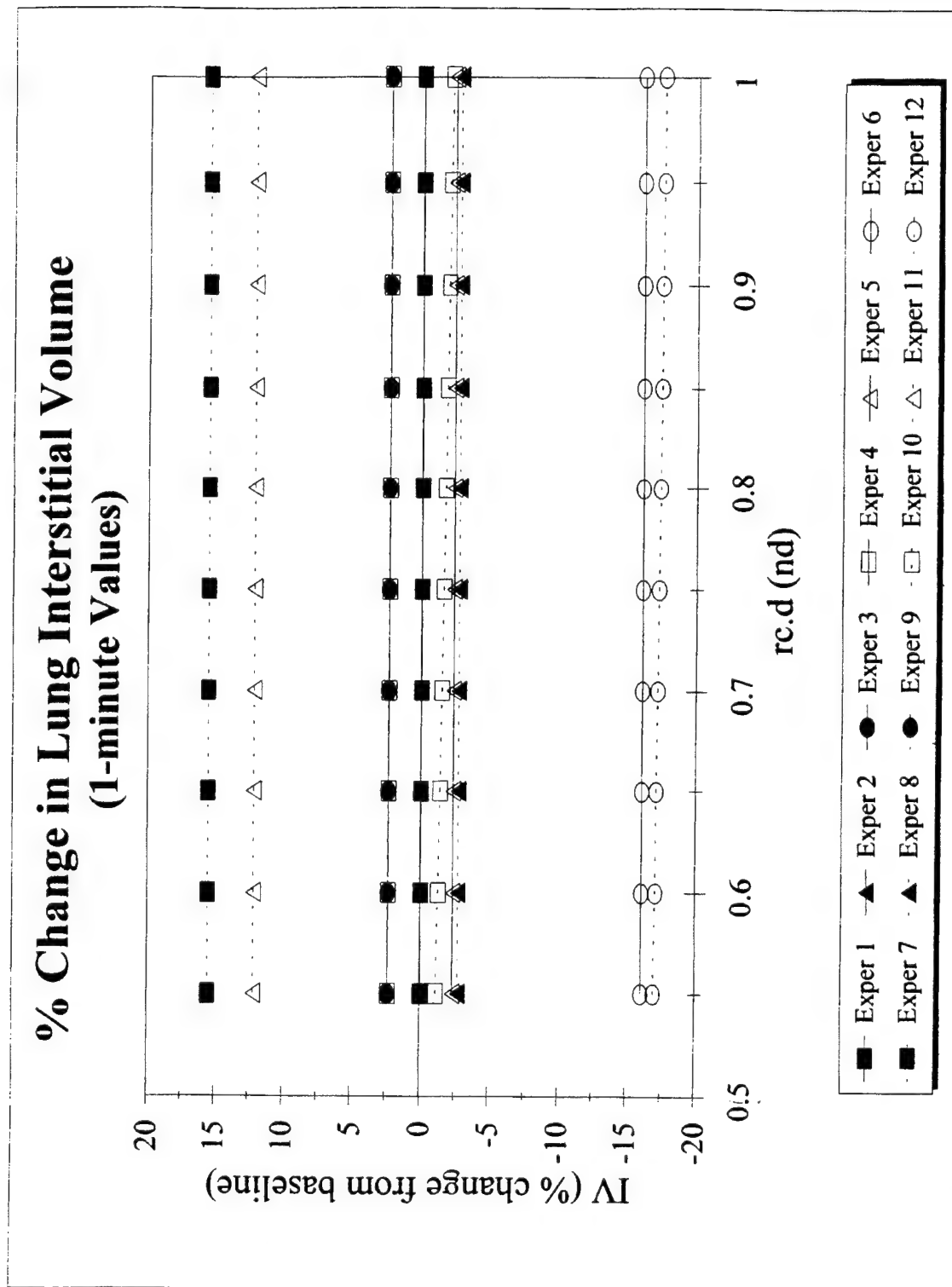


Figure C82

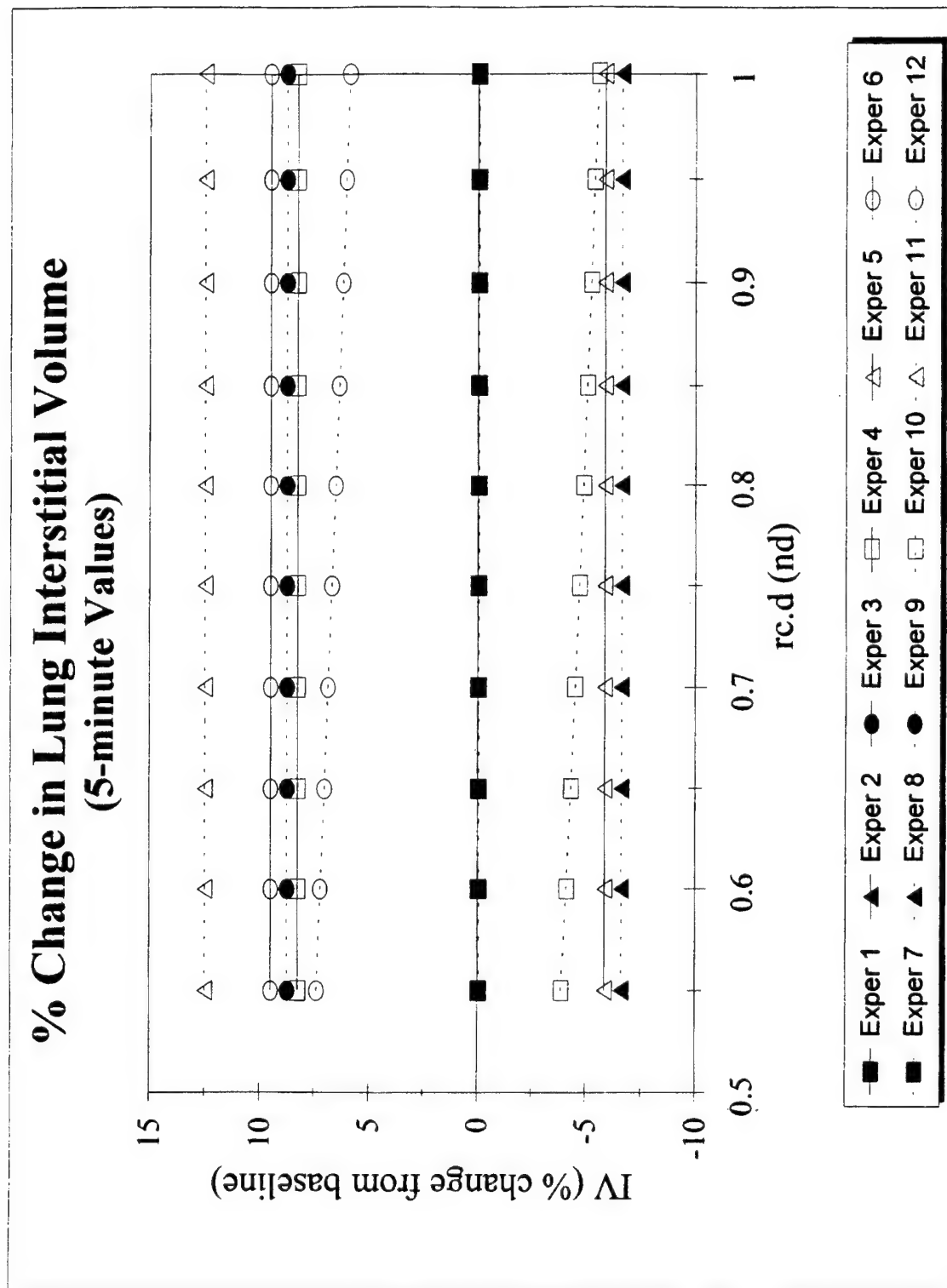


Figure C83

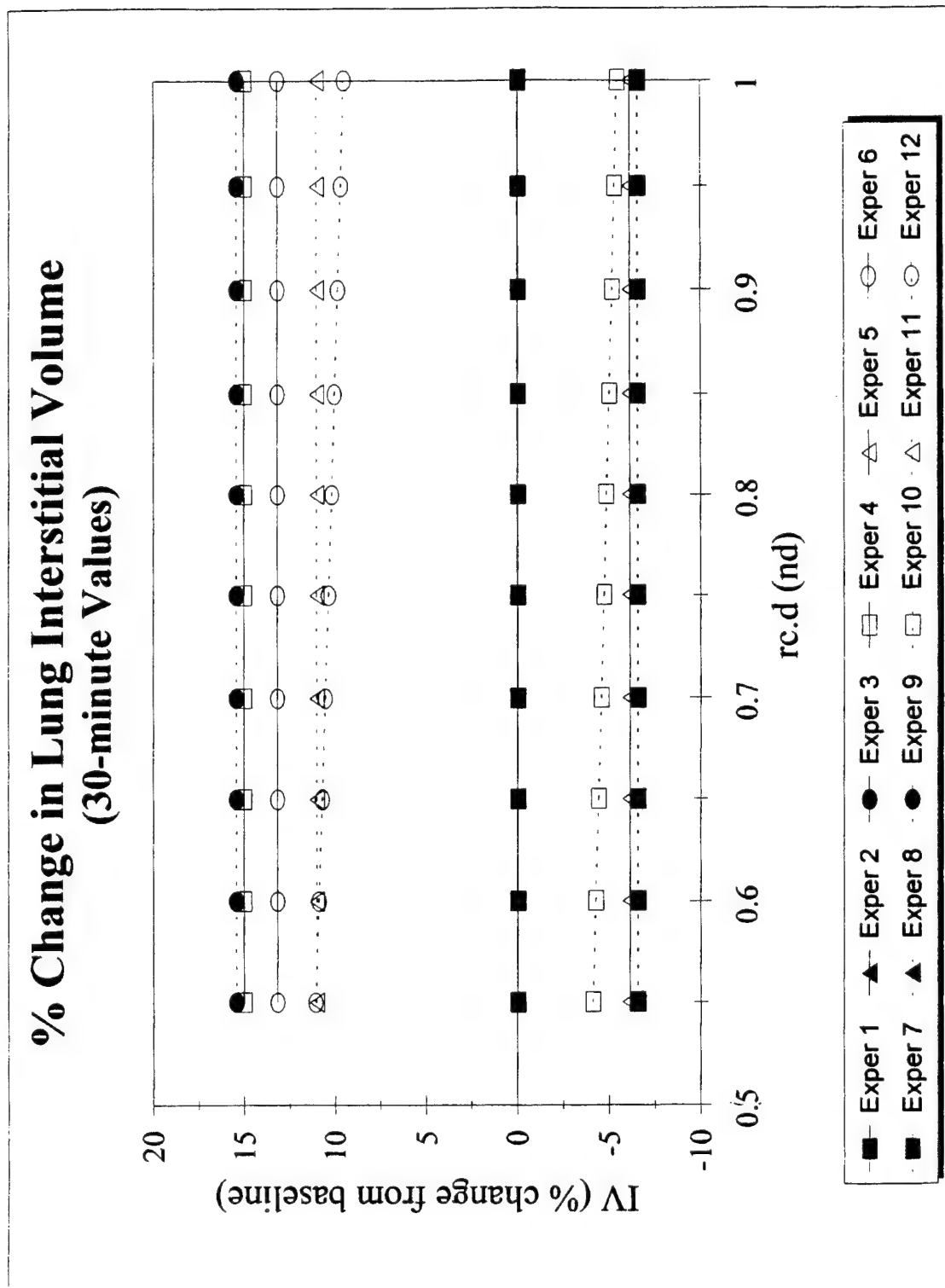


Figure C84

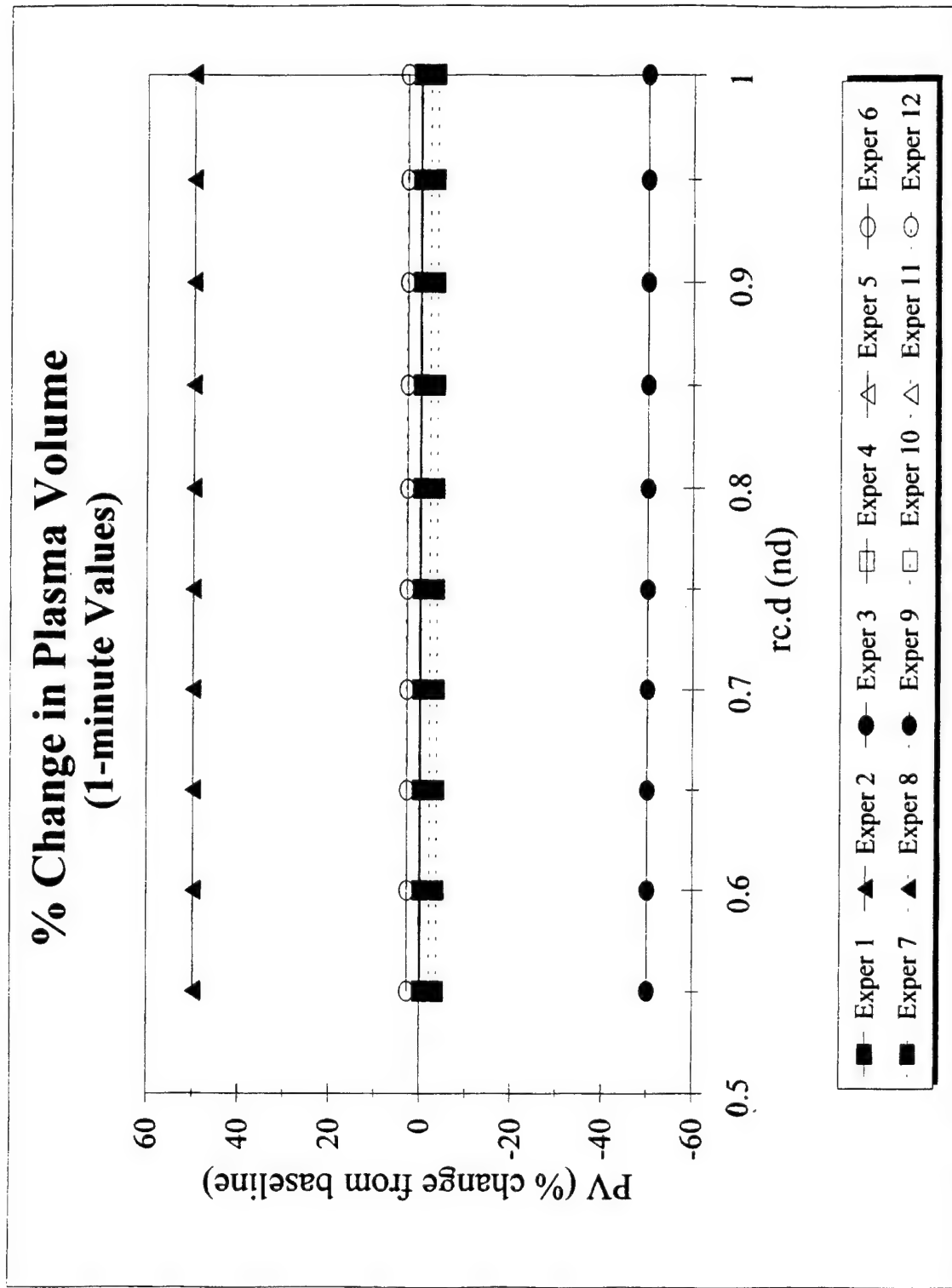


Figure C85

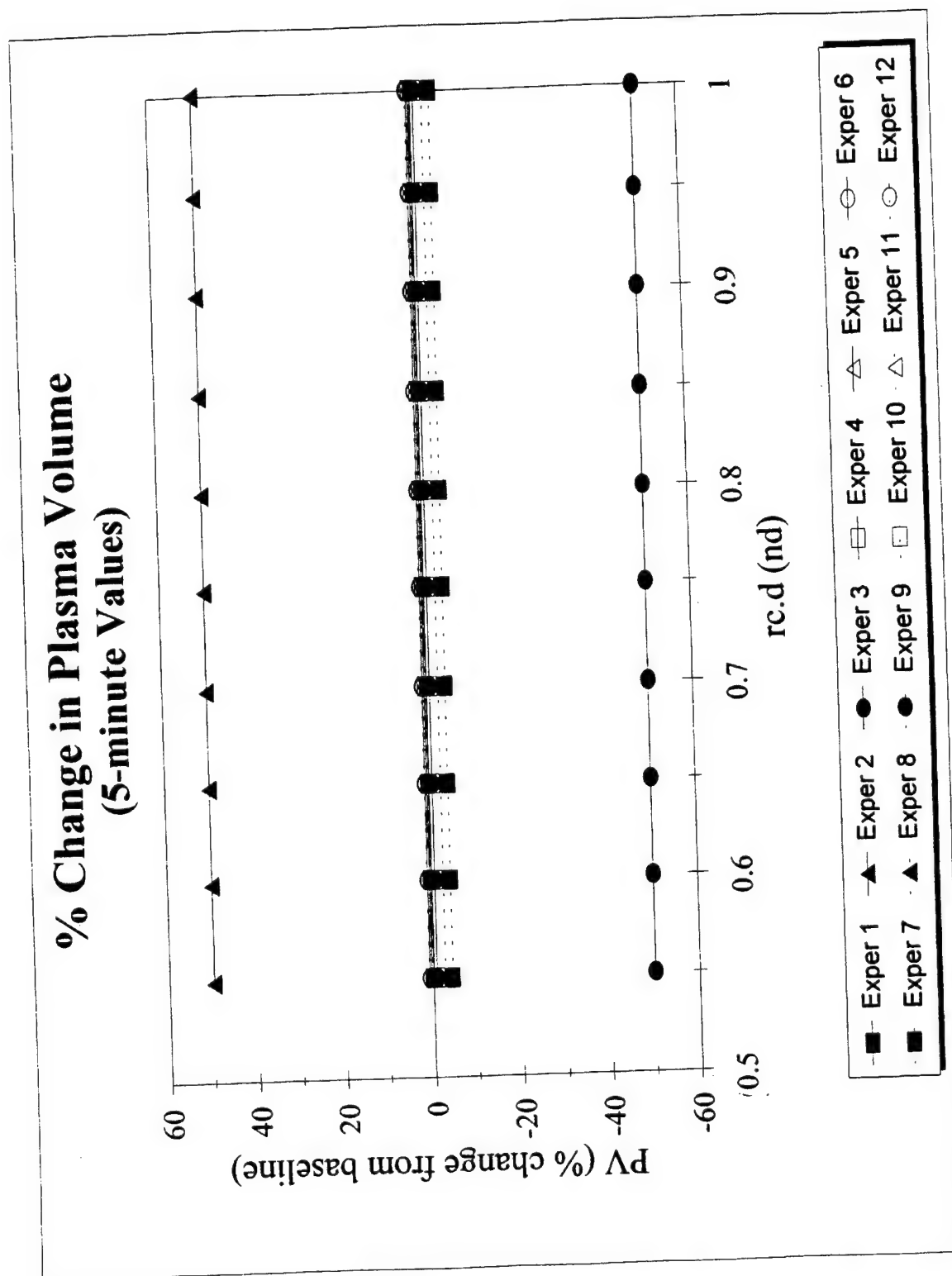


Figure C86

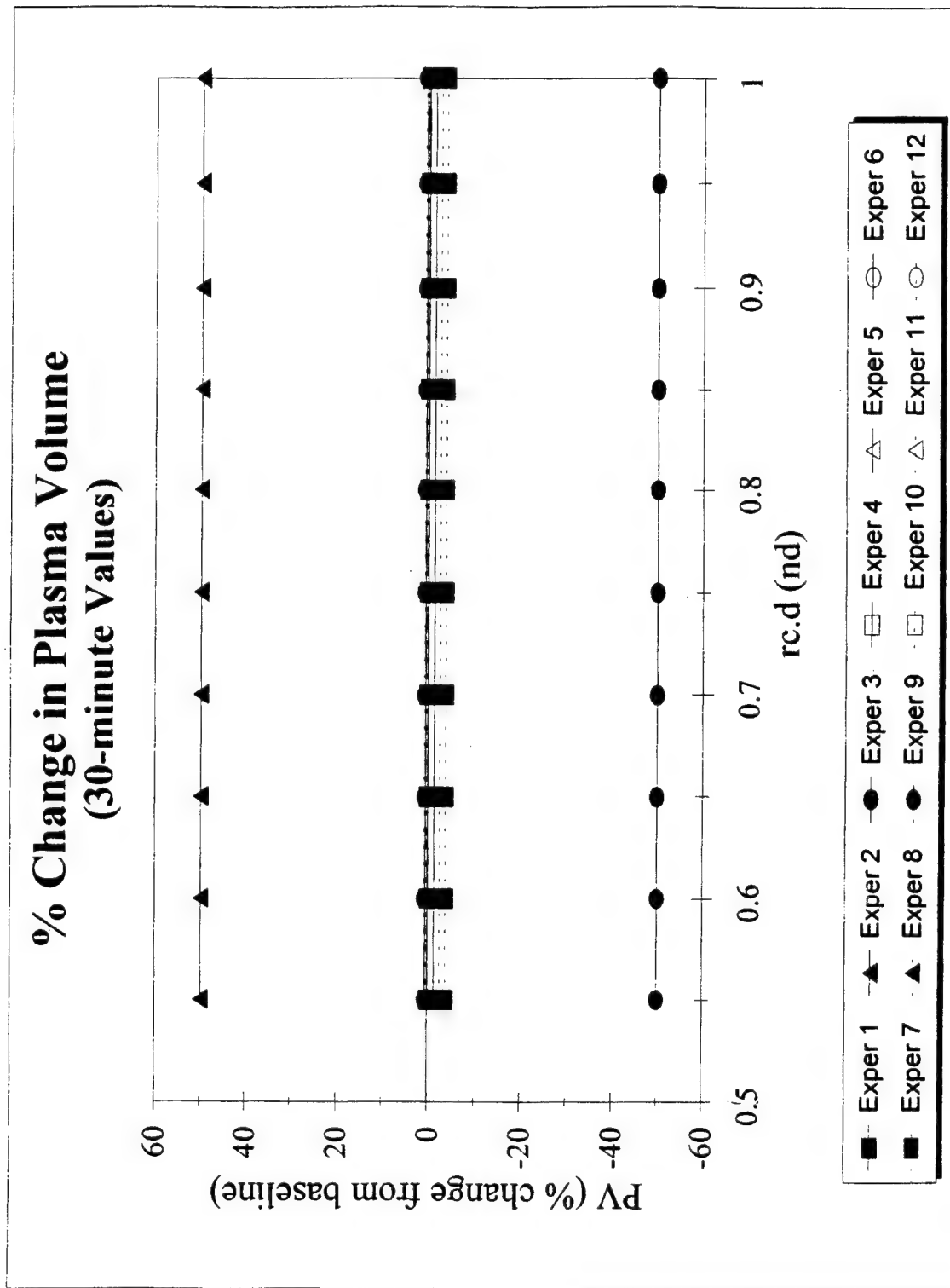


Figure C87

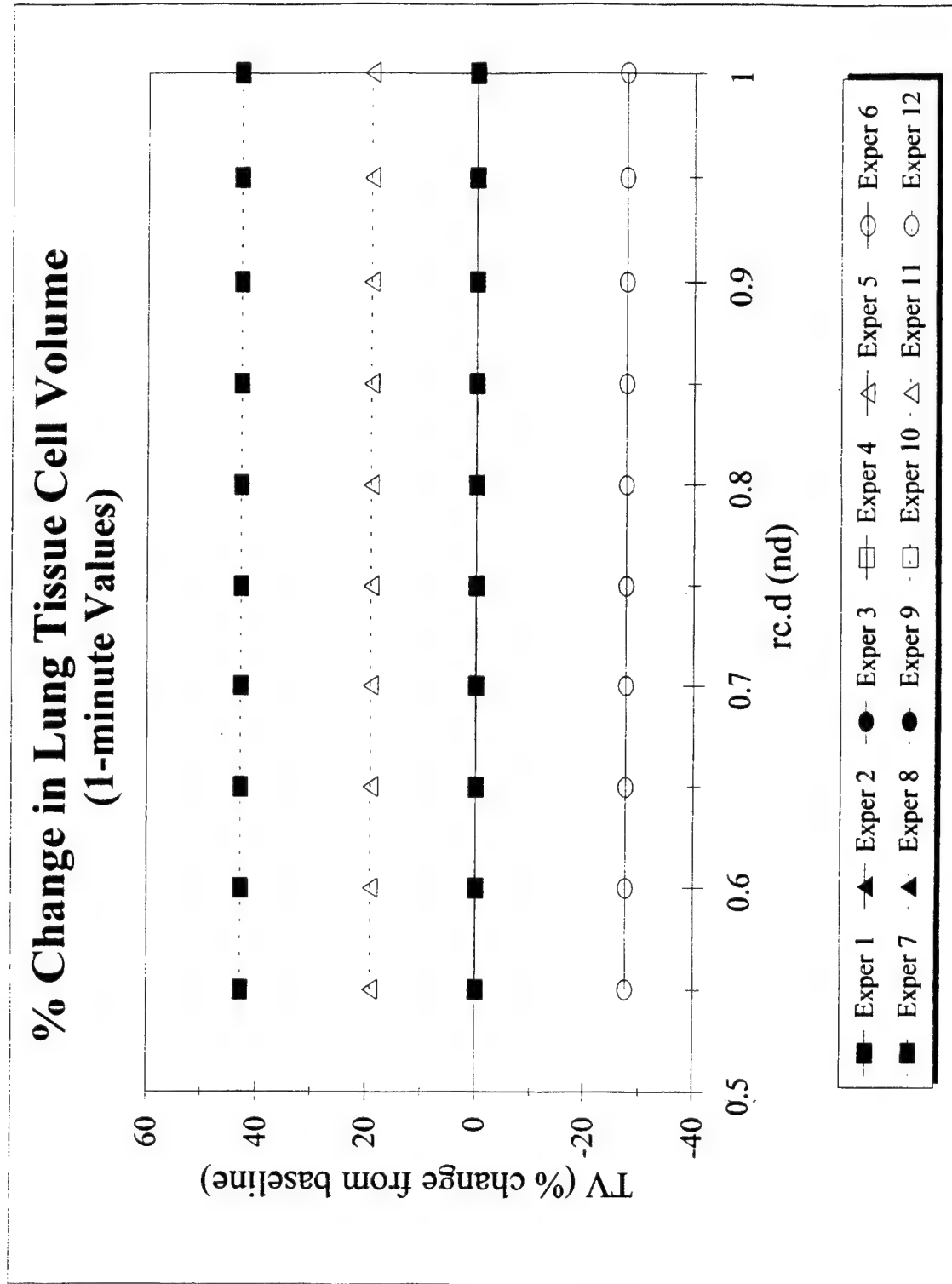


Figure C88

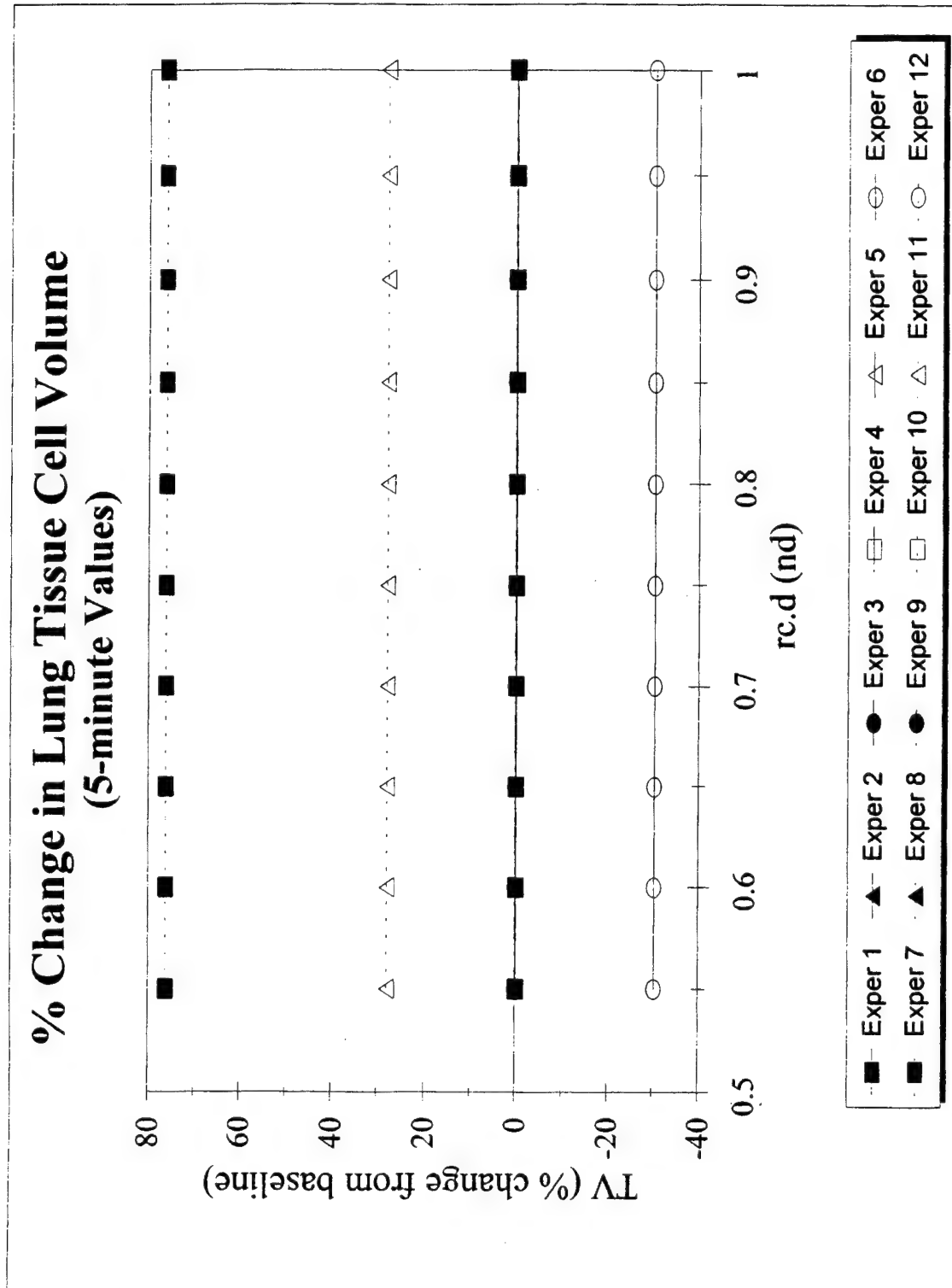


Figure C89

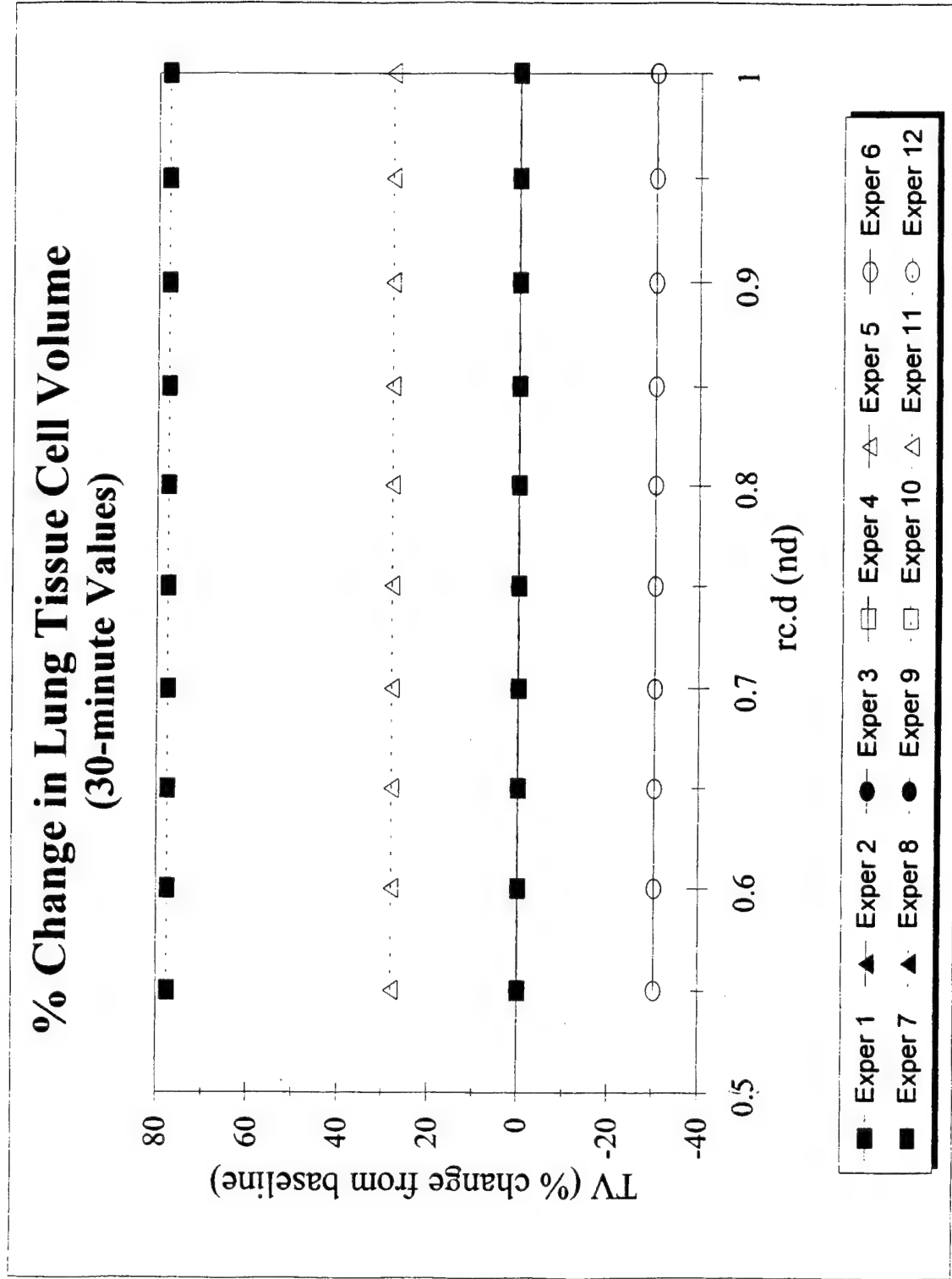


Figure C90

APPENDIX D

Model Predictions of Plasma, Pulmonary Interstitial, and Tissue Cell Volume Responses to Changes in Plasma NaCl

Preliminary Report 12/15/94
Contract # DAMD17-94-C4126

% Change in Interstitial Volume $k.p2i = 0.004$

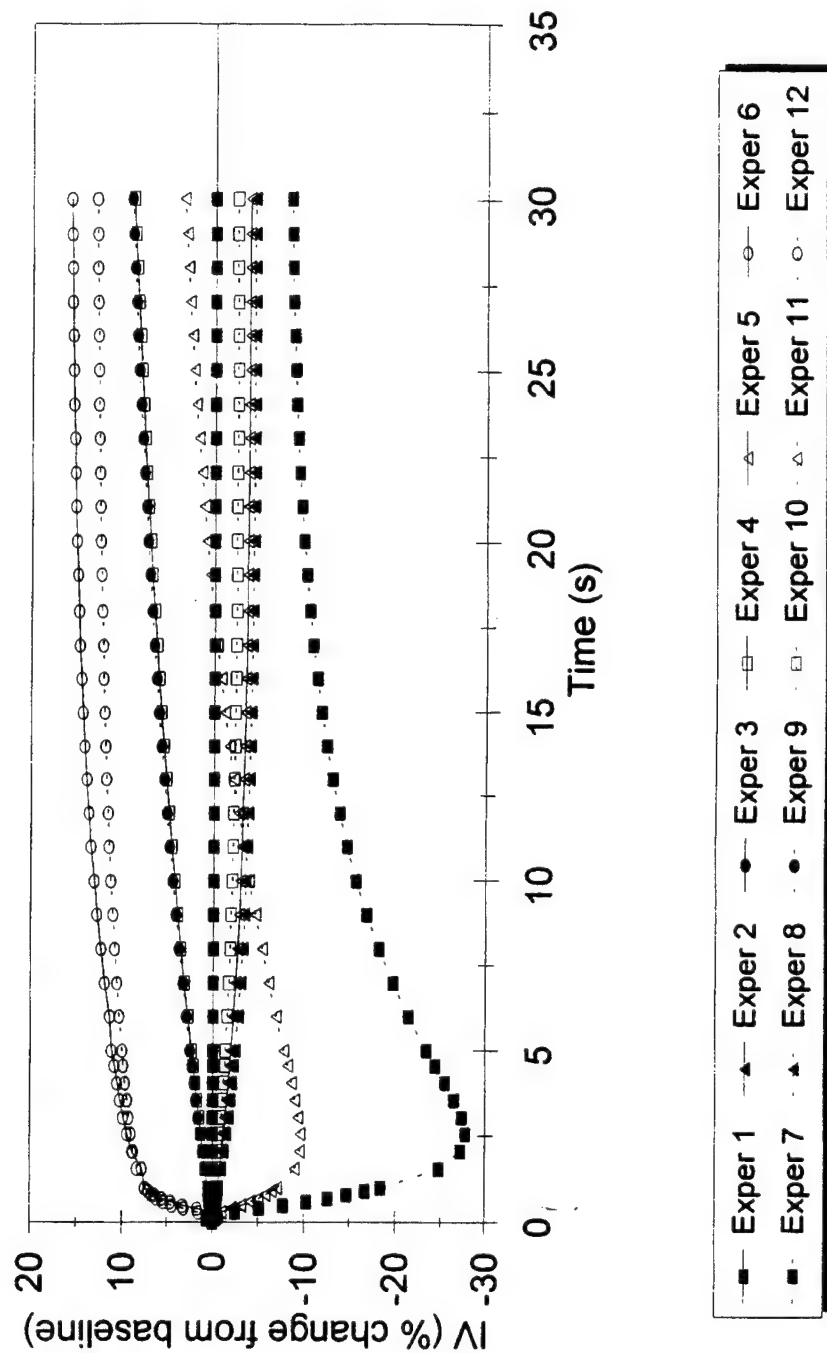


Figure D1

% Change in Interstitial Volume

$k.p2i = 0.04$

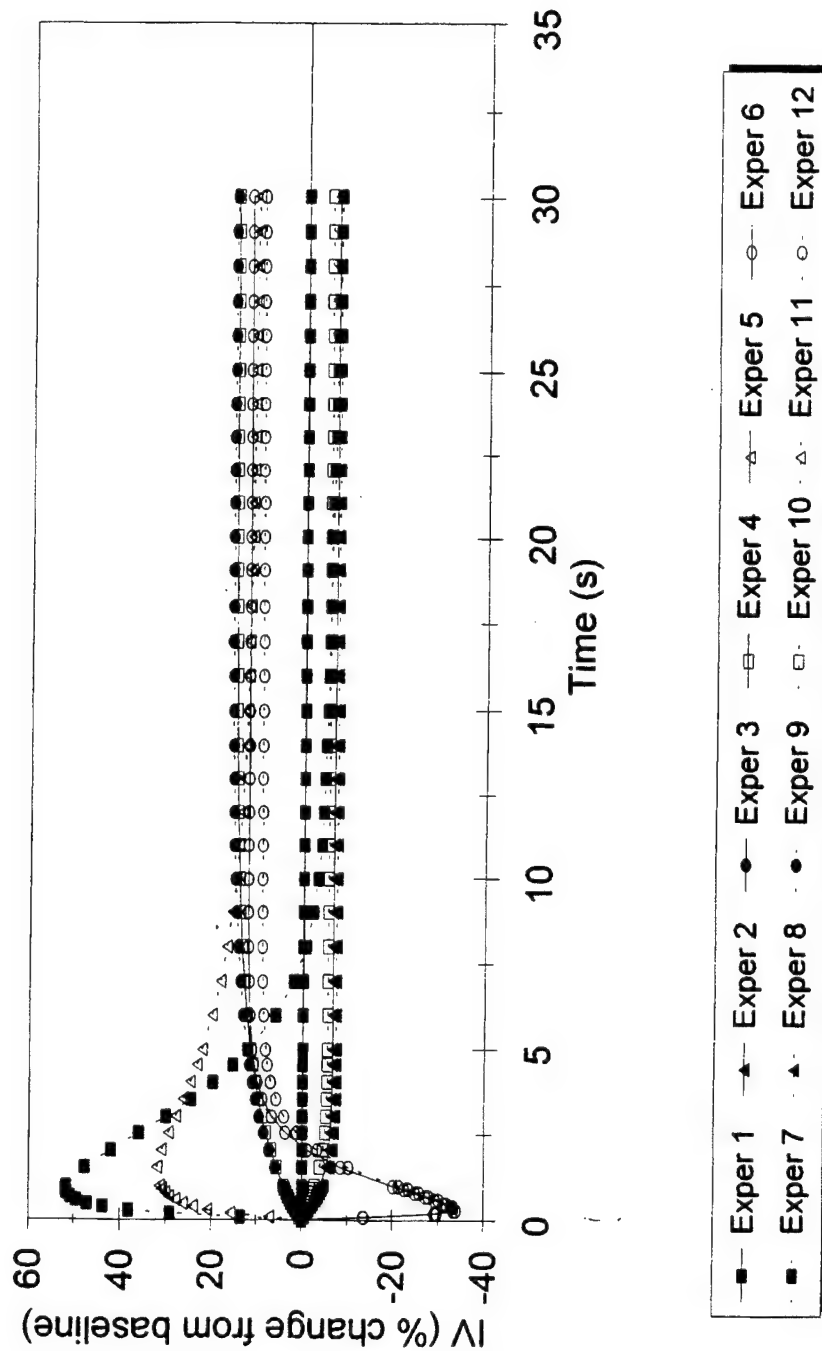


Figure D2

% Change in Plasma Volume

$k.p2i = 0.004$

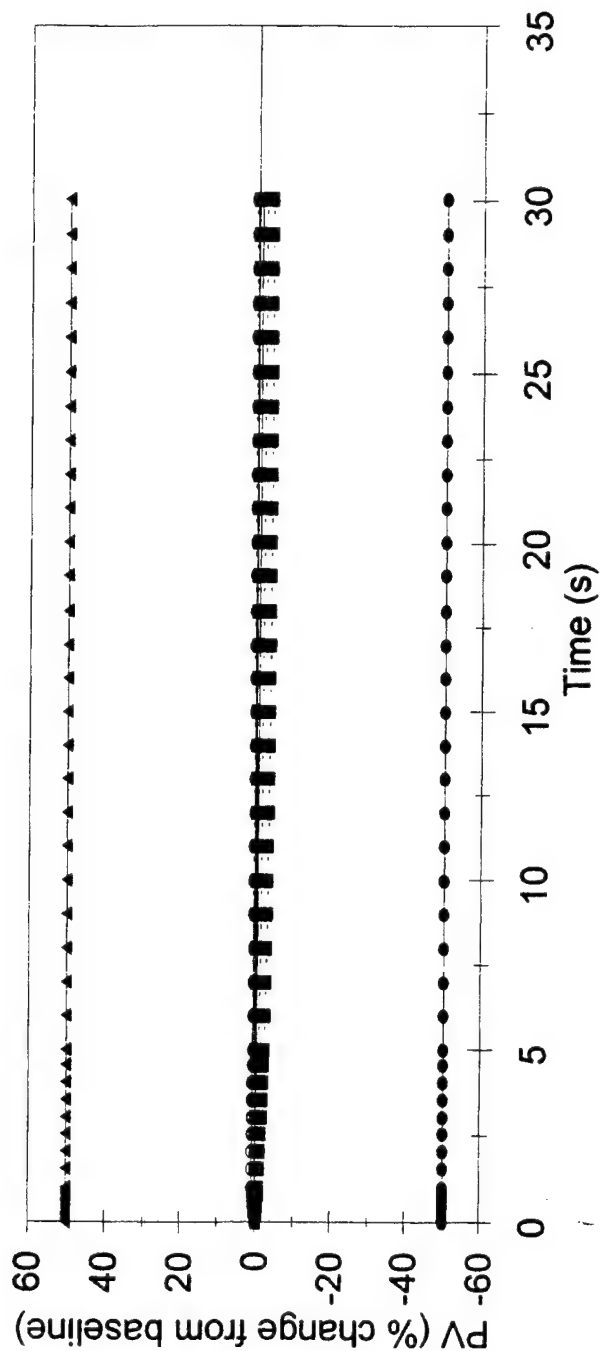


Figure D3

% Change in Plasma Volume

$k.p2i = 0.04$

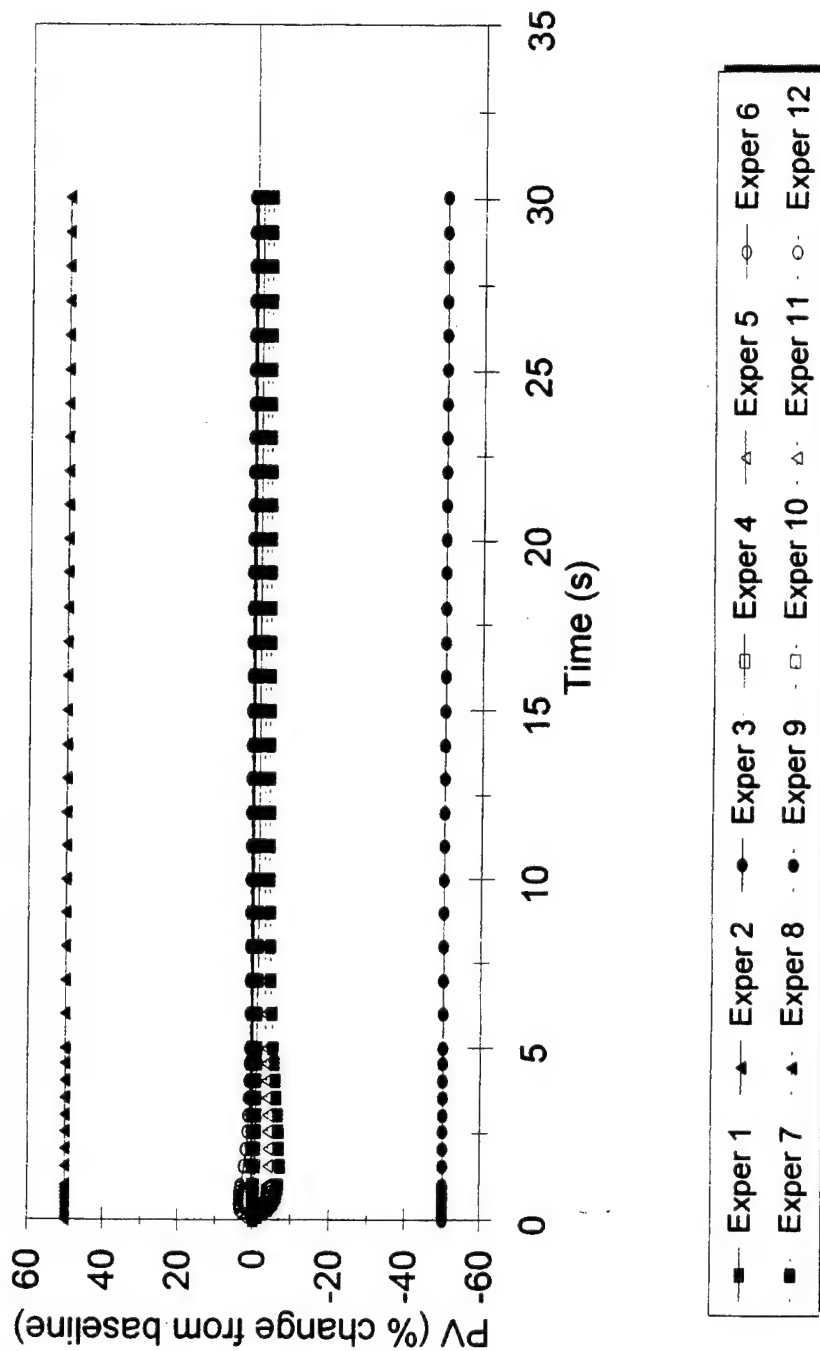


Figure D4

% Change in Lung Tissue Volume

$k.p2i = 0.004$

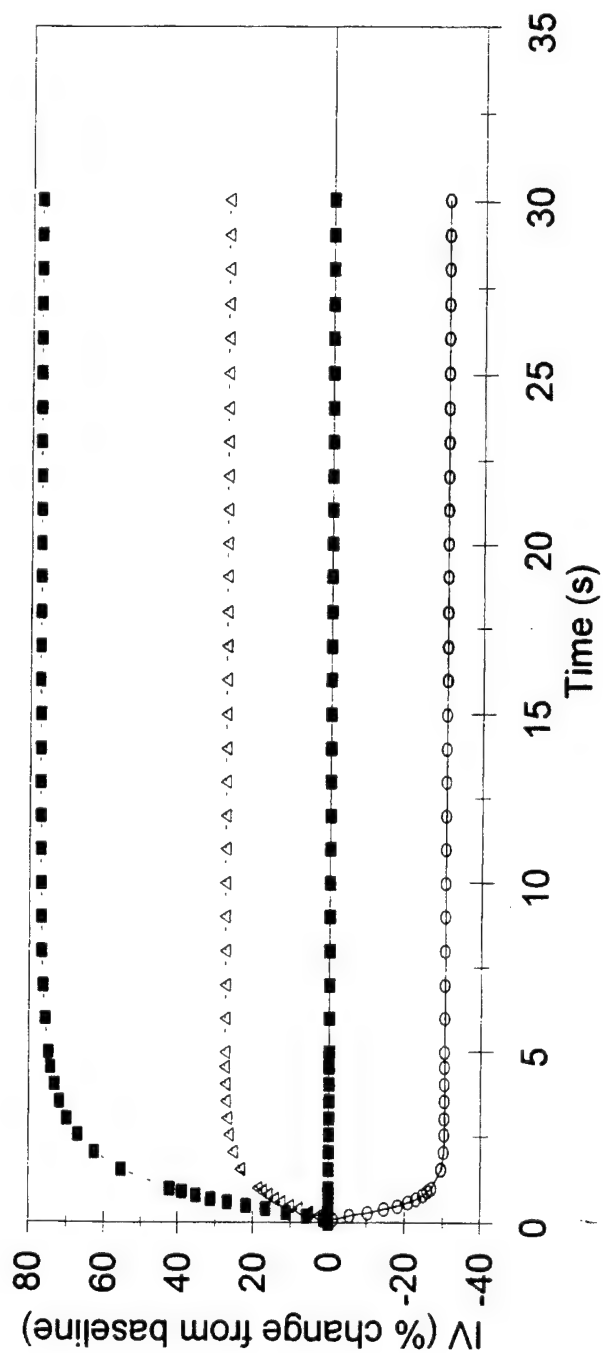


Figure D5

% Change in Lung Tissue Volume

$k.p2i = 0.04$

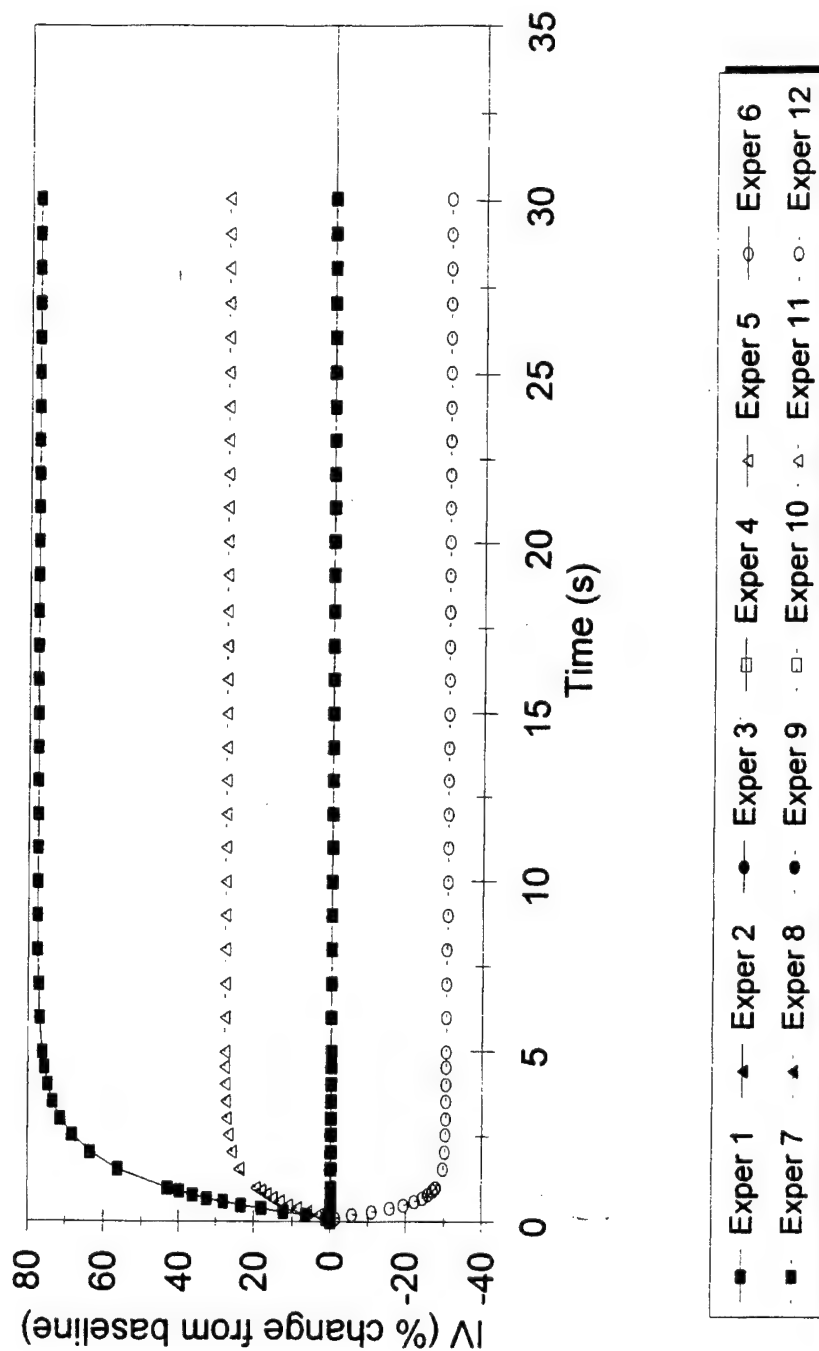


Figure D6

SOUTHWEST RESEARCH INSTITUTE

6220 CULEBRA ROAD • POST OFFICE DRAWER 28510 • SAN ANTONIO, TEXAS, USA 78228-0510 • (210) 684-5111 • TELEX 244846

March 9, 1995

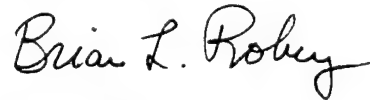
Donald P. Jenkins
Deputy Director for Defense Healthcare Technologies
ARPA/Defense Sciences Office
3701 North Fairfax Drive
Arlington, VA 22203-1714

Dear Sir,

Enclosed is the second quarterly report for work performed under contract no. DAMD17-94-C4126. This report covers the period from 1 December, 1994 to 3 March, 1995. Most of the work performed during this period focused on porting the existing cardiovascular and lung flux system models into the "C" language.

Please feel free to contact me at (210) 522-5115 if you have any questions or concerns regarding the technical aspects of this report. Please contact Ms. Sharon Rowe in our contracting office at (210) 522-3026 for any contractual or financial matters.

Sincerely,



Brian L. Robey
Project Manager

Enclosure



SAN ANTONIO, TEXAS
HOUSTON, TEXAS • DETROIT, MICHIGAN • WASHINGTON, DC

Quarterly Progress Report

1. Contract No. DAMD17-94-c4126
2. Report Date 15 March, 1995
- SwRI Project No. 12-6711
3. Reporting Period from 1 December, 1994 to 3 March, 1995.
4. PI Brian Robey
5. Phone (210) 522-5115
6. Institution Southwest Research Institute, San Antonio, Texas
7. Project Title Model for Trauma Patient Simulation and Automated Fluid Resuscitation
8. Current staff with percent effort of each on project

Brian Robey 1%

Jian Ling 48 %

Tammy Doherty 22 %

Jennifer Peacock 15 %

9. Contract expenditures to date (as applicable):

	this qtr/cumulative		this qtr/cumulative
Personnel	<u>10,338.52 / 14,848.22</u>	Travel	<u>0.00 / 0.00</u>
Fringe Benefits	<u>4,517.93 / 6,488.66</u>	Equipment/Supplies	<u>101.22 / 7,671.17</u>
Overhead	<u>17,530.62 / 25,177.53</u>	Facilities Capital	<u>1,545.06 / 2,219.02</u>

	this qtr/cumulative
Subtotal	<u>34,033.35 / 56,404.60</u>
Indirect Costs	<u> / </u>
Fee	<u>2,599.09 / 4,334.89</u>
Total	<u>36,632.44 / 60,739.49</u>

10. Administrative and Logistical Matters

During this reporting period, SwRI transferred principal investigating (PI) responsibilities from Tammy Doherty to Brian Robey. (Dr. Doherty accepted a position with the Army at Ft. Sam Houston, San Antonio). Mr. Robey co-authored the proposal and has had extensive coursework, both undergraduate and graduate, in mathematical modeling of physiological systems. Jian Ling, who has played a key role in model development since the beginning of the project, will continue to provide model programming under the guidance of Mr. Robey as well as Dr. Dean Winter, Manager of Bioengineering at SwRI. Mr. Robey plans to commit 25% of his time to this effort during the next quarter. Mr. Ling will continue to commit approximately 50% of his time.

Much of the effort during this reporting period concentrated on converting existing software to the "C" language. This conversion is intended to meet the real-time system requirements of simulating hemorrhage and resuscitation. In addition, the increased execution speed will permit faster refinement and training of the model control systems.

11. Scientific Progress

Task 1 - Passive System Model Development/Refinement:

The passive system models (i.e., cardiovascular flux and lung flux) were reviewed. We began refining the cardiovascular flux model through implementation in the "C" language. The lung flux model was ported to C (from Microsoft Quick BASIC) to speed model execution for real-time implementation. (See Task 10). The lung model port is complete except for testing. All coding is being performed to permit simple integration of both the cardiovascular and lung flux models.

Task 2 - Acquire Existing Data

SwRI continued to obtain hemorrhage data to support model development. At this time we have obtained literature with animal hemorrhagic data (primarily from the Letterman Army Institute of Research). This data, after tabulation, will allow us to initially refine the combined passive system models with the neural network and deterministic control systems (as part of developing the trauma patient simulator - TPSIM). We plan to obtain additional data from Dr. Fred Pearce at WRAIR to complete TPSIM development.

Task 3 - Deterministic Control System Model Development

As discussed in the last quarterly progress report, we began implementing the deterministic control system in C++ numerically using the Downhill Simplex method. We have delayed refinement of the deterministic control system while we convert the passive cardiovascular system model into C. Upon conversion of the cardiovascular system model, we will integrate this model with the deterministic control system and execute the models to obtain model coefficients, and consequently define the deterministic system.

Task 4 - Deterministic Model Refinement and Testing

Not started.

Task 5 - Neural Network Control System Development

We found that the NeuralWare software package would not meet our integration requirements with the passive system models. We designed and implemented a custom neural network program in C. As with the deterministic control system development, work toward refining/training the neural network will continue once the cardiovascular system model has been ported to C.

Task 6 - Neural Network Model Refinement and Testing

Not started.

Task 7 - Model Reliability and Accuracy Studies

Not started.

Task 8 - Control System Model Selection

Not started.

Task 9 - Development of Fluid Resuscitation Optimization Algorithm

Not started.

Task 10 - Real-Time System Development

We continued coding the lung flux model, cardiovascular system flux model, and neural network control model in C. This will allow fast run-time execution of these modules for system deployment as well as for training/refining the neural network and deterministic control systems.

Task 11 - Prototype System Development

Not started.

Task 12 - Review Clinical Data

Not started.

12. Plans For Next Quarter

- a. Finish coding the passive cardiovascular system flux model in C.
- b. Integrate the cardiovascular system flux model with the lung flux model.
- c. Integrate the deterministic control system model with the overall passive system model.
- d. Integrate the neural network control system with the overall passive system model.
- e. If time permits, begin optimizing and training both the deterministic and neural network control system models.
- f. Continue to acquire data for hemorrhage and resuscitation.

June 12-6711

SOUTHWEST RESEARCH INSTITUTE

6220 CULEBRA ROAD • POST OFFICE DRAWER 28510 • SAN ANTONIO, TEXAS, USA 78228-0510 • (210) 684-5111 • TELEX 244846

June 15, 1995

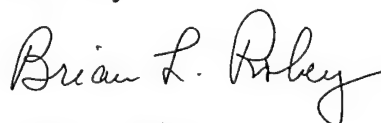
Donald P. Jenkins, Ph.D.
Deputy Director for Defense Healthcare Technologies
ARPA/Defense Sciences Office
3701 North Fairfax Drive
Arlington, VA 22203-1714

Dear Dr. Jenkins:

Enclosed is the ^{third} second quarterly report for work performed under contract no. DAMD17-94-C4126. This report covers the period from 4 March, 1995 to 26 May, 1995.

Please feel free to contact me at (210) 522-5115 if you have any questions or concerns regarding the technical aspects of this report. Please contact Ms. Sharon Rowe in our contracting office at (210) 522-3026 for any contractual or financial matters.

Sincerely,



Brian L. Robey
Project Manager
Biosciences & Bioengineering Department

Enclosure



SAN ANTONIO, TEXAS
HOUSTON, TEXAS • DETROIT, MICHIGAN • WASHINGTON, DC

Quarterly Progress Report

1. Contract No. DAMD17-94-c4126 2. Report Date 15 June, 1995
SwRI Project No. 12-6711
3. Reporting Period from 4 March, 1995 to 26 May, 1995.
4. PI Brian Robey 5. Phone (210) 522-5115
6. Institution Southwest Research Institute, San Antonio, Texas
7. Project Title Model for Trauma Patient Simulation and Automated Fluid Resuscitation
8. Current staff with percent effort of each on project

Brian Robey 5 %

Dean Winter 3 %

Jian Ling 37 %

9. Contract expenditures to date (as applicable):

	this qtr/cumulative		this qtr/cumulative
Personnel	<u>4,958.31 / 19,806.53</u>	Travel	<u>0.00 / 0.00</u>
Fringe Benefits	<u>2,166.79 / 8,655.45</u>	Equipment/Supplies	<u>58.50 / 7,729.67</u>
Overhead	<u>8,407.60 / 33,585.13</u>	Facilities Capital	<u>740.98 / 2,960.00</u>

	this qtr/cumulative
Subtotal	<u>16,332.18 / 72,736.78</u>
Indirect Costs	<u>/</u>
Fee	<u>1,247.32 / 5,582.21</u>
Total	<u>17,579.50 / 78,318.99</u>

10. Administrative and Logistical Matters

None to report during this period.

11. Scientific Progress

During this reporting period, the passive cardiovascular system model was implemented in the "C" language. The model was then run and compared against experimental swine data found in the literature. The model was then integrated with the neural network system control system model. The neural network model was trained using reinforcement procedures. The integrated model was then re-run and compared against the same experimental data. The model compared favorably with the experimental data. A preliminary report is attached which details the results of integrating the passive system model with the neural network control system.

Task 1 - Passive System Model Development/Refinement:

The passive system model of cardiovascular hemodynamics and fluid exchange was implemented in the "C" language. The passive model includes both the system circulation model and the lung circulation model. All coding was performed to permit easy integration with the adaptive cardiovascular system control model.

The stability of the passive model was tested. The passive system model was used to estimate the blood volume, mean blood pressure, hematocrit, and cardiac output after hemorrhage for experimental data found in the literature.

Task 2 - Acquire Existing Data:

Uncontrolled hemorrhage experimental data from swine were collected from the literature. The data included both conscious and anesthetized swine. The data were used to evaluate the passive system model and train the adaptive neural network-based cardiovascular control system model. Additional data is required for further refinement of the neural network model.

Task 3 - Deterministic Control System Model Development:

No work was performed toward integration of the passive system model with the deterministic control system. An initial deterministic cardiovascular control system was developed during the first quarter of this project. The next step in this task is integration of the deterministic model with the passive system model and evaluation of performance against the experimental data.

Task 4 - Deterministic Model Refinement and Testing:

Not started.

Task 5 - Neural Network Control System Development:

The feed-forward neural network was refined and integrated with the passive system model. The neural network was trained using one set of experimental data. A reinforcement-

based learning algorithm was utilized to train the network. Favorable preliminary results are included in the attached report.

Tasks 6-9:

Not started.

Task 10 - Real Time System Development:

The lung circulation model, cardiovascular system circulation model, and deterministic control system model have all been implemented in the "C" language. This work was the logical first step toward development of a real-time system.

Task 11- Prototype System Development:

Not started.

Plans For Next Quarter

- Additional experimental data will be collected through contacts at ARPA.
- The reliability and accuracy of the passive system will be tested using any additional acquired data.
- The neural network control system will be further trained and tested.
- The deterministic control system will be integrated with the passive system.
- The deterministic control system will be refined and tested.
- The results of the deterministic control system and neural network control system will be compared.

Preliminary Report on

**Model for Trauma Patient Simulation and Automated Fluid
Resuscitation: Implementation and Integration of a
Passive Cardiovascular System Model and a
Neural Network Control System**

June 15, 1995

**SwRI Project No. 12-6711
Contract No. DAMD17-94-C4126**

Prepared for:

**Director, U.S. Army Research Acquisition Activity
ATTN: SGRD-RMA-RC
Fort Detrick, MD 21702-5014
and
Deputy Director for Defense Healthcare Technologies
ARPA/Defense Sciences Office
3701 North Fairfax Drive
Arlington, VA 22203-1714**

Prepared by:

**Jian Ling and Brian L. Robey
Southwest Research Institute
San Antonio, Texas**



**SAN ANTONIO, TEXAS
HOUSTON, TEXAS • DETROIT, MICHIGAN • WASHINGTON, DC**

MODEL FOR TRAUMA PATIENT SIMULATION AND AUTOMATED FLUID RESUSCITATION: IMPLEMENTATION AND INTEGRATION OF A PASSIVE CARDIOVASCULAR SYSTEM MODEL AND A NEURAL NETWORK CONTROL SYSTEM

INTRODUCTION

This report describes the implementation and initial testing of a passive system model of cardiovascular hemodynamics and fluid exchange, a portion of the work being performed under contract no. DAMD17-94-C4126. The report also includes a description of the integration of the passive system model with an adaptive, neural network-based cardiovascular control system. Results from the initial training of the neural network are included as well. An integrated model, such as the one described in this report, will form the basis for the trauma patient simulator (TPSIM). All figures and diagrams for this report may be found in the Appendix.

This is a preliminary report. It is expected that the neural network control system will be further refined with additional experimental data. A final version of this report will be incorporated into the final project report to be submitted at the conclusion of this project.

Southwest Research Institute (SwRI) has also developed a preliminary adaptive deterministic model of the cardiovascular control system. After integrating the deterministic system with the passive system, SwRI will prepare an additional report. Both approaches will be compared and a control system approach will be selected for the TPSIM.

OVERALL PASSIVE SYSTEM MODEL

An arterial hemorrhage causes numerous hemodynamic changes to the circulatory system [1]. The change of blood volume causes blood pressure changes in all branches of the circulatory system. Changes in arterial or venous blood pressure will affect end-systolic volume and end-diastolic volume of the heart. Consequently, changes occur in cardiac output and mean arterial blood pressure. Capillary blood volume and plasma volume are also changed. This loss of blood also causes changes in solution concentrations which results in fluid and solution exchange among the capillaries, interstitial space, and tissue cells. The fluid movement from the interstitial space and tissue cells compensates for the blood loss but lowers the blood hematocrit. A significant decrease in hematocrit and cardiac output creates an oxygen debt to all organ systems.

It is the purpose of this mathematical modeling research to develop methods for predicting these changes in hemodynamic parameters. Prediction of hemodynamic parameters based on blood volume changes is the first step in the development of an automated fluid resuscitation system.

The passive cardiovascular system model [1] is comprised of three components: 1) cardiac ventricular mechanics, 2) systemic circulation, and 3) fluid and solute exchange between the capillaries, interstitial space, and tissue cells. The overall model is illustrated in Figure 1. In this model, the cardiac pump (or heart) is divided into right and left ventricles. The ventricles connect to a two-segment lung model to form the pulmonary circulation. For the systemic circulation, a single vascular pathway is used to represent all vital organs, the non-muscle vasculature, and the muscle vasculature. The purpose of this simplification is to reduce the overall complexity during initial development of a cardiovascular control system model. Inclusion of the three parallel vascular pathways described in [1] does not significantly alter cardiovascular hemodynamic responses, but only redistributes the blood flow during hemorrhage. For a similar reason, lung microvascular fluid exchange is also not included in this model. However, these vascular pathways as well as the lung-flux model will be included in the final TPSIM to determine detailed blood distribution among the vasculatures after hemorrhage, and to detect pulmonary edema during resuscitation.

Appropriate modeling techniques have been employed in the development of each component of the passive system model. For example, a compartmental modeling approach has been used for a large portion of the circulatory system. Compartments are described by blood volume, blood pressure, and compliance. Resistance to blood flow is included for all inter-connected compartments. A three-compartment (plasma, interstitial fluid, and tissue cell) model was used to simulate microvascular fluid and solute exchange. An overall passive system flow chart depicting computational procedures is illustrated in Diagram 1. The following sections provide detailed descriptions of the techniques used for all passive system model components.

Cardiac Ventricular Mechanics

A viscoelastic wall model [1] was used to model the heart as a pump to determine stroke volume. (Stroke volume is used to calculate cardiac output). In the diastolic period, the relationship of the right and left ventricular pressure $p(t)$ and volume $v(t)$ can be described by the following differential equation system:

$$\begin{cases} \frac{dp(t)}{dt} = -\frac{\kappa}{\xi} \cdot p + (\alpha + \kappa) \cdot \left(\frac{P - p(t)}{R} \right) + \frac{\kappa}{\xi} \cdot \alpha \cdot (v - V_0) \\ \frac{dv(t)}{dt} = \frac{P - p(t)}{R} \end{cases} \quad 1)$$

where κ is the heart spring coefficient, ξ is the heart damping coefficient, α is the heart fill coefficient, V_0 is the unstressed heart volume, P is the venous pressure for right heart computation and the pulmonary pressure for left heart computation, R is the venous to right heart resistance for the right heart and the pulmonary to left heart resistance for left heart. For the systolic period, an "active" function, Ψ_{t+1} , is included in the equations to simulate the contraction of the heart. The system of equations for systole are:

$$\begin{cases} \frac{dp(t)}{dt} = -\frac{\kappa}{\xi} \cdot p + (\alpha \cdot \psi \cdot t + \alpha + \kappa) \cdot \left(\frac{P - p(t)}{R}\right) + \left(\alpha \cdot \psi + \frac{\kappa}{\xi} \cdot (\alpha \cdot \psi \cdot t + \alpha)\right) \cdot (v - V_0) \\ \frac{dv(t)}{dt} = \begin{cases} \frac{P - p(t)}{R} & P < p(t) \\ 0 & P \geq p(t) \end{cases} \end{cases} \quad 2)$$

where ψ is the systolic emptying coefficient, which has a larger value for the left heart and smaller value for the right heart. For the right heart, P is the pulmonary pressure and R is the right heart to pulmonary resistance. For the left heart, P is the arterial pressure and R is the left heart to arterial resistance.

According to the equations, any change of venous, pulmonary, or arterial pressure (i.e., the preload and afterload of the right heart and of the left heart) will cause changes in the right and left heart end-systolic and end-diastolic volumes. These volume changes determine stroke volume. Figure 2 illustrates the determination of the right and left heart stroke volumes and cardiac output based on current hemodynamic conditions.

Systemic Circulation

The blood out-flow from the right and left ventricles provides the blood in-flow to the lung (via the pulmonary artery) and systemic circulation (via the aorta), respectively. The blood in-flow and out-flow of a compartment (i.e., lung, arteries, capillaries, or veins) determine the blood volume change of that compartment. The compliance (or capacitance) of a compartment defines the blood pressure decrease that occurs when blood volume decreases. The blood pressure affects the in- and out-flow of the compartment. Figure 3 illustrates the interdependency of blood flow, blood volume, and blood pressure with the resistance and compliance of compartments. These physical relationships can be represented by the following set of equations:

$$Q_{i,i+1} = \frac{P_i - P_{i+1}}{R_{i,i+1}} \quad 3)$$

$$\frac{dV_i}{dt} = Q_{i-1,i} - Q_{i,i+1} \quad 4)$$

$$P_i = \frac{V_i - V_{0i}}{C_i} \quad 5)$$

where $i-1$ indicates an up-stream compartment, and $i+1$ indicates a downstream compartment. Q , V , and P are the blood flow, blood volume, and blood pressure of the compartment. V_0 is the unstressed volume of the compartment. R and C are the resistance and compliance, respectively. Solutions to these equations provide necessary input to calculations of cardiac output, mean arterial pressure, fluid flux across the capillary and interstitial walls, oxygen debt, as well as other hemodynamic parameters.

Fluid and Solute Exchange between the Capillaries, Interstitial Space, and Tissue Cells

Capillaries, interstitial space, and tissue cells were studied as a three-compartment model. Plasma exchange and solute exchange continually occur among these three compartments [1]. The plasma out-flow from the tissue cells and from the interstitial space into the capillaries compensates for blood loss during hemorrhage. The plasma exchange rate is determined by both compartmental and osmotic pressures. The osmotic pressure is determined by solute concentration. This fluid exchange (or movement) between the individual compartments is illustrated in Figure 4. The plasma, interstitial, and tissue volume changes can be described by the following mass balance equations:

$$\begin{aligned}\frac{dV_P}{dt} &= L_v - J_{v,CI} \\ \frac{dV_I}{dt} &= J_{v,CI} - L_v - J_{v,IT} \\ \frac{dV_T}{dt} &= J_{v,IT}\end{aligned}\tag{6}$$

where the subscripts P, C, I, and T indicate the plasma, capillary, interstitial, and tissue, respectively. L_v is the rate of lymph flow and J_v is the rate of fluid flux from compartment i to j. The Kedem-Katchalsky equations are used to describe the fluid flux across the capillary and interstitial walls:

$$J_{v,CI} = k_{v,CI} \cdot \left[(P_C - P_I) - \sum \sigma_{s,CI} \cdot (\Pi_{s,P} - \Pi_{s,I}) \right]\tag{7}$$

$$J_{v,IT} = k_{v,IT} \cdot \left[(P_I - P_T) - \sum \sigma_{s,IT} \cdot (\Pi_{s,I} - \Pi_{s,T}) \right]\tag{8}$$

where Π indicates the osmotic pressure. Similar equations are used to model solute exchange for determination of osmotic pressures.

Calculation of Systemic Hemodynamic Parameters

1) Total Blood Volume (V_B), Hematocrit (Hct), and Blood Viscosity (σ_B)

During hemorrhage, the total blood volume change is determined by the arterial hemorrhage rate, venous hemorrhage rate, lymphatic return rate, capillary-interstitial fluid exchange rate, and fluid resuscitation rate. The hematocrit can be determined by the current blood volume and current red blood cell volume (after accounting for red blood cell loss through hemorrhage). The blood viscosity is closely related to the hematocrit. The empirical formula [2] used to estimate blood viscosity is:

$$\sigma_B = 1.14 + 0.0235 \cdot Hct\tag{9}$$

2) Cardiac Output (CO) and Mean Arterial Blood Pressure (MAP)

Cardiac output is the average left heart to arterial blood flow per minute. It is the product of left heart stroke volume and heart rate. Mean arterial blood pressure can be estimated through cardiac output and left heart to arterial resistance.

3) Oxygen Debt (O_2 Debt)

Oxygen debt level is the critical parameter which must be controlled during hemorrhage for survival of the trauma patient. Oxygen debt is the accumulated difference between the maximum oxygen available for consumption and minimum oxygen required [2]. It can be estimated by the following formula:

$$\frac{dO_2 Debt}{dt} = MinO_2R - E_{O_2} \cdot C_{O_2} \cdot Q_{AV} \quad 10)$$

$$\text{where } C_{O_2} = (1.36) \cdot (0.97) \cdot (0.335) \cdot Hct + 0.003 \quad 11)$$

and $MinO_2R$ indicates the minimum oxygen required, E_{O_2} is the maximum oxygen extraction ratio, C_{O_2} is the arterial oxygen concentration, and Q_{AV} is the arterial-venous blood flow rate.

Solution of Equations and Model Implementation

Model differential equations were solved numerically using the fourth order Runge-Kutta formula. A time step of 0.014 minutes was used to obtain stable solutions. The overall passive system model was written in the "C" language and implemented on a 486-100Mhz personal microcomputer. Initial conditions and constants were obtained from [1].

NEURAL NETWORK CONTROL MODEL

A cardiovascular control system model was designed to simulate the effects of baroreceptor-mediated sympathetic activity, vaso-active hormones, and oxygen debt on hemodynamics during hemorrhage (see Figure 5). A neural network system was used as the cardiovascular controller. Neural networks are able to handle nonlinear relationships between inputs and outputs. The oxygen debt, the change in blood volume, the change in mean blood pressure, and the change in blood viscosity were assumed as the causes of the change in heart rate, heart strength (right and left heart end-systolic volume), arteriolar resistance, venous resistance, and venous compliance during hemorrhage. The former were inputs to the neural network controller and the latter were outputs of the controller. During execution of the overall combined system (i.e., passive system plus cardiovascular control system), the outputs of the controller are passed to the passive system which then calculates and updates hemodynamic parameters. Diagram 2 illustrates the overall flow of a TPSIM system that incorporates a neural network approach.

In this preliminary design, a three-layer feed-forward neural network with four input nodes, three hidden nodes, and six output nodes was used (see Figure 6). Existing experimental animal data was used to train the weights of the neural network. During "training" of the neural network, the outputs of the network were supplied as inputs to the passive system for calculation of cardiovascular parameters. The cardiovascular parameters MAP, Hct, and CO calculated by the passive system model as well as heart rate (HR) as determined by the neural network were compared to experimental data. The error of the comparison was used to adjust the weights of the neural network. Since the direct output of the neural network was not easy to measure (except HR), a back-propagation algorithm was not used. Instead, a reinforcement learning algorithm that incorporates directed random search was used in the design.

Neural Network Implementation

The neural network model was written and implemented in the "C" language. No neural network software packages were used. This approach provided increased flexibility in both network development and integration with the passive system model.

MODEL TESTING AND RESULTS

Passive System Only

Responses of both conscious and anesthetized swine to an uncontrolled aortotomy hemorrhage have been studied by Brickell et al. [3, 4]. The uncontrolled hemorrhage lasted about five minutes with an estimated 33% (23.1 ml per kg body weight) loss in normal blood volume. There was no fluid resuscitation during Brickell's experiment. If we assume that the hemorrhage rate declines exponentially with a time constant (τ) of one minute, the hemorrhage rate can be described as follows [2]:

$$\begin{aligned}
 H(t) &= H_0 \cdot e^{-kt} + (R/k) \cdot (1 - e^{-kt}) \\
 k &= \ln(2)/\tau \\
 R &= (23.1) \cdot k^2 / (5 \cdot k + (1 - e^{5k})) \\
 H_0 &= R \cdot (1 - e^{5k}) / k
 \end{aligned}
 \tag{12}$$

The MAP, CO, HR, and hematocrit were measured at 0, 10, 20, 35, 65, 95 and 125 minutes after the start of hemorrhage. The experimental data were compared with data calculated by the passive system model. The cardiovascular control system was not included in the calculation. Therefore, the heart rate, the arterial resistance, the venous resistance, and the venous compliance remained constant during model execution. Figure 7 shows the calculated changes in hemodynamic parameters after the onset of hemorrhage. The blood volume (BV or V_B) decreased to about 70% of the normal value after five minutes of hemorrhage, and then gradually returned to approximately 83% of normal. The plasma exchange among the capillary, interstitial space, and tissue cells partially compensated for a portion of the changes in blood volume. The MAP and CO

decreased to about 5% of the normal value immediately after the hemorrhage and then gradually recovered to approximately 50% of normal. The hematocrit decreased to about 80% of the normal value. The oxygen debt steadily increased from 0 mlO₂/kg to about 60 mlO₂/kg during the hemorrhage (primarily due to Hct decrease). The debt continued to increase even after the MAP and CO were stabilized at 60 minutes after the hemorrhage. Data from hemorrhaged dogs indicates that an oxygen debt of 160 mlO₂/kg is almost always fatal [5].

Individual parameter comparisons between the experimental data and the calculated data are shown in Figures 8 (MAP), 9 (Hct), and 10 (CO) for conscious swine and Figures 11 (MAP), 12 (Hct), and 13 (CO) for anesthetized swine. For conscious swine, there are larger differences between the experimental data and model calculated data (except hematocrit). However, the trends compared favorably between experimental and calculated data. The larger difference is not surprising since the neural and hormonal control system was not yet included in the model. For anesthetized swine, there are relatively small differences between the experimental data and model calculated data. Given these results, it is hypothesized that the cardiovascular neural and hormonal control system may have greater influence on conscious swine than anesthetized swine.

Integrated System: Passive System Plus Neural Network Control System

The three-layer neural network control system was trained with the conscious swine experimental data that were used above. The batch training method was used to insure that the trained neural network control system would fit all of the data. Initially, an arbitrary set of connection weights were assigned to the nodes in the network. The weights were adjusted after each pass of the combined model through all 125 minutes of hemorrhage data (see Figure 6). With each pass, the passive system model calculated MAP, CO, Hct, O₂ debt, blood volume, and blood viscosity using HR, compliance, and resistance values supplied by the neural network. Values were calculated every 14 ms (baseline pulse period) from 0 to 125 minutes. Overall model calculated values at 0, 10, 20, 35, 65, 95, and 125 minutes were compared to the corresponding experimental data. The root mean squared error of the differences between calculated and measured values was used to adjust the neural network weights between data passes. The goal was to obtain an error value close to zero.

The iteration procedure was time consuming. In this preliminary study, the number of data passes (with weight adjustments) was limited to 400. These iterations required approximately six days of continuous execution on a PC-486DX-100MHz computer. A completely converged (trained) neural network control system was not obtained prior to the writing of this report. The results of further training will be included in the final report as well as in the next quarterly progress report. If available, an even faster computer will be used for additional neural network development.

Figures 14 through 18 illustrate the results of executing the combined passive system and trained neural network on the same conscious swine data used to train the

network. The Figure 14 provides a time series graph of calculated changes in hemodynamic parameters (similar to Figure 7) after onset of hemorrhage. Individual parameter calculations are shown in Figures 15 (HR), 16 (MAP), 17 (Hct), and 18 (CO). The combined model calculations of MAP and CO agree more favorably to the experimental data than the model without the control system. However, relatively large differences are also present. Further training of the neural network control system is expected to improve these results.

SUMMARY

SwRI has implemented a cardiovascular passive system model, integrated the model with a neural network control system, and conducted preliminary training and testing of the combined model. The results of testing showed that the passive system model provided reasonable estimates the trends of hemodynamic changes after hemorrhage. The addition of the neural network as a control model improved the results by accounting for neural and hormonal regulation of the hemodynamic changes after hemorrhage. Though these results are encouraging, the TPSIM model must provide better predictions of hemodynamic changes as input for decision making by the automated fluid resuscitation model.

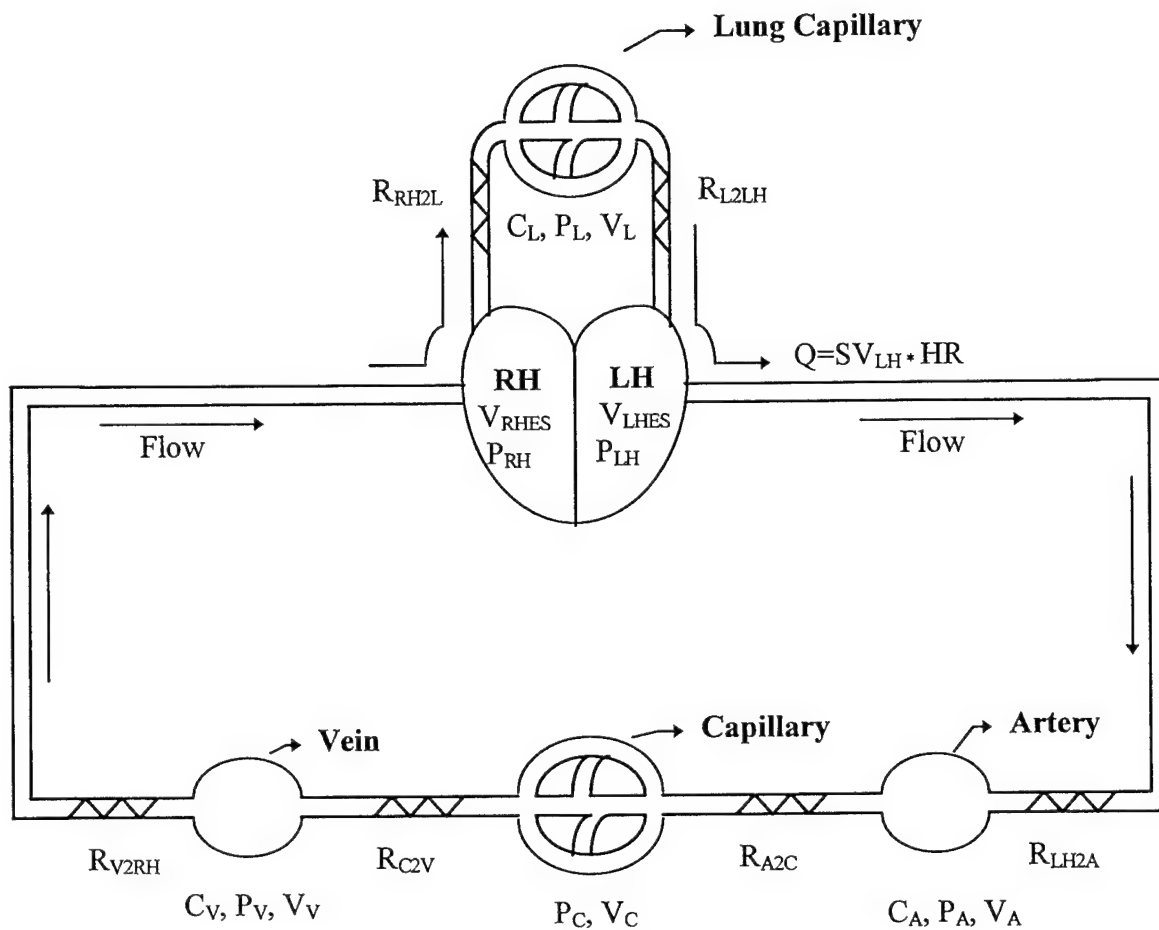
During the next quarterly reporting period, the neural network control system will continue to be trained with additional iterations of the conscious swine data. Results will be compared with the experimental data. The neural network control system will also be trained and tested with additional data (once identified and obtained).

REFERENCES

- [1] Doherty T.J., "A mathematical model of the circulation for the study of hemorrhagic shock and fluid resuscitation", Ph.D. dissertation, University of California at Berkeley, 1993.
- [2] Doherty T.J., Bruttig S.P., Bickell W.H., "Controlled response to aortotomy hemorrhage in swine: effects of anesthesia," Letterman Army Institute of Research internal report.
- [3] Bickell W.H., O'benar J., Bruttig S.P., Wade C.E., Hannon J.P., Tillman F., Rodkey W., "The hemodynamic response to aortotomy in the conscious chronically instrumented swine," *The Physiologist*, 30, 228, 1987.
- [4] Bickell W.H., Bruttig S.P., Wade C.E., "Hemodynamic response to abdominal aortotomy in the anesthetized swine," *Circ. Shock*, 28, 321-332, 1989.
- [5] Crowell, J.W., Smith, E.E., "Oxygen deficit and irreversible hemorrhagic shock," *Am J Physiol*, 206:313, 1964.

APPENDIX: FIGURES AND DIAGRAMS

Figure 1. Cardiovascular Passive System



Notes :

- Subscript A, C, V, L, LH, RH indicate Artery, Capillary, Vein, Lung, Left Heart, Right Heart, respectively. "2" means "to".
- P, V, C, R indicate Blood Pressure, Blood Volume, Compliance, and Resistance, respectively.
- Q indicates blood flow; SV indicates Stroke Volume; HR indicates Heart Rate.

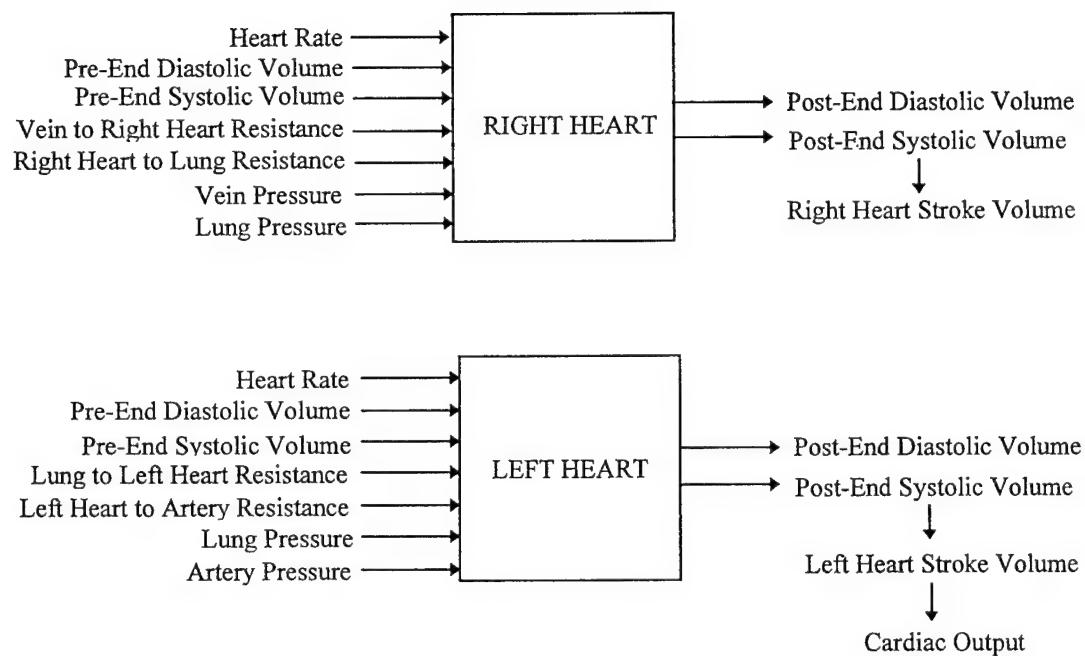
Figure 2. Right Heart and Left Heart Modules

Figure 3. Dependency among the Blood Volume, Blood Pressure and Blood Flow

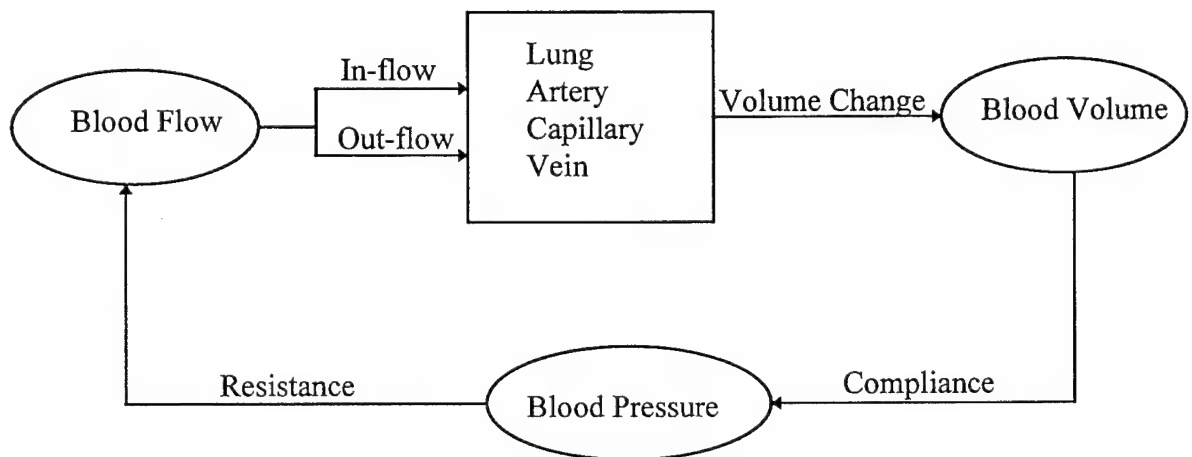


Figure 4. Microvascular Fluid and Solution Exchange

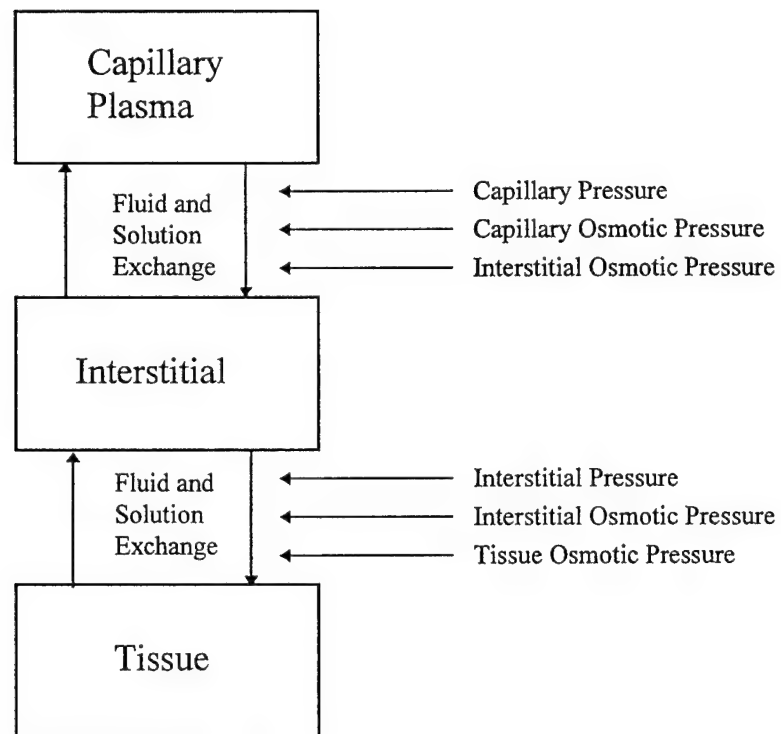
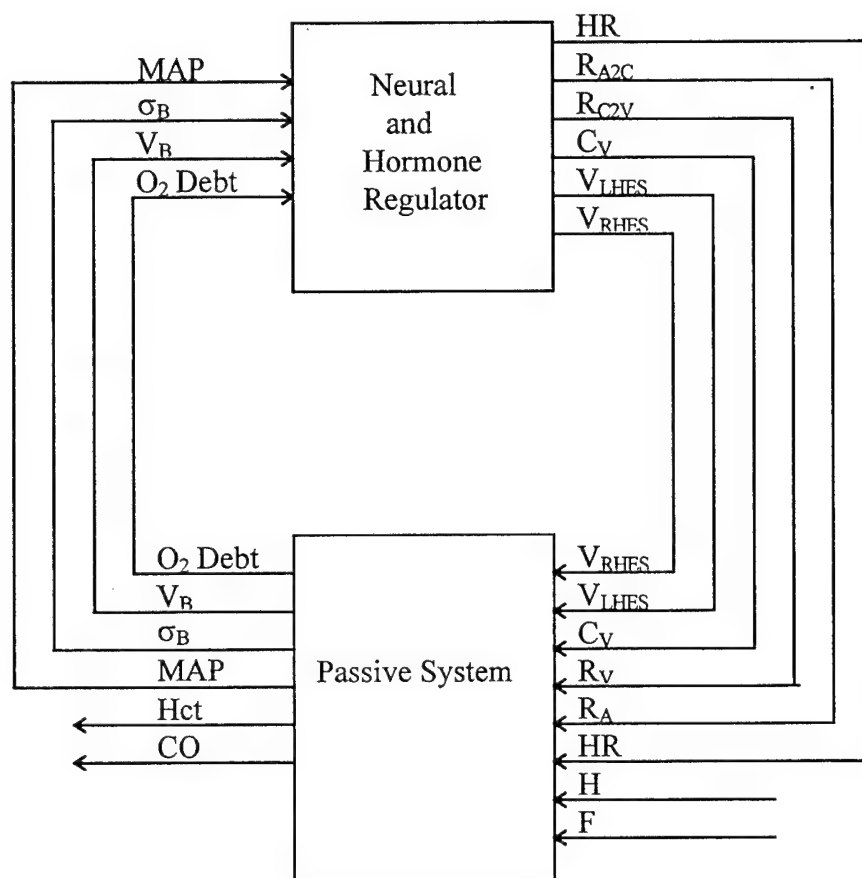
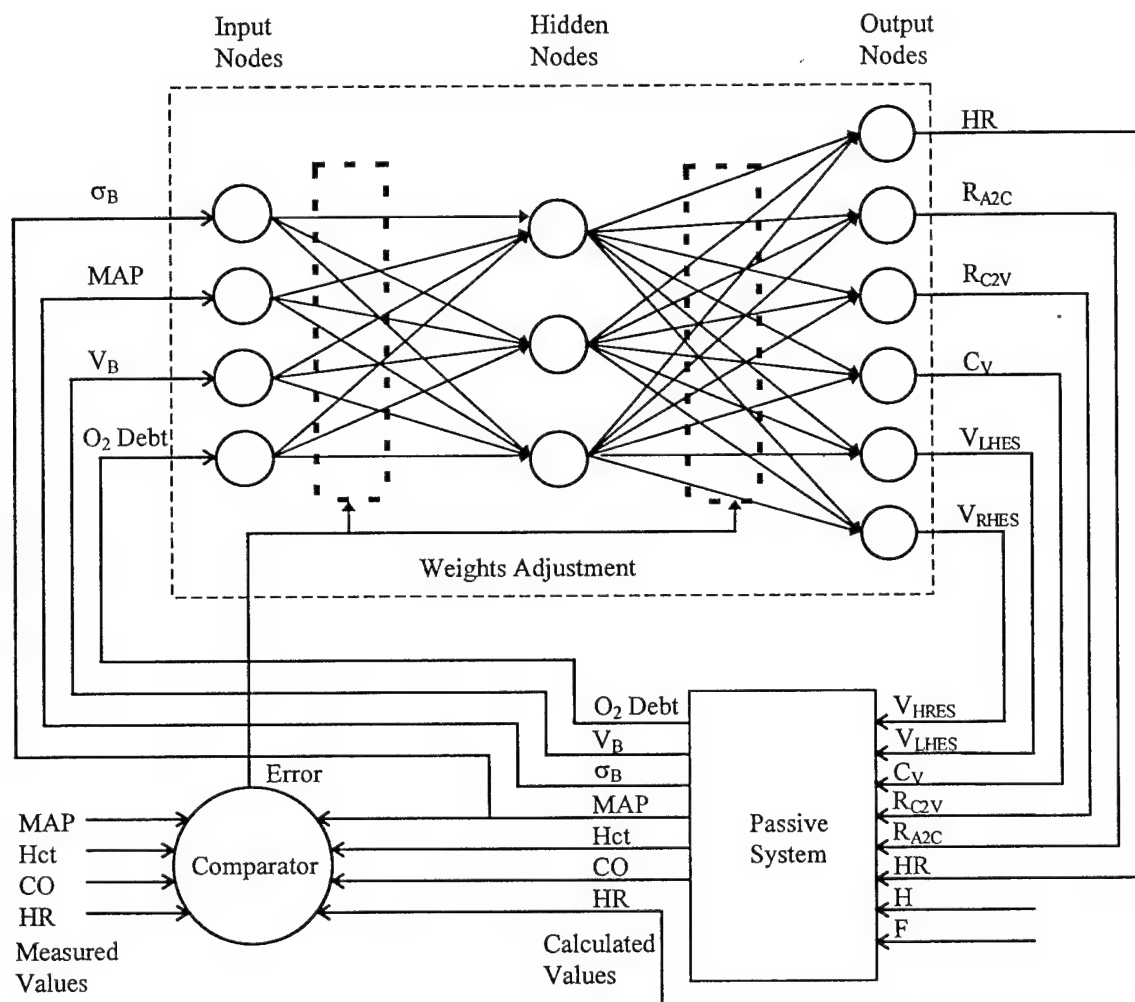


Figure 5. Diagram of the Trauma Patient Simulator



$O_2 Debt$: Oxygen Debt;
 V_B : Blood Volume;
 MA : Mean Blood Pressure;
 σ_B : Blood Viscosity;
 Hct : Hematocrit;
 CO : Cardiac Output;
 V_{RHES} : Right Heart End-Systolic Volume;
 V_{LHES} : Left Heart End-Systolic Volume;
 C_V : Vein Compliance;
 R_{A2C} : Artery to Capillary resistance;
 R_{C2V} : Capillary to Vein Resistance;
 HR : Heart Rate;
 H : Hemorrhage;
 F : Fluid Resuscitation.

Figure 6. Neural Network Control System Training Diagram



$O_2 \text{ Debt}$: Oxygen Debt;
 V_B : Blood Volume;
MA: Mean Blood Pressure;
 σ_B : Blood Viscosity;
Hct: Hematocrit;
CO: Cardiac Output;
 V_{RHES} : Right Heart End-Systolic Volume;
 V_{LHES} : Left Heart End-Systolic Volume;
 C_V : Vein Compliance;
 R_{A2C} : Artery to Capillary resistance;
 R_{C2V} : Capillary to Vein Resistance;
HR: Heart Rate;
H: Hemorrhage;
F: Fluid Resuscitation.

Figure 7. Passive System Test
Calculated Data After Hemorrhage

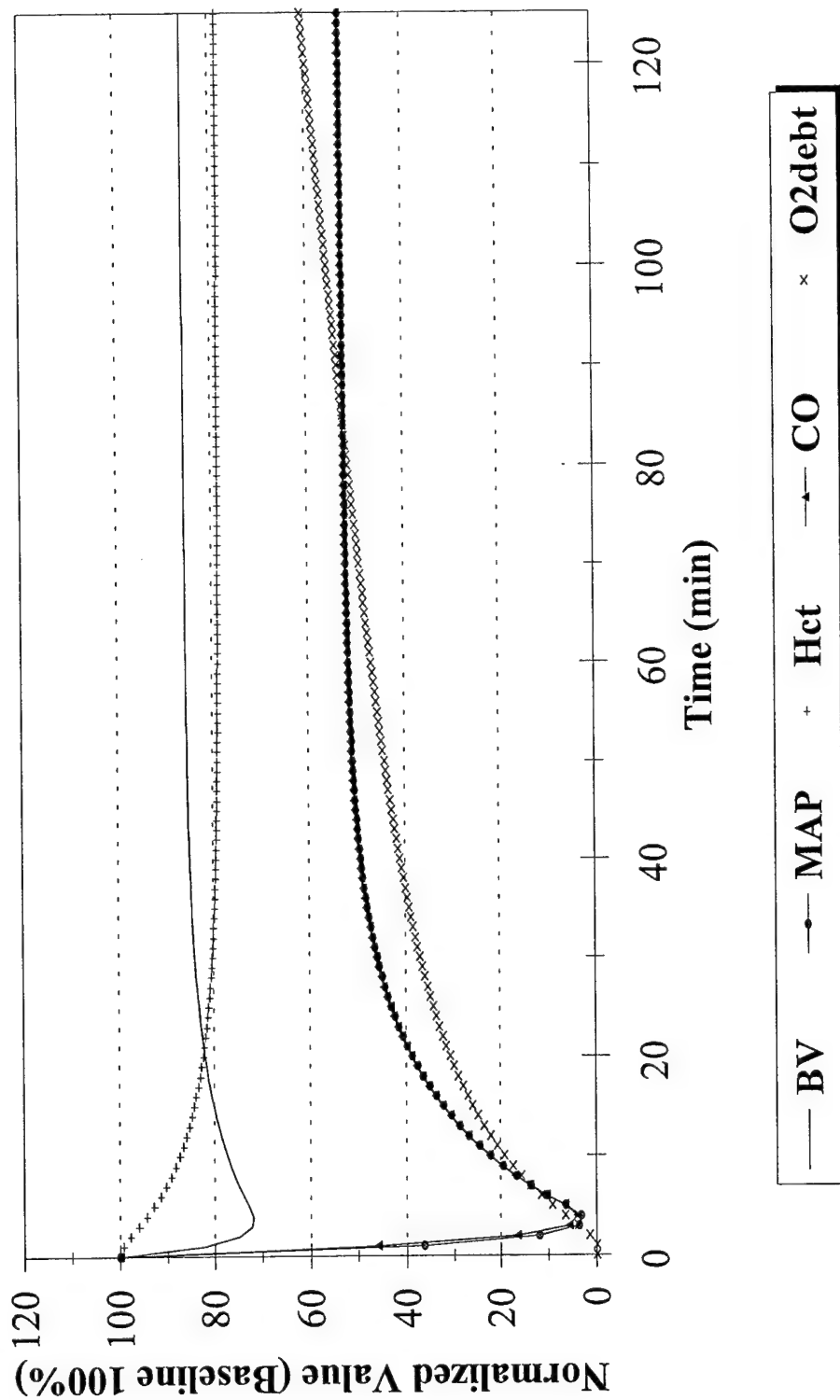


Figure 8. Passive System Test
MAP - Conscious Swine

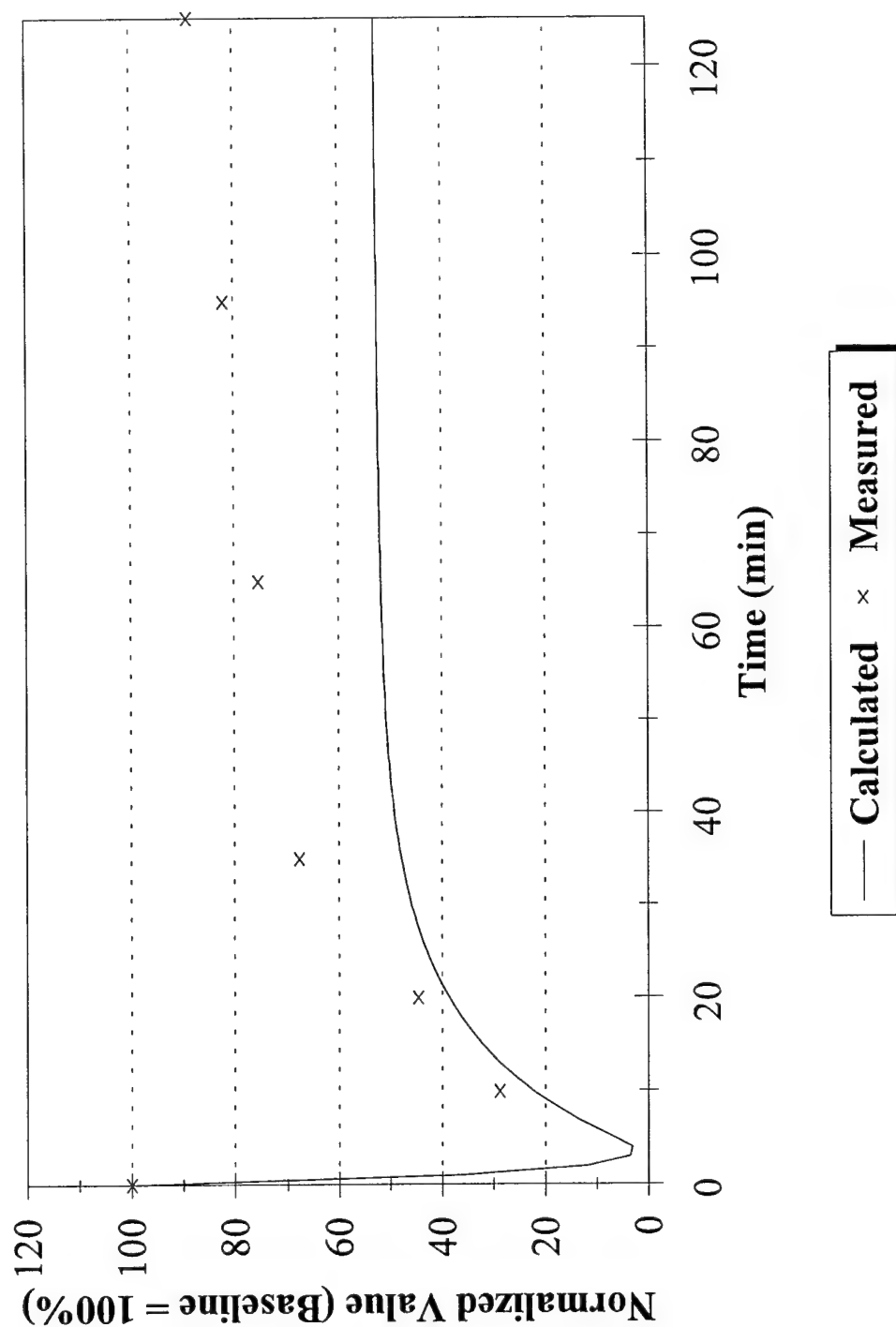


Figure 9. Passive System Test
Hct - Conscious Swine

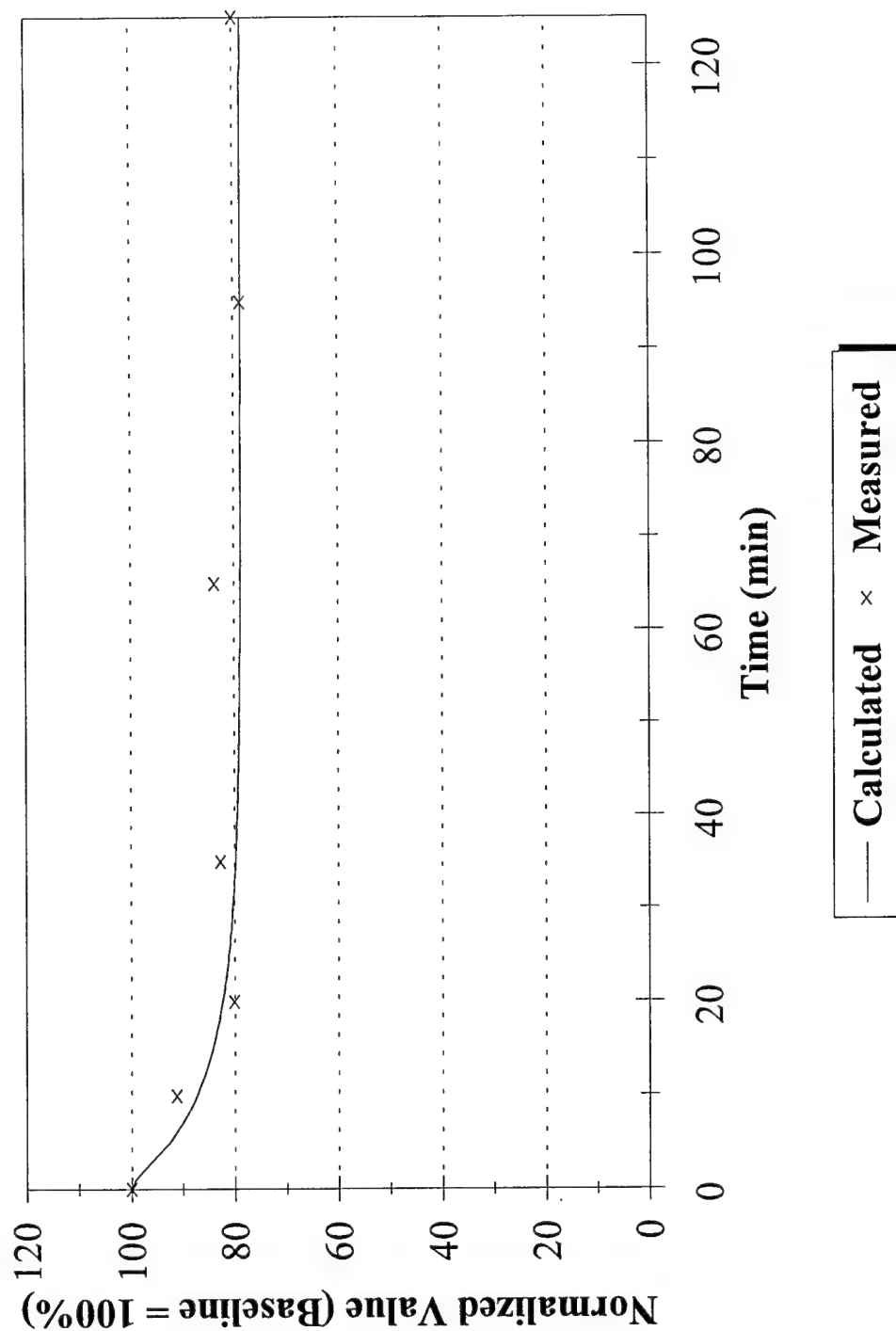


Figure 10. Passive System Test
CO - Conscious Swine

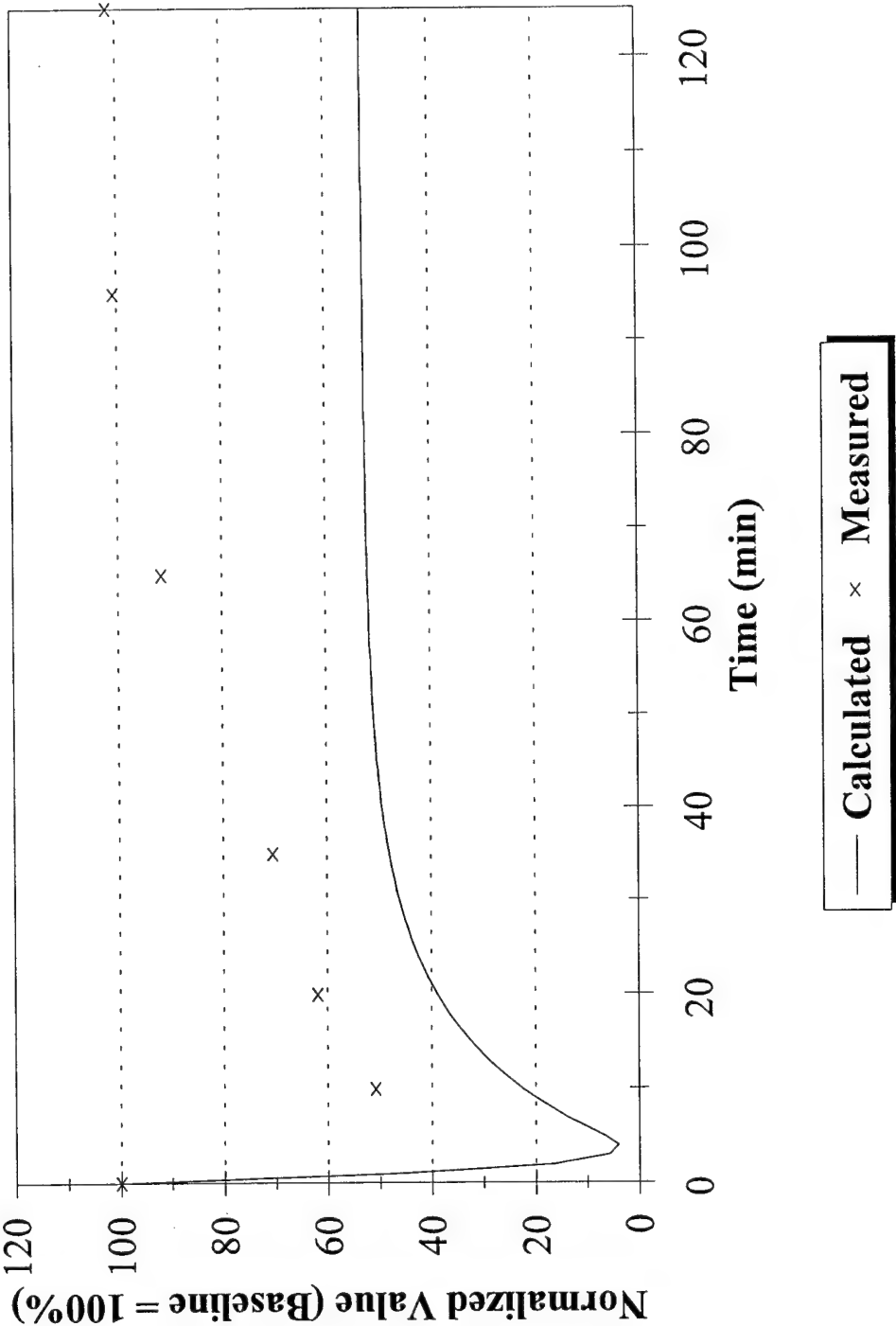


Figure 11. Passive System Test
MAP - Anesthetized Swine

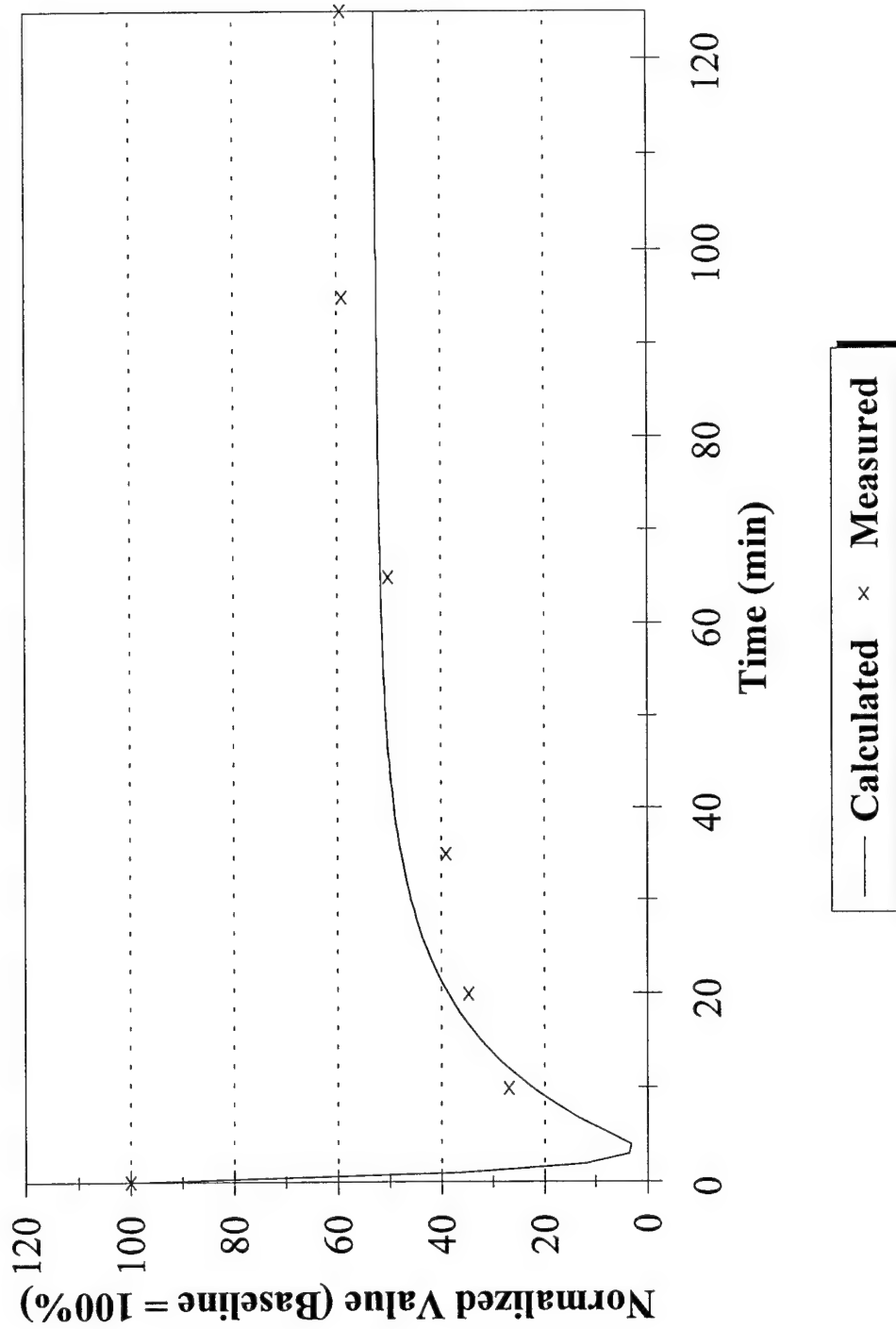


Figure 12. Passive System Test
Hct - Anesthetized Swine

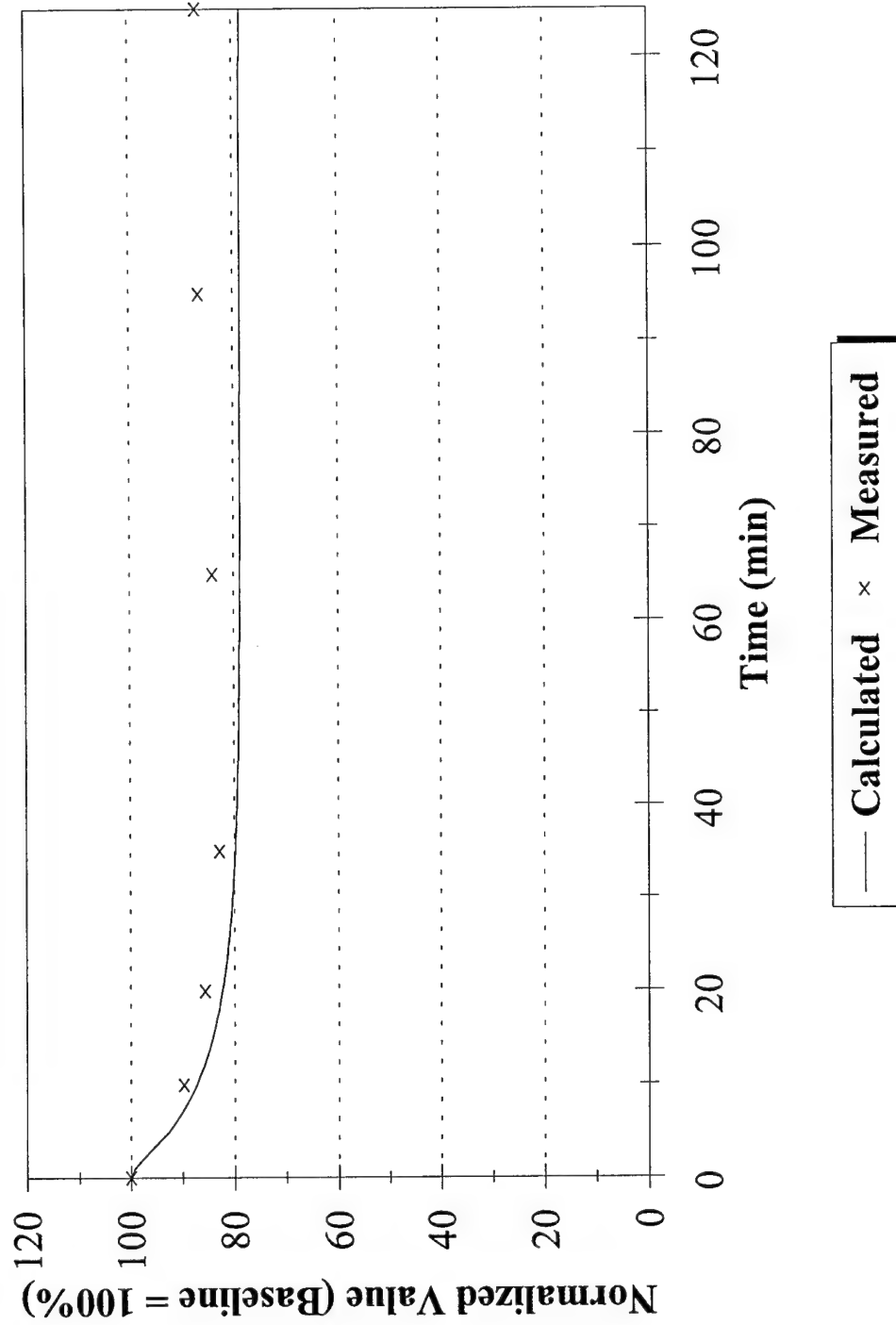


Figure 13. Passive System Test
CO - Anesthetized Swine

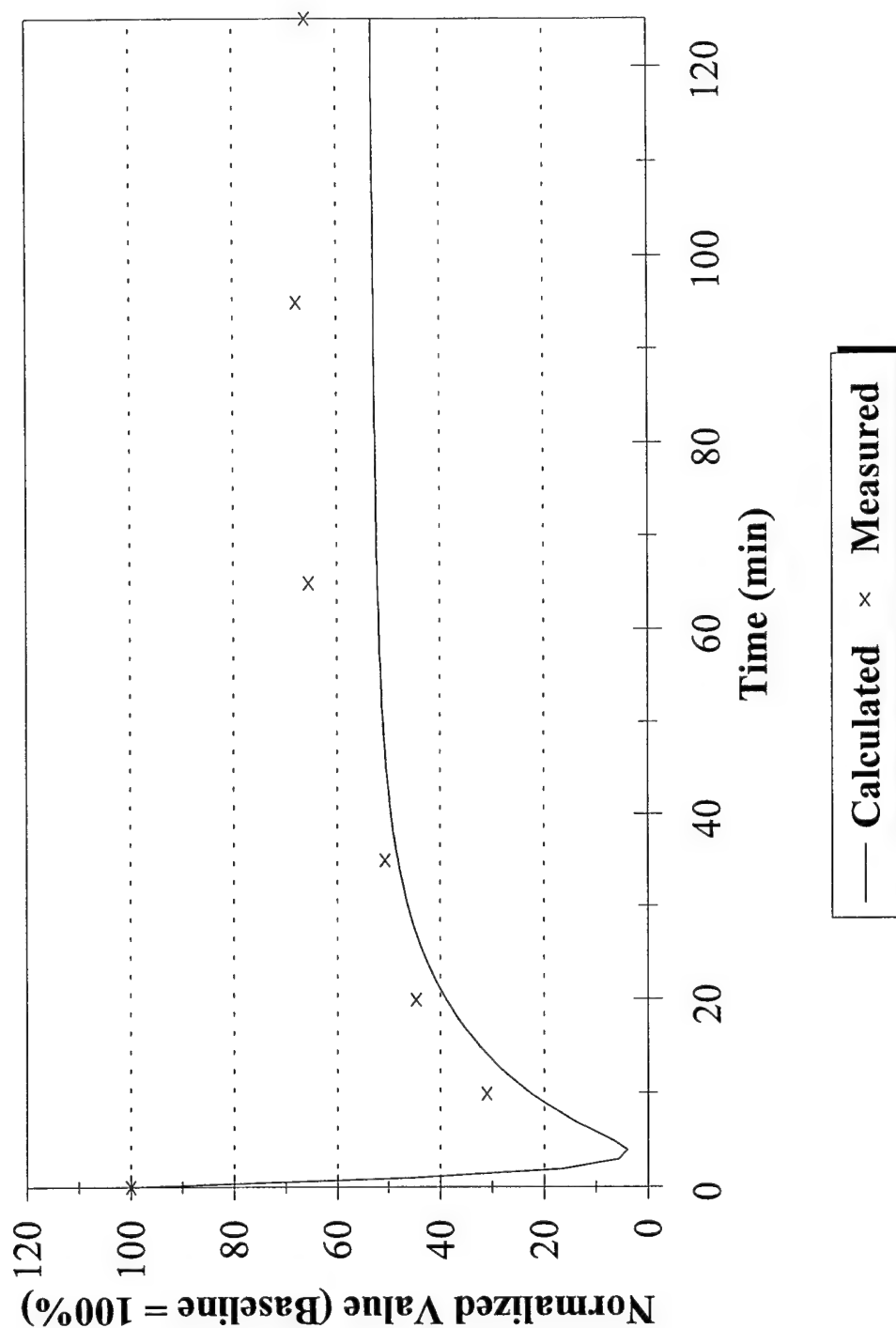


Figure 14. TPSIM System Test
Physiological Data After Hemorrhage

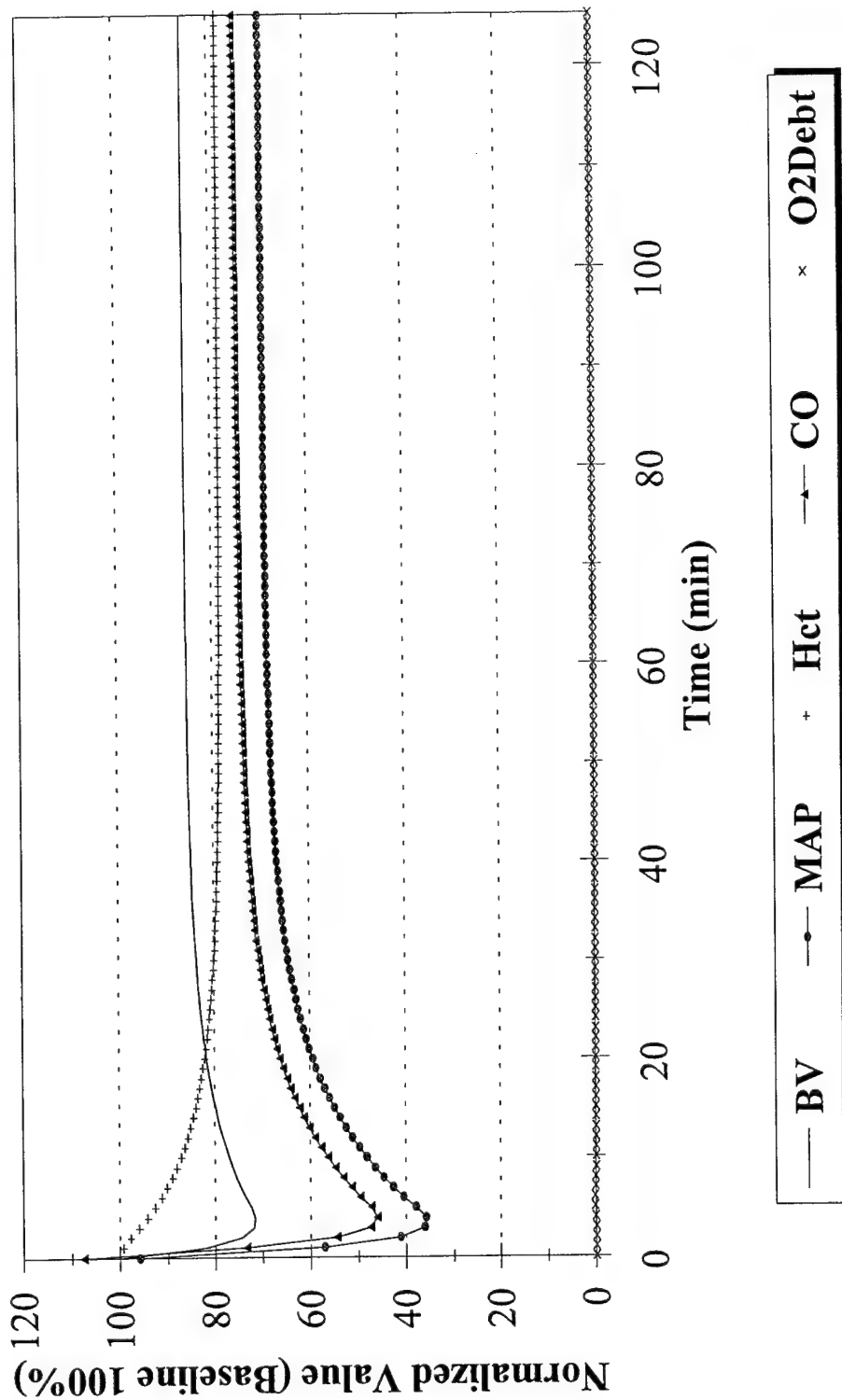


Figure 15. Passive System Test
HR - Conscious Swine

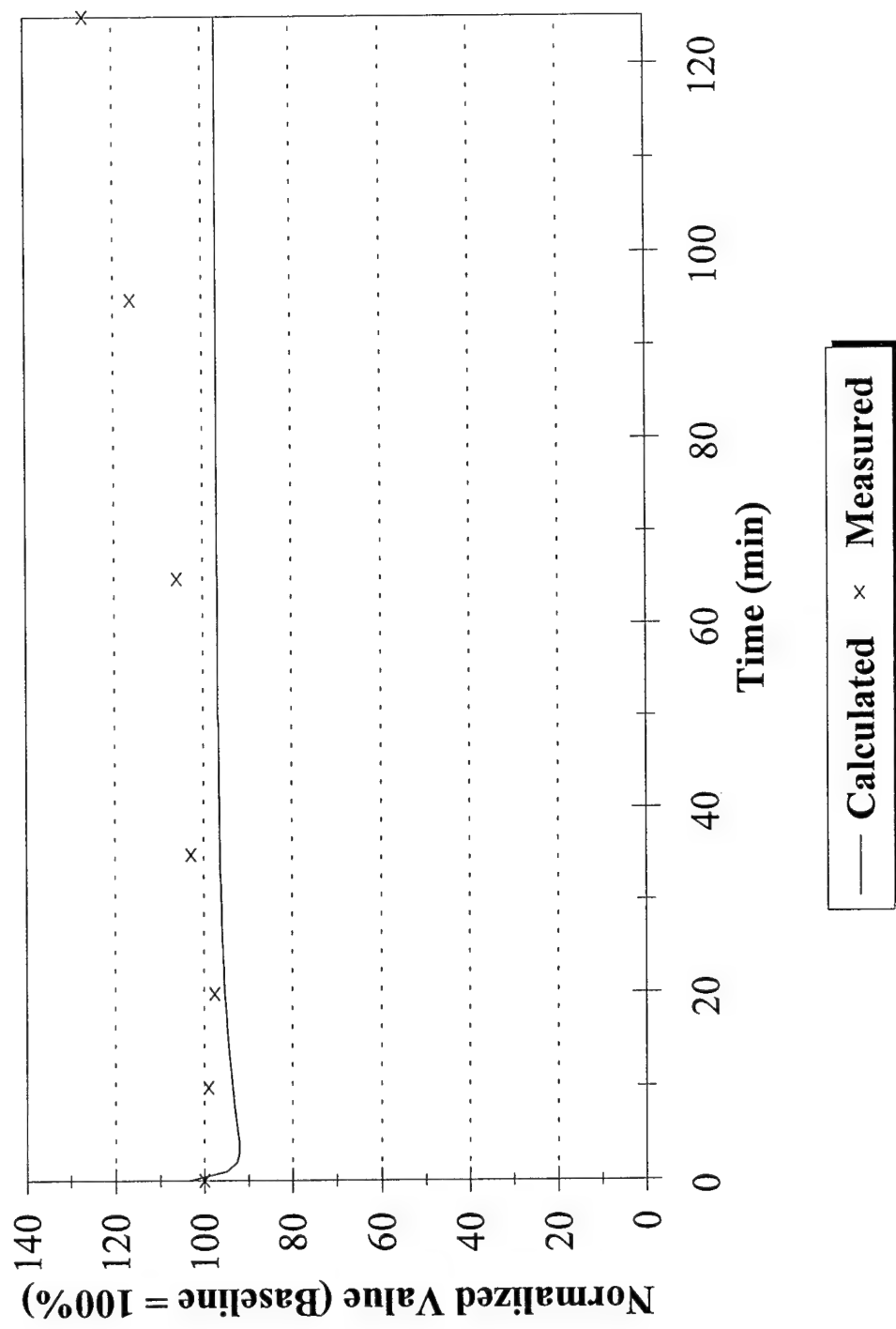


Figure 16. TPSIM System Test
MAP - Conscious Swine

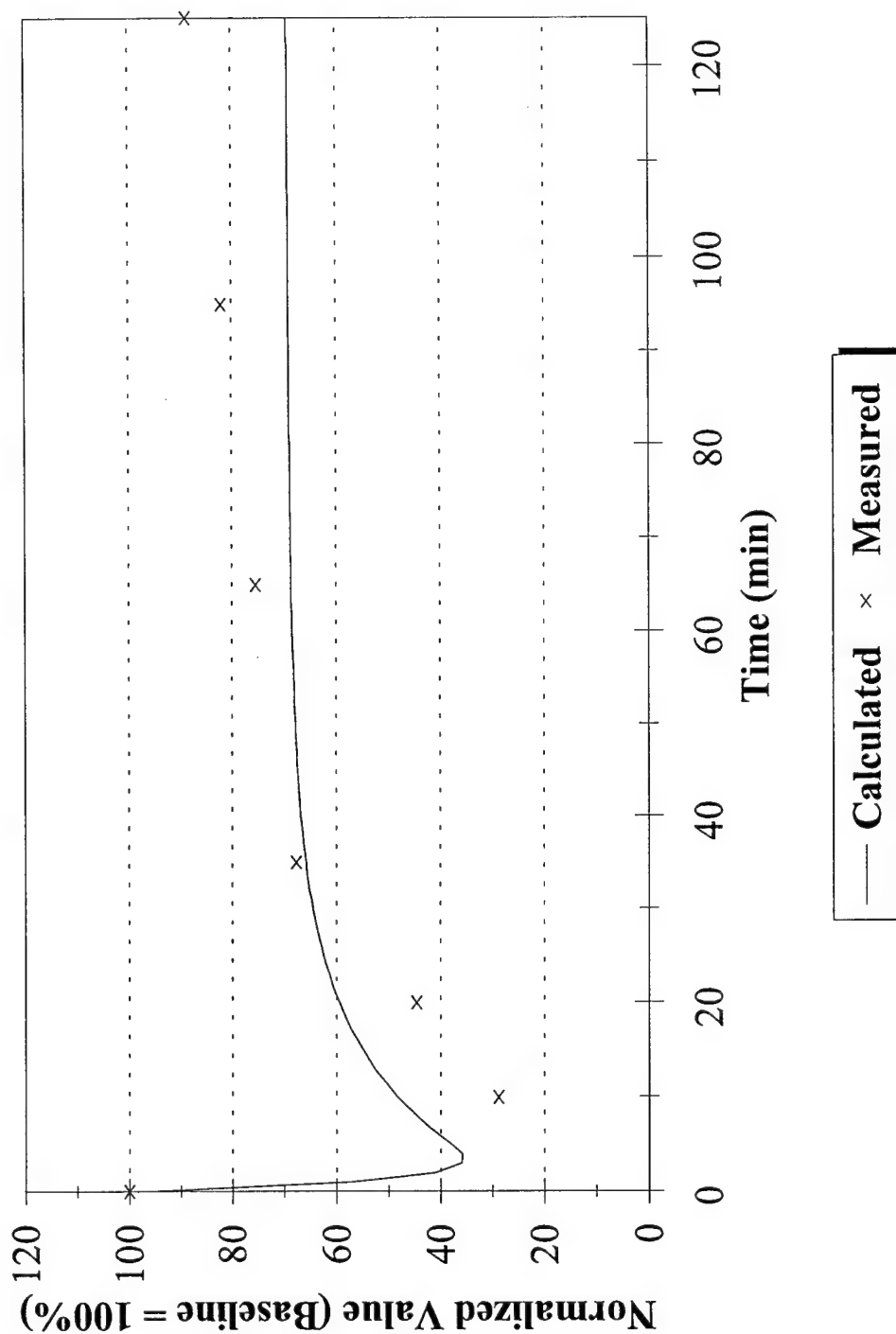


Figure 17. Passive System Test
Hct - Conscious Swine

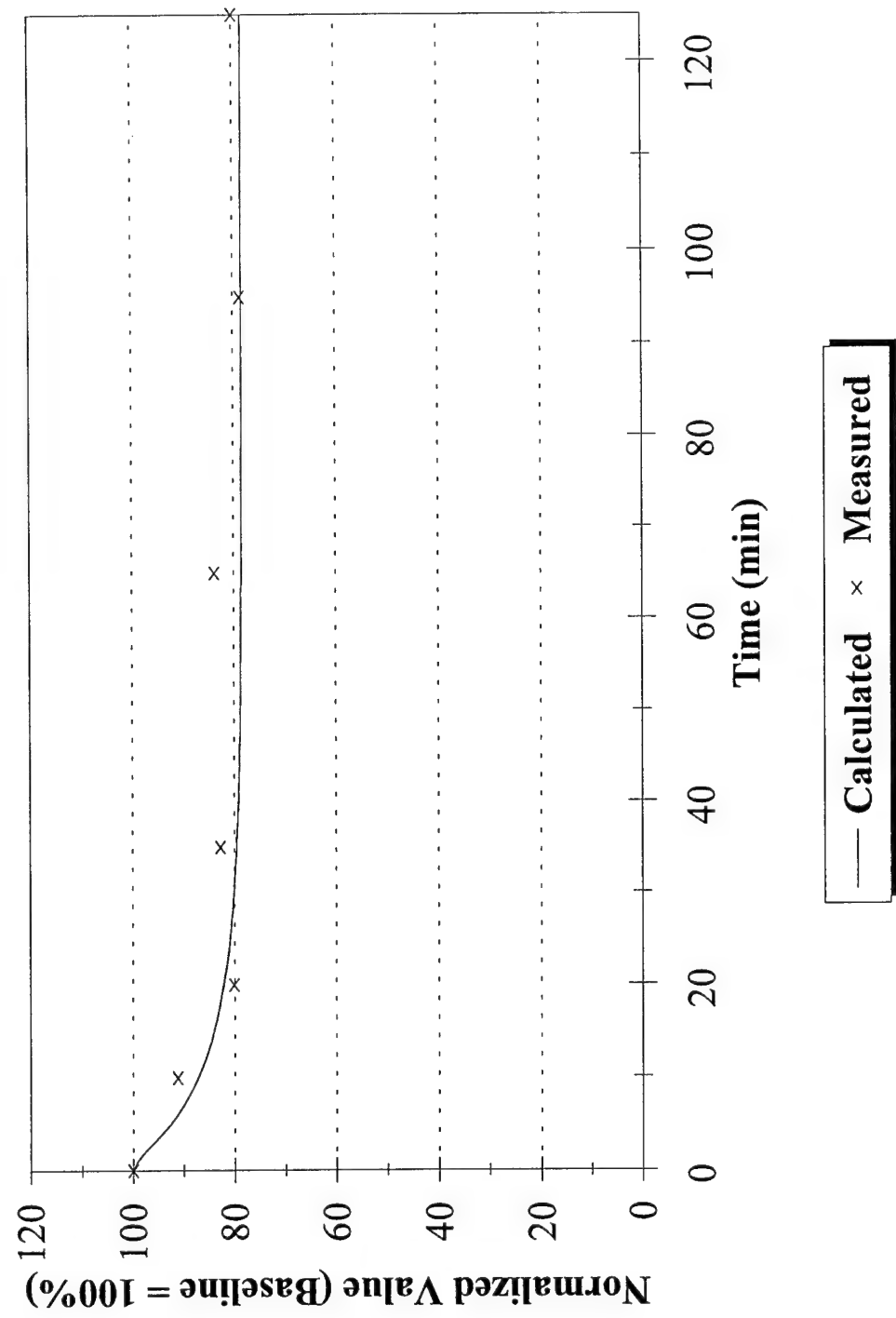


Figure 18. Passive System Test
CO - Conscious Swine

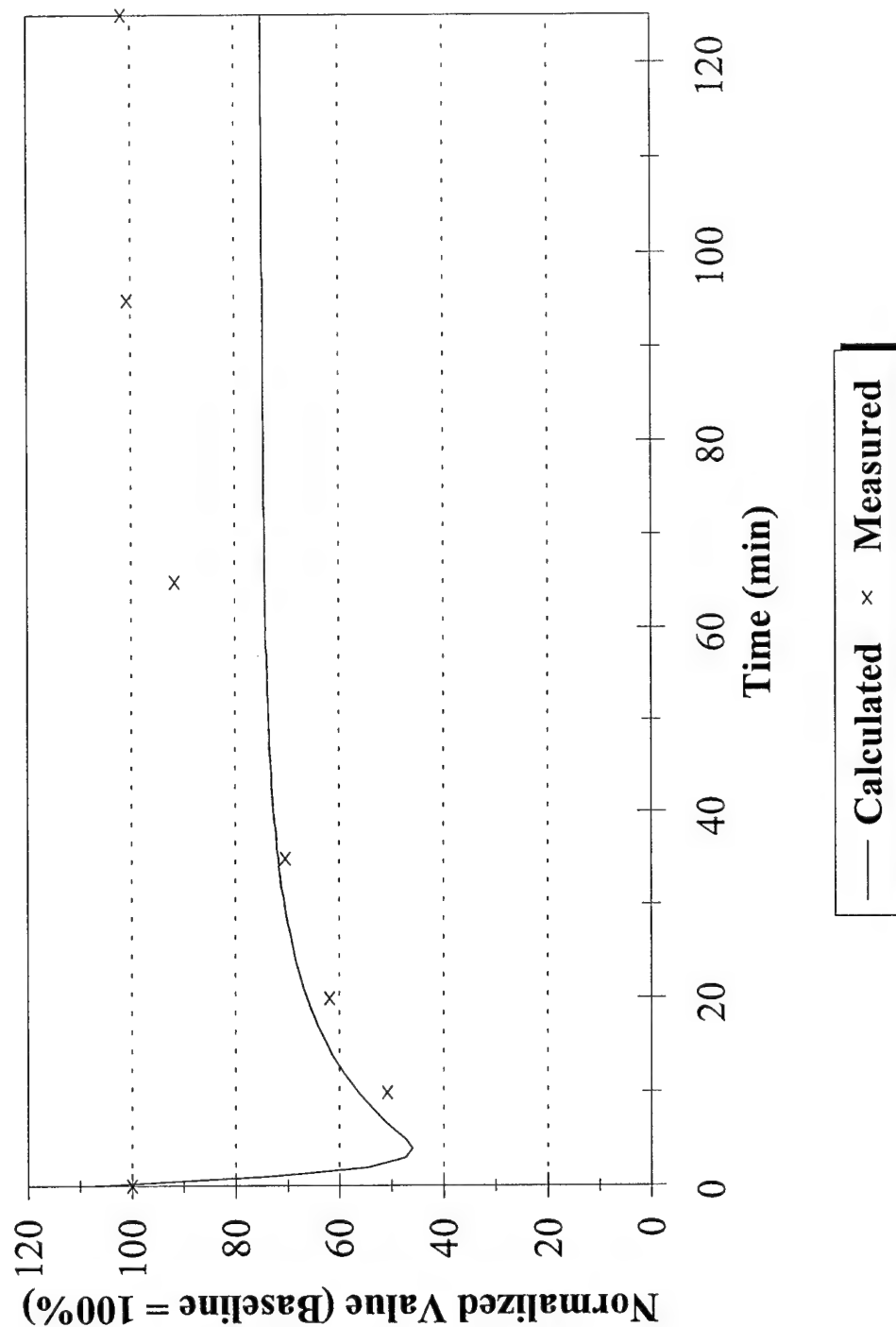


Diagram 1. Passive System Simulator

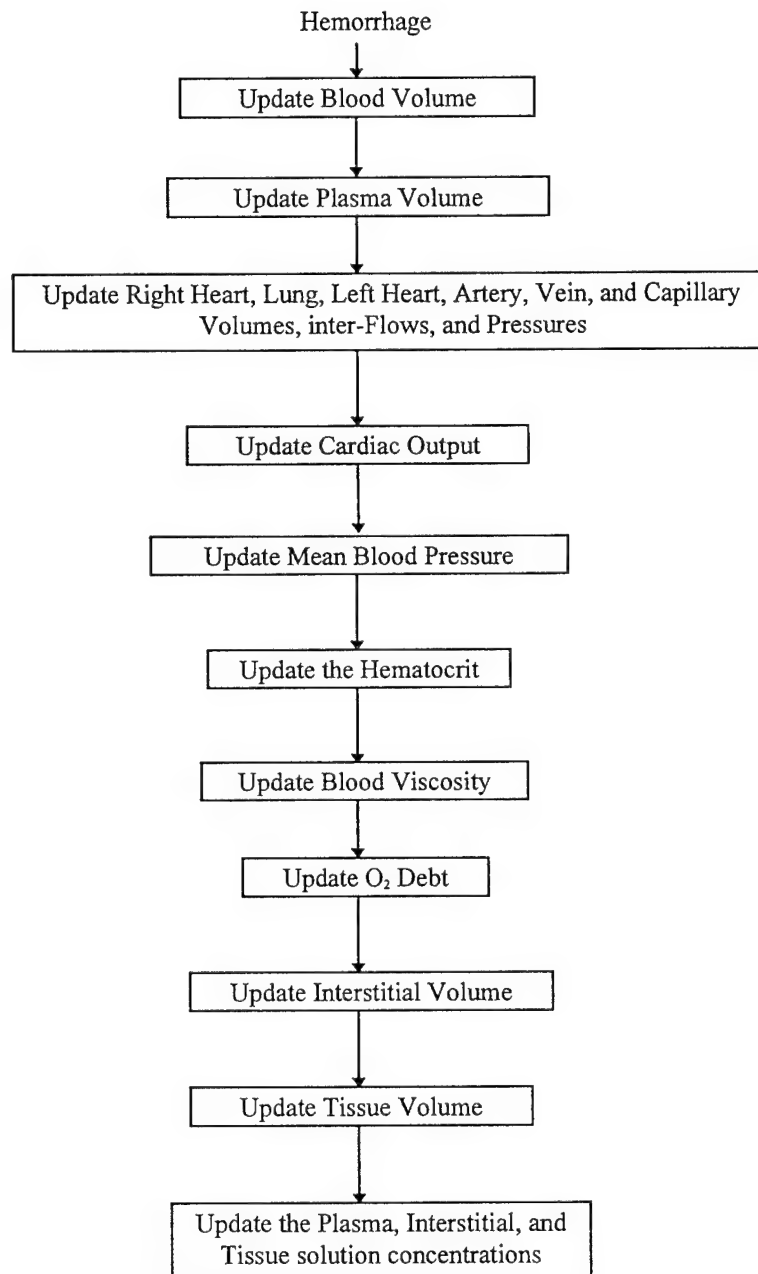
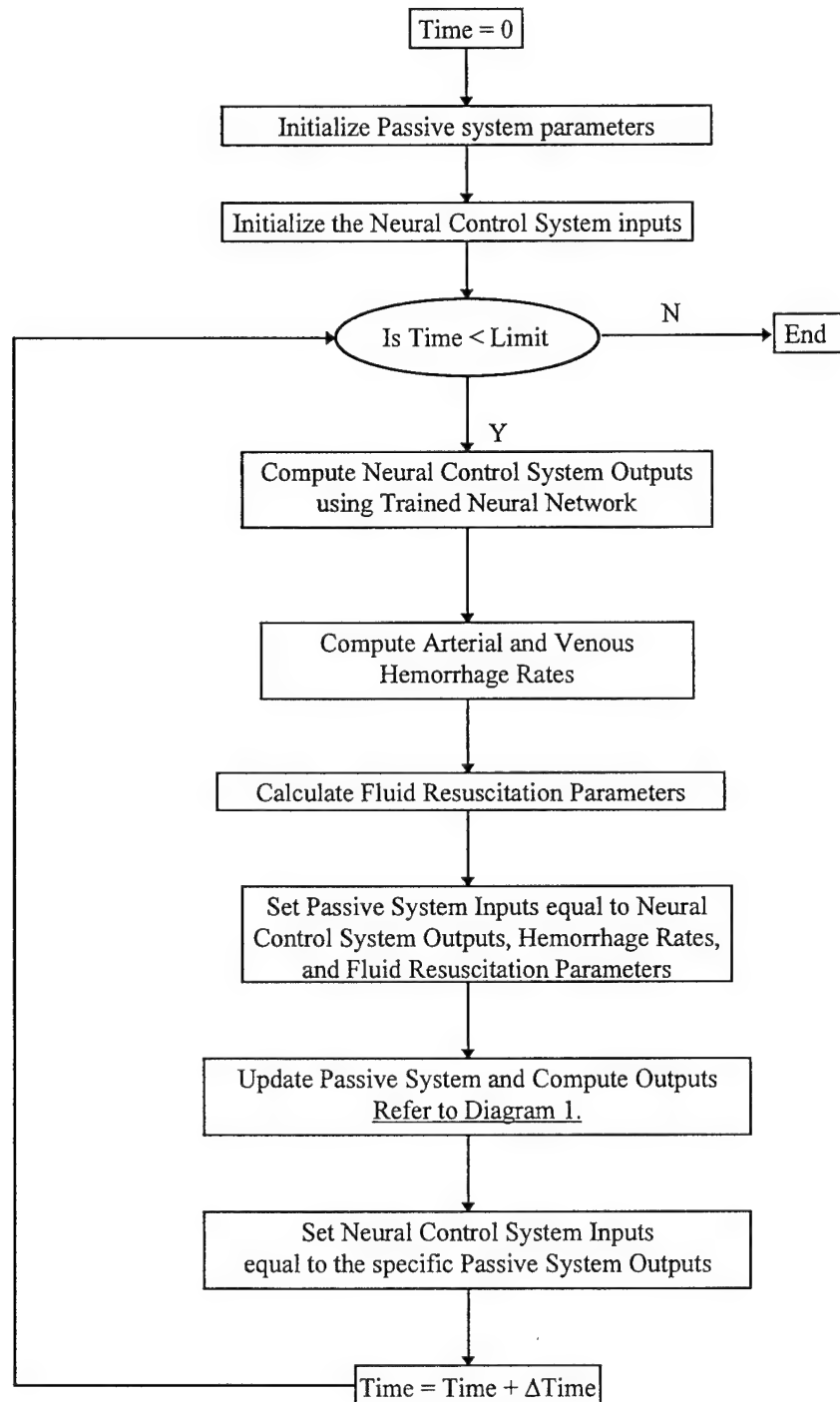


Diagram 2. Trauma Patient Simulator (TPSIM)

SOUTHWEST RESEARCH INSTITUTE

6220 CULEBRA ROAD • POST OFFICE DRAWER 28510 • SAN ANTONIO, TEXAS, USA 78228-0510 • (210) 684-5111 • TELEX 244846

September 14, 1995

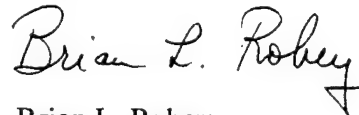
Donald P. Jenkins, Ph.D.
Deputy Director for Defense Healthcare Technologies
ARPA/Defense Sciences Office
3701 North Fairfax Drive
Arlington, VA 22203-1714

Dear Dr. Jenkins:

Enclosed is the fourth quarterly report for work performed under contract no. DAMD17-94-C4126. This report covers the period from 27 May, 1995 to 1 September, 1995.

Please feel free to contact me at (210) 522-5115 if you have any questions or concerns regarding the technical aspects of this report. Please contact Ms. Sharon Rowe at (210) 522-3026 for any contractual or financial matters.

Sincerely,



Brian L. Robey
Project Manager
Biosciences & Bioengineering Department

Enclosure



SAN ANTONIO, TEXAS
HOUSTON, TEXAS • DETROIT, MICHIGAN • WASHINGTON, DC

File
12-6711

SOUTHWEST RESEARCH INSTITUTE

6220 CULEBRA ROAD • POST OFFICE DRAWER 28510 • SAN ANTONIO, TEXAS, USA 78228-0510 • (210) 684-5111 • TELEX 244846

September 14, 1995

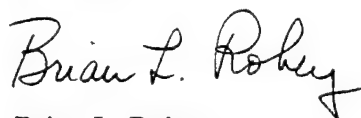
Director
U.S. Army Medical Research Acquisition Activity
ATTN: SGRD-RMA-RC
Fort Detrick
Frederick, MD 21702-5014

Dear Sir:

Enclosed is the fourth quarterly report for work performed under contract no. DAMD17-94-C4126. This report covers the period from 27 May, 1995 to 1 September, 1995.

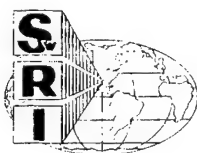
Please feel free to contact me at (210) 522-5115 if you have any questions or concerns regarding the technical aspects of this report. Please contact Ms. Sharon Rowe at (210) 522-3026 for any contractual or financial matters.

Sincerely,



Brian L. Robey
Project Manager
Biosciences & Bioengineering Department

Enclosure



SAN ANTONIO, TEXAS
HOUSTON, TEXAS • DETROIT, MICHIGAN • WASHINGTON, DC

Quarterly Progress Report

1. Contract No. DAMD17-94-c4126 2. Report Date 15 June, 1995
- SwRI Project No. 12-6711
3. Reporting Period from 27 May, 1995 to 1 September, 1995.
4. PI Brian Robey 5. Phone (210) 522-5115
6. Institution Southwest Research Institute, San Antonio, Texas
7. Project Title Model for Trauma Patient Simulation and Automated Fluid Resuscitation
8. Current staff with percent effort of each on project

Brian Robey 14 %

Dean Winter 7 %

Jian Ling 40 %

9. Contract expenditures to date (as applicable):

	this qtr/cumulative		this qtr/cumulative
Personnel	<u>8,428.49 / 28,235.02</u>	Travel	<u>1,882.43 / 1,882.43</u>
Fringe Benefits	<u>3,683.26 / 12,338.71</u>	Equipment/Supplies	<u>71.00 / 7,800.67</u>
Overhead	<u>14,291.88 / 47,877.01</u>	Facilities Capital	<u>1,270.08 / 4,230.08</u>

	this qtr/cumulative
Subtotal	<u>29,582.14 / 102,318.92</u>
Indirect Costs	<u> / </u>
Fee	<u>2,265.00 / 7,847.21</u>
Total	<u>31,847.14 / 110,166.13</u>

10. Administrative and Logistical Matters

During 19-20 June, Mr. Brian Robey and Dr. Dean Winter traveled to ARPA to meet with Dr. Don Jenkins to provide a status update of the project and to discuss the status of monitoring systems on the LSTAT. Mr. Robey and Dr. Winter also met with Dr. Fred Pearce at Walter Reed for a project review as well as to identify sources of animal and clinical data for model development and validation. Dr. Jenkins recommended that SwRI contact Dr. Champion, a D.C. trauma physician.

During a planned trip to Los Angeles on unrelated business, Mr. Robey met with Dr. William Shoemaker (Chairman of Emergency Medicine at Martin Luther King Hospital and Professor of Surgery at Los Angeles County/USC Medical Center) to discuss availability of clinical data for model development and testing. Dr. Shoemaker and his staff have extensive experience with fluid resuscitation and have also developed decision-making algorithms. They also maintain a large database of data for trauma patients treated at the hospital. Mr. Robey scheduled a follow-up meeting with Dr. Shoemaker and Dr. Mike Bishop (an attending ER physician who maintains the database) to obtain data. (See attached follow-up letter to Dr. Demetriades, Director of Trauma and Dr. Shoemaker's department head at Los Angeles County).

On 7-8 September, Mr. Robey and Mr. Jian Ling traveled to Los Angeles to meet with Dr. Shoemaker and Dr. Bishop to initiate collection of data for model development. (SwRI attempted to schedule this trip in late July or early August; however, Dr. Shoemaker was not available until early September). During these meetings, an example data set from one patient was obtained (based on the type of data required to develop and validate the model). Additional data sets may be obtained from Dr. Bishop for a fee (approximately \$250-\$500 per data set). Approximately 50 data sets will be required to finish development and to validate the model.

As discussed with Dr. Jenkins and Dr. Pearce, SwRI has begun working to revise the project statement of work to accommodate the costs for data collection and further model refinement. Based on discussions with Dr. Jenkins, SwRI understands that other contractors are responsible for developing the integrated hardware system for the LSTAT. SwRI plans to re-direct the hardware development budget to data collection and further model refinement.

SwRI requested an increase in the travel budget to cover expenses required for travel to Los Angeles on 7-8 September, as well as for future trips to Los Angeles and to other national trauma centers as needed for data collection (e.g., Dr. Champion in Washington, D.C.) A formal request to increase the budget by \$5,000 was requested in writing to C. Susan Rupprecht at USAMRAA, Fort Detrick.

11. Scientific Progress

Task 1 - Passive System Model Development/Refinement:

No major modifications were made to the passive cardiovascular system model.

Task 2 - Acquire Existing Data:

As described above, SwRI has begun acquiring clinical data from Martin Luther King (MLK) Hospital in Los Angeles. The model has yet to be refined and tested with clinical data. The acquisition of large amounts of data (from MLK) is dependent upon approval of a revised

statement of work that provides funds to purchase data sets. Until this revised statement of work is approved, SwRI plans to purchase at least four data sets from MLK; this data will allow continued development of the Trauma Patient Simulator (TPSIM).

Task 3 - Deterministic Control System Model Development:

The passive cardiovascular system model was integrated with a deterministic control system to form a TPSIM. (An initial deterministic cardiovascular control system was developed during the first quarter of this project). Results of this work may be found in the attached report.

Task 4 - Deterministic Model Refinement and Testing:

The Trauma Patient Simulator (TPSIM) (that incorporates a deterministic control system) was refined using the same swine data used to refine the neural network-based control system model. Results of this work may be found in the attached report.

Task 5 - Neural Network Control System Development:

A preliminary version of the neural network control system software was completed during the last reporting period. Minor modifications were made to the neural network and are described in the attached report.

Task 6 - Neural Network Model Refinement and Testing:

The TPSIM (that incorporates a neural network control system) was modified and re-trained using conscious swine data. Results of this work may be found in the attached report.

Task 7 - Model Reliability and Accuracy Studies:

Not started.

Task 8 - Control System Model Selection:

Not started.

Task 9 - Development of a Fluid Resuscitation Optimization Algorithm:

SwRI has begun to review Dr. Shoemaker's fluid resuscitation algorithm (through discussions and literature review). A portion of this algorithm may form the basis of the LSTAT volume resuscitation optimization system (VROS).

Task 10 - Real Time Software System Development:

All software continues to be developed in the C-language for ease of portability.

Task 11- Prototype System Development:

Not started.

Plans For Next Quarter

- Additional clinical data will be obtained from Martin Luther King Hospital.
- The reliability and accuracy of the passive system will be evaluated using additional acquired data.
- The neural network control system will be further refined and tested using clinical data.
- The deterministic control system will be further refined and tested using clinical data.
- The results of further testing with the deterministic control system and neural network control system will be compared.

Status Report on

**The Development of a Deterministic Control Model and
a Neural Network Control Model for Trauma Patient
Simulation and Automated Fluid Resuscitation**

September 15, 1995

**SwRI Project No. 12-6711
Contract No. DAMD17-94-C4126**

Prepared for:

**Director, U.S. Army Research Acquisition Activity
ATTN: SGRD-RMA-RC
Fort Detrick, MD 21702-5014
and
Deputy Director for Defense Healthcare Technologies
ARPA/Defense Sciences Office
3701 North Fairfax Drive
Arlington, VA 22203-1714**

Prepared by:

**Jian Ling and Brian L. Robey
Southwest Research Institute
San Antonio, Texas**



**SAN ANTONIO, TEXAS
HOUSTON, TEXAS • DETROIT, MICHIGAN • WASHINGTON, DC**

THE DEVELOPMENT OF A DETERMINISTIC CONTROL MODEL AND A NEURAL NETWORK CONTROL MODEL FOR TRAUMA PATIENT SIMULATION AND AUTOMATED FLUID RESUSCITATION

INTRODUCTION

This report describes the development status of models that simulate the neural and hormonal control of the cardiovascular system during hemorrhage. Two model approaches have been implemented - deterministic and neural network. Each has been integrated with the passive system model of cardiovascular hemodynamics and fluid exchange to form independent trauma patient simulators (TPSIMs). Each TPSIM was trained with conscious swine hemorrhage data. The results from training each TPSIM are discussed in detail. Since the results are reasonably favorable for both approaches, additional data and model training is necessary before a formal comparison and selection of a final control system for the TPSIM can be made. All figures and diagrams for this report may be found in the Appendix.

This is a preliminary report. It is expected that both control systems will be further refined with additional clinical data. A final version of this report will be incorporated into the final project report to be submitted at the conclusion of this project.

THE NEURAL AND HORMONAL CARDIOVASCULAR CONTROL SYSTEM

Neural and hormonal regulation have both short-term and intermediate effects on the passive cardiovascular system during hemorrhage. Short-term, neural regulation typically acts within seconds or minutes. It includes the baroreceptor feedback control mechanism, the chemoreceptor control mechanism, and the central nervous system ischemic control mechanism. When the arterial blood pressure decreases after severe hemorrhage, the baroreceptor system in the walls of most of the great arteries elicit powerful stimulation to the sympathetic vasoconstrictor system throughout the body. This increases the total peripheral resistance to maintain arterial blood pressure. The sympathetic constriction of the veins attempts to maintain adequate venous return and restrict cardiac output from decreasing to lethal levels. The sympathetic system also increases the heart rate and contractility of the heart. Chemoreceptors detect decreased oxygen content (as well as increased carbon dioxide and hydrogen ions). They then excite the vasomotor center to elevate blood pressure. Chemoreceptors, however, do not come into play until arterial pressure falls below 80 mmHg. When the arterial blood pressure falls below 50 mmHg, the central nervous system invokes a strong sympathetic response as a last ditch effort to prevent brain blood flow from decreasing to a lethal level. Some peripheral vessels can become totally or almost totally occluded [1, 2].

Intermediate, hormonal regulation requires 10 minutes to an hour for a response to occur. It includes the formation of angiotensin which constricts the peripheral arteries. The hypothalamus secretes vasopressin (also called the antidiuretic hormone) which even

further constricts the peripheral arteries and veins and also greatly increases water retention by the kidneys. In addition to neural and hormonal control, changes in blood viscosity and blood volume during hemorrhage affect the peripheral resistance. Figure 1 illustrates the various arterial pressure control mechanisms versus time after a sudden change in blood pressure [1, 2].

Southwest Research Institute (SwRI) has attempted to include the effects of neural and hormonal control mechanisms in both TPSIM control system models (deterministic and neural network). Changes in mean arterial blood pressure (MAP), blood viscosity (σ_B), blood volume (V_B), and oxygen debt (O_2Debt) are input parameters for the neural and hormonal control system. The changes in heart rate (HR), right and left heart contractility (CC_{RH} and CC_{LH}), arterial to capillary resistance (R_{A2C}), capillary to venous resistance (R_{C2V}), and venous compliance (C_V) are output parameters of each control system. Previously (as described in SwRI's 15 June, 1995, preliminary report), right and left heart end-systolic volumes were considered output parameters. However, upon further review, these parameters have been replaced with right and left heart contractility. As described above, heart contractility is directly affected by sympathetic stimulation. The diagram of the complete TPSIM system is shown in Figure 2.

DETERMINISTIC CONTROL MODEL

The following system of equations were developed to represent the cardiovascular deterministic control system model:

$$\begin{aligned}
 \Delta HR &= G1 \cdot \Delta MAP + G2 \\
 \Delta CC_{LH} &= G3 \cdot \Delta MAP + G4 \cdot \Delta V_B + G5 \cdot O_2Debt + G6 \\
 \Delta CC_{RH} &= G7 \cdot \Delta MAP + G8 \cdot \Delta V_B + G9 \cdot O_2Debt + G10 \\
 \Delta R_{A2C} &= G11 \cdot \Delta MAP + G12 \cdot O_2Debt + G13 \cdot \frac{\Delta \sigma_B}{\Delta V_B^2} + G14 \\
 \Delta R_{C2V} &= G15 \cdot \Delta MAP + G16 \cdot O_2Debt + G17 \cdot \frac{\Delta \sigma_B}{\Delta V_B^2} + G18 \\
 \Delta C_V &= G19 \cdot \Delta MAP + G20 \cdot \Delta V_B + G21 \cdot O_2Debt + G22.
 \end{aligned} \tag{1}$$

where Δ indicates a change in a parameter. In these equations, it is assumed that a change in heart rate is directly related to a change in MAP. Changes in heart contractility, the arterial to capillary resistance, the capillary to venous resistance, and the venous compliance were considered directly related to changes in MAP as well as oxygen debt. Peripheral resistance was also assumed to be directly related to changes in blood viscosity and inversely related to the square of changes in blood volume.

Figure 3 illustrates the training process used to build a TPSIM that includes a deterministic control system model. To train the deterministic model, the weights (i.e., G1...G22) were initialized to baseline values, such that without changes in inputs, the output values remain unchanged. Other than this restriction, the initial weights were assigned based on experience solving numerical models. The outputs of the control model were supplied as inputs to the passive cardiovascular system for calculation of hemodynamic parameters. Changes in MAP, Hct, CO, (calculated by the passive system model) and HR (calculated by the deterministic control model) were compared incrementally (in time) to the experimental data. The Simplex method [3] was used to optimize the weights G1, G2, ... G22 by minimizing the following cost function:

$$L = \sum_i^N [(HR_M - HR_C)^2 + (MAP_M - MAP_C)^2 + (Hct_M - Hct_C)^2 + (CO_M - CO_C)^2] \quad 2)$$

where N is the total number of measurements (in this case, seven); Hct indicates the blood hematocrit; CO indicates the cardiac output; the subscript M indicates experimentally measured values and the subscript C is the notation for calculated values. The final weights for the deterministic model were chosen once the cost function reached a minimum value.

The deterministic control system model was implemented in the "C" language on a Sun Sparcstation 10 computer running UNIX (Solaris operating system). The deterministic model was integrated with the previously developed passive cardiovascular system model. All code was written for portability and ease of modification. Approximately 500 passes of the swine data were executed to determine the final deterministic model weights. The results of executing the model with the final weights are presented below.

NEURAL NETWORK CONTROL MODEL

The neural network control model was refined to better simulate neural and hormonal control during hemorrhage. The details of the neural network control model design were described in the 15 June, 1995, preliminary report. However, changes have been made to improve performance results. A change was made to replace left and right heart end-systolic volumes with right and left heart contractility. Absolute values of MAP, blood volume, blood viscosity were also added as inputs to the neural network. Changes in these values remained as inputs. The modified design includes a total of seven input nodes, four hidden nodes, and six output nodes. An updated training diagram for the TPSIM that includes a neural network control model is shown in Figure 4. Approximately 700 data passes were executed on a Sun Sparcstation 10 computer to train the neural network. The results of this training are presented below.

TPSIM MODEL TESTING AND RESULTS

Responses of conscious swine to an uncontrolled aortotomy hemorrhage have been studied by Bickell et al [4]. The uncontrolled hemorrhage lasted about five minutes with an estimated 33% (23.1 ml per kg body weight) loss in normal blood volume. There was no fluid resuscitation during Bickell's experiment. If we assume that the hemorrhage rate declines exponentially with a time constant (τ) of one minute, the hemorrhage rate can be described as follows [5]:

$$\begin{aligned} H(t) &= H_0 \cdot e^{-kt} + (R/k) \cdot (1 - e^{-kt}) \\ k &= \ln(2)/\tau \\ R &= (23.1) \cdot k^2 / (5 \cdot k + (1 - e^{5k})) \\ H_0 &= R \cdot (1 - e^{5k}) / k \end{aligned} \quad 3)$$

The MAP, CO, HR, and hematocrit were measured at 0, 10, 20, 35, 65, 95 and 125 minutes after the start of hemorrhage. The experimental data were compared with data calculated by the passive system model combined with the deterministic-based cardiovascular control system as well as the passive system combined with the neural network-based cardiovascular control system.

A incremental time step of 0.86 seconds was used to train (and test) the models. This represents about one heart beat period (assuming the baseline heart rate is 70 beats/minute). For each model, the calculated values of MAP, CO, HR, and Hct at time 0, 10, 20, 35, 65, 95 and 125 minutes were compared with the corresponding experimentally measured values using the cost function described in Equation 2 above. Weights were adjusted after each pass of all the data (125 minutes, 0.86 second increments). This iterative process continued until a minimal change in the cost function was observed. Using these final weights, hemodynamic parameters were calculated for comparison against the experimental swine data.

TPSIM with Deterministic Cardiovascular Control System

Figures 5 to 10 illustrate the results from executing the TPSIM model with the final deterministic control system weights. Figure 5 shows the changes in blood volume, MAP, Hct, and CO relative to their baseline values after hemorrhage. This figure also shows that oxygen debt increases immediately after hemorrhage and decreases with recovery of cardiac output. The neural and hormonal controlling parameters such as heart rate, right and left heart contractility, arterial and venous resistance, and venous compliance changed immediately after the onset of hemorrhage, then settled to new baseline values. These time series changes are shown in Figure 6. The arterial and venous resistance increased to maintain the arterial pressure, then fell to new values. At the same time, the venous compliance decreased to compress blood volume from the veins into the circulation. However, heart rate did not increase whereas heart contractility decreased. Figures 7 through 10 compare the model estimated heart rate, Hct, MAP, and

CO with experimentally measured values. The differences between the calculated values and measured values for MAP and CO are less than those seen with the TPSIM model without a control system (Figures 17 to 22).

TPSIM with Neural Network Cardiovascular Control System

Figures 11 to 16 illustrate the results from executing the TPSIM model with the revised neural network control system. Figure 11 shows similar trends for blood volume, MAP, Hct, CO, and oxygen debt as found in Figure 5 (from the deterministic model). However, several of the neural and hormonal controlling parameters shown in Figure 12 displayed somewhat different trends than those found with the deterministic model (Figure 6). As expected physiologically, the right and left heart contractility increased after hemorrhage to increase the cardiac output. However, the venous resistance did not increase nor did the venous compliance decrease. As seen in the deterministic model, the arterial resistance increased to maintain the arterial blood pressure.

Figures 13 to 16 compared the TPSIM model calculated heart rate, Hct, MAP, and CO with their experimentally measured values. As reported in June, 1995, and as seen with the deterministic-based model, the results are better with a control system model than without one (Figures 17 to 22).

SUMMARY

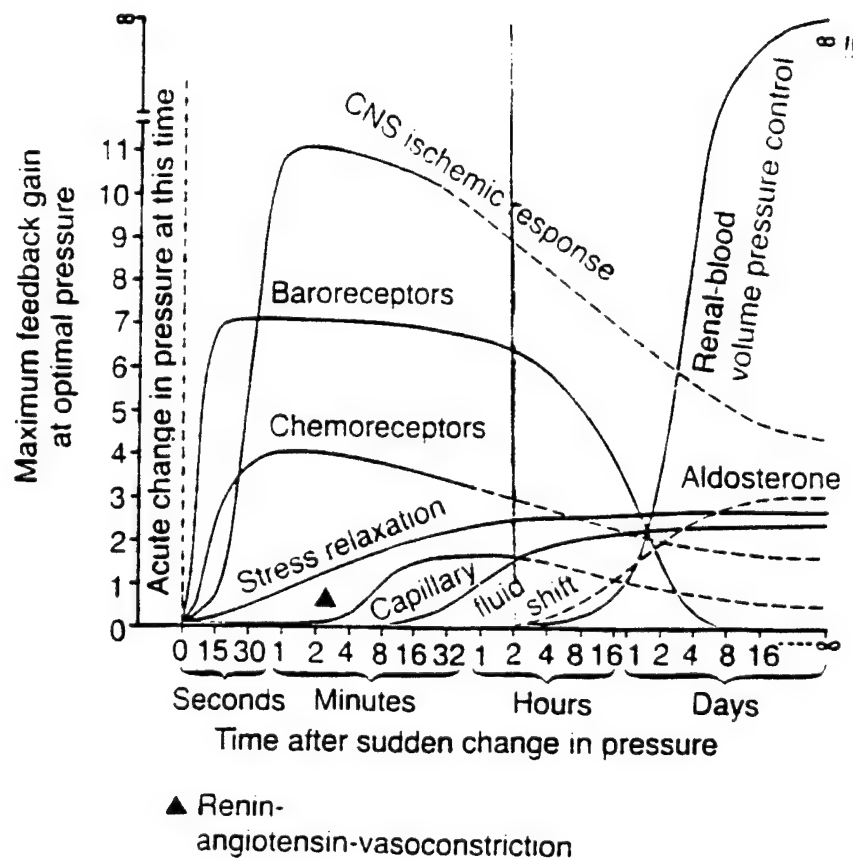
SwRI has implemented two versions of the trauma patient simulator (TPSIM), one that combines the passive system model with a neural network control system and one that combines the passive model with a deterministic control system. Both TPSIMs have been trained and tested using experimental animal hemorrhage data. The neural network-based TPSIM has received refinement and testing. The results of the latest testing with the refined neural network-based TPSIM showed improved performance. Results from preliminary testing with the deterministic-based TPSIM showed performance similar to the neural network-based TPSIM for determination of hemodynamic changes. Both approaches provided reasonable estimates of the trends of hemodynamic changes after hemorrhage. However, the trends for neural and hormonal controlled parameters varied between the two models. Since only one data set was used to train and test the two approaches, it can be expected that the results would exhibit inconsistencies. However, these inconsistencies must be significantly reduced for a fair comparison and evaluation of the two approaches. Further, the trends for the neural and hormonal control variables must better represent the physiology of trauma. Training both models with additional data is expected to decrease the inconsistencies. Training and testing of both TPSIMs with additional data is necessary before a final control system approach can be determined.

REFERENCES

- [1] Guyton A.C., "Summary of the integrated, multifaceted system for arterial pressure regulation", in Textbook of Medical Physiology, W.B. Saunders Co., 1991, pp. 218 - 219.
- [2] Guyton A.C., "Shock caused by hypovolemia - hemorrhagic shock", in Textbook of Medical Physiology, W.B. Saunders Co., 1991, pp. 264 - 265.
- [3] Press W.H., Teukolsky S.A., Vetterling W.T., Flannery B.P., "Downhill Simplex method in multidimensions", in Numerical Recipes in C, Cambridge, 1992, pp. 408 - 411.
- [4] Bickell W.H., O'benar J., Bruttig S.P., Wade C.E., Hannon J.P., Tillman F., Rodkey W., "The hemodynamic response to aortotomy in the conscious chronically instrumented swine," *The Physiologist*, 30, pp. 228, 1987.
- [5] Doherty T.J., Bruttig S.P., Bickell W.H., "Controlled response to aortotomy hemorrhage in swine: effects of anesthesia," Letterman Army Institute of Research internal report.

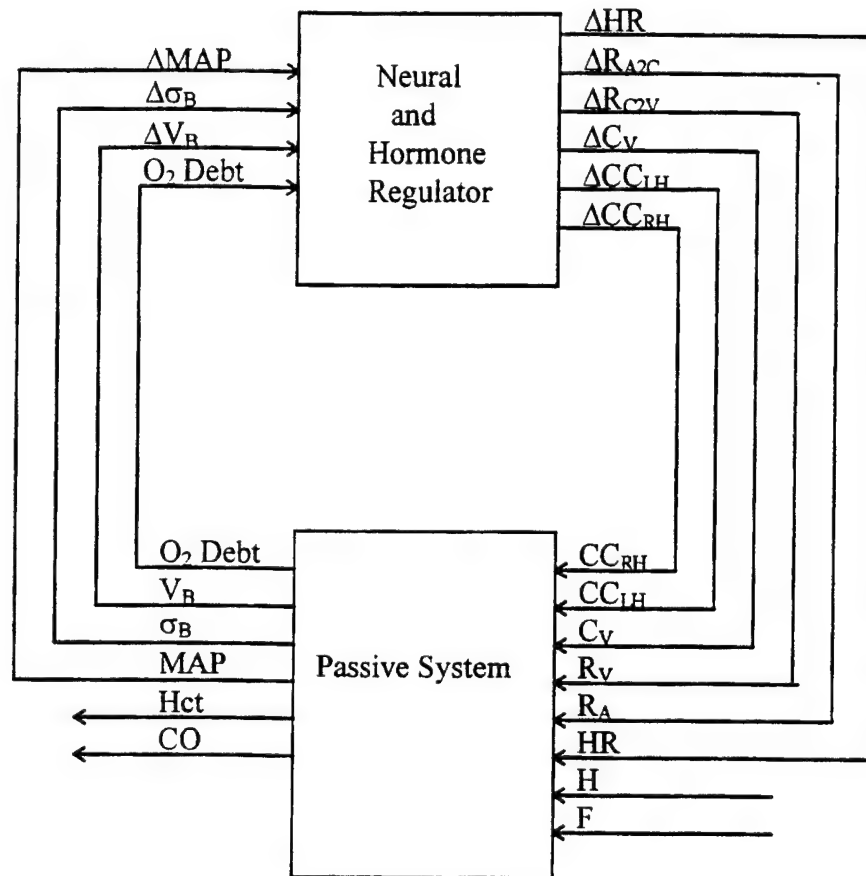
APPENDIX: FIGURES AND DIAGRAMS

Figure 1. Arterial Blood Pressure Control Mechanisms



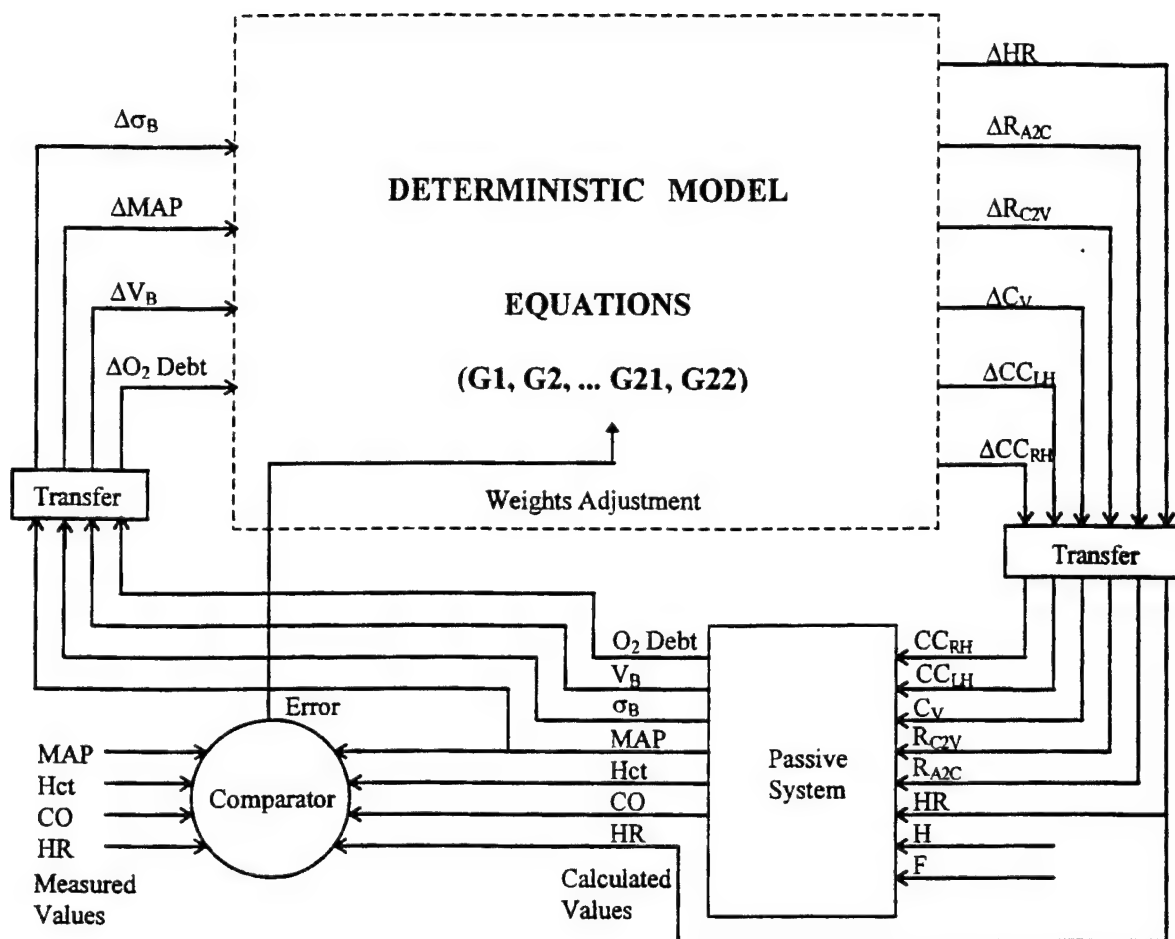
Approximate potency of various arterial pressure control mechanisms at different time intervals after the onset of a disturbance to the arterial pressure. (from Guyton: Textbook of Medical Physiology. Philadelphia, W.B. Saunders Company, 1991).

Figure 2. Diagram of the Trauma Patient Simulator



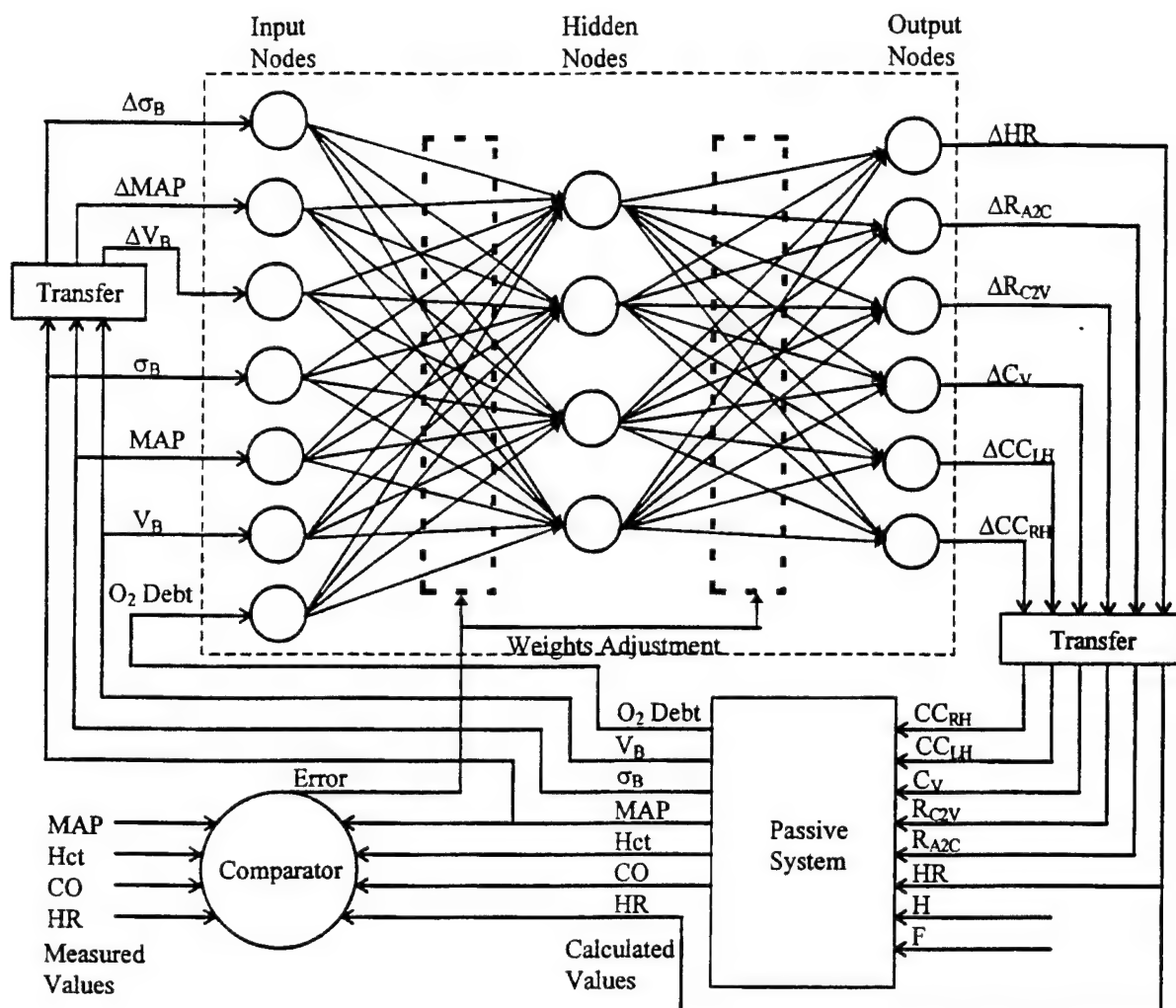
$O_2 \text{ Debt}$: Oxygen Debt;
 V_B : Blood Volume;
 MA : Mean Blood Pressure;
 σ_B : Blood Viscosity;
 Hct : Hematocrit;
 CO : Cardiac Output;
 CC_{RH} : Right Heart Contractility;
 CC_{LH} : Left Heart Contractility;
 C_V : Vein Compliance;
 R_{A2C} : Artery to Capillary resistance;
 R_{C2V} : Capillary to Vein Resistance;
 HR : Heart Rate;
 H : Hemorrhage Rate;
 F : Fluid Resuscitation Rate.

Figure 3. Deterministic Control System Training Diagram



O₂ Debt: Oxygen Debt;
V_B: Blood Volume;
MAP: Mean Blood Pressure;
σ_B: Blood Viscosity;
Hct: Hematocrit;
CO: Cardiac Output;
CC_{RH}: Right Heart Contractility;
CC_{LH}: Left Heart Contractility;
C_V: Vein Compliance;
R_{A2C}: Artery to Capillary resistance;
R_{C2V}: Capillary to Vein Resistance;
HR: Heart Rate;
H: Hemorrhage Rate;
F: Fluid Resuscitation Rate.

Figure 4. Neural Network Control System Training Diagram



$O_2 Debt$: Oxygen Debt;
 V_B : Blood Volume;
 MAP : Mean Blood Pressure;
 σ_B : Blood Viscosity;
 Hct : Hematocrit;
 CO : Cardiac Output;
 CC_{RH} : Right Heart Contractility;
 CC_{1H} : Left Heart Contractility;
 C_V : Vein Compliance;
 R_{A2C} : Artery to Capillary resistance;
 R_{C2V} : Capillary to Vein Resistance;
 HR : Heart Rate;
 H : Hemorrhage Rate;
 F : Fluid Resuscitation Rate.

Figure 5. TPSIM System Test - DET Control
Physiological Data After Hemorrhage

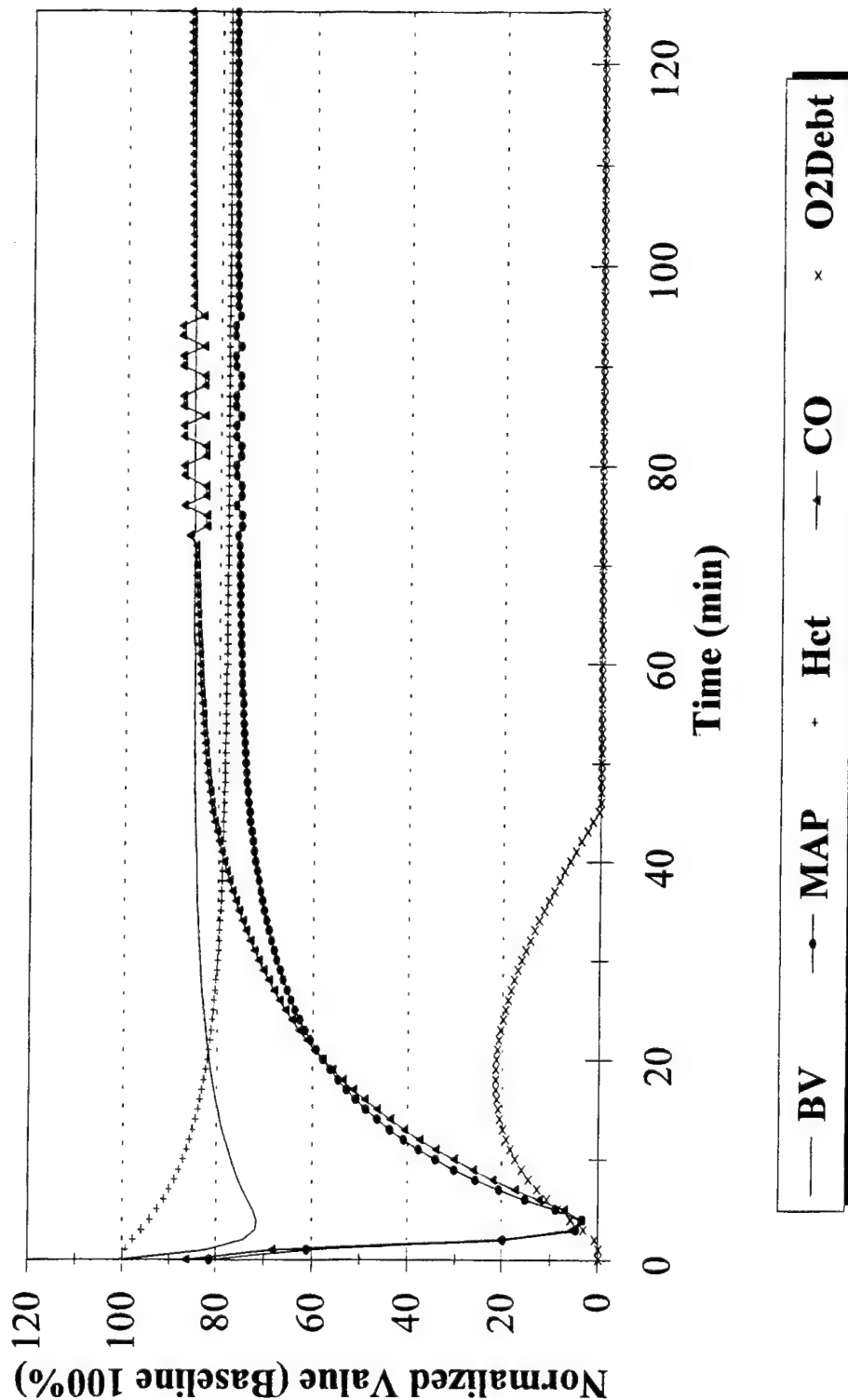


Figure 6. TPSIM System Test - DET Control
Control Data After Hemorrhage

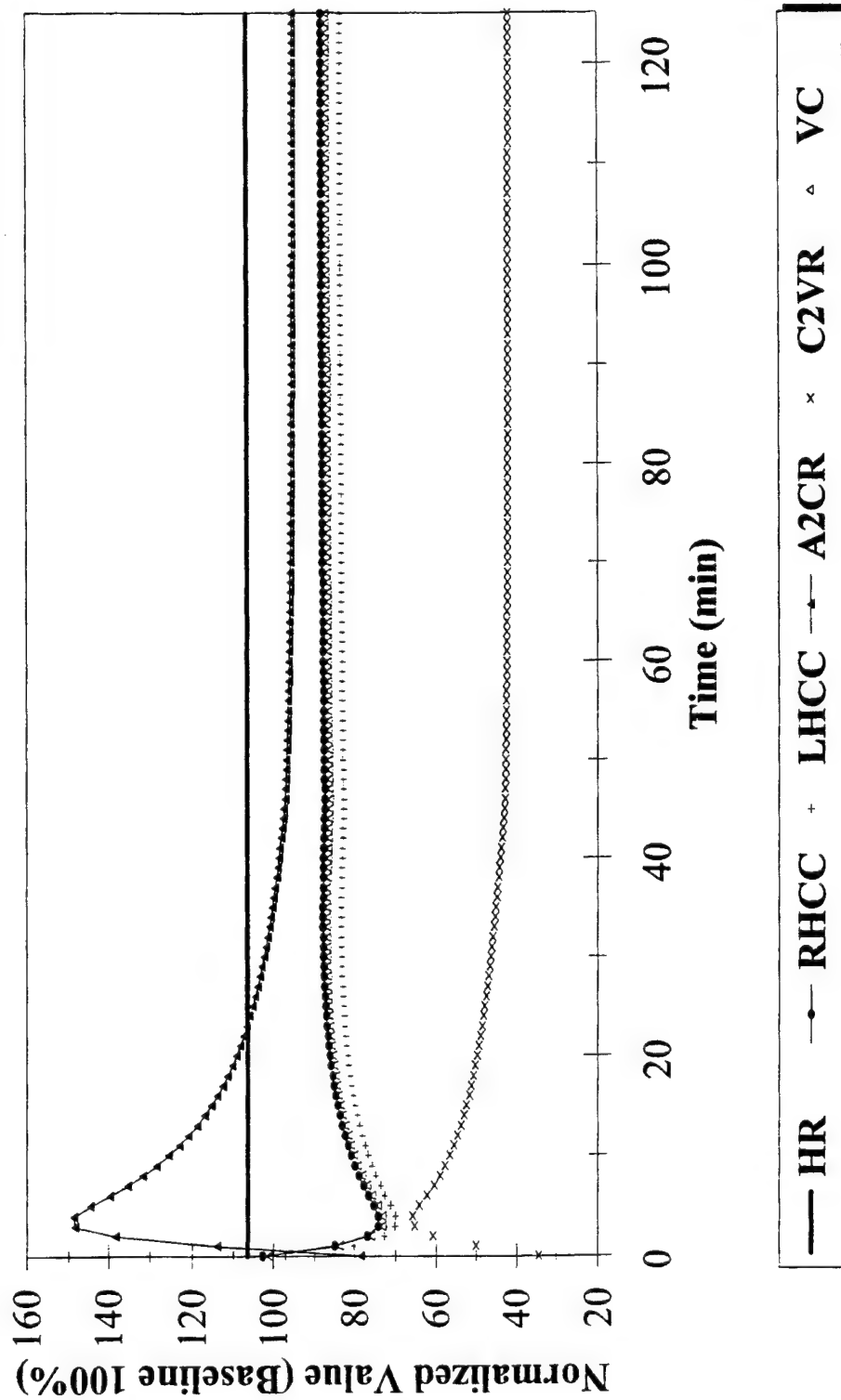


Figure 7. TPSIM System Test - DET Control
HR - Conscious Swine

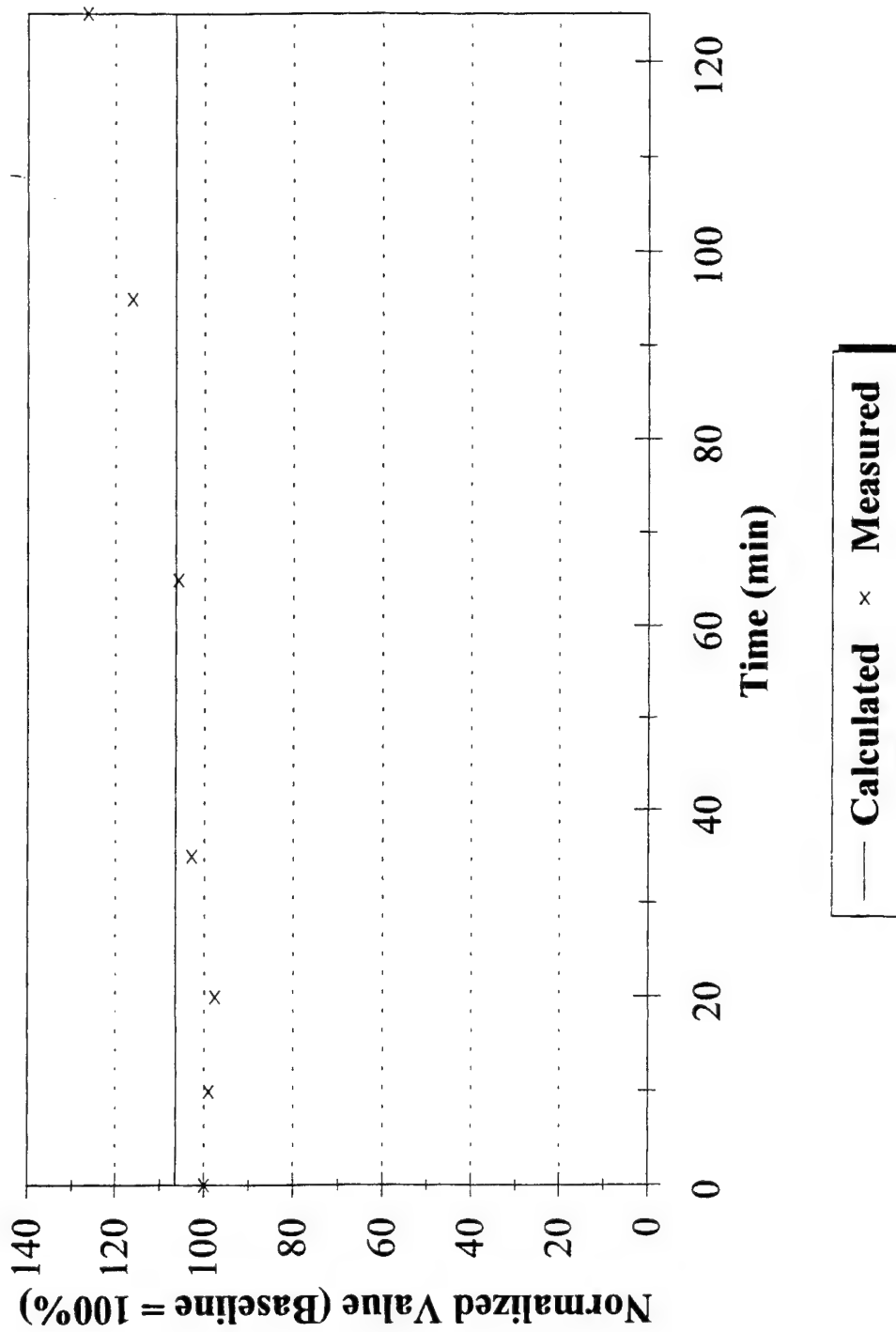


Figure 8. Passive System Test - DET Control
Hct - Conscious Swine

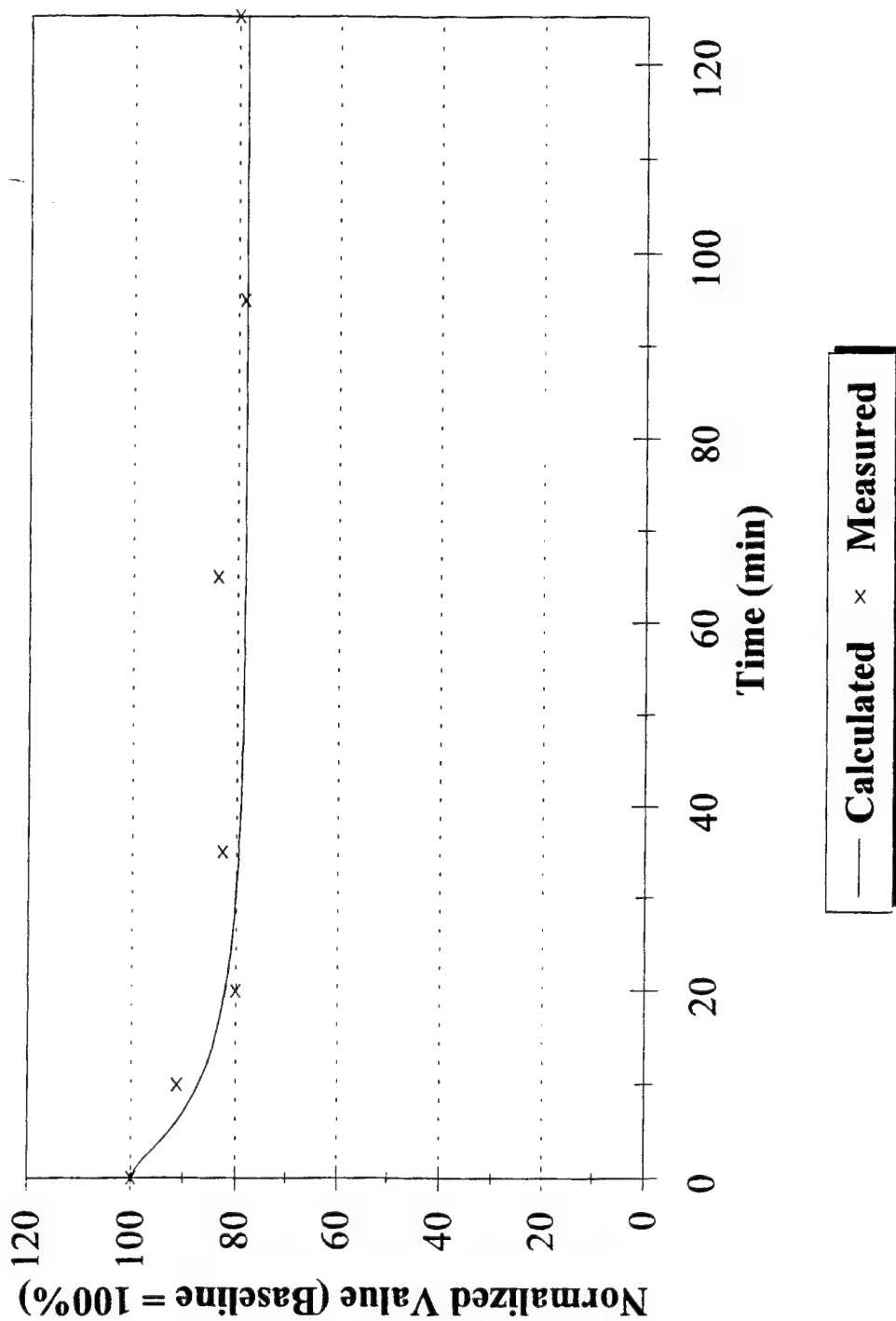


Figure 9. TPSIM System Test - DET Control
MAP - Conscious Swine

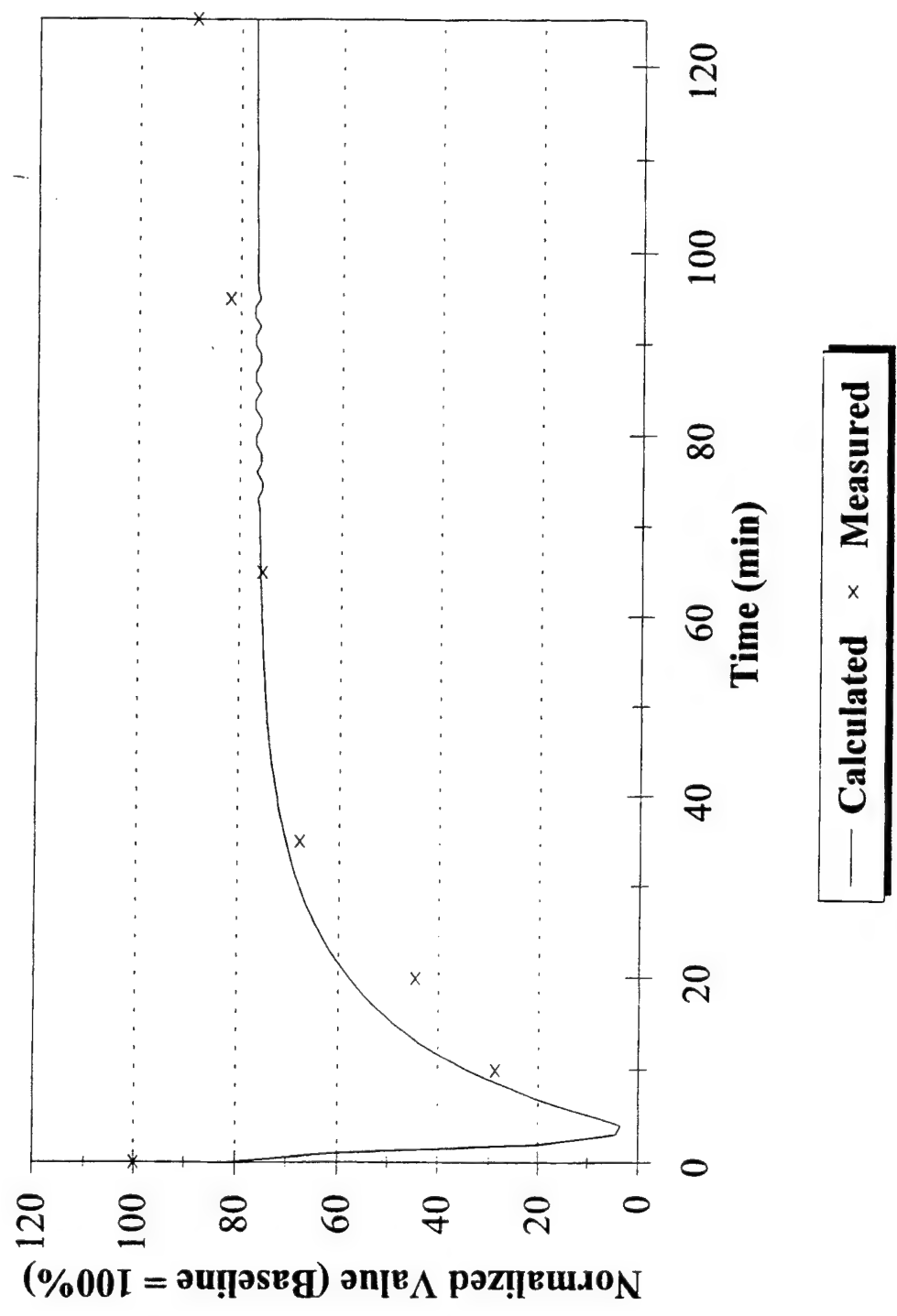


Figure 10. Passive System Test - DET Control
CO - Conscious Swine

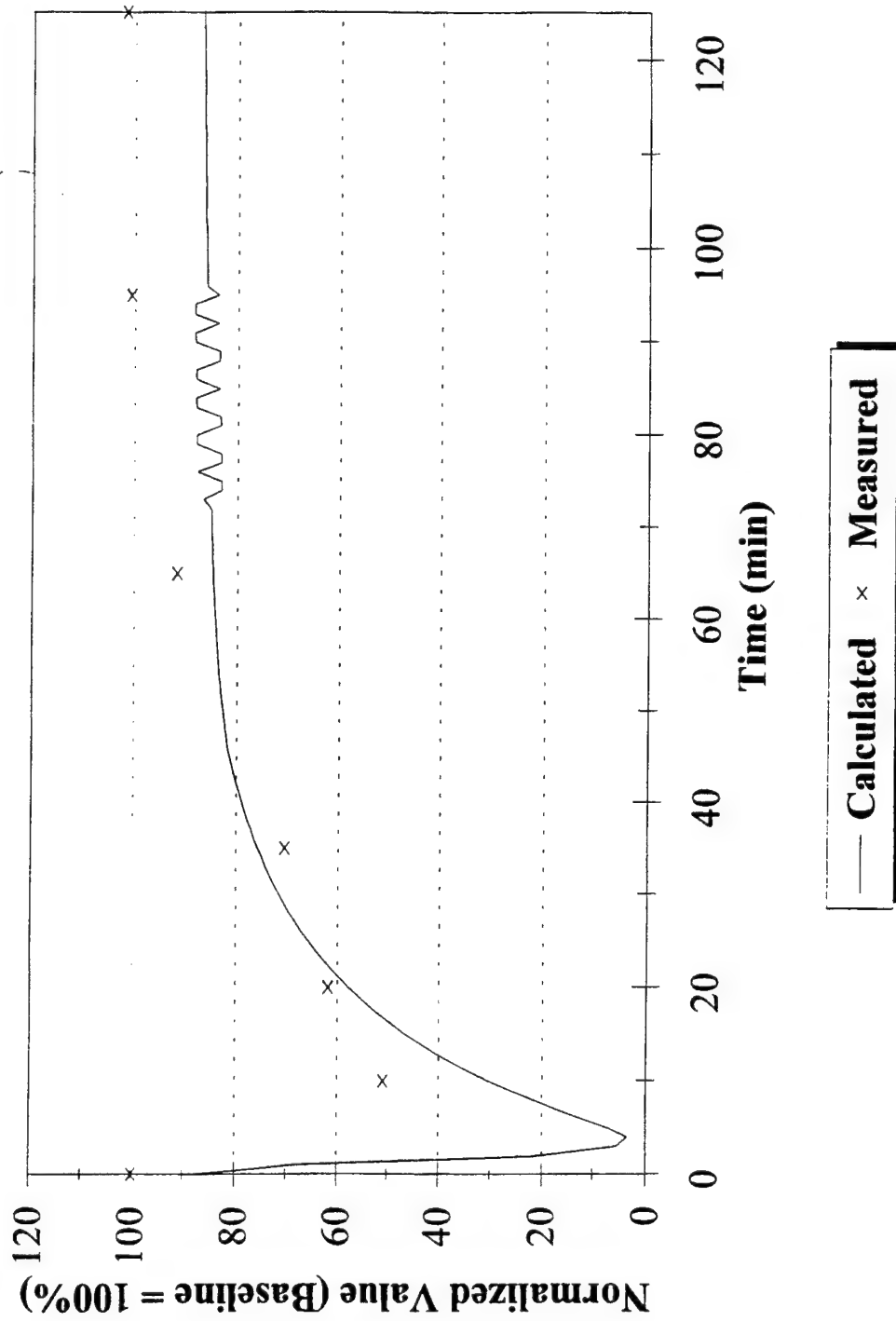


Figure 11. TPSIM System Test - NN Control
Physiological Data After Hemorrhage

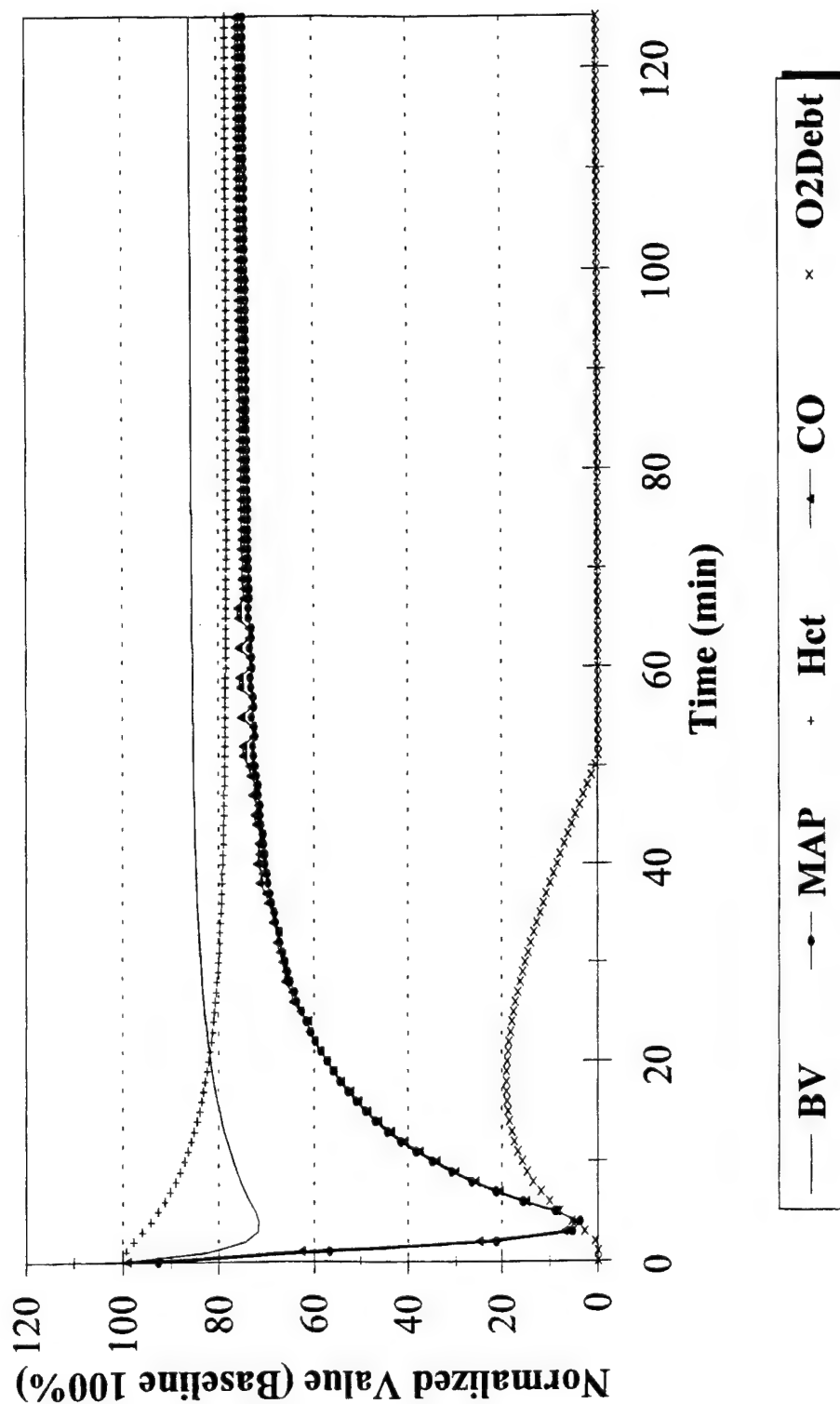


Figure 12. TPSIM System Test - NN Control
Control Data After Hemorrhage

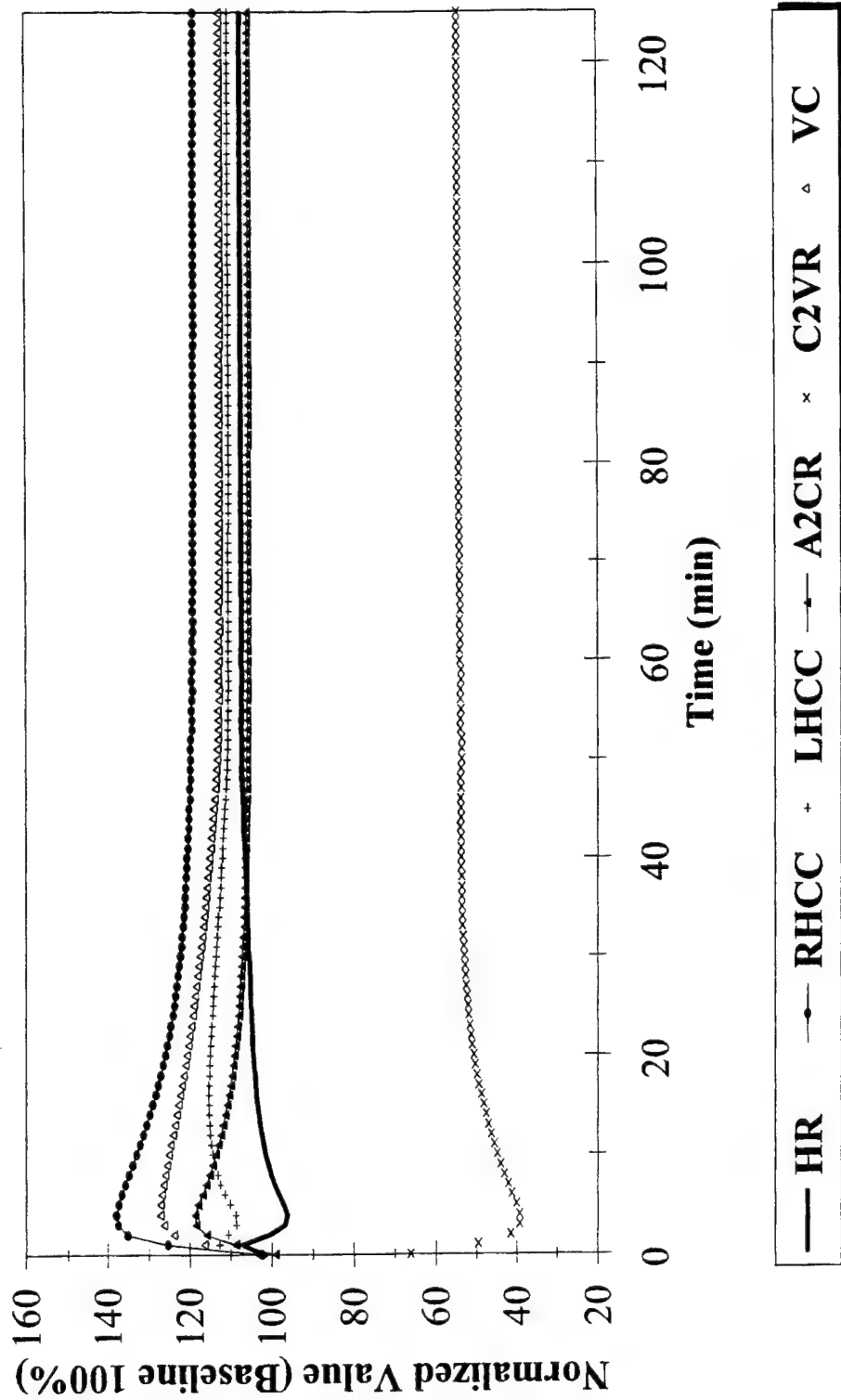


Figure 13. TPSIM System Test - NN Control
HR - Conscious Swine

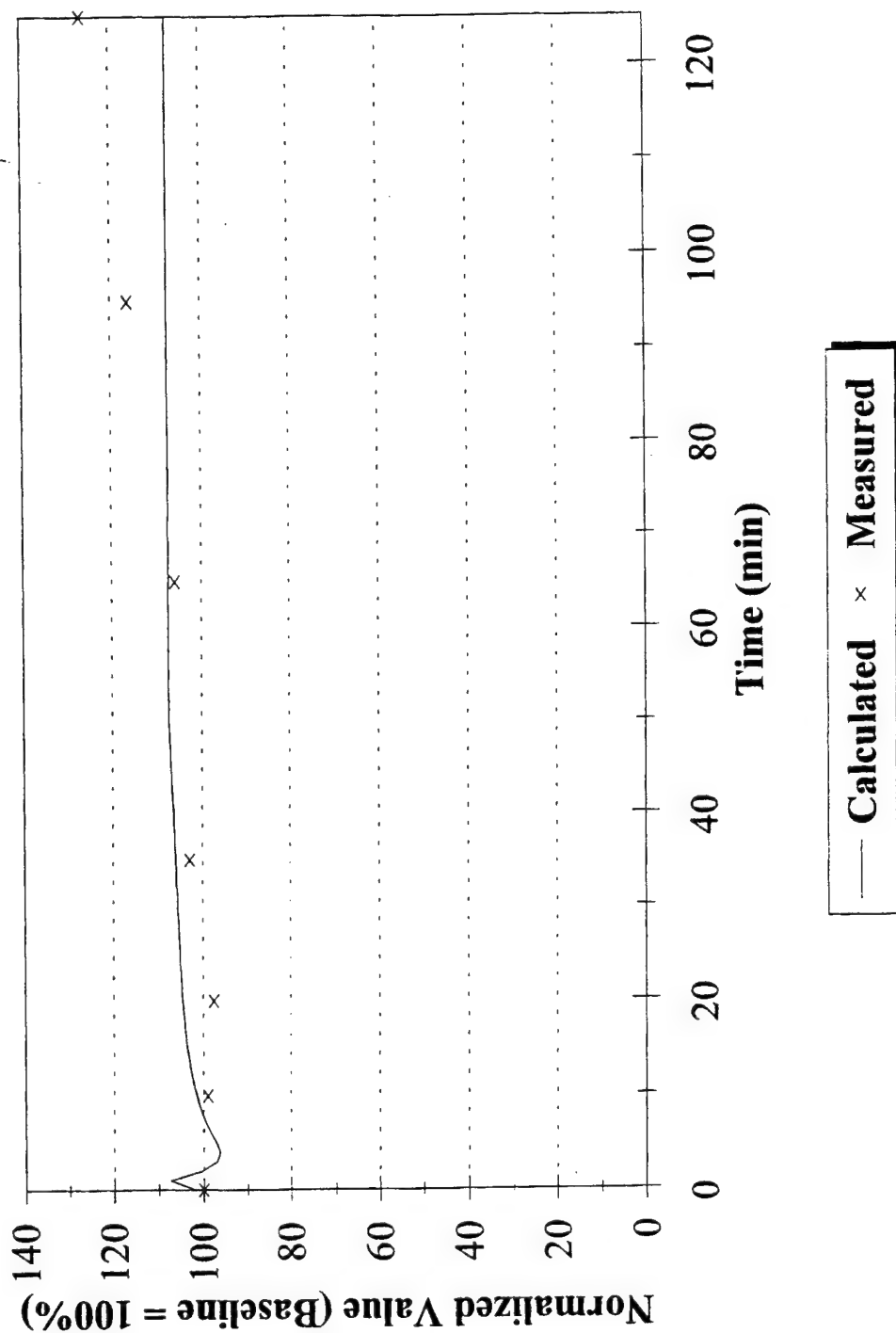


Figure 14. Passive System Test - NN Control
Hct - Conscious Swine

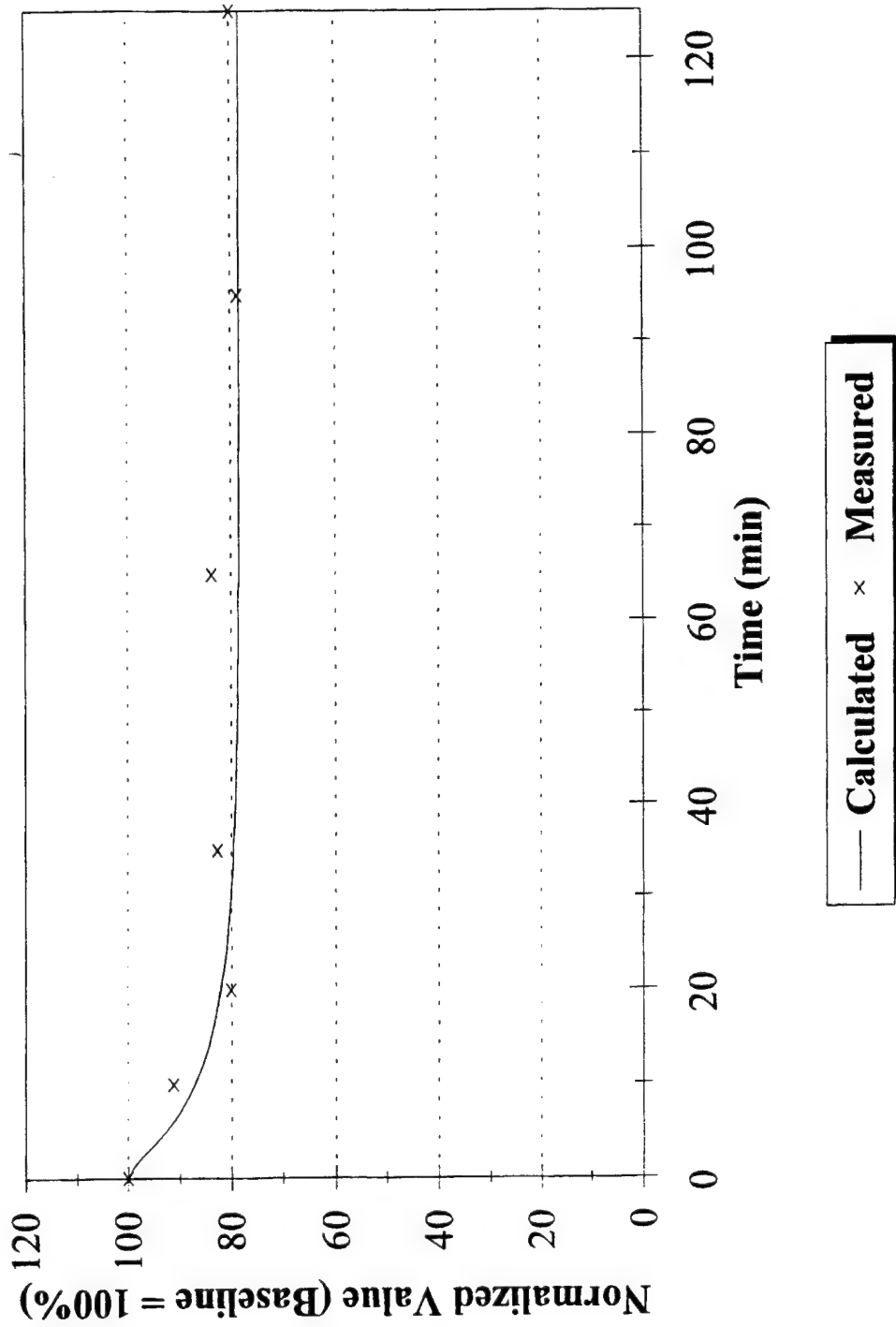


Figure 15. TPSIM System Test - NN Control
MAP - Conscious Swine

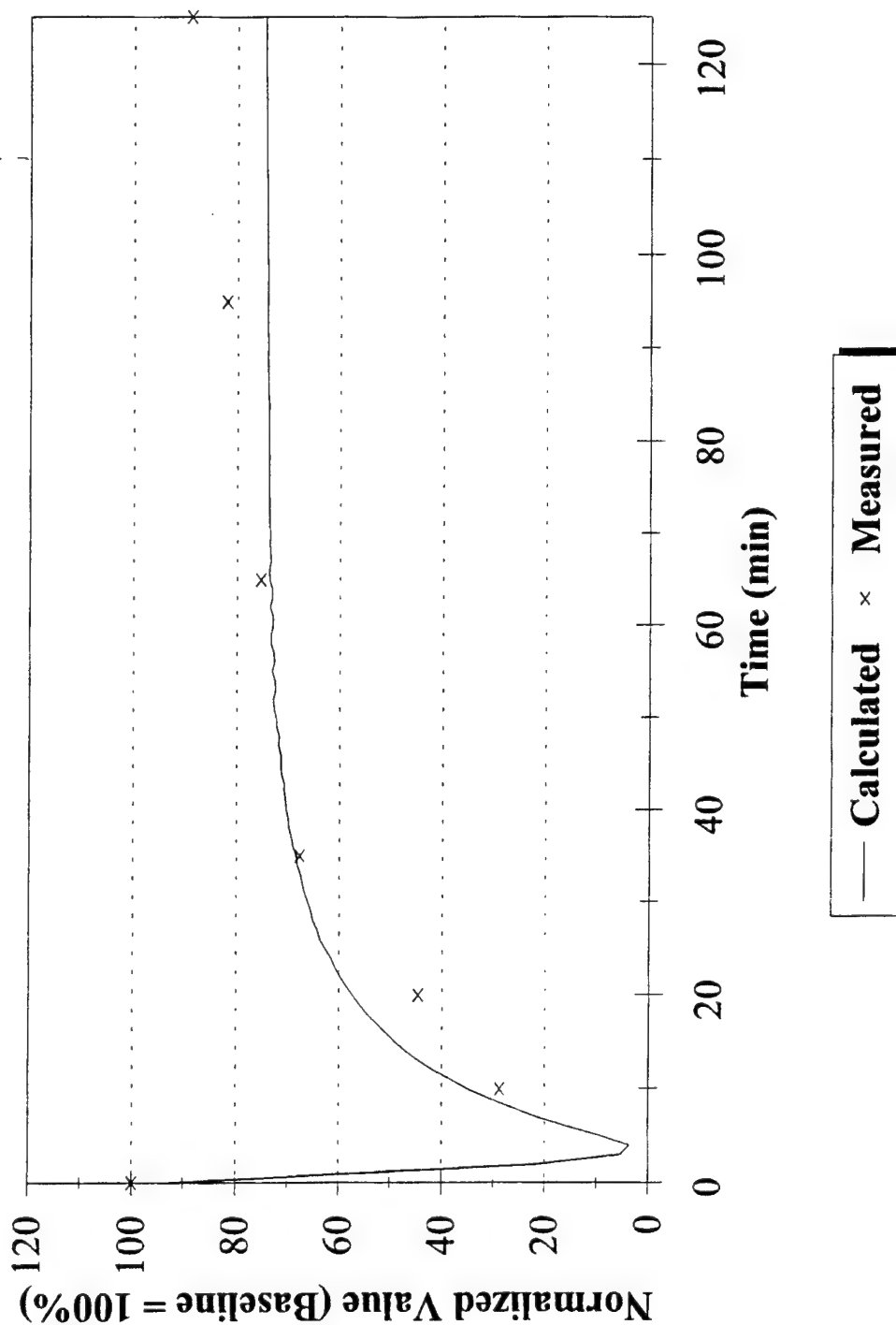


Figure 16. Passive System Test - NN Control
CO - Conscious Swine

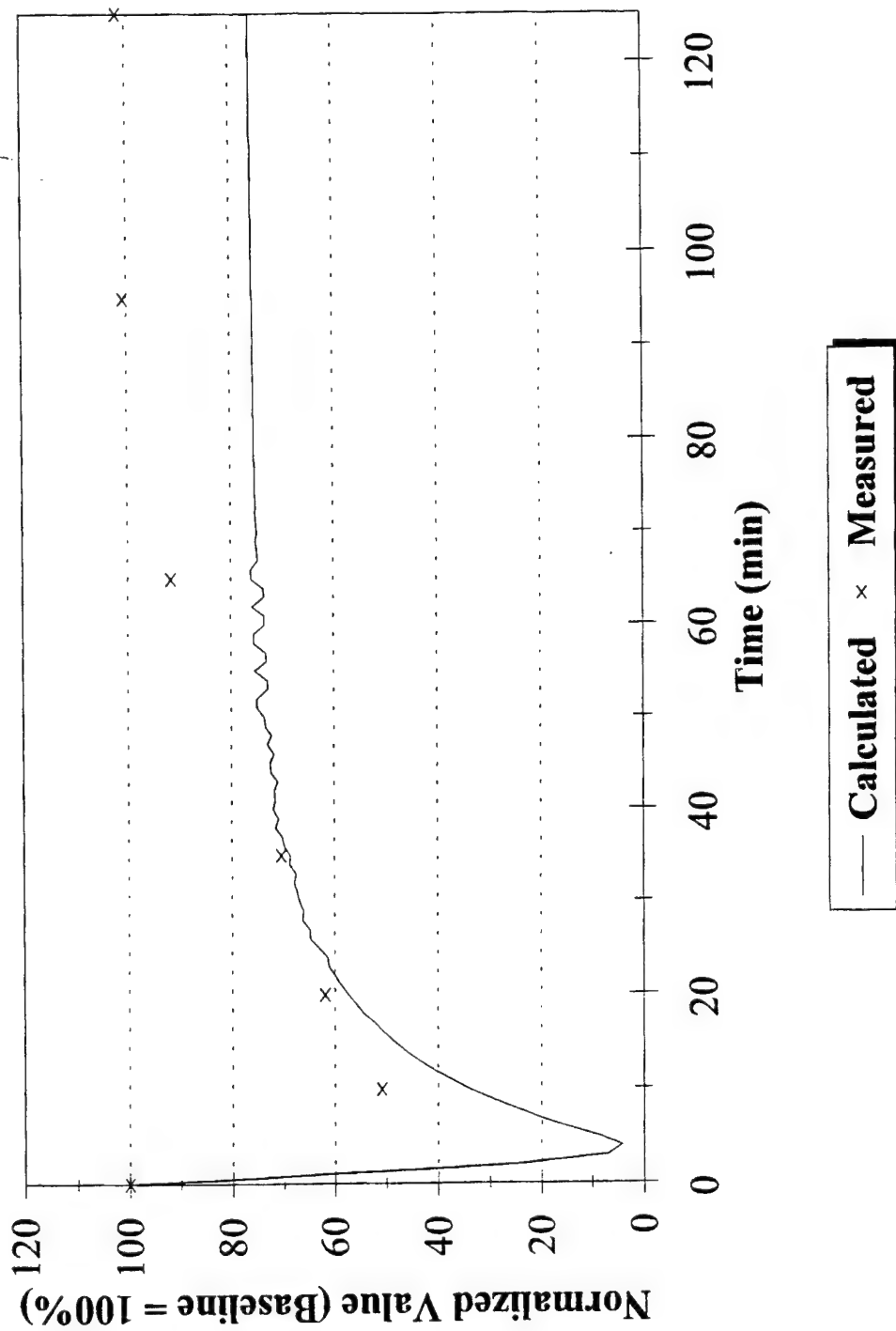


Figure 17. TPSIM System Test - No Control
Physiological Data After Hemorrhage

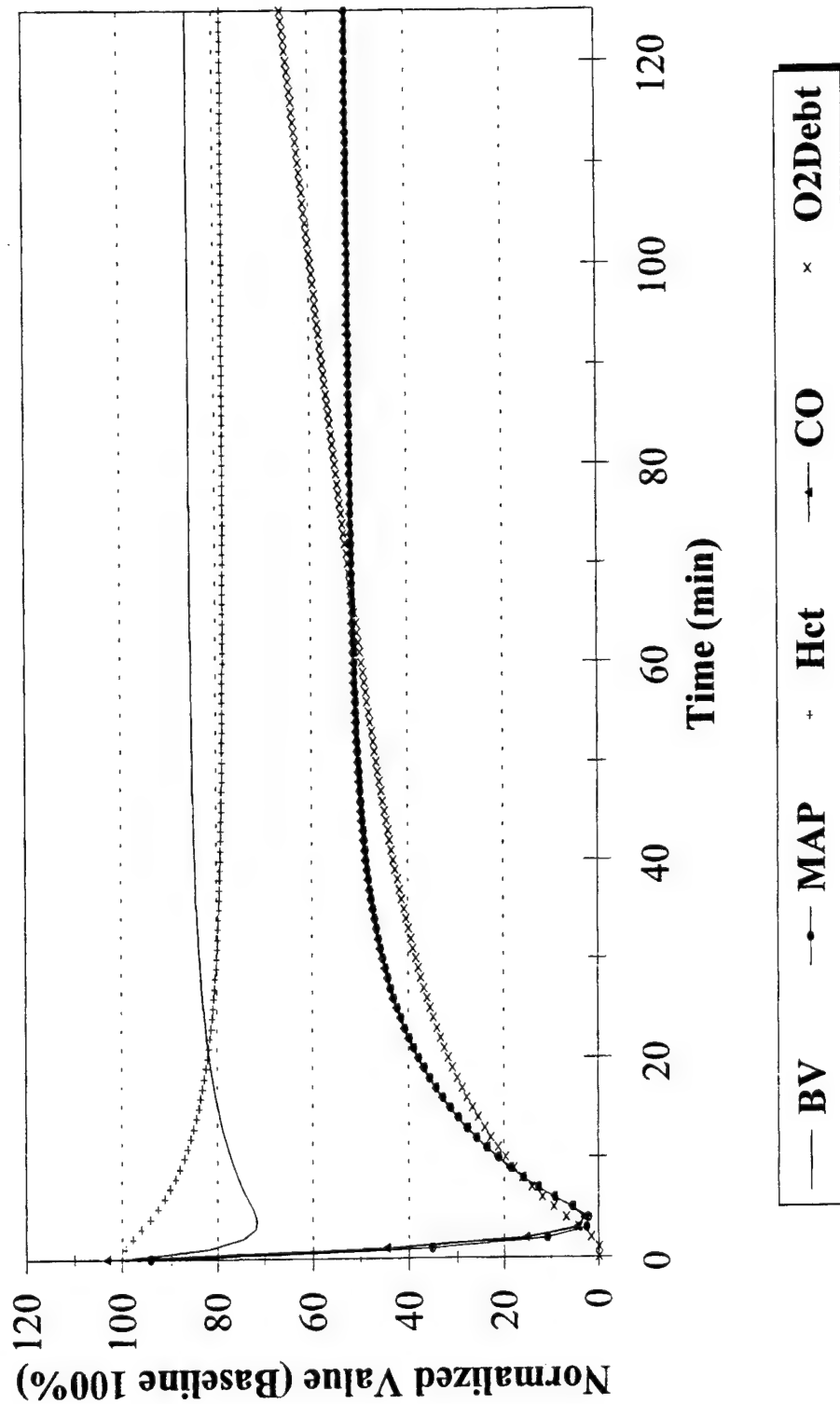


Figure 18. TPSIM System Test - No Control
No Control After Hemorrhage

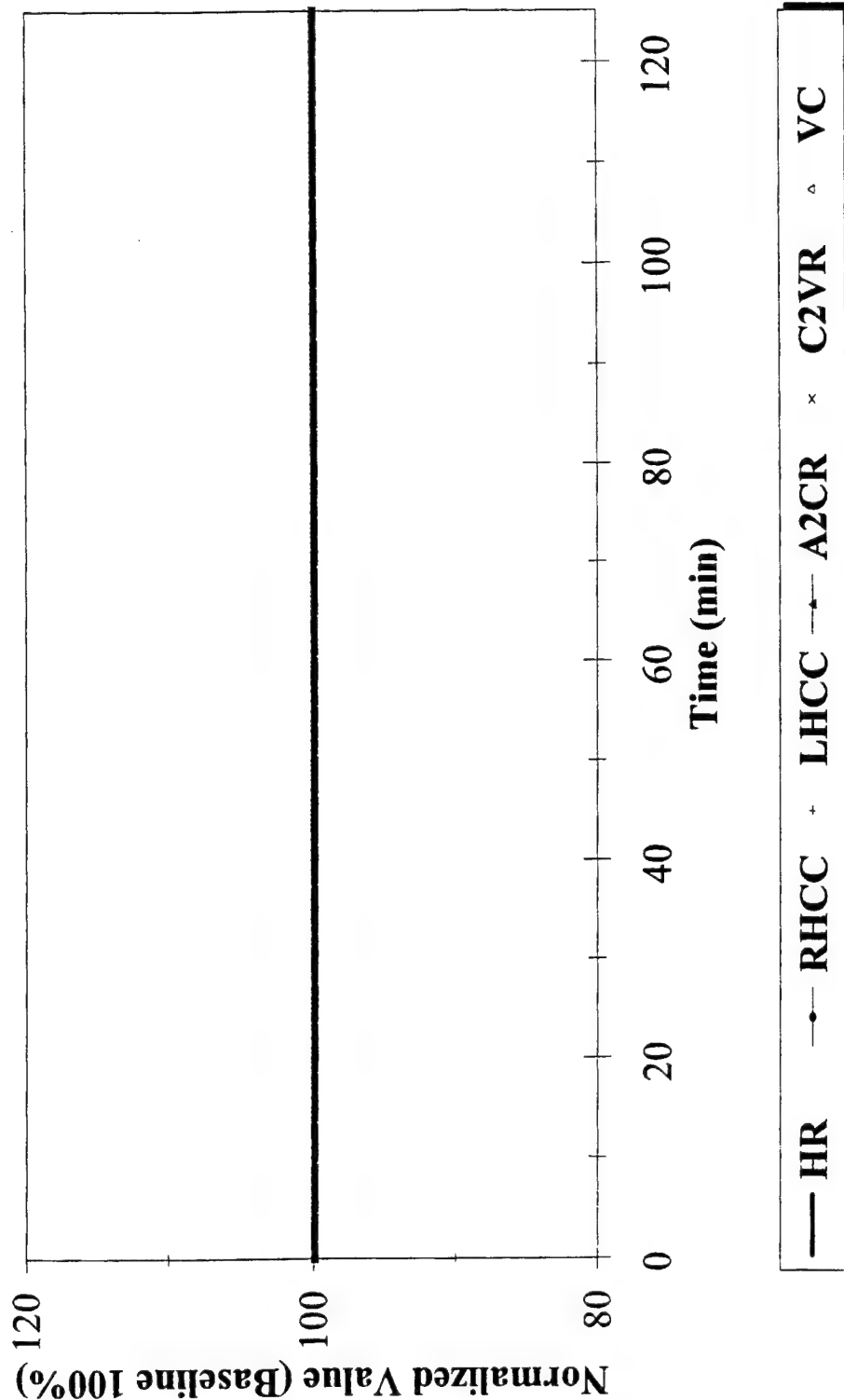


Figure 19. TPSIM System Test - No Control
HR - Conscious Swine

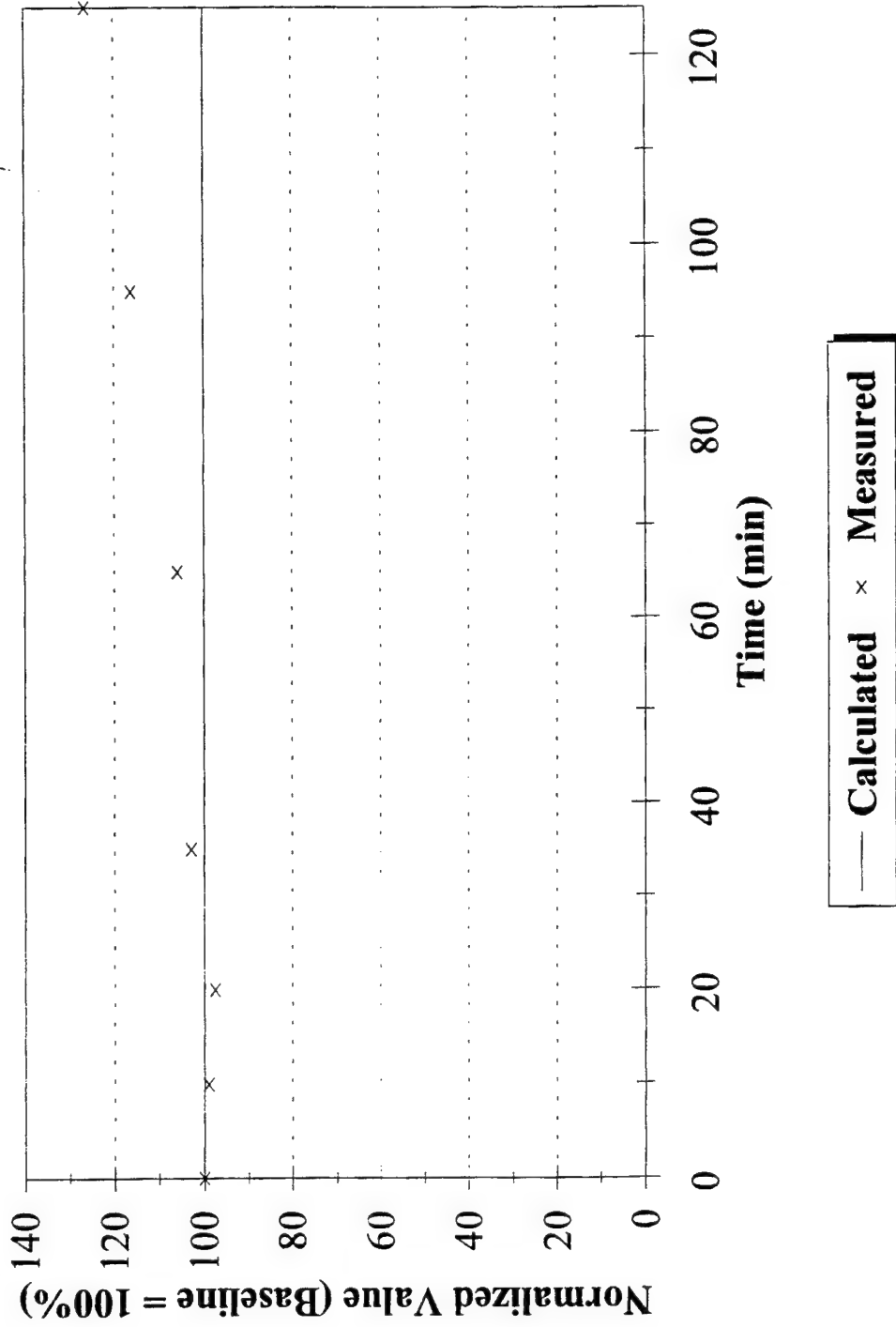


Figure 20. Passive System Test - No Control
Hct - Conscious Swine

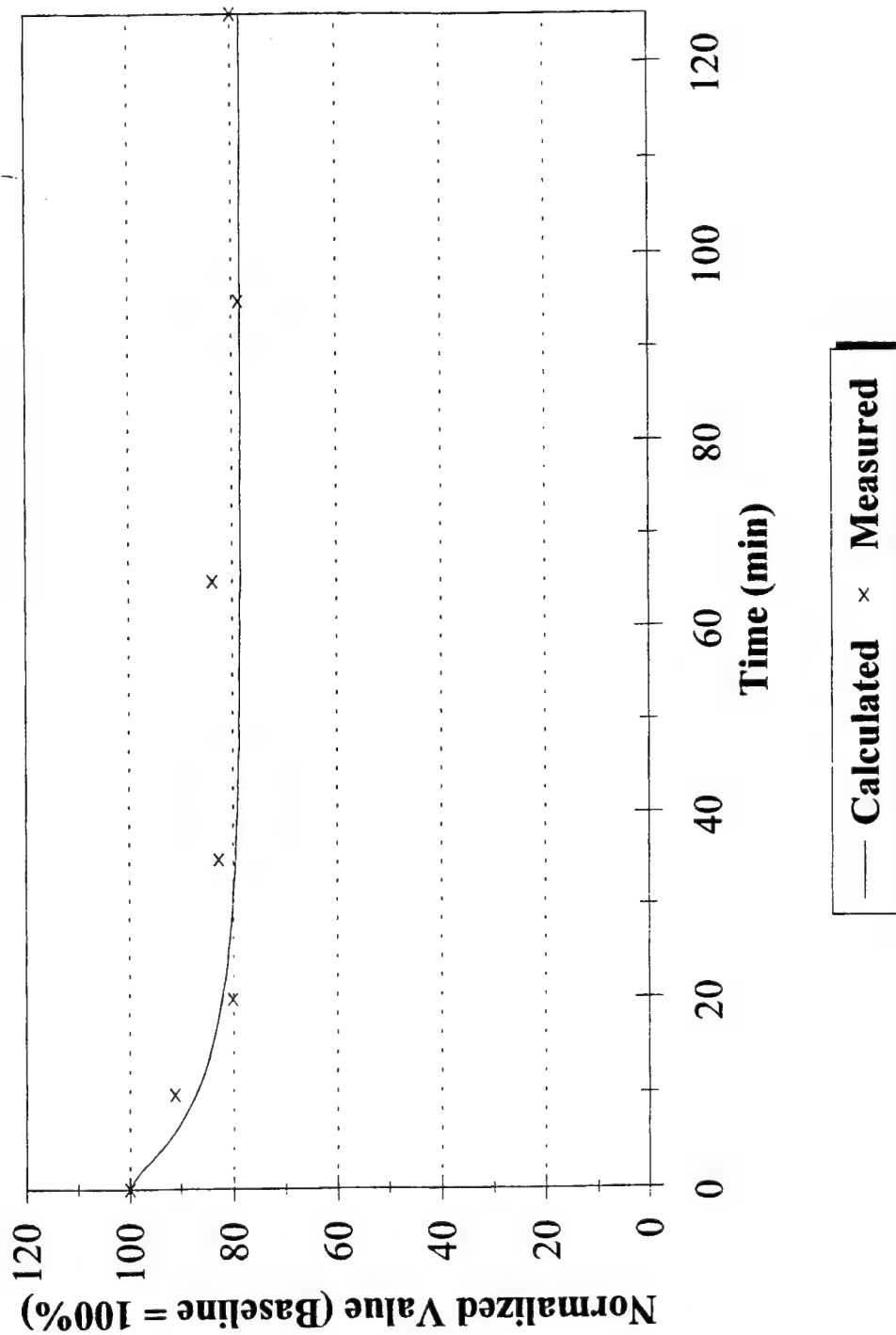


Figure 21. TPSIM System Test - No Control
MAP - Conscious Swine

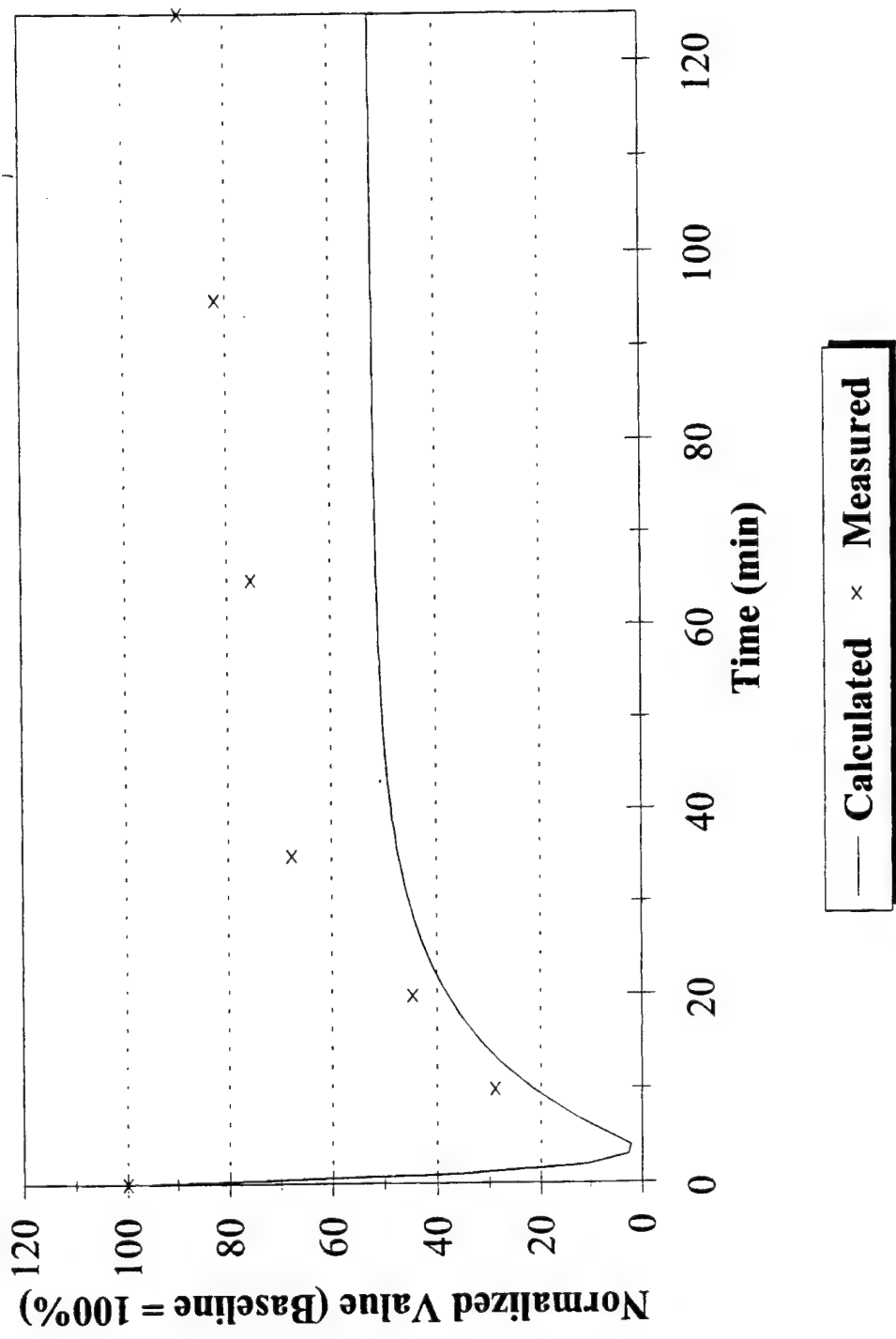
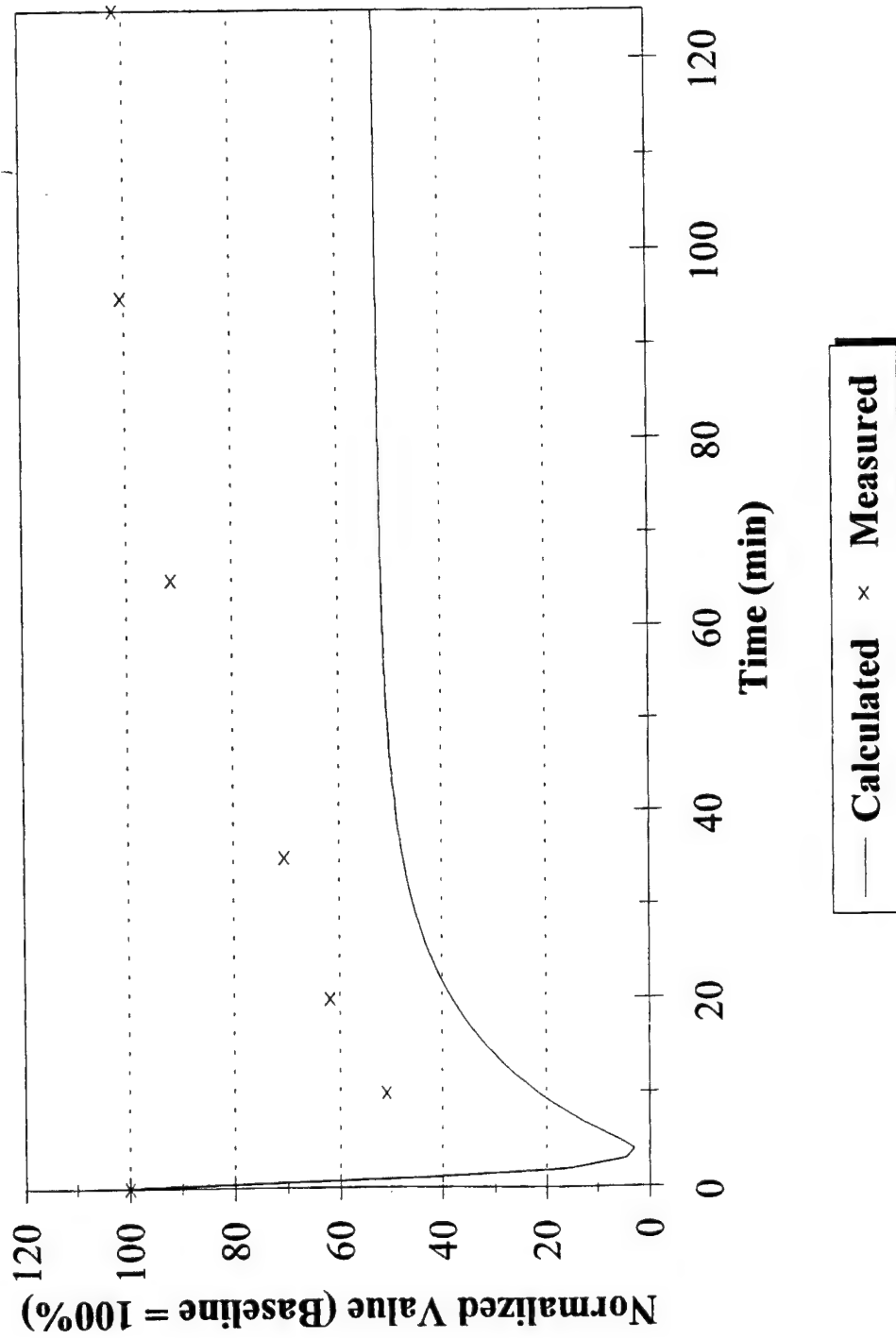


Figure 22. Passive System Test - No Control
CO - Conscious Swine



Copy A
12-6711

SOUTHWEST RESEARCH INSTITUTE

6220 CULEBRA ROAD • POST OFFICE DRAWER 28510 • SAN ANTONIO, TEXAS, USA 78228-0510 • (210) 684-5111 • TELEX 244846

December 14, 1995

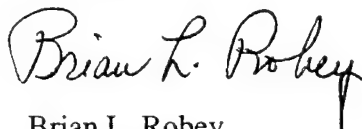
Frederick Pearce, Ph.D.
Director, Division of Surgery
Walter Reed Army Institute of Research
16th St., Building 40
Washington, D.C. 20307-5100

Dear Dr. Pearce:

Enclosed is the fifth quarterly report for work performed under contract no. DAMD17-94-C4126. This report covers the period from 2 September, 1995 to 24 November, 1995.

Please feel free to contact me at (210) 522-5115 if you have any questions or concerns regarding the technical aspects of this report. Please contact Ms. Sharon Rowe at (210) 522-3026 for any contractual or financial matters.

Sincerely,



Brian L. Robey
Project Manager
Biosciences & Bioengineering Department

Enclosure



SAN ANTONIO, TEXAS
HOUSTON, TEXAS • DETROIT, MICHIGAN • WASHINGTON, DC

Quarterly Progress Report

1. Contract No. DAMD17-94-c4126 2. Report Date 15 December, 1995
SwRI Project No. 12-6711
3. Reporting Period from 2 September, 1995 to 24 November, 1995.
4. PI Brian Robey 5. Phone (210) 522-5115
6. Institution Southwest Research Institute, San Antonio, Texas
7. Project Title Model for Trauma Patient Simulation and Automated Fluid Resuscitation
8. Current staff with percent effort of each on project

Brian Robey 14 %

Dean Winter 4 %

Jian Ling 63 %

9. Contract expenditures to date (as applicable):

	this qtr/cumulative		this qtr/cumulative
Personnel	<u>9,378.72 / 37,613.74</u>	Travel	<u>2,909.65 / 4,792.08</u>
Fringe Benefits	<u>4,098.51 / 16,437.22</u>	Equipment/Supplies	<u>1,062.82 / 8,818.49</u>
Overhead	<u>15,903.12 / 63,780.13</u>	Facilities Capital	<u>1,100.31 / 5,330.39</u>

	this qtr/cumulative
Subtotal	<u>29,886.01 / 132,204.93</u>
Indirect Costs	<u> / </u>
Fee	<u>2,302.85 / 10,150.06</u>
Total	<u>32,188.86 / 142,354.99</u>

10. Administrative and Logistical Matters

On 11 October, Mr. Brian Robey and Mr. Jian Ling traveled to Washington D.C. to meet with Dr. Howard Champion at the National Study Center for Trauma and EMS. The purpose of this visit was to determine the availability of clinical data that could be used for continued model development and validation. Dr. Champion can provide data similar to that provided by Dr. Michael Bishop at Martin Luther King Hospital in Los Angeles.

Also, on 11 October, Mr. Robey and Mr. Ling met with Dr. Fred Pearce at Walter Reed for a project review. Dr. Pearce recommended that we use animal data from his laboratory for continued model development and validation. SwRI agreed with Dr. Pearce's recommendation and has delayed plans to obtain clinical data from Drs. Bishop and Champion. SwRI will proceed with model development and validation once the animal data is received from Dr. Pearce. Until this data is received, SwRI is unable to continue work on this project.

SwRI revised the project statement of work to accommodate the costs for further model refinement. Based on discussions with Dr. Don Jenkins at ARPA, SwRI understands that other contractors are responsible for developing the integrated hardware system for the LSTAT. SwRI plans to re-direct the hardware development budget to data collection and further model refinement. The table below summarizes the cost to complete the project according to the revised statement of work.

Work Area	Original Budget	Costs incurred as of 27 October	Cost to Complete
Project Administration	\$57,178	\$35,616	\$34,039
Model Development and Testing (TPSIM and VROS)	\$154,670	\$90,381	\$94,389
Prototype Hardware Development	\$41,659	\$0	\$0
Prototype Real-Time Software Development	\$61,589	\$2,889	\$62,700
Equipment/Supplies	\$29,257	\$8,176	\$500
Phone/FAX	\$130	\$117	\$500
Travel	\$2,910	\$5,176	\$12,910
Total	\$347,393	\$142,355	\$205,038

These costs do not reflect an overall increase in the project budget. The revised statement of work has been sent to the contract officer for review and approval. A copy is attached to this progress report.

SwRI arranged a consulting agreement with Dr. Evangelia Micheli-Tzanakou, Professor and Chairperson for the Department of Biomedical Engineering at Rutgers University. She is considered by many researchers to be an authority on neural networks, particularly in biomedicine. Mr. Robey and Mr. Ling met with Dr. Tzanakou on 12 October, to discuss our neural network design and development approach. The results of this meeting are described in Task 6 below.

11. Scientific Progress

Task 1 - Passive System Model Development/Refinement:

No major modifications were made to the passive cardiovascular system model.

Task 2 - Acquire Existing Data:

During our October 12 meeting with Dr. Pearce, he recommended that we use animal hemorrhage data for model development. Dr. Pearce offered to provide animal hemorrhage data from rats. The rat data provides continuously recorded hemorrhage data (from onset) of the necessary physiological parameters whereas the clinical hospital data only provides intermittent recording of data. Continuous data may provide useful information that is otherwise not available from intermittent recordings. Clinically available data also does not include recordings immediately after a hemorrhage begins.

Prior to the meeting with Dr. Pearce, SwRI purchased two clinical data sets from Dr. Michael Bishop (Martin Luther King Hospital - Los Angeles) at a cost of \$1,000. SwRI began using these data sets to continue development of the TPSIM model. After the meeting with Dr. Pearce, SwRI delayed model evaluation with clinical data.

Task 3 - Deterministic Control System Model Development:

No modifications were made to the deterministic control system.

Task 4 - Deterministic Model Refinement and Testing:

Testing of the deterministic model is described in the Attachment to this progress report.

Task 5 - Neural Network Control System Development:

No major modifications were made to the neural network control system.

Task 6 - Neural Network Model Refinement and Testing:

Mr. Robey and Mr. Ling visited Dr. Tzanakou at Rutgers University on 12 October. We presented our neural network design and approach to her for critical review. She agreed with the overall design and made several recommendations. She suggested that we consider simulating additional data (based on the swine data) to for use in training and testing the network. Based on Dr. Tzanakou's recommendation, we generated simulated data for further training and testing of the neural network. This work is described in the Attachment.

Task 7 - Model Reliability and Accuracy Studies:

Not started.

Task 8 - Control System Model Selection:

We began comparing performance between the deterministic and neural network control system models. Since animal data had not been received, simulated data were generated by supplying the existing neural network (and passive system model) with different hemorrhage rates. This provided additional data sets similar to the swine hemorrhage data. We then used these data sets to train and test both the deterministic and neural network-based TPSIMs. This work is further described in the Attachment. We will continue evaluating the two control system models with the rat data from Dr. Pearce.

Task 9 - Development of a Fluid Resuscitation Optimization Algorithm:

No work was performed on this task.

Task 10 - Real Time Software System Development:

No work was performed on this task.

Task 11- Prototype System Development:

Not started.

Plans For Next Quarter

- Animal data will be obtained from Dr. Fred Pearce at Walter Reed.
- The reliability and accuracy of the passive system will be evaluated using additional acquired data.
- The neural network control system will be further refined and tested using the animal data.
- The deterministic control system will be further refined and tested using the animal data.
- The results of further testing with the deterministic control system and neural network control system will be compared.

ATTACHMENT

TESTS OF THE DETERMINISTIC CONTROL MODEL AND NEURAL NETWORK CONTROL MODEL USING SIMULATED DATA

This attachment describes the tests performed on the deterministic and neural network-based TPSIM models using simulated data. The training times for both methods were compared. This work was performed to provide a preliminary indication of the performance of both approaches with additional data. Further comparisons will be performed using animal data to be provided by Dr. Fred Pearce at Walter Reed.

The ten simulation data sets were created with the neural network-based TPSIM model that was originally trained with swine data. Minute-by-minute time-series data for heart rate (HR), mean blood pressure (MAP), cardiac output (CO), and hematocrit (Hct) were obtained for ten different hemorrhage rates. The hemorrhage rate was calculated, as described in previous reports, using the following formula:

$$H(t) = H_0 \cdot e^{-kt} + (R/k) \cdot (1 - e^{-kt})$$

$$k = \ln(2)/\tau$$

$$R = (Total\ Blood\ Loss\% \cdot Total\ Blood\ volume) \cdot k^2 / (5 \cdot k + (1 - e^{5k}))$$

$$H_0 = R \cdot (1 - e^{5k}) / k$$

Total bleeding time was assumed constant (i.e. 5 minutes). The hemorrhage rate was determined based on the total amount of blood lost during this period. In this study, we let the amount of blood loss be 10%, 13%, 15%, 17%, 20%, 23%, 25%, 27%, 30%, and 33% of total blood volume. The data sets were named data1 through data10, corresponding to increasing blood loss. One data set was obtained for each hemorrhage rate (see Figure 1). The corresponding data for all ten data sets of heart rate (HR), mean arterial pressure (MAP), cardiac output (CO), and hematocrit (Hct) are shown in Figures 2, 3, 4, and 5, respectively.

To compare performance of the two control system approaches, the ten data sets were divided into two parts. Data1, 3, 5, 7, and 9 were used as training sets and data2, 4, 6, 8, and 10 were used as test sets. For the training data sets, data points at time 0, 10, 20, ..., 120 minutes (i.e., 10 minutes interval) were selected to simulate discrete measurements. Therefore, the training data was composed of five sets, each with 13 points for a total of 65 points.

Prior to training, the connection weights for both the deterministic and the neural network models were re-initialized. They were then trained using the simulated training data sets described above. After 600 iterations, the neural network-based TPSIM converged to a root mean squared error (RMS) of 6.7%. (All 65 data points were used in this calculation). The TPSIM with the deterministic control system finished learning (without convergence) after 180 iterations. The RMS error was 27%. The time required to train the deterministic model using the simplex method was longer than that required for the neural network. We utilized a batch reinforcement learning method to train the neural network.

The re-trained neural network-based TPSIM model was tested with the simulated test data. HR, MAP, CO, Hct and O₂ debt estimated from the model were compared minute by minute with the test data from 0 to 125 minutes. For this comparison, the RMS was 0.8%.

Figures 6, 7, 8, and 9 provide comparison results from the 23% blood loss test data (i.e., data6). The neural control parameters (i.e., the heart contractility coefficients CC_{RH} and CC_{LH} , artery to capillary resistance R_{A2C} , capillary to venous resistance R_{C2V} , and venous compliance C_V) calculated by the re-trained model were different from the corresponding test data values.

Two conclusions can be drawn from the neural network re-training and testing. First, the neural network model adjusted the neural control parameters to cause the physiological parameters (HR, MAP, CO and Hct) to converge to their correct values. Second, the neural network model was not able to adjust the neural control parameters CC_{RH} , CC_{LH} , R_{A2C} , R_{C2V} , and C_V to the original training data values. This may be because the passive system was not unique for the neural control inputs. Different combinations of neural control inputs may have the same output from the passive system. For example, an increase in vessel resistance and a decrease in vessel compliance may cause the same change in cardiac output. One possible solution to this problem is to train the neural network with additional data.

In conclusion, our preliminary analysis indicates that the neural network-based TPSIM model will perform better than the deterministic-based model. Additional training and testing with animal data are expected to provide supporting evidence toward this conclusion. We expect to perform similar tests with data provided by Dr. Pearce. In addition, SwRI will investigate the cause of the non-convergence experienced with the deterministic control system model.

Figure 1. Different Hemorrhage Rates for Ten Data Sets

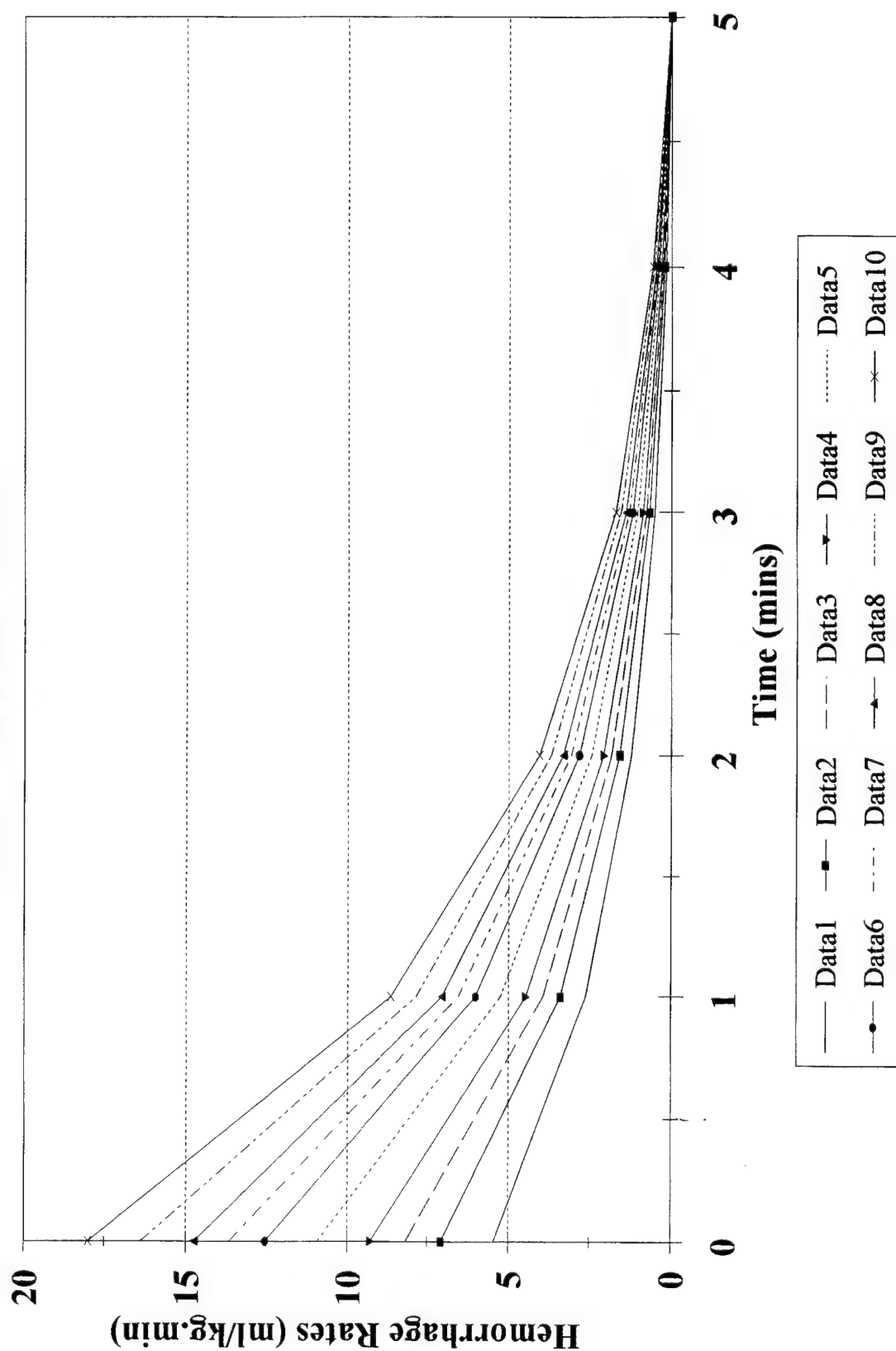
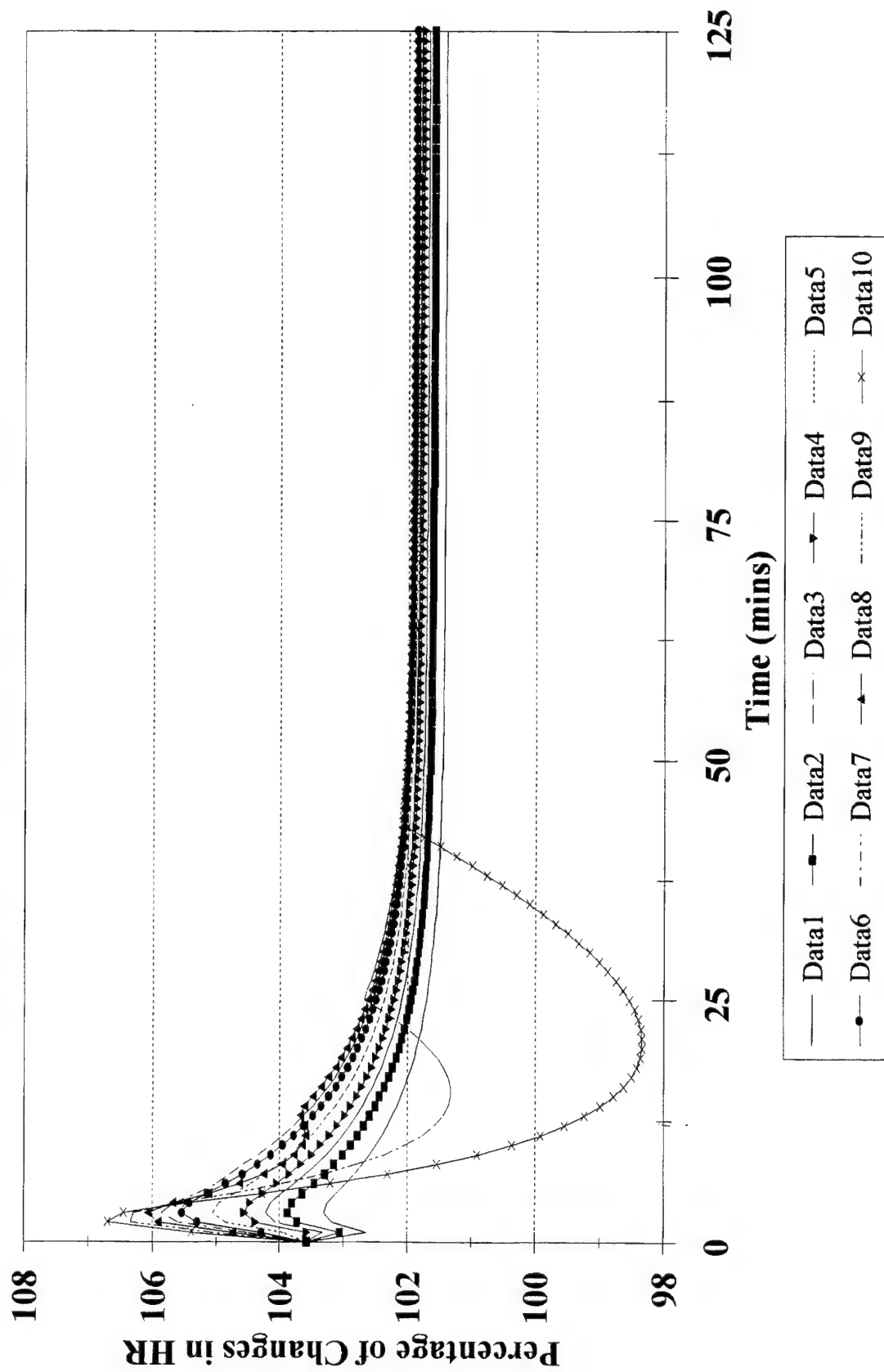
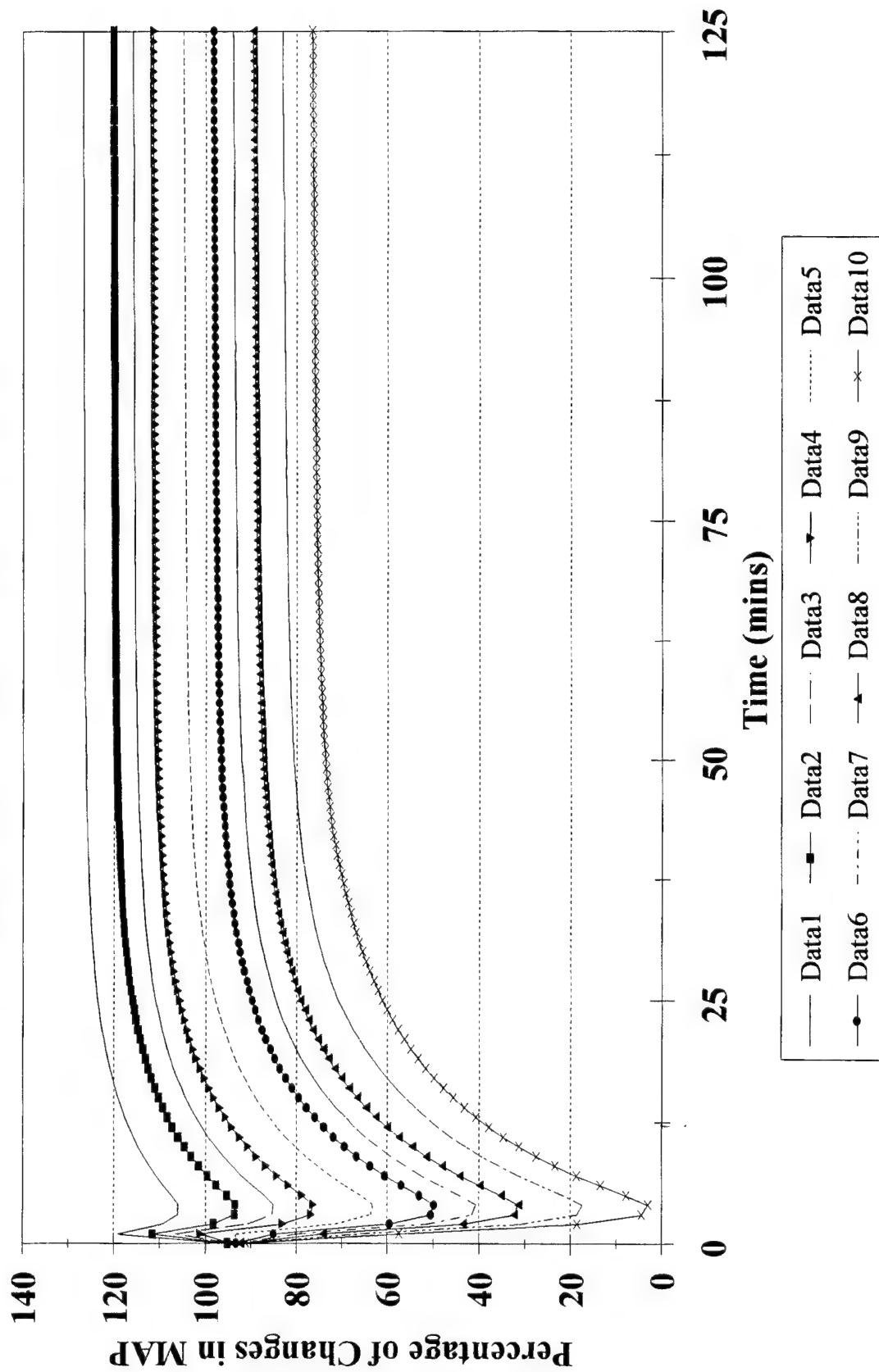


Figure 2. HR Changes Corresponding to Different Hemorrhage Rates



**Figure 3. MAP Changes Corresponding
to Different Hemorrhage Rates**



**Figure 4. CO Changes Corresponding
to Different Hemorrhage Rates**

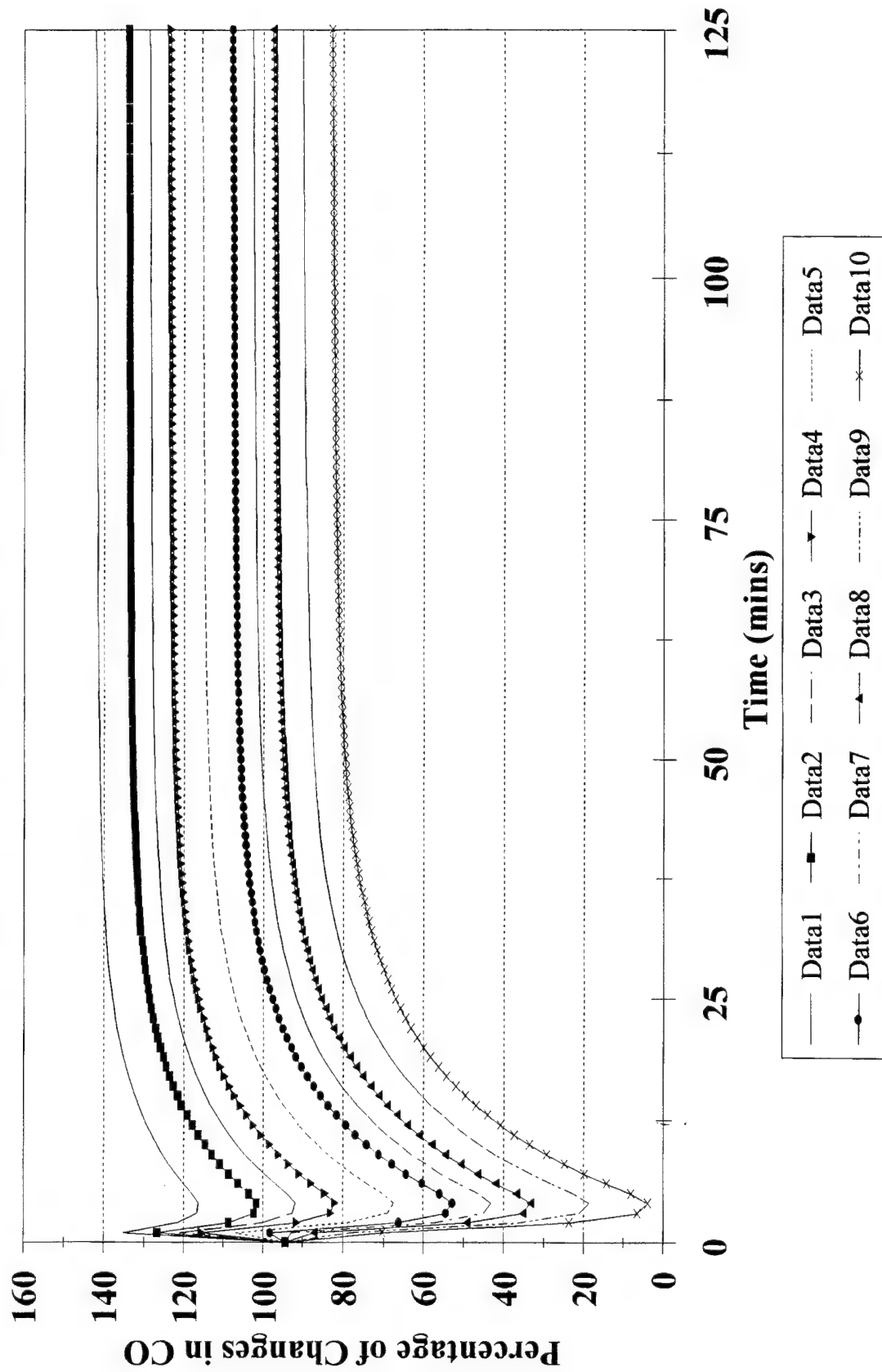
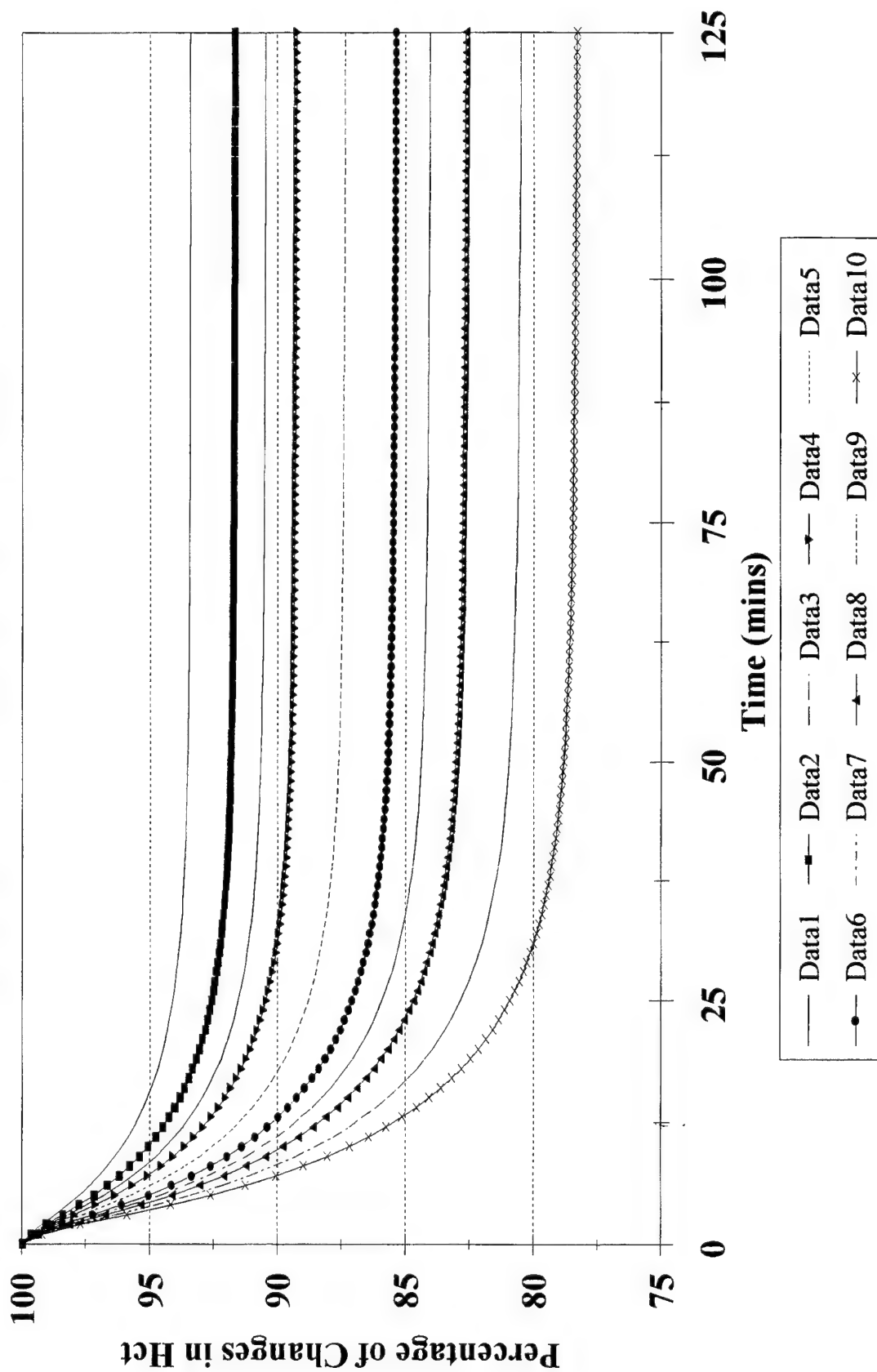


Figure 5. Hct Changes Corresponding to Different Hemorrhage Rates



**Figure 6. Comparison of Test Data and
Estimate Data for HR (23% Blood Loss)**

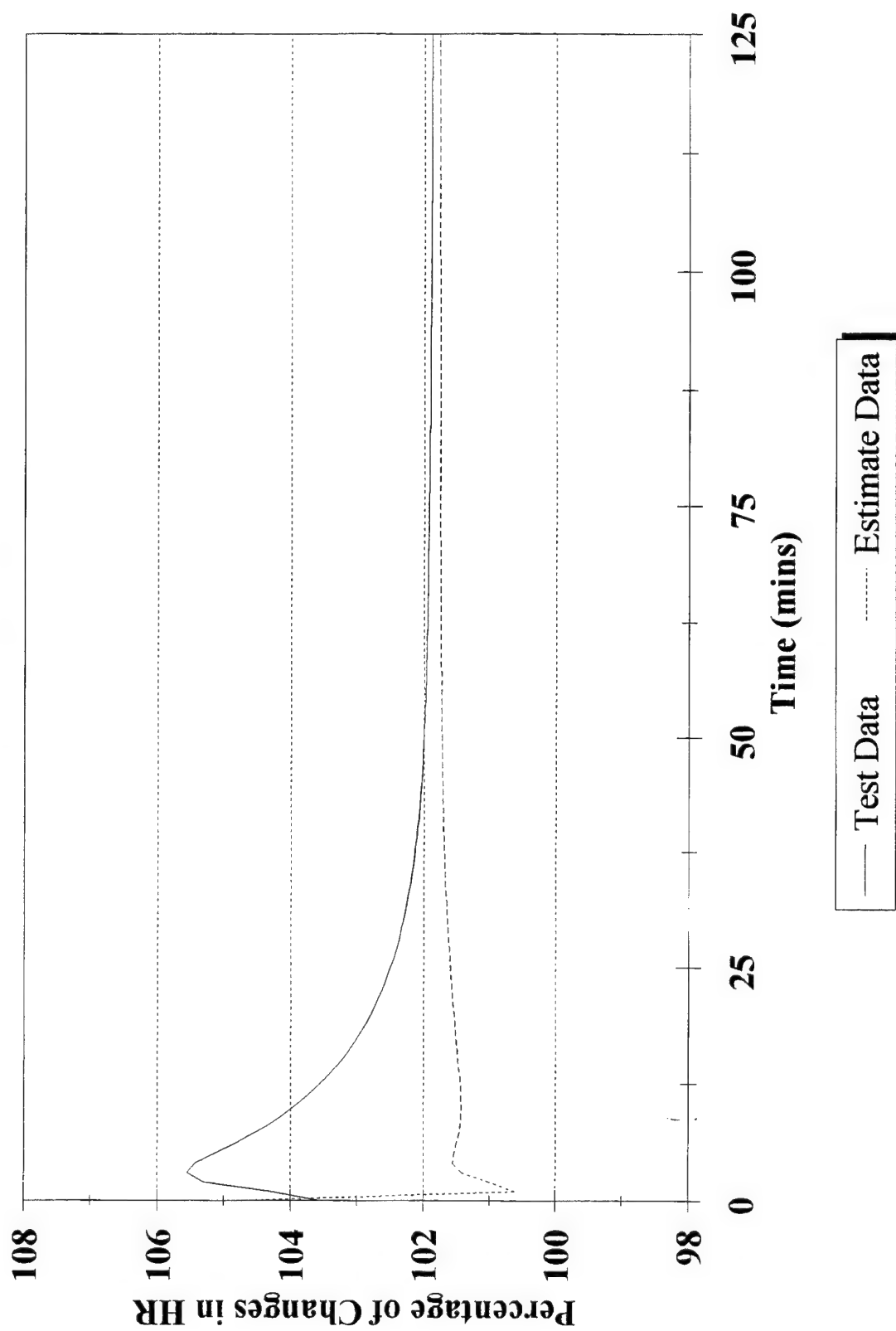
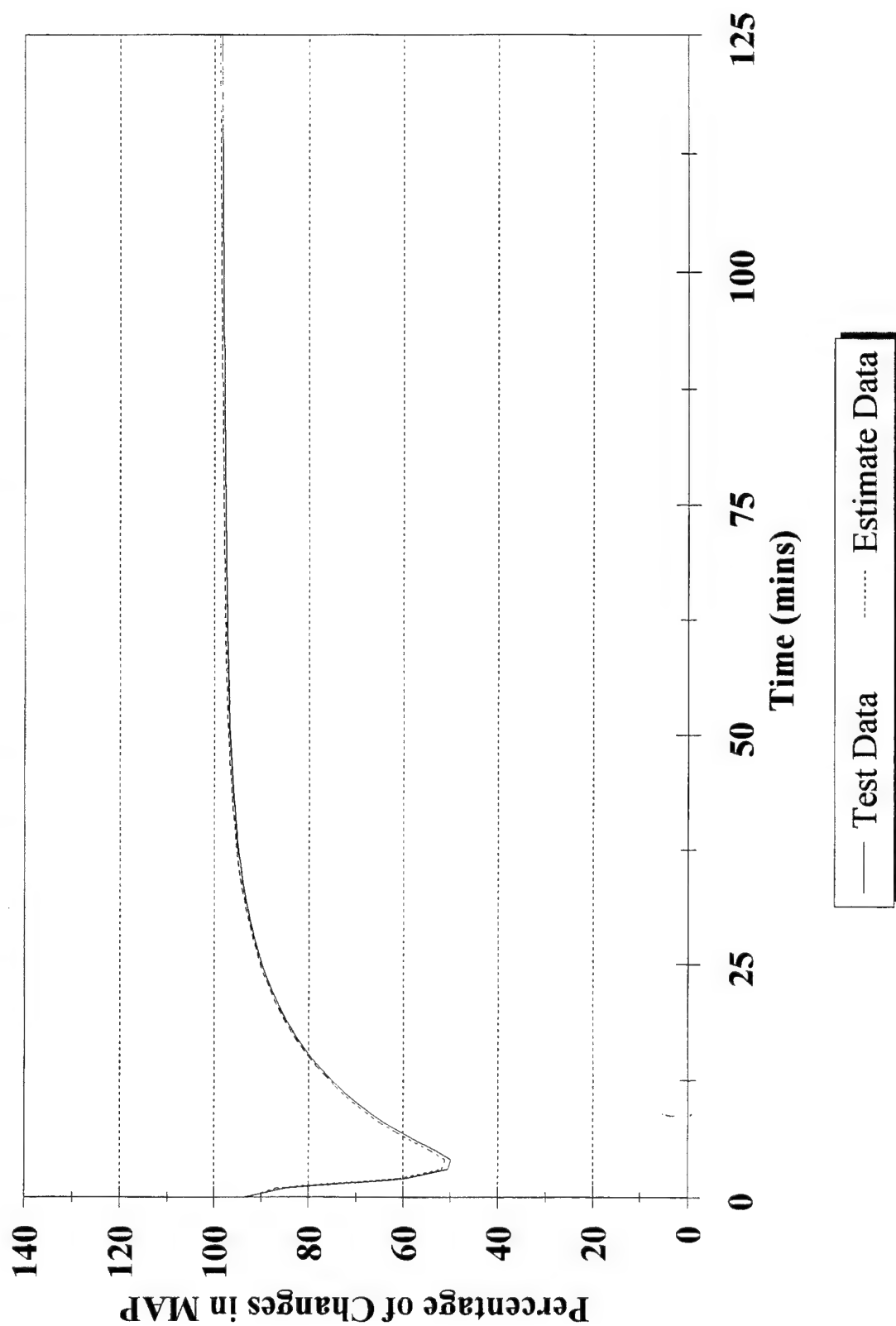
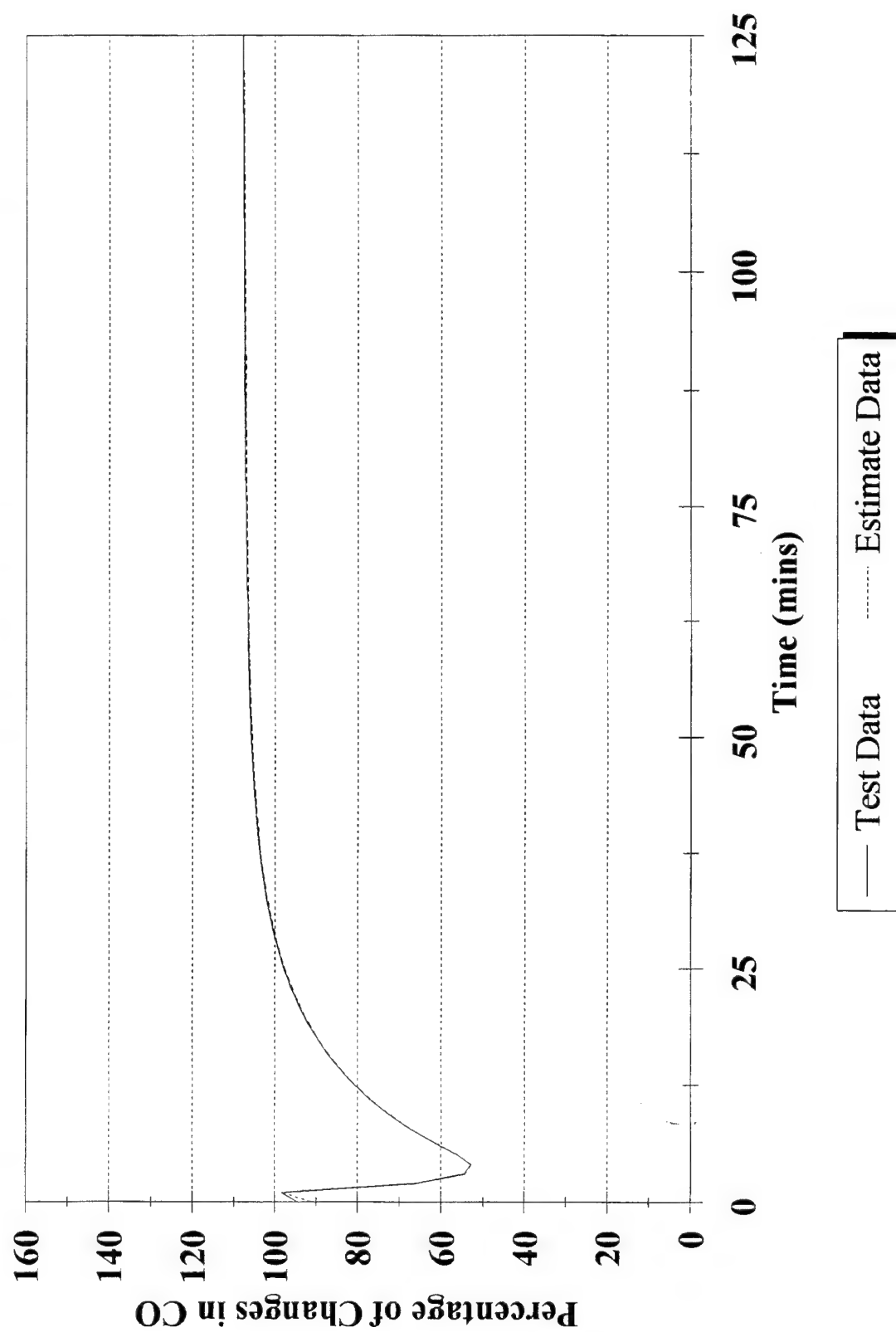


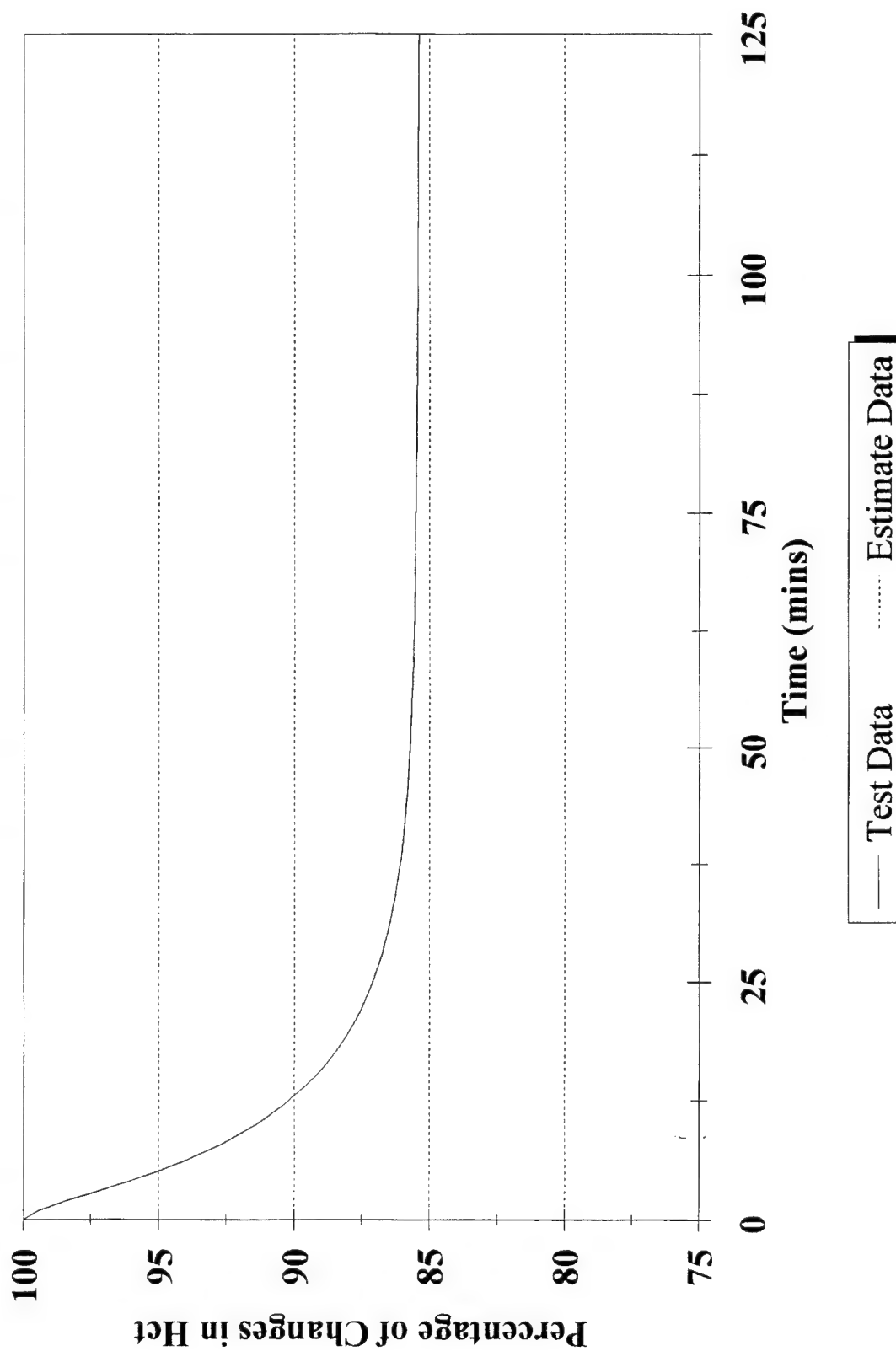
Figure 7. Comparison of Test Data and Estimate Data for MAP (23% Blood Loss)



**Figure 8. Comparison of Test Data and
Estimate Data for CO (23% Blood Loss)**



**Figure 9. Comparison of Test Data and
Estimate Data for Hct (23% Blood Loss)**



Revised Technical Approach and Statement of Work

**Adaptive Mathematical Model for Trauma Patient Monitoring and
Automated Fluid Resuscitation**

Contract No. DAMD17-94-C4126
Southwest Research Institute Project No. 12-6711

November 10, 1995

Contact:

Brian L. Robey
Department of Biosciences and Bioengineering
Southwest Research Institute
Post Office Drawer 28510
San Antonio, Texas 78228-0510
Tel: (210) 522-5115
Fax: (210) 684-6147
E-mail: brobey@swri.edu



SAN ANTONIO, TEXAS
HOUSTON, TEXAS • DETROIT, MICHIGAN • WASHINGTON, DC

Adaptive Mathematical Model for Trauma Patient Monitoring and Automated Fluid Resuscitation

Key Words: Combat Casualty Care, Mathematical Model, Hemorrhage, Volume Resuscitation, Physiological Monitoring

To increase survivability of soldiers wounded on the battlefield, casualties should be monitored and treated as early as possible. Plans for a self-contained evacuation platform for combat casualties include advanced communications, physiological monitoring, and life-support systems. To enhance the utility and effectiveness of the evacuation platform, we propose to develop a system to assess the physiological state of the casualty, to identify the optimal volume resuscitation strategy for the individual casualty, and to control and monitor automated fluid/drug delivery systems for resuscitation. The first component of this proposed system is a trauma patient simulator (TPSIM) which will be used to interpret physiological measurements and to estimate oxygen debt, blood loss, and hemostasis. TPSIM will incorporate a mathematical representation of the passive physical components of the cardiovascular system, as well as an adaptive model of the cardiovascular control system (to account person-to-person variability and responses to head injury, shock, and pharmacological intervention) made up of either deterministic or neural network components. Trauma patient simulation would involve "fitting" the model to on-line physiological measurements in real-time, similar to the process used to fit simpler models, such as polynomials or straight lines, to sets of measured data. Once the fitting process is successful, the model may be used to estimate values for variables which cannot be measured directly, but which are important indices of level of shock and effectiveness of volume resuscitation. The second component of the proposed system, the volume resuscitation optimization system (VROS) will use the TPSIM system to predict the cardiovascular system response to volume resuscitation, and a numerical optimization algorithm to determine the optimum resuscitation strategy (i.e., amount of fluid delivered, the start time for fluid delivery and the rate of fluid delivery) for the individual patient. The third and final component of the

proposed system would include the software required for data acquisition, communication with on-site and remote medical personnel, and control of automated fluid/drug delivery systems.

Ideally, the proposed system would frequently query physiological measurement/monitoring systems for data, assess the patient's physiological status, determine the "best" resuscitation strategy for an individual patient, and relay this information to on-site and remote medical personnel. Medical personnel would command the system to implement either the "optimal" resuscitation strategy or some other treatment strategy. The proposed system, which would control and monitor an automated fluid/drug delivery system, would then initiate and monitor the resuscitation process automatically. Overall, the proposed system would be expected to enhance the quality of combat casualty care while conserving medical resources.

Table of Contents

Statement of Problem.	Page 1
Technical Objectives and Rationale	Page 2
Innovative Claims	Page 7
Deliverables	Page 7
Statement of Work.	Page 7

Adaptive Mathematical Model for Trauma Patient Monitoring and Automated Fluid Resuscitation

STATEMENT of PROBLEM

Hemorrhage is the leading cause of death on the battlefield. Severe blood loss is accompanied by a decrease in blood flow to tissues and, consequently, a decrease in oxygen delivery. Data from hemorrhaged dogs suggests that a whole-body oxygen debt of 100 ml/kg is survivable, whereas an oxygen debt of 160 ml/kg is nearly always fatal¹. To improve survivability on the battlefield, bleeding must first be controlled. Then, if evacuation is delayed or prolonged, volume resuscitation should be attempted to curtail or reverse the level of oxygen debt.

Because oxygen debt is difficult to estimate, a speedy return of arterial pressure to "normal" levels is the most often used criteria for resuscitation efficacy. However, arterial pressure is affected by many factors in addition to blood volume. Following hemorrhage and resuscitation, arterial blood pressure may lag behind recovery of variables directly associated with oxygen delivery, such as cardiac output. Thus, resuscitating to normal values of mean arterial pressure may be inefficient (resulting in greater amounts of fluids used than are actually required), and could lead to fluid overload. Speedy return to normal mean arterial pressure has also been shown to be fatal (through increased blood loss) when hemorrhage is not well controlled^{2,3,4}. Even if oxygen debt could be easily measured, the human cardiovascular system is complex, and effects of resuscitation on oxygen debt may not become apparent until long after the fluid is administered. If total blood loss is known, then the amount of fluid required to replace lost blood may be determined. However, the minimum amount of fluid that could be used, and the rate of fluid replacement that would safely keep oxygen debt within tolerable

¹ J.W. Crowell and E.E. Smith. Oxygen deficit and irreversible hemorrhagic shock. *Am J Physiol* 206:313, 1964.

² W.H. Bickell, S.P. Bruttig, M.A. Millnamow et al. The detrimental effects of intravenous crystalloid after aortotomy in swine. *Surgery* 110: 529-536, 1991.

³ D. Gross, E.H. Landau, et al. Is hypertonic saline resuscitation safe in uncontrolled hemorrhagic Shock? *J Trauma* 28:751-756, 1988.

⁴ G. Miles, C.J. Koucky, and H.G. Zacheis. Experimental uncontrolled hemorrhage. *Surgery* 60:434-442, 1966.

limits, cannot be estimated by intuition or simple calculation. Finally, reinitiation of hemorrhage must be watched for throughout resuscitation.

The self-contained evacuation platform is expected to include advanced communications, physiological monitoring, and life-support systems. These advanced systems by themselves, however, will do little to resolve current problems in resuscitation therapy. To enhance the utility and effectiveness of this system while preserving medical resources, the evacuation platform must also include a system to assess the physiological state of the casualty (e.g., blood loss, level of oxygen debt, hemostasis), to determine the optimal volume resuscitation strategy, to present this information to remote medical personnel, and to control and monitor automated fluid/drug delivery systems.

TECHNICAL OBJECTIVES and RATIONALE

The main objectives of the proposed project are to develop a system to assess the physiological state of the casualty, to identify the optimal volume resuscitation strategy for the individual casualty, and to communicate with on-site or remote medical personnel, physiological measurement/monitoring equipment, and other biomedical instruments. For practical purposes, we have divided the proposed, comprehensive system into three subsystem components: 1) a Trauma Patient Simulator (TPSIM) for physiological assessment, 2) a Volume Resuscitation Optimization System (VROS), and 3) supporting software for communication, data acquisition, and instrument control.

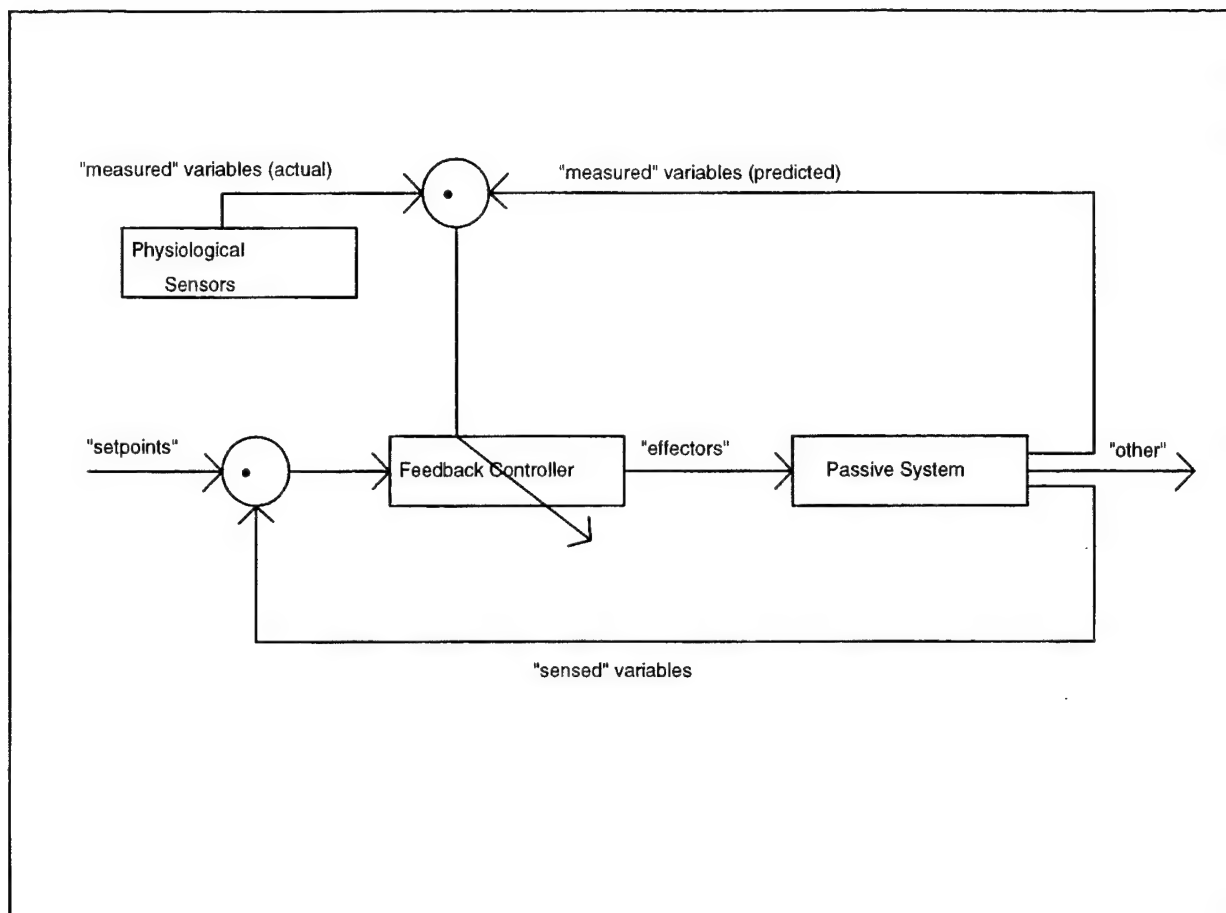
Trauma Patient Simulator (TPSIM)

The first objective of the proposed project is to assess the hemodynamic state of the patient or casualty in real time, taking advantage of whatever physiological sensors and monitoring equipment are available in the evacuation platform. This means estimating variables such as blood loss, instantaneous rate of blood loss, and level of oxygen debt from measured values of variables such as arterial blood pressure, noninvasive cardiac output, and on-line hematocrit. To accomplish this objective, we propose to use a hybrid mathematical model

incorporating a passive model of cardiovascular hemodynamics and fluid exchange, and an adaptive model of cardiovascular system control.

The cardiovascular control system model will be made up of either a deterministic model (i.e., a fixed set of model equations) with adaptable parameter values, or a neural network model with adaptable connection weights. Initial control system parameter values (for the deterministic system), or connection weights (for the neural network system) will be pre-specified, based on prior simulations of existing laboratory data. During patient simulation, parameter values or connection weights will be continuously adjusted based on differences between model estimates and actual values of "measured" variables. Deterministic control system models, based on empirical observations of control system behavior have been used exclusively in the past. Alternative neural network models have been used successfully in the development of "adaptive" robotic system controllers. Based on this work in robotics, use of a neural network controller may result in shorter simulation times and more robust model predictions.

Whether the control system is deterministic or neural network based, system components and the relationships between them may be represented by the schematic below. Differences between predicted and observed values of "measured" variables would act as error signals for control system adjustment. The control system would determine values for "effector" variables, such as heart rate, heart strength, vascular resistance, and venous compliance, and would pass these values on to the passive system. The passive system model would incorporate the physical relationships between cardiac, vascular, and extravascular compartment pressures, volumes, flow rates, and gas or solute concentrations. Passive system estimates of "measured" variables (e.g., noninvasive blood pressure and cardiac output) would be used to adjust control system parameter values or network connection weights. Passive system estimates of variables "sensed" by cardiovascular mechano- and chemoreceptors (i.e., aortic and carotid artery wall stretch, cardio-pulmonary wall stretch, and arterial O_2 and CO_2 concentration) would be passed as inputs to the control system.



A mathematical model of the "passive" circulation has already been developed for the study of hemorrhage and fluid resuscitation⁵. An earlier version of this model was used with a deterministic model of the cardiovascular control system to simulate a set of uncontrolled hemorrhage experiments in swine⁶. A single control system model (i.e., set of equations) was identified that was valid for conscious and anesthetized animals. However, parameter values (which were optimized for "best fit" between model predictions and observed values of mean arterial pressure, cardiac output, and hematocrit) differed between the two groups. Based on these results, we would expect that a single control system model may be identified for a wide range of conditions, but that control system parameter values may require adjustment to compensate for changes in the neurological or physiological state of the patient.

⁵ T.J. Doherty. A mathematical model for the study of hemorrhagic shock and fluid resuscitation. Institute Reports # 476-479, Letterman Army Institute of Research, Presidio of San Francisco, CA, 1993.

⁶ T.J. Doherty, S.P. Bruttig, and W.H. Bickell. Model analysis: controlled response to aortotomy hemorrhage in swine. *Physiologist* 34(4): 231, 1991.

The difference between the model described by the schematic above, and a more-typical mathematical prediction model, is in the adaptation of control system parameter values. In a typical prediction model, control system parameter values are preset or vary using predetermined equations. Such models generally are valid over only a limited range of physiological conditions. Using adaptable control system parameter values, based on actual observed patient responses, alleviates this shortcoming.

Expert systems, empirical models, and other approaches that use empirically-derived relationships between measured variables and other variables of interest have been used in the past to relate "degree of shock" to other measurable parameters. These relationships are usually highly dependent on the sets of data used in their construction. Thus, they may not be valid for different hemorrhage models, different fluid resuscitation schemes, different animal species, or different physiological states from those used to construct the relationships. Because traumatic hemorrhage in humans differs greatly from experimental hemorrhage models in all respects except perhaps resuscitation strategy, empirically-derived relationships are not expected to resolve current problems in monitoring the combat casualty and do not address the need to optimize volume resuscitation strategy. Use of a mathematical model, based on physical as well as empirical observations of cardiovascular system behavior, would enable the system to work over a greater range of conditions. The adaptive mathematical modeling approach has the additional benefit that different sets of "measured" variables may be used for parameter value adaptation. Loss of a particular sensor due to malfunction, addition of sensors, or exchange of one type of sensor (e.g., noninvasive) for another, would not be expected to affect system reliability. Thus, the system may be used in many different military and civilian settings in which the sets of measured variables are likely to be different.

Volume Resuscitation Optimization System (VROS)

The second objective of the proposed project is to develop a system that may be used to identify the optimum volume resuscitation strategy for an individual. At any time, once initial simulation is successful (i.e., predicted and observed values for "measured" variables match), the model described above may be used to predict future events, including the cardiovascular

response to resuscitative fluid administration. Optimization of the fluid resuscitation strategy for a particular fluid would be accomplished using existing numerical algorithms that automatically adjust optimization parameters (e.g., fluid volume and rate of administration) until optimization criteria are met (e.g., minimization of total fluid volume and oxygen debt). Rates of arterial pressure increase limits on the rate of fluid delivery, and limits on the total fluid volume may also be considered in the optimization scheme.

Supporting, Communications Software

To complete the system, the third objective of the proposed project is to develop software for external communications, data acquisition, and control of automated fluid/drug delivery systems. This software support subsystem will enable data from monitoring/measurement equipment within the evacuation platform to be passed to the TPSIM system, and 1) enable information regarding physiological status and optimum fluid resuscitation strategy to be relayed to remote medical personnel, 2) enable remote medical personnel to command the system, and 3) enable the system to implement volume resuscitation (specified by remote medical person) using automated fluid/drug delivery systems. Device communications protocols must be specified by ARPA project managers for successful accomplishment of this objective.

System Validation

The system described above, consisting of the TPSIM, VROS, and supporting, communications software will be designed for compatibility with other life support, physiological monitoring, and communications systems within the trauma pod. We expect that efforts in development of these other systems will include clinical trials and demonstrations, as appropriate. We do not intend to duplicate this effort by conducting our own laboratory or clinical trials. Rather, we will demonstrate the validity of our system using either experimental or clinical data generated by these other system developers, or comparable data from the literature. Data will also be collected from national trauma centers (e.g., Drew/King Medical Center, Los Angeles) and other sources (e.g., Uniformed Services of the Health Sciences,

Bethesda, MD). Compatibility with these other systems will be demonstrated during development of a prototype system for the self-contained evacuation platform.

INNOVATIVE CLAIMS

Development of adaptive models (specifically of hybrid mathematical/neural network models) is a new field. To our knowledge, there have been no attempts to develop such a model for patient monitoring and exploration of treatment options.

DELIVERABLES

- A prototype software system for incorporation into the self-contained evacuation platform. This will include software components (to include the adaptive trauma patient simulator, fluid resuscitation, and communications algorithms).
- Seven quarterly reports and one final report describing all software components of the system, as well as results of system validity and reliability studies.

STATEMENT of WORK

The technical objectives identified above may be accomplished by completing the following tasks. A time line (Gant Chart) showing estimated start and end dates for each task is attached to this proposal.

TASK 1: PASSIVE SYSTEM MODEL DEVELOPMENT/REFINEMENT.

- Identify and resolve (if necessary) limitations on the current passive system model.

TASK 2: ACQUIRE EXISTING DATA

- Acquire existing data from animal experiments of controlled hemorrhage, uncontrolled hemorrhage and volume resuscitation. Attempt to acquire data that includes head injury, trauma, and/or pharmacological intervention.
- Acquire existing clinical data from national trauma centers, if appropriate. Attempt to acquire data that includes time series measurements of critical resuscitation parameters (e.g., blood pressure, heart rate, blood loss/hemorrhage rate, hematocrit, cardiac output, fluids/drugs administered - amounts and rates, etc.) SwRI will travel, as necessary, to trauma centers for collection of data.

TASK 3. DETERMINISTIC CONTROL SYSTEM MODEL DEVELOPMENT

- Develop General Deterministic Control System Software (i.e., sets of fixed equations with variable parameter values).

TASK 4. DETERMINISTIC MODEL REFINEMENT AND TESTING

- Through model fitting using existing laboratory data, identify the "best" set of control system equations (i.e., the set that is valid over the entire range of available experimental data and that which uses the smallest number of variable parameters).
- Through model fitting using human clinical data (if appropriate), refine the model and identify a set of initial parameter values for this model.

TASK 5. NEURAL NETWORK CONTROL SYSTEM DEVELOPMENT.

- Develop one or more neural network model(s) of the cardiovascular control system.

TASK 6. NEURAL NETWORK MODEL REFINEMENT AND TESTING

- Through model fitting using existing laboratory animal data, identify the minimal neural network architecture that is valid over the entire range of existing laboratory data.

- Through model fitting using human clinical data (if appropriate), identify a set of starting connection weights for this model.

TASK 7: MODEL RELIABILITY AND ACCURACY STUDIES

- Estimate control system parameter value reliability using Monte-Carlo simulations.
- Determine which measured variables are important or necessary for model fitting.
- If data are available (i.e., both oxygen uptake and oxygen consumption), estimate the accuracy of oxygen debt.
- Using the control system parameter values from above, estimate blood loss and rate of hemorrhage for existing animal data (for which blood loss and rate of hemorrhage are known); compute the accuracy of blood loss and rate of hemorrhage estimates.
- Demonstrate that the adaptive model is able to simulate a wide range of clinical data including hemorrhage and volume resuscitation. The goal is to simulate these responses when head injury, trauma, and/or pharmacological intervention are also involved.

TASK 8. CONTROL SYSTEM MODEL SELECTION

- Based on comparisons of parameter value reliability (over different sets of laboratory and clinical data), as well as the amount of time required for parameter value adjustment and successful simulation, determine whether the deterministic or neural network model would be more appropriate for real-time simulation of the combat casualty.

TASK 9. DEVELOPMENT OF FLUID RESUSCITATION OPTIMIZATION ALGORITHM.

- Identify criteria and considerations for optimal fluid resuscitation.
- If possible, identify resuscitation criteria using existing data from previous laboratory experiments and clinical outcomes.
- Implement an existing numerical algorithm for optimization. A knowledge-based system may be combined with the numerical algorithm to assist in narrowing the run-time search for the optimal resuscitation strategy.

- Assess the reliability of predicted optimal volume resuscitation strategies. Results will be compared against clinical outcomes (from trauma center data).

TASK 10. REAL-TIME SYSTEM DEVELOPMENT

- Identify system modifications required for real-time trauma patient simulation (e.g., change in language, methods of solution).
- Implement system modifications required for real-time trauma patient simulation.

TASK 11. PROTOTYPE SYSTEM DEVELOPMENT

- Acquire (from ARPA project managers) the set of measured variables that will be made available to the system and the communications protocol necessary for data acquisition.
- Acquire (from ARPA project managers) communication protocols for system output to displays and/or remote communications equipment within the trauma pod.
- Acquire (from ARPA project managers) protocols for communications with automated drug/fluid delivery systems within the trauma pod.
- Develop and test software algorithms for communication with measurement devices, sensors, and/or other data acquisition systems within the trauma pod. Integrate the software into the main software module.
- Develop and test software algorithms for communication with display units and/or remote medical personnel via communications equipment within the trauma pod. Integrate the software into the main software module.
- Develop and Test software algorithms for communication with measurement devices, sensors, and/or other data acquisition systems within the trauma pod. Integrate the software into the main software module.
- Implement all trauma patient simulation and resuscitation software on trauma pod hardware system (which is being developed by other project teams).

TASK 12. REVIEW CLINICAL DATA

- Acquire laboratory and clinical data from other project teams developing physiological monitoring equipment or fluid/drug delivery systems.
- Demonstrate that the adaptive model is able to successfully simulate this data in real-time.

File 12-6711-004

SOUTHWEST RESEARCH INSTITUTE

6220 CULEBRA ROAD • POST OFFICE DRAWER 28510 • SAN ANTONIO, TEXAS, USA 78228-0510 • (210) 684-5111 • TELEX 244846

March 14, 1996

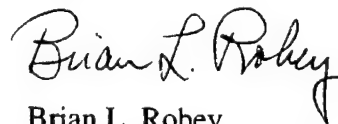
Frederick Pearce, Ph.D.
Director, Division of Surgery
Walter Reed Army Institute of Research
16th St., Building 40
Washington, D.C. 20307-5100

Dear Dr. Pearce:

Enclosed is the sixth quarterly report for work performed under contract no. DAMD17-94-C4126. This report covers the period from 25 November, 1995 to 3 March, 1996.

Please feel free to contact me at (210) 522-5115 if you have any questions or concerns regarding the technical aspects of this report. Please contact Ms. Sharon Rowe at (210) 522-3026 for any contractual or financial matters.

Sincerely,



Brian L. Robey
Project Manager
Biosciences & Bioengineering Department

Enclosure



SAN ANTONIO, TEXAS
HOUSTON, TEXAS • DETROIT, MICHIGAN • WASHINGTON, DC

SOUTHWEST RESEARCH INSTITUTE

6220 CULEBRA ROAD • POST OFFICE DRAWER 28510 • SAN ANTONIO, TEXAS, USA 78228-0510 • (210) 684-5111 • TELEX 244846

March 14, 1996

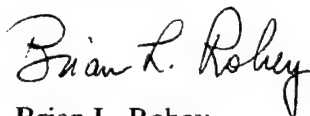
Director
U.S. Army Medical Research Acquisition Activity
ATTN: SGRD-RMA-RC
Fort Detrick
Frederick, MD 21702-5014

Dear Sir:

Enclosed is the sixth quarterly report for work performed under contract no. DAMD17-94-C4126. This report covers the period from 25 November, 1995 to 3 March, 1996.

Please feel free to contact me at (210) 522-5115 if you have any questions or concerns regarding the technical aspects of this report. Please contact Ms. Sharon Rowe at (210) 522-3026 for any contractual or financial matters.

Sincerely,



Brian L. Robey
Project Manager
Biosciences & Bioengineering Department

Enclosure



SAN ANTONIO, TEXAS
HOUSTON, TEXAS • DETROIT, MICHIGAN • WASHINGTON, DC

SOUTHWEST RESEARCH INSTITUTE

6220 CULEBRA ROAD • POST OFFICE DRAWER 28510 • SAN ANTONIO, TEXAS, USA 78228-0510 • (210) 684-5111 • TELEX 244846

March 14, 1996

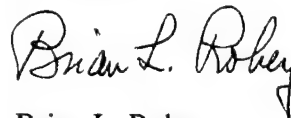
Donald P. Jenkins, Ph.D.
Deputy Director for Defense Healthcare Technologies
ARPA/Defense Sciences Office
3701 North Fairfax Drive
Arlington, VA 22203-1714

Dear Dr. Jenkins:

Enclosed is the sixth quarterly report for work performed under contract no. DAMD17-94-C4126. This report covers the period from 25 November, 1995 to 3 March, 1996.

Please feel free to contact me at (210) 522-5115 if you have any questions or concerns regarding the technical aspects of this report. Please contact Ms. Sharon Rowe at (210) 522-3026 for any contractual or financial matters.

Sincerely,



Brian L. Robey
Project Manager
Biosciences & Bioengineering Department

Enclosure



SAN ANTONIO, TEXAS
HOUSTON, TEXAS • DETROIT, MICHIGAN • WASHINGTON, DC

Quarterly Progress Report

1. Contract No. DAMD17-94-c4126 2. Report Date 15 March, 1996
- SwRI Project No. 12-6711
3. Reporting Period from 25 November, 1995 to 3 March, 1996.
4. PI Brian Robey 5. Phone (210) 522-5115
6. Institution Southwest Research Institute, San Antonio, Texas
7. Project Title Model for Trauma Patient Simulation and Automated Fluid Resuscitation
8. Current staff with percent effort of each on project

Brian Robey 2 %

Dean Winter 1 %

Jian Ling 12 %

9. Contract expenditures to date (as applicable):

	this qtr/cumulative		this qtr/cumulative
Personnel	<u>2,120.69 / 39,734.43</u>	Travel	<u>0.00 / 4,792.08</u>
Fringe Benefits	<u>926.75 / 17,363.97</u>	Equipment/Supplies/ Consultants	<u>936.01 / 9,754.50</u>
Overhead	<u>3,595.97 / 67,376.10</u>	Facilities Capital	<u>294.60 / 5,827.51</u>

	this qtr/cumulative
Subtotal	<u>7,874.02 / 144,848.59</u>
Indirect Costs	<u> / </u>
Fee	<u>606.36 / 11,121.79</u>
Total	<u>8,480.38 / 155,970.38</u>

10. Administrative and Logistical Matters

Last quarter, Mr. Brian Robey and Mr. Jian Ling met with Dr. Fred Pearce at Walter Reed for a project review. Dr. Pearce recommended the use of rat hemorrhage data from his laboratory for continued model development and validation. The data were received on 29 January, 1996. Unfortunately, there was an insufficient amount of information and data provided to justify the use of these data for further model development. A description of the data is presented in Task 2 below. SwRI is in the process of locating additional physiological data to continue work on this project.

On 30 January, 1996, Mr. Jian Ling contacted Dr. William Traverso at the Mason Medical Center in Seattle, Washington. In the late 1980's, Dr. William Traverso published two companion papers on fluid resuscitation in the unanesthetized swine, simulating human exsanguination. The companion papers compared and contrasted the ability of different crystalloid and colloid solutions to prevent death after otherwise fatal hemorrhages. Mr. Ling approached Dr. Traverso in effort to gain some input or data for the development of the fluid resuscitation optimization algorithm. Unfortunately, Dr. Traverso has since changed his focus of research and was unable to provide any assistance.

On 8 February, 1996, Mr. Jian Ling contacted Dr. William Bickell of Saint Francis Hospital in Tulsa, Oklahoma. In 1989, Dr. Bickell studied the hemodynamic response to uncontrolled hemorrhage in the anesthetized swine. These data were used for initial training of the hemorrhage model. More recently, Dr. Bickell has been studying the effect of fluid resuscitation with lactated Ringer's solution following a hemorrhage in the swine. He has agreed to provide SwRI with some of the data from these experiments for the development of the fluid resuscitation optimization algorithm. These data have not been received at this time.

11. Scientific Progress

Task 1 - Passive System Model Development/Refinement:

No major modifications were made to the passive cardiovascular system model.

Task 2 - Acquire Existing Data:

During last quarter's meeting with Dr. Fred Pearce, he recommended that SwRI use animal hemorrhage data for model development. At the meeting, Dr. Pearce offered to provide animal hemorrhage data from rats. The data that Dr. Pearce forwarded to SwRI included measurements of heart rate, systolic blood pressure, and diastolic blood pressure immediately after a hemorrhage. The data were collected in 5 second intervals for up to 2 hours after the hemorrhage. Unfortunately, we were only able to obtain data collected in one rat and did not have access to any information pertaining to the nature of the hemorrhage. Also, there are large fluctuations in the data, suggesting that these data are not appropriate for the model development. The empirical data are plotted in Attachment A and smoothed versions, using a moving average, are plotted in Attachment B.

Task 3 - Deterministic Control System Model Development:

No modifications were made to the deterministic control system.

Task 4 - Deterministic Model Refinement and Testing:

No modifications were made to the deterministic model.

Task 5 - Neural Network Control System Development:

No major modifications were made to the neural network control system.

Task 6 - Neural Network Model Refinement and Testing:

No major modifications were made to the neural network control system.

Task 7 - Model Reliability and Accuracy Studies:

Not started.

Task 8 - Control System Model Selection:

No further tests were performed due to the insufficient amount of data available for model training.

Task 9 - Development of a Fluid Resuscitation Optimization Algorithm:

Extensive literature reviews were performed to initiate the development of the fluid resuscitation optimization algorithm. The literature reviews focused on fluid resuscitation studies using various crystalloid and colloid solutions comparing the advantages and disadvantages of administering these solutions on the battlefield.

SwRI contacted two potential sources for fluid resuscitation data in the swine, Drs. William Traverso and William Bickell. Dr. Traverso was unable to assist SwRI because he has changed the focus of his research. Dr. Bickell was receptive to our request for resuscitation data. SwRI has yet to receive the data.

Task 10 - Real Time Software System Development:

No work was performed on this task.

Task 11 - Prototype System Development:

Not started.

Plans for Next Quarter

- Additional data will be obtained to assess the two different control systems.
- Fluid resuscitation data will be obtained from Dr. William Bickell for the development of the fluid resuscitation optimization algorithm.

Attachment A

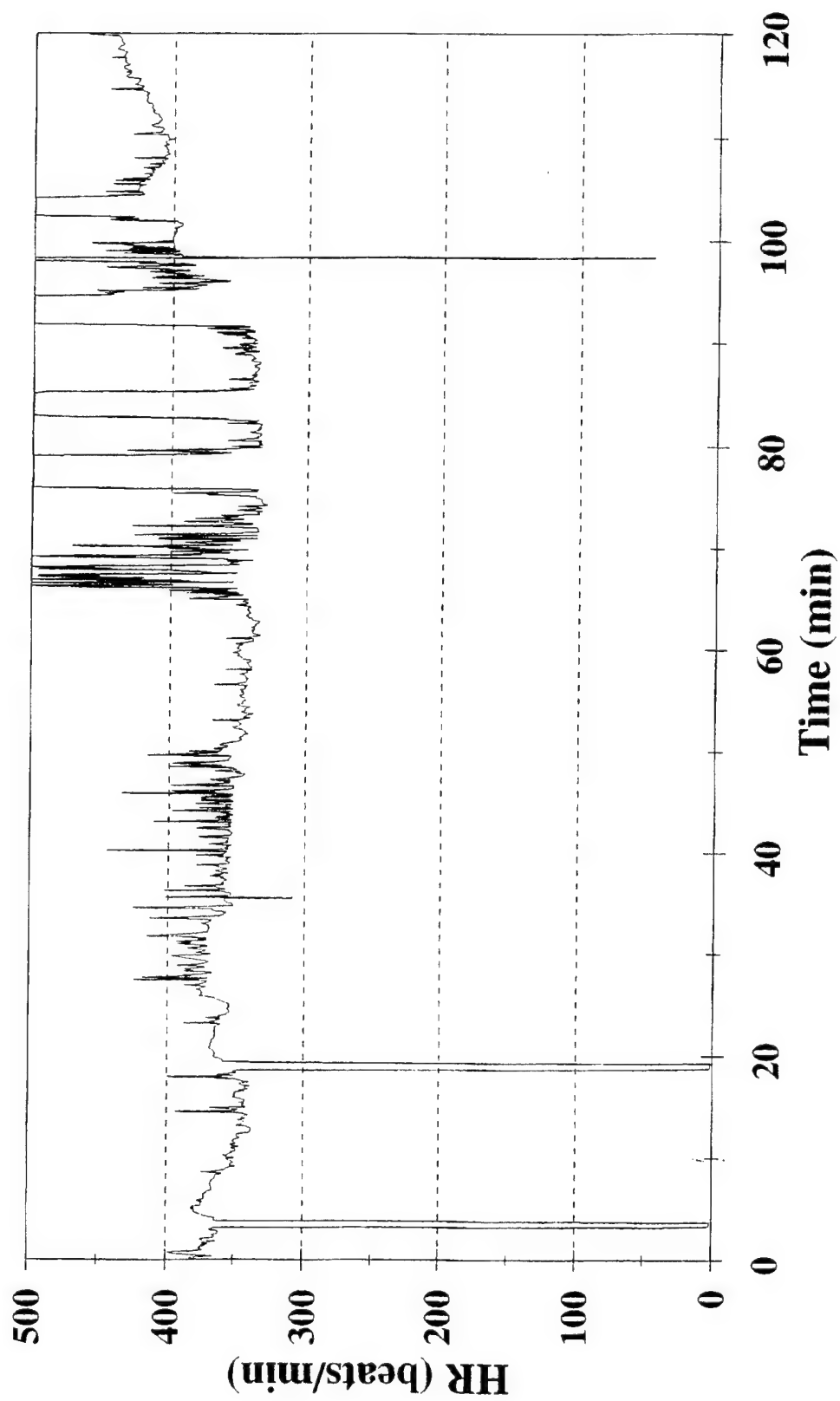
Empirical Hemorrhage Data for the Rat

(obtained from Dr. Fred Pearce, Walter Reed Hospital)

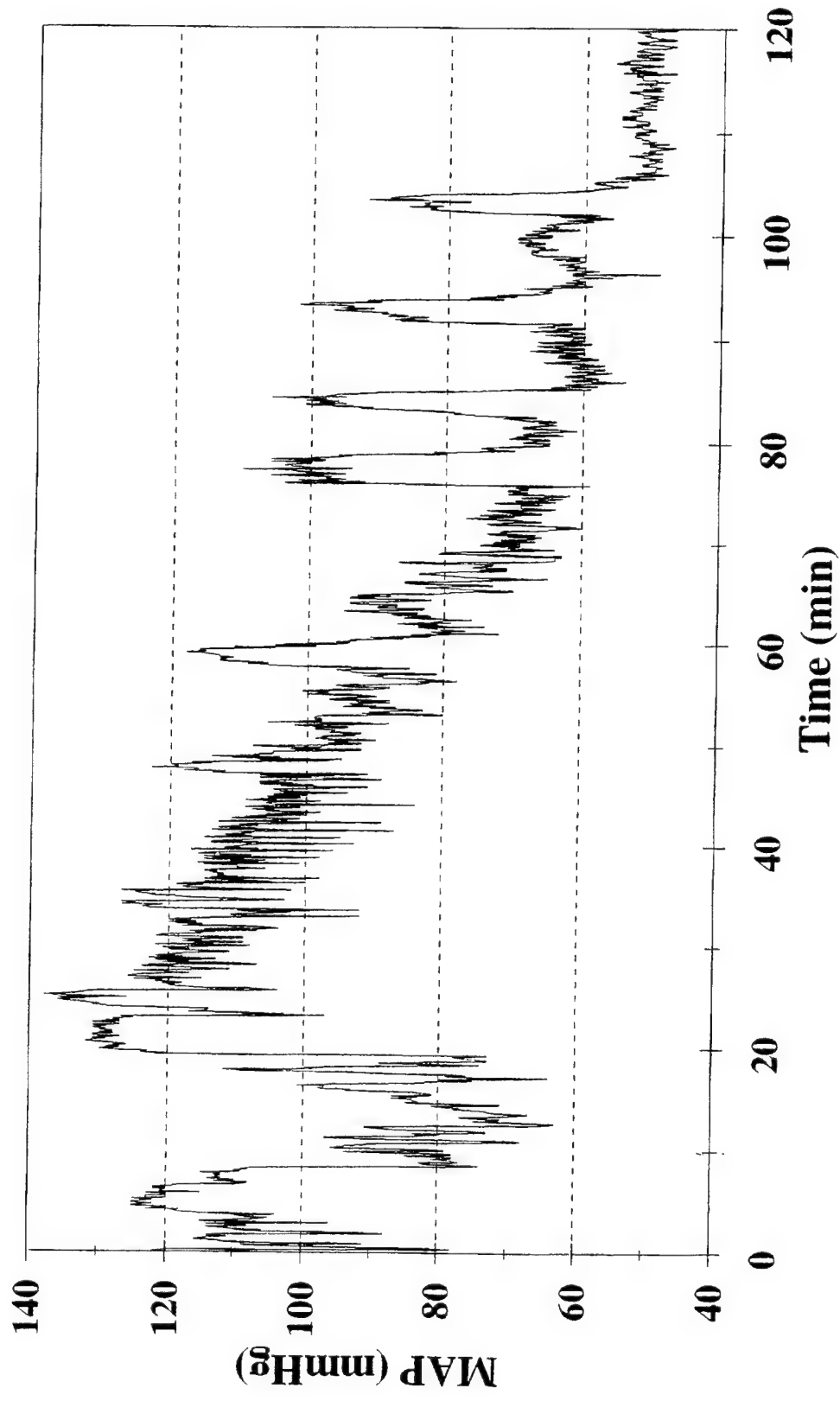
Note: HR = Heart rate

MAP = Mean arterial pressure

HR Changes After Hemorrhage In Rats



MAP Changes After Hemorrhage In Rats

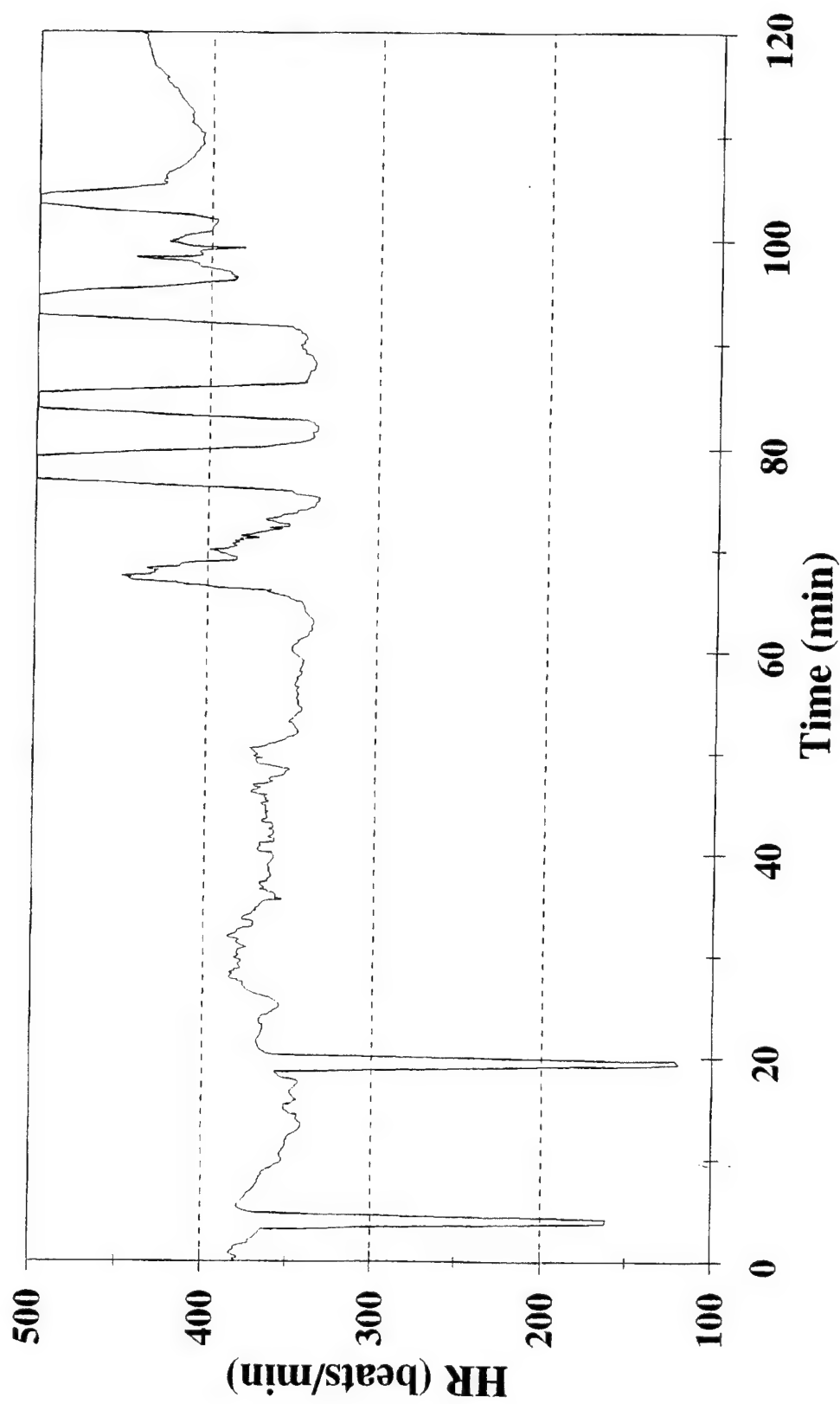


Attachment B

Smoothed (Moving Average) Hemorrhage Data for the Rat

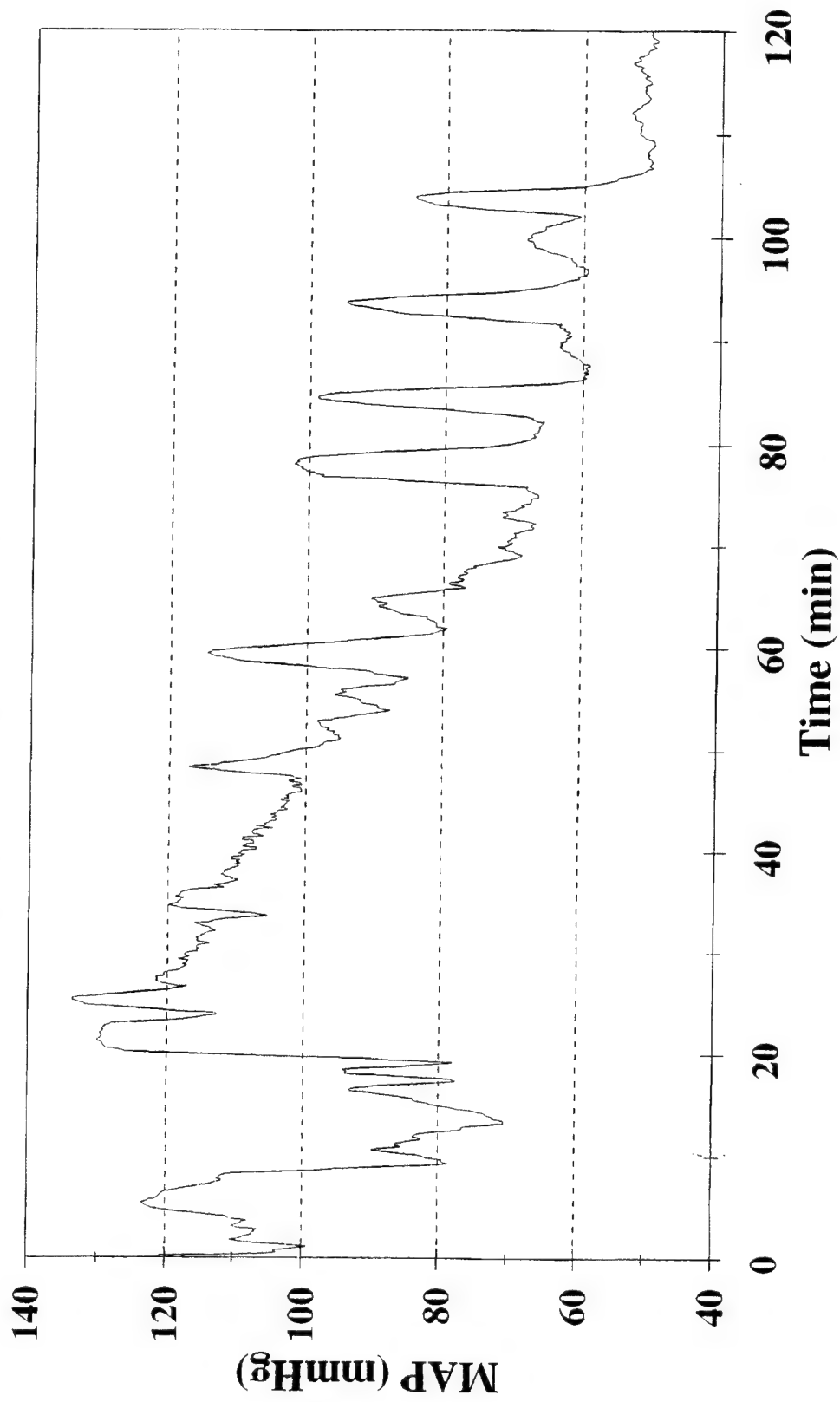
HR Changes After Hemorrhage In Rats

One Minute Moving Average Values



MAP Changes After Hemorrhage In Rats

One Minute Moving Average Values



SOUTHWEST RESEARCH INSTITUTE

6220 CULEBRA ROAD • POST OFFICE DRAWER 28510 • SAN ANTONIO, TEXAS, USA 78228-0510 • (210) 684-5111 • TELEX 244846

June 14, 1996

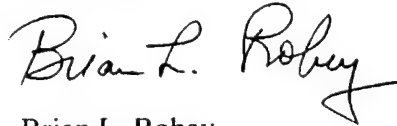
Frederick Pearce, Ph.D.
Director, Division of Surgery
Walter Reed Army Institute of Research
16th St., Building 40
Washington, D.C. 20307-5100

Dear Dr. Pearce:

Enclosed is the seventh quarterly report for work performed under contract no. DAMD17-94-C4126. This report covers the period from 2 March, 1996 to 24 May, 1996.

Please feel free to contact me at (210) 522-5115 if you have any questions or concerns regarding the technical aspects of this report. Please contact Ms. Sharon Rowe at (210) 522-3026 for any contractual or financial matters.

Sincerely,



Brian L. Robey
Project Manager
Biosciences & Bioengineering Department

Enclosure



SAN ANTONIO, TEXAS
HOUSTON, TEXAS • DETROIT, MICHIGAN • WASHINGTON, DC

SOUTHWEST RESEARCH INSTITUTE

6220 CULEBRA ROAD • POST OFFICE DRAWER 28510 • SAN ANTONIO, TEXAS, USA 78228-0510 • (210) 684-5111 • TELEX 244846

June 14, 1996

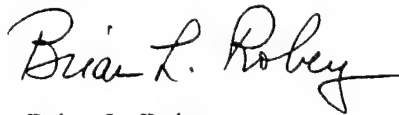
Donald P. Jenkins, Ph.D.
Deputy Director for Defense Healthcare Technologies
DARPA/Defense Sciences Office
3701 North Fairfax Drive
Arlington, VA 22203-1714

Dear Dr. Jenkins:

Enclosed is the seventh quarterly report for work performed under contract no. DAMD17-94-C4126. This report covers the period from 2 March, 1996 to 24 May, 1996.

Please feel free to contact me at (210) 522-5115 if you have any questions or concerns regarding the technical aspects of this report. Please contact Ms. Sharon Rowe at (210) 522-3026 for any contractual or financial matters.

Sincerely,



Brian L. Robey
Project Manager
Biosciences & Bioengineering Department

Enclosure



SAN ANTONIO, TEXAS
HOUSTON, TEXAS • DETROIT, MICHIGAN • WASHINGTON, DC

SOUTHWEST RESEARCH INSTITUTE

6220 CULEBRA ROAD • POST OFFICE DRAWER 28510 • SAN ANTONIO, TEXAS, USA 78228-0510 • (210) 684-5111 • TELEX 244846

June 14, 1996

Director
U.S. Army Medical Research Acquisition Activity
ATN: SGRD-RMA-RC
Fort Detrick
Frederick, MD 21702-5014

Dear Sir:

Enclosed is the seventh quarterly report for work performed under contract no. DAMD17-94-C4126. This report covers the period from 2 March, 1996 to 24 May, 1996.

Please feel free to contact me at (210) 522-5115 if you have any questions or concerns regarding the technical aspects of this report. Please contact Ms. Sharon Rowe at (210) 522-3026 for any contractual or financial matters.

Sincerely,



Brian L. Robey
Project Manager
Biosciences & Bioengineering Department

Enclosure



SAN ANTONIO, TEXAS
HOUSTON, TEXAS • DETROIT, MICHIGAN • WASHINGTON, DC

Quarterly Progress Report

1. Contract No. DAMD17-94-c4126

2. Report Date 15 June, 1996

SwRI Project No. 12-6711

3. Reporting Period from 2 March, 1996 to 24 May, 1996.

4. PI Brian Robey

5. Phone (210) 522-5115

6. Institution Southwest Research Institute, San Antonio, Texas

7. Project Title Model for Trauma Patient Simulation and Automated Fluid Resuscitation

8. Current staff with percent effort of each on project

Brian Robey 2 %

Dean Winter 1%

Jian Ling 15%

Aileen Huang 43%

9. Contract expenditures to date (as applicable):

	this qtr/cumulative		this qtr/cumulative
Personnel	<u>7,439.98 / 47,174.41</u>	Travel	<u>0.00 / 4,792.08</u>
Fringe Benefits	<u>3,251.26 / 20,615.23</u>	Equipment/Supplies/ Consultants	<u>183.24 / 9,937.74</u>
Overhead	<u>12,615.66 / 79,991.76</u>	Facilities Capital	<u>1,033.52 / 6,861.03</u>

	this qtr/cumulative
Subtotal	<u>24,523.66 / 169,372.25</u>
Indirect Costs	<u> / </u>
Fee	<u>1,879.22 / 13,001.01</u>
Total	<u>26,402.88 / 182,373.26</u>

10. Administrative and Logistical Matters

Presently, SwRI has successfully completed the development of the passive cardiovascular model and developed three separate models for implementing the neural and hormonal control for the trauma patient simulator (TPSIM). The first two control models, the deterministic and neural network models, have been discussed in past quarterly reports. Both the deterministic and neural network models were plagued with a number of limitations. The deterministic control model (detailed in quarterly report September 1995) was less successful because the model is a linear approximation of a nonlinear response and takes a long time to train (refer to quarterly report December 1995). Conversely, the neural network model requires more individual swine data than is presently available to obtain realistic model parameters (detailed in quarterly report September 1995). The third model, a fuzzy logic model, was developed this quarter. It is the third model may be the most appropriate method for modeling the neural and hormonal control in the TPSIM. Parameters for the new TPSIM were obtained by training the model with fluid resuscitation data obtained from Dr. William Bickell of St. Francis Hospital in Tulsa, Oklahoma. As of this quarter, the development of the TPSIM has focused on fluid resuscitation with normal saline. Additional fluids will be studied once SwRI has determined what fluids will be available to the soldier in the battlefield. This issue will be addressed at the IMAGE/DARPA Annual Principal Investigator Workshop on June 27, 1996.

A paper describing the development of the fuzzy logic model has been submitted to the 1996 IEEE Engineering in Medicine and Biology (EMBS) Conference by Jian Ling and Brian Robey, "A Fuzzy Logic Model for Neural and Hormonal Compensation in Hemorrhagic Shock" (Attachment).

Dr. Aileen Y. Huang joined SwRI on March 4, 1996 and has been assigned to assist the research efforts on the LSTAT project. Dr. Huang joined SwRI after completing her doctorate at The Johns Hopkins University in the Department of Biomedical Engineering.

11. Scientific Progress

Task 1 - Passive System Model Development/Refinement:

No modifications were made to the passive cardiovascular system model.

Task 2 - Acquire Existing Data:

Last quarter, Mr. Jian Ling contacted Dr. William Bickell at the St. Francis Hospital in Tulsa, Oklahoma. In his 1989 Circulatory Shock paper, Dr. Bickell described his work on the hemodynamic response to non-fatal uncontrolled hemorrhage in the anesthetized swine. These mean hemodynamic values published in the 1989 paper were used for the initial training of the hemorrhage model. Since then, Dr. Bickell has begun studying the effect of fluid resuscitation on non-fatal and fatal uncontrolled hemorrhages in the anesthetized swine. The fluids used for his studies include: normal saline, lactated Ringer's, different concentrations of diaspirin crosslinked hemoglobin, fresh whole blood and stored red blood cells with 5% albumin. This quarter Dr. Bickell generously provided SwRI with the individual swine data collected during his present set of experiments. SwRI also inquired about the individual swine data collected for the 1989 study which were collected at Letterman Army Institute of Research. Although Dr. Bickell was more than willing to share that data, he did not have a copy of the data since Letterman disbanded. He suggested that Major Stephen Bruttig of the U.C. Army Medical Reserve and Materiel Command would be able to locate the data.

On April 15, 1996, Dr. Aileen Huang contacted Major Bruttig. Major Bruttig is under the impression that he can locate the individual swine data collected for the 1989 study; although the data have yet been received.

Task 3 - Deterministic Control System Model Development:

No modifications were made to the deterministic control system.

Task 4 - Deterministic Model Refinement and Testing:

No modifications were made to the deterministic control system.

Task 5 - Neural Network Control System Development:

No modifications were made to the neural network control system.

Task 6 - Neural Network Model Refinement and Testing:

No modifications were made to the neural network control system.

Task 7 - Model Reliability and Accuracy Studies:

No modifications were made to the neural network control system.

Task 8 - Control System Model Selection:

At the onset of this quarter, SwRI had developed two different models for the neural and hormonal control in the trauma patient simulator (TPSIM), a deterministic control model and a neural network model. Although both models produced positive results, both models are limited by a number of constraints. The deterministic control model (detailed in quarterly report September 1995) is limited because it is a linear approximation of a nonlinear function and a lengthy training procedure is required (refer to quarterly report December 1995). Although the neural network model is a nonlinear model, the model is limited by the minimal amount of animal data presently available. Furthermore, the black box nature of neural network models makes it difficult to interpret the physiological mechanism of the neural and hormonal control. Taking these constraints into consideration, this quarter, SwRI developed a third control system for the TPSIM which is based on fuzzy logic.

Fuzzy logic is a relatively new modeling technique used by bioscientists for controlling and modeling biological systems. Fuzzy logic systems incorporate the domain knowledge of neural and hormonal regulation and can be used to model nonlinear systems. With the incorporation of the domain knowledge, the demand for additional data is lessened and the training procedure is accelerated.

Task 9 - Development of a Fluid Resuscitation Optimization Algorithm:

The fuzzy logic control model was integrated with the passive system model of cardiovascular hemodynamics and fluid exchange to form the independent trauma patient TPSIM. The TPSIM was trained with swine hemorrhage and fluid resuscitation data. A number of assumptions have been made for these initial tests:

1. The hemorrhaging has been stopped by a medic in the field.

2. The available resuscitation fluid is normal saline.
3. The wound is a penetrating trauma to the torso with no head trauma.

It was necessary to make these assumptions for the initial tests to eliminate the complications of secondary hemorrhaging due to fluid infusion and the additional factors involved in the event of trauma to the head. The predicted changes in heart rate, heart contractility, peripheral resistance, and venous compliance were consistent with the physiological results. The trends in predicted mean arterial blood pressure, cardiac output, and hematocrit were also in agreement with physiological results, although the model tended to overestimate predicted magnitudes. This may be due to the individual differences between the swine. Also, the passive component of the fuzzy logic TPSIM model was found to be too sensitive to the blood loss and fluid resuscitation. The fuzzy logic TPSIM model provided meaningful results about hemodynamic changes during hemorrhage. However, additional training should be performed once the passive model has been refined to incorporate a broader range of blood loss and additional fluids.

Task 10 - Real Time Software System Development:

Not started.

Task 11- Prototype System Development:

Not started.

Plans For Next Quarter

- Refine the passive model.
- Refine the fuzzy logic model to decrease the amount of oscillations.
- Determine the available fluids on the LSTAT Trauma Pod for resuscitation.
- Use different resuscitation fluids to continue training the model.
- Study the affect of different rates and volume of resuscitation fluids on the model to further develop the fluid resuscitation optimization algorithm.

ATTACHMENT

PAPER SUBMITTED TO IEEE EMBS CONFERENCE 1996

A Fuzzy Logic Model for Neural and Hormonal Compensation in Hemorrhagic Shock

Jian Ling and Brian L. Robey

Southwest Research Institute, San Antonio, Texas, 78238 U.S.A.

E-mail: jling@swri.edu, brobey@swri.edu

Abstract - Southwest Research Institute (SwRI) has developed a fuzzy logic model to simulate neural and hormonal compensation (NHC) mechanisms during hemorrhagic shock. This NHC model is a component in a larger trauma patient simulation model under development that predicts changes in hemodynamic parameters during and after hemorrhage. These predicted variables may then be used to determine and automate fluid resuscitation. To develop the fuzzy logic model, SwRI combined physiological knowledge about NHC with experimental hemorrhage data obtained from swine. Plausible predictions for physiological variables were obtained.

I. INTRODUCTION

Southwest Research Institute (SwRI) is developing an automated fluid resuscitation system for the Advanced Research Projects Agency (ARPA) and the U.S. Army. This system is composed of two components: a trauma patient simulation model for prediction of changes in hemodynamic parameters during and after a hemorrhage (with and without fluid resuscitation) and a decision-making system for selection of optimal fluid resuscitation strategies based on model predictions. This overall system is intended to enhance the quality of trauma care on the battlefield while conserving medical resources.

During hemorrhage, compensation mechanisms play an important role in maintaining blood pressure and cardiac output during hemorrhage. These mechanisms include baroreceptor feedback control, chemoreceptor control, central nervous system ischemic control, and hormonal regulation [1]. When arterial blood pressure decreases after severe hemorrhage, the baroreceptors in the walls of the great arteries elicit powerful stimulation to the sympathetic

vasoconstrictor system throughout the body. This increases peripheral resistance to maintain arterial blood pressure. The sympathetic constriction of the veins attempts to increase the venous return and restrict cardiac output. The sympathetic system also increases the heart rate and contractility of the heart. Chemoreceptors in the walls of blood vessels detect decreased oxygen content and then excite the vasomotor center to elevate blood pressure. The central nervous system invokes a strong sympathetic response as a final effort to prevent brain blood flow from decreasing to a lethal level.

Hormonal regulation includes the formation of angiotensin which constricts the peripheral arteries, thereby raising blood pressure. The hypothalamus secretes vasopressin which even further constricts the peripheral arteries and veins [1].

SwRI is developing a model for these neural and hormonal compensation (NHC) mechanisms during hemorrhage. This NHC model, in combination with a passive cardiovascular system model, forms the basis for the trauma patient simulator. This paper describes the use of fuzzy logic to simulate these complex and inter-related NHC mechanisms.

II. METHODS

The effects of NHC are adjustments of heart rate (HR), heart contractility (CT), peripheral resistance (PR), and venous compliance (VC) to return blood pressure and blood oxygen content to normal levels. To develop the fuzzy logic model, changes in mean arterial pressure (MAP) and oxygen debt (O2D) (the difference between oxygen consumption and oxygen delivery) were selected as NHC model inputs, and HR, CT, PR, and VC as model outputs (Fig. 1).

A. Fuzzy Logic System

A fuzzy logic system was chosen to model the NHC system. Fuzzy logic systems are able to handle nonlinear

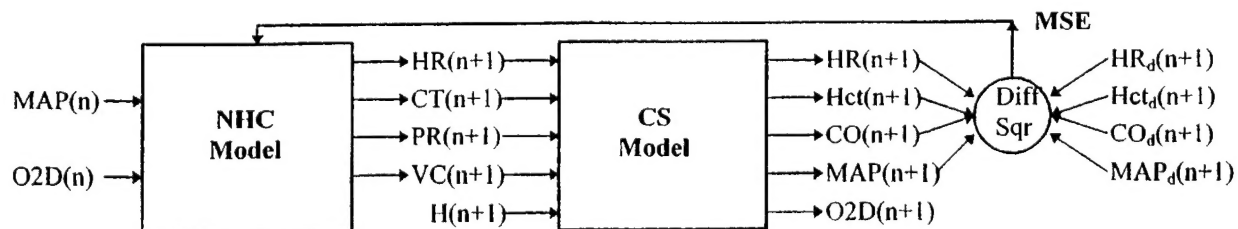


Fig. 1. Flow diagram for the trauma patient simulator comprised of both a neural and hormonal compensation (NHC) model and a cardiovascular system (CS) model [2]. The mean squared error (MSE) between the estimation and measurements (indicated by subscript d) for HR, Hct, CO, and MAP was used to optimize the NHC model.

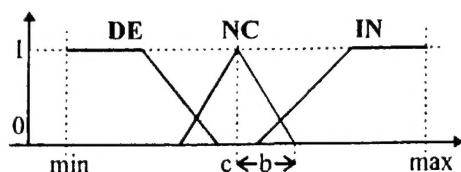


Fig. 2. Membership functions (MBFs) for "Decreased" (DE), "No Change" (NC), and "Increased" (IN). The variable c represents the center of the MBF; b is one-half of MBF's base width; min and max are the limits of the variable inputs and outputs.

Table 1. Four rules based on physiological compensation mechanisms.

IF (Inputs)		THEN (Outputs)			
MAP	O2D	HR	CT	PR	VC
DE	NC	IN	IN	IN	DE
DE	IN	IN	IN	IN	DE
NC	NC	NC	NC	NC	NC
IN	NC	DE	DE	DE	IN

relationships between inputs and outputs. Such systems can also incorporate domain-specific knowledge useful in problem solving. Previous attempts to model NHC with a neural network were less successful; predictions for PR and CT were unrealistic. To develop the NHC fuzzy logic model, three linguistic variables, *Decreased* (DE), *No Change* (NC), and *Increased* (IN), were used to describe the changes between inputs and outputs. The membership function (MBF) used to represent changes in inputs and outputs is illustrated in Fig. 2. Four fuzzy rules were developed to describe the physiological effects on HR, CT, PR, and VC based on changes in MAP and O2D (Table 1).

The fuzzy singleton approach was used to fuzzify the input values. Fuzzy MIN and MAX operators were adopted for the fuzzy inference engine [3]. The center-of-gravity defuzzifier was used to defuzzify the outputs from the NHC model.

B. Training the NHC Model

Optimal membership functions (i.e., the center and width of each MBF) were obtained by training the model with experimental data. Data was obtained from uncontrolled hemorrhage experiments on five swine performed by Bickell et al. [4]. The HR, MAP, CO, and Hct were measured at 0, 5, 15, 30, 60, 90, and 120 minutes after the start of each hemorrhage. The modified random search (MRS) optimization method [5] was used to train the model with averaged experiment data.

III. RESULTS AND DISCUSSION

Figs. 3 and 4 illustrate changes in HR, CT, PR, VC, MAP, CO, and O2D calculated by the trauma patient simulator with NHC for 33% blood loss in 5 minutes. Trends for PR, CT, and VC follow physiological expectations. In particular, PR doubled during hemorrhage. The results also show a decrease in CT after an initial increase. This may suggest that a

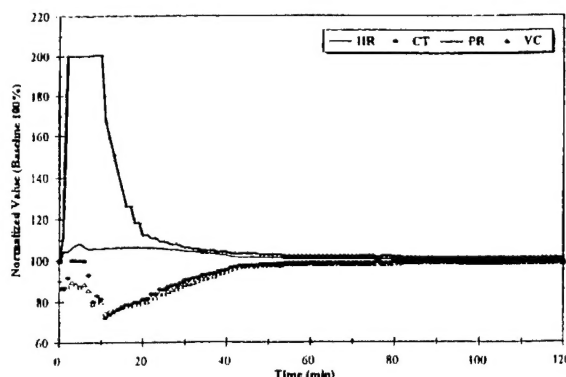


Fig. 3. Changes in heart rate (HR), heart contractility (CT), peripheral resistance (PR), and venous compliance (VC) during and after hemorrhage as predicted by the neural and hormonal compensation model.

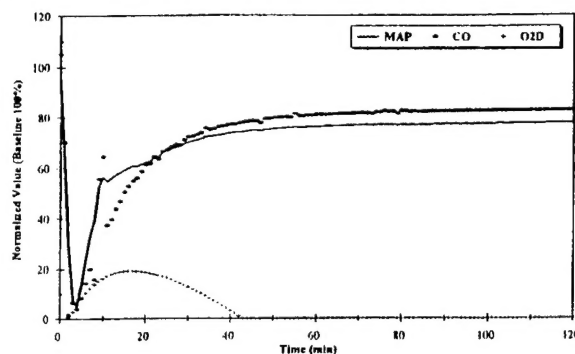


Fig. 4. Changes in mean arterial pressure (MAP), cardiac output (CO), and oxygen debt (O2D, in absolute value) during and after hemorrhage as predicted by the cardiovascular model with NHC.

reduction in heart muscle oxygen content prevents normal functioning. In conclusion, the fuzzy logic approach provides a means to include domain-specific knowledge required for solving many complex non-linear problems.

REFERENCES

- [1] A.C. Guyton, *Medical Physiology*. Philadelphia: W.B. Saunders Co., 1991.
- [2] T.J. Doherty, *A Mathematical Model of the Circulation for the Study of Hemorrhagic Shock and Fluid Resuscitation*. Ph.D. Dissertation, University of California at Berkeley, 1993.
- [3] L.X. Wang, *Adaptive Fuzzy Systems and Control*. Prentice Hall, Englewood Cliffs, 1994.
- [4] W.H. Bickell, J. O'Benar, S.P. Bruttig, C.E. Wade, J.P. Hannon, F. Tillman, W. Rodkey, "The hemodynamic response to aortotomy in the conscious chronically instrumented swine," *The Physiologist*, vol. 30, pp.228, 1987.
- [5] N. Baba, "A new approach for finding the global minimum of error function of neural networks," *Neural Networks*, Vol. 2, pp.367-373, 1989.